Complete Reading and Problem Assignments for Physics 243A
Surface Physics of Materials: Spectroscopy, Fall, 2016

READING:

- **WOODRUFF AND DELCHAR, "MODERN TECHNIQUES OF SURFACE SCIENCE", 2ND EDITION--**
  - **Chapter 1**
  - **Chapter 2: Sections 2.1, pp.22 (bottom)-23(top) on Wood notation for surface structures, 2.4, and 2.5 (pp. 31-37), 2.9.6 on standing waves**
  - **Chapter 6: 6.9, 6.10, 6.11**
  - **Chapter 3: Sections 3.1, 3.2, 3.3, 3.5**
- **ZANGWILL, "PHYSICS AT SURFACES", DOWNLOADABLE CHAPTERS 1-5 (SEE COURSE WEBSITE)--**
  - **Chapter 1: Everything except "The roughening transition"**
  - **Chapter 3: pp. 28-34, pp. 49-52 on STM, Pages 85-8, 192-196, 204-212**
  - **Chapter 2: All**
  - **Chapter 4: Introduction, with lighter reading of *The jellium model*, *One-dimensional band theory, and Three-dimensional band theory*, and detailed reading of *Photoelectron spectroscopy, Metals, and Alloys***
- **IBACH, "PHYSICS OF SURFACES AND INTERFACES", DOWNLOADABLE BOOK (SEE COURSE WEBSITE)—**
  - **Chapter 2: 2.1, 2.2**
  - **Chapter 8: 8.2**
- **DESJONQUERES AND SPANJAARD, "CONCEPTS OF SURFACE PHYSICS", EXCERPTS DOWNLOADABLE FROM COURSE WEBSITE:**
  - **On equilibrium shapes of surfaces, thermodynamics, kinetics and adsorption isotherms,STM current calculation, photoelectron diffraction and Debye-Waller factors. No need to follow every step, but as needed to fill in the line of arguments in lecture and Zangwill**
- **FADLEY, "BASIC CONCEPTS OF XPS", HANDED OUT, BUT ALSO DOWNLOADEABLE—**
  - **Read all of it**
- **FADLEY, "THE STUDY OF SURFACE STRUCTURES BY PHOTOELECTRON DIFFRACTION AND AUGER ELECTRON DIFFRACTION", PAGES 421-450 only, DOWNLOADABLE FROM COURSE WEBSITE with other examples and exercises using the EDAC web program introduced in lecture**
- **ATTWOOD, DOWNLOADEABLE EXCERPT ON SYNCHROTRON RADIATION FROM THE BOOK "Soft X-Rays and Extreme Ultraviolet Radiation" (see course website)**
- **SIX READING DOWNLOADS FROM THE COURSE WEBSITE: <u>If needed for comprehension at level of lectures or to use programs</u>**
  - **1) Molecular orbital basics**
  - **2) Tight-binding basics**
  - **3) Core-Hole Multiplets with Charge Transfer--Basic Theory, or similar pages from Book by de Groot and Kotani**
  - **4) Brief Manual for SESSA spectral simulation program**
  - **5) Brief Manual for CTM4XAS20 charge-transfer multiplet simulation program**
  - **[7) <u>Optional only for physics students</u>: Basic theory for the Hubbard Model of bonding }**

PROBLEM ASSIGNMENT 4-FINAL: Not all problems assigned

Problem Asst. 4—4.5, 4.7(a) only, 5.1, 5.2, 5.3. 5.4, 5.7, 5.8, 5.9, 5.10, due Friday, December 2nd

REMAINING LECTURE SCHEDULE:

22 November, Happy Thanksgiving!, 29 November and 1 December

FINAL EXAMINATION: TUESDAY, DECEMBER 6TH, 10:30-12:30 PM, PHYSICS 185

Open book: You may use lecture notes, copies of lecture slides, textbooks, and laptops, with signed affirmation as follows:

I will not make use of any hardcopy or online material from prior versions of this course that is not posted at the current course website.

Copying from such material will be considered as cheating.

Some basic measurements:

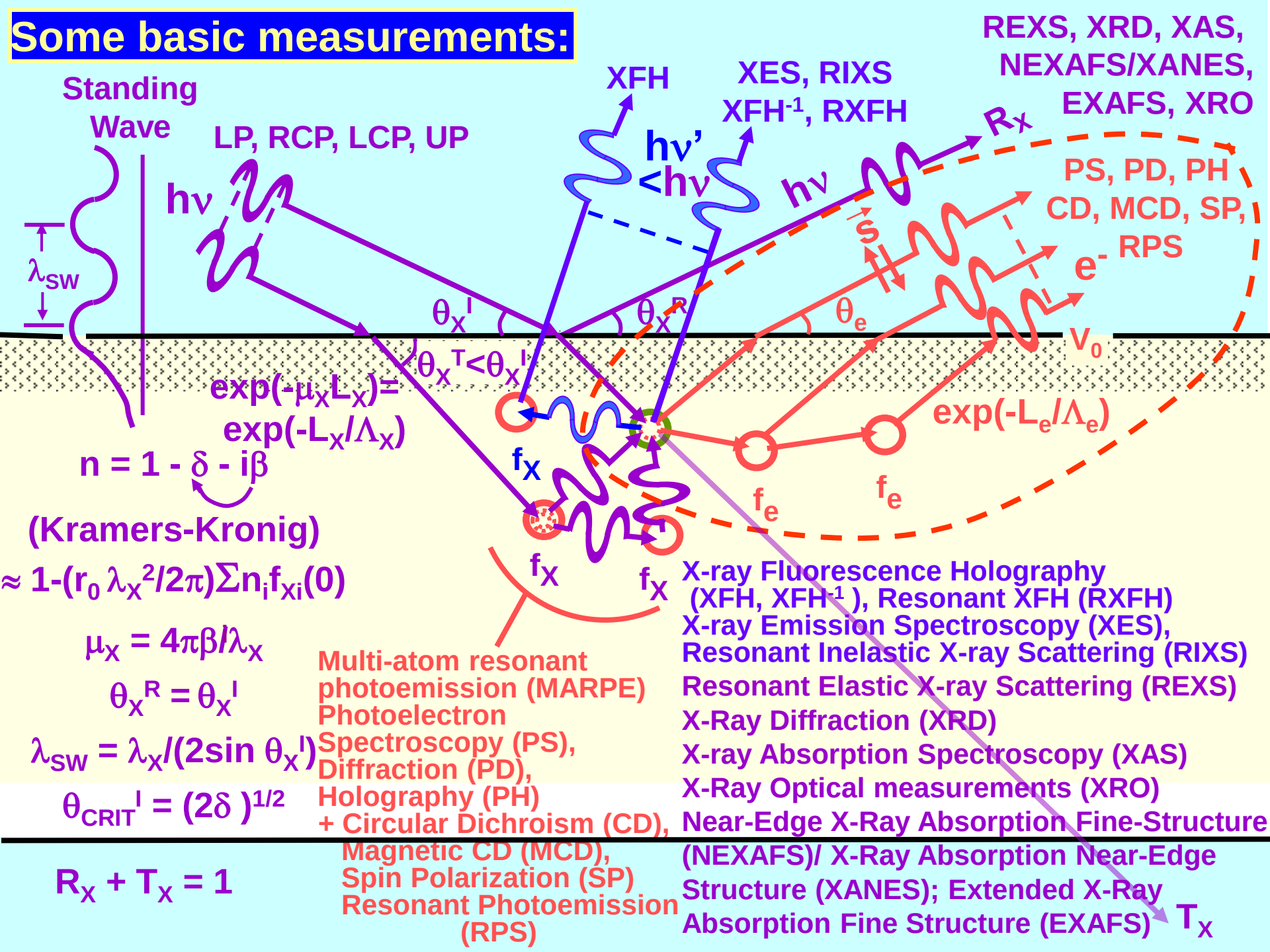

Outline—Here to end of quarter

- Core-level chemical shifts: Koopmans', relaxation, the potential model
- Various other final state effects providing information in core-level spectra
- Photoelectron diffraction, extended x-ray absorption fine structure (EXAFS, XAFS)
- Photoelectron spectroscopy at realistic pressures in the multi-Torr range
- Photoelectron microscopy: adding lateral spatial resolution in 2 dimensions
- Valence-band spectra: low-energy UPS limit and high-energy XPS limit

PHOTOELECTRON SPECTRA

OXIDIZED SILICON

CHEMICAL SHIFTS OF CORE LEVELS

EXACTLY WHAT IS STRUCTURE OF INTERFACE? NEED STATE-SPECIFIC STRUCTURAL INFORMATION!

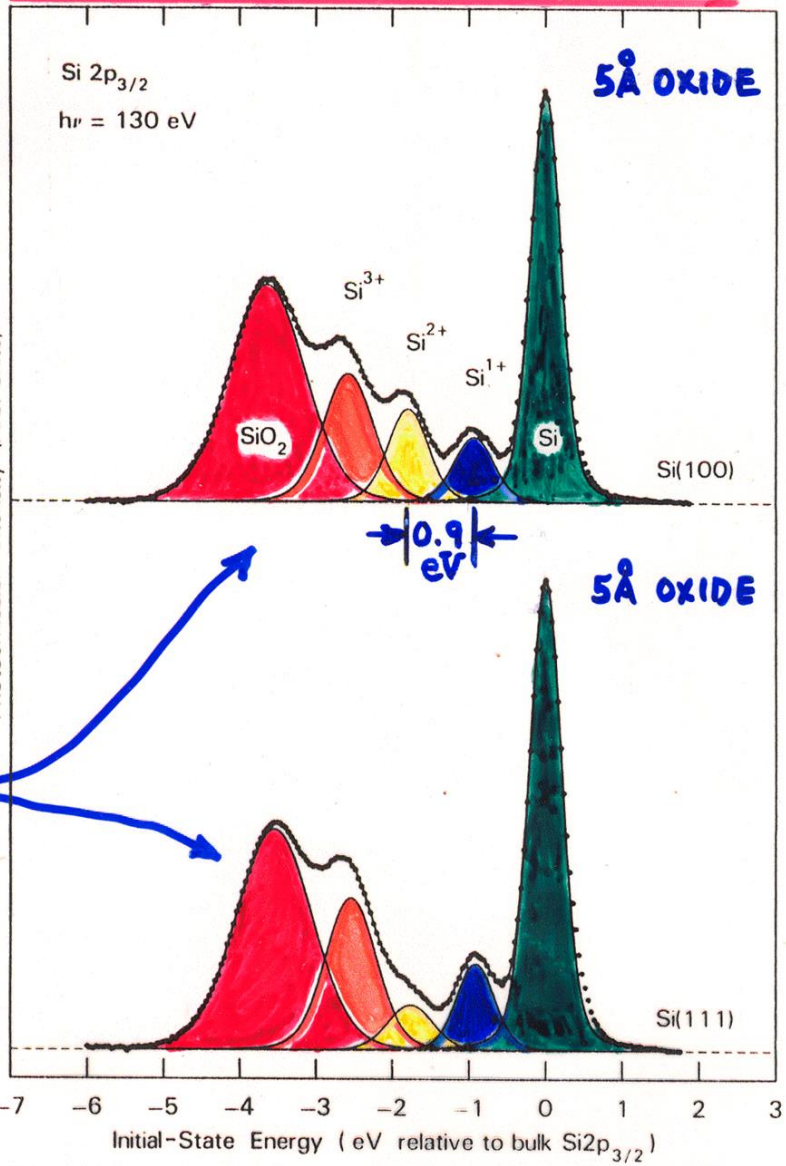

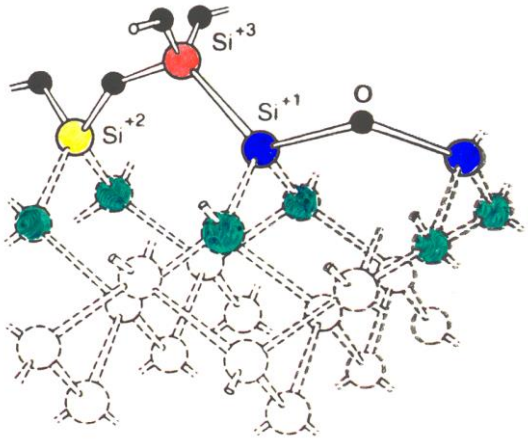

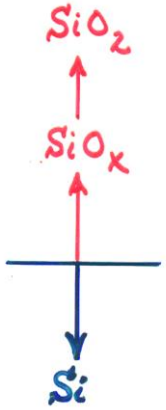

HIMPSEL ET AL., PHYS. REV. B, 38, 6084('90)

CHEMICAL SHIFTS IN ADSORBATE & SUBSTRATE

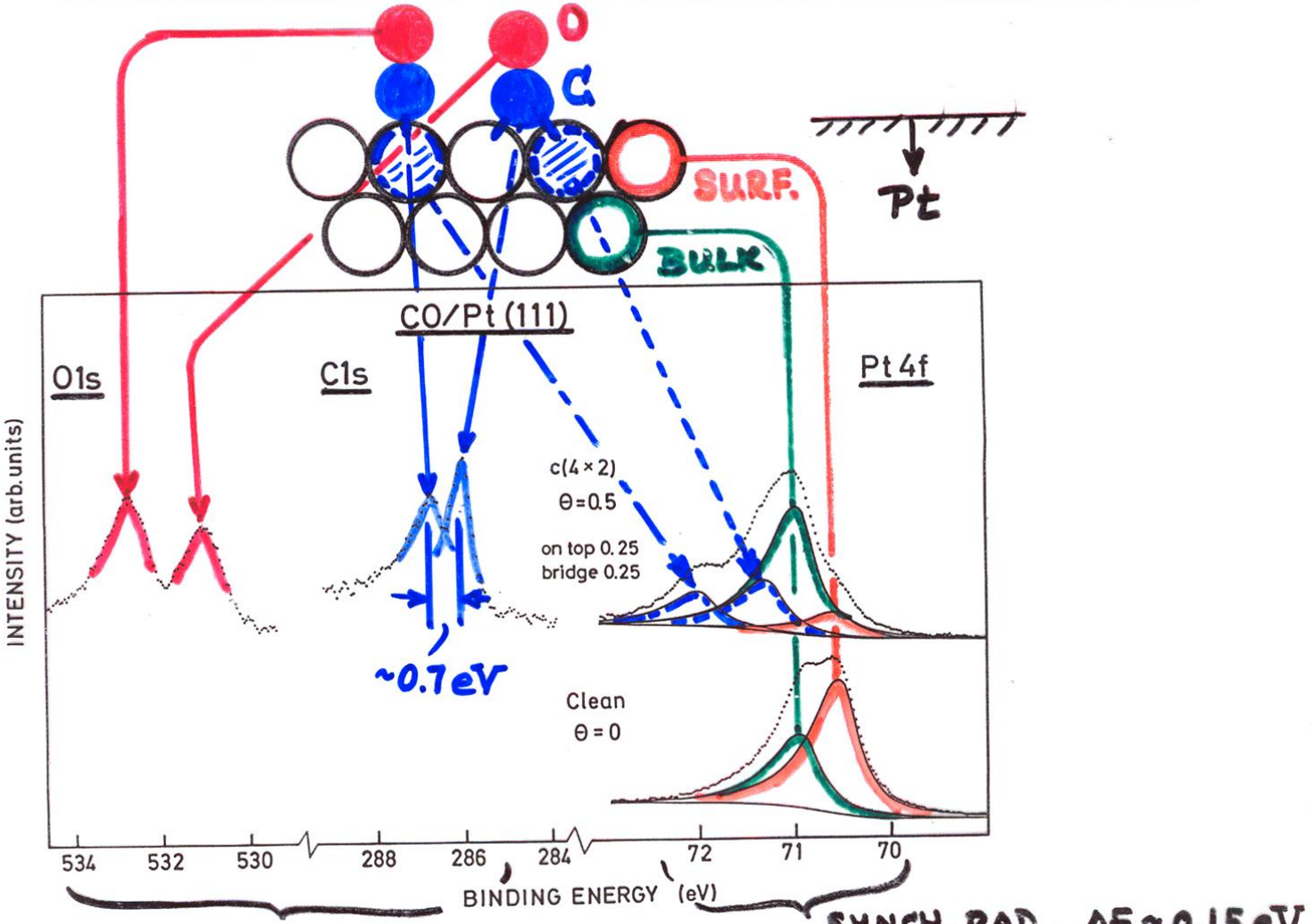

MONOCH. XPS,
ΔE ~ 0.3 eV

SYNCH. RAD., ΔE ~ 0.15 eV

BJÖRNEHOLM
ET AL.
(NILSSON GRP.,
UPPSALA)

Be(0001)-Surface core-level shifts

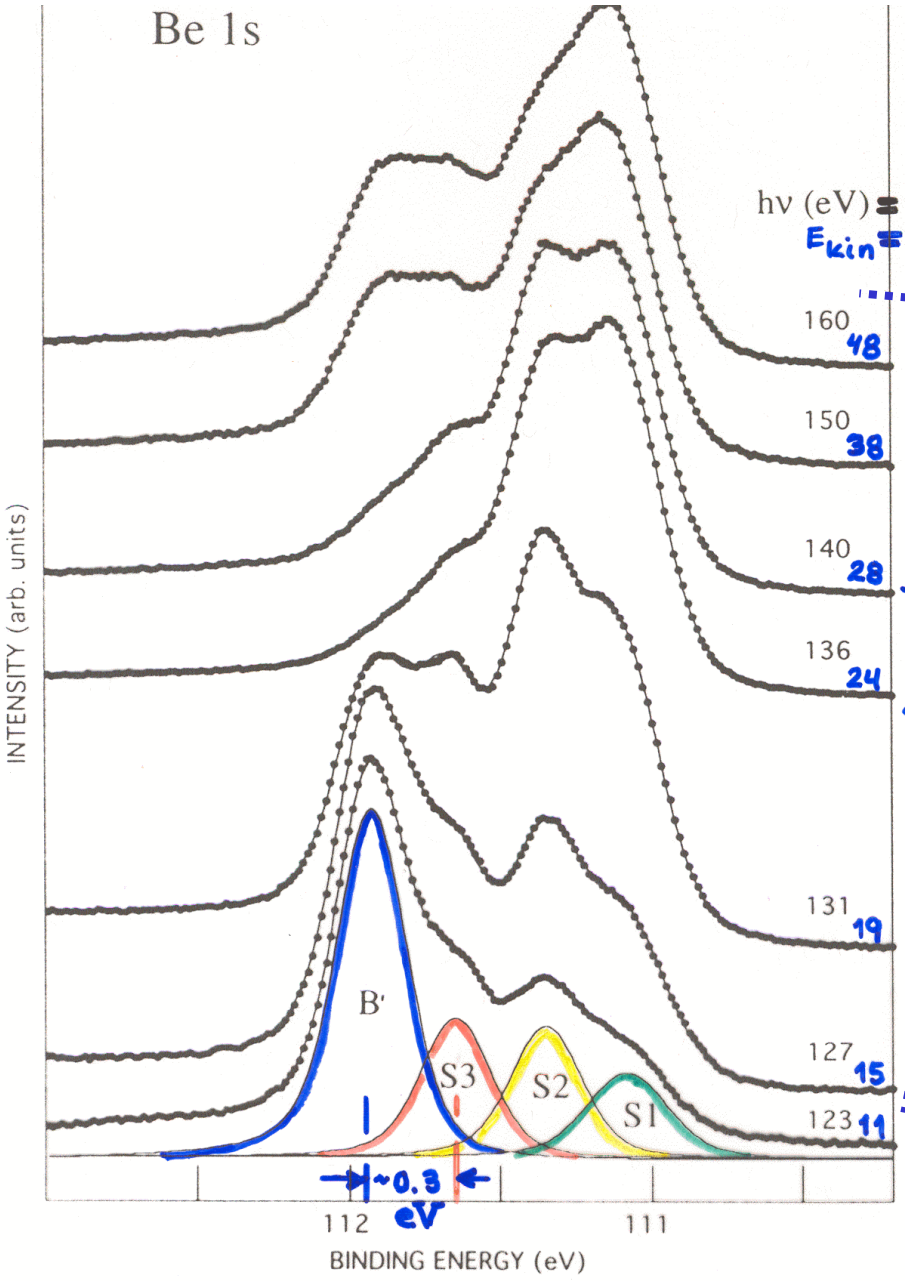

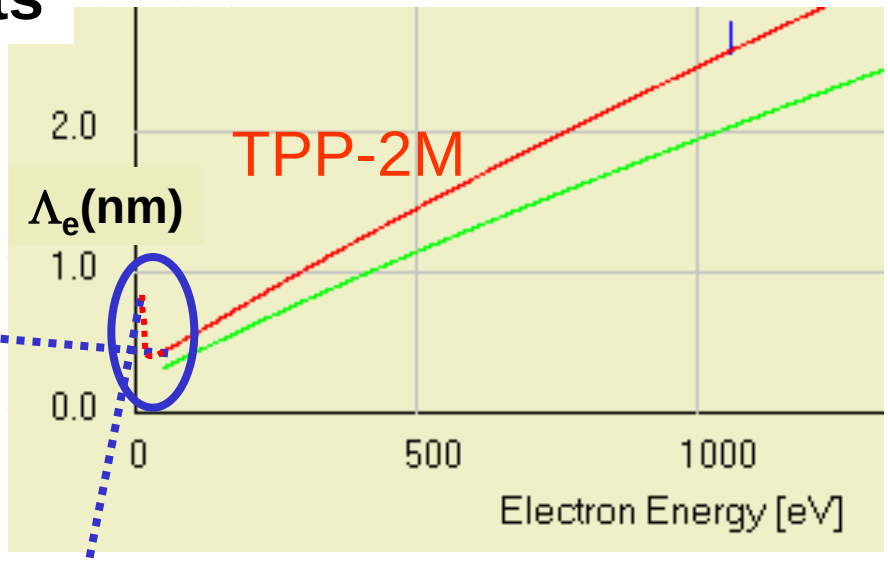

MINIMUM IN e⁻ ESCAPE DEPTH

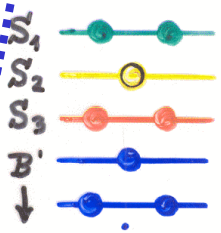

JOHANSSON ET. AL., P.R.L. 71, 2453('93)

Changing photon energy sweeps through IMFP minimum, changes surface and bulk sensitivity dramatically

Basic energetics—Many e⁻ picture

Photoelectron emission: $n\ell j \rightarrow$ photoelectron at $E_{kinetic}$

$$h\nu = E_{binding}^{Vacuum} + E_{kinetic} = E_{binding}^{Fermi} + \varphi_{spectrometer} + E_{kinetic}$$

$$E_{binding}^{Vacuum}(Qn\ell j, K) = E_{final}(N-1, Qn\ell j \text{ hole}, K) - E_{initial}(N)$$

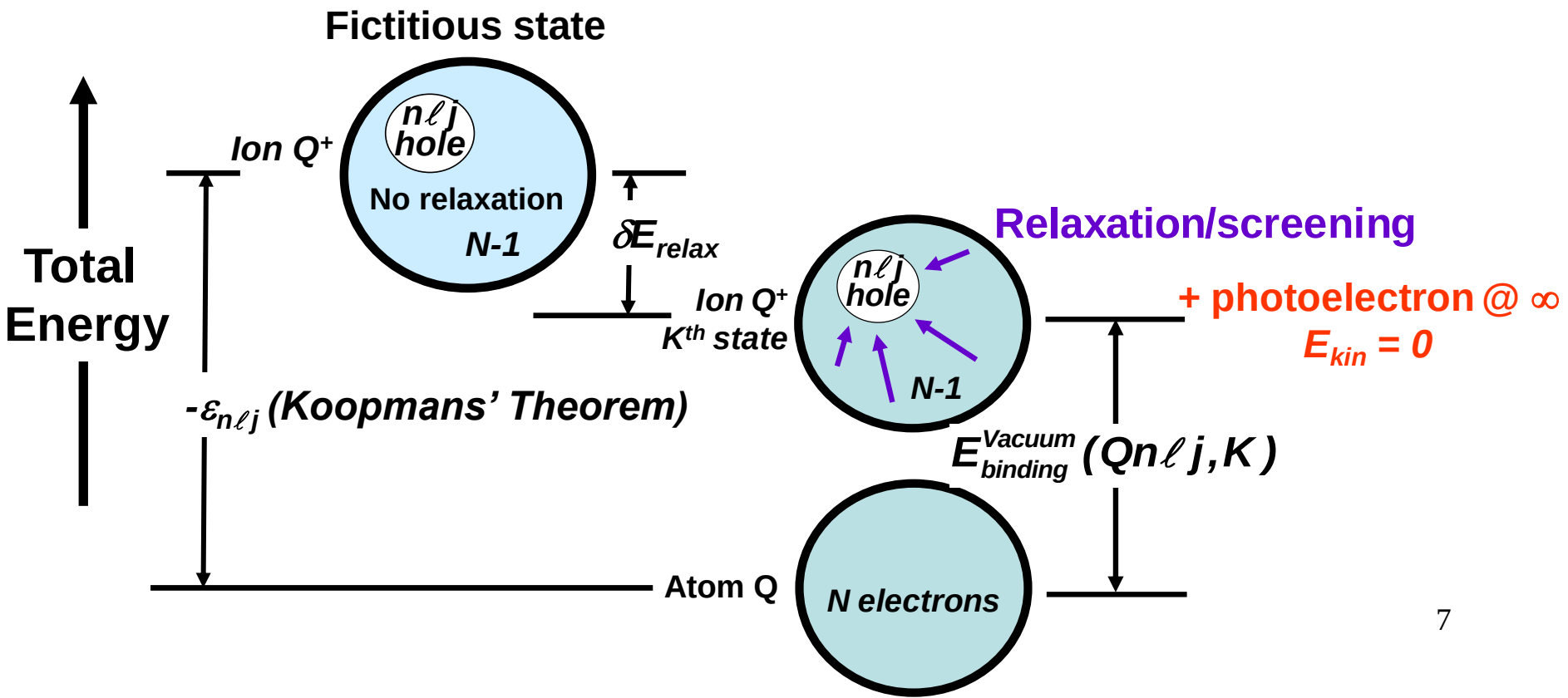

Koopmans' Theorem Calculation of C 1s Chemical Shifts in Small C-Containing Molecules

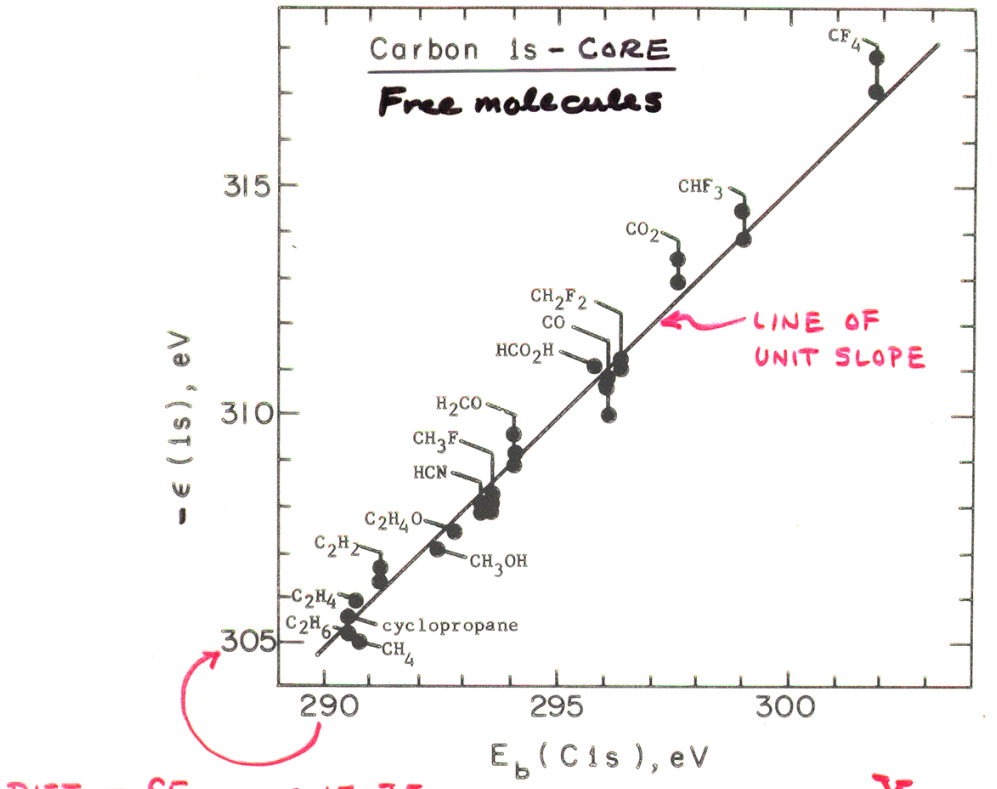

Figure 18 -- Plot of carbon 1s binding energies calculated via Koopmans' Theorem against experimental binding energies for several carbon-containing gaseous molecules. For some molecules, more than one calculated value is presented. The slope of the straight line is unity. The two scales are shifted with respect to one another by 15 eV, largely due to relaxation effects. All of the theoretical calculations were of roughly double-zeta accuracy or better. (From Shirley, reference 7.)

"Basic Concepts of XPS"
Figure 18

GROUND-STATE POTENTIAL MODEL FOR CORE-LEVEL CHEMICAL SHIFTS

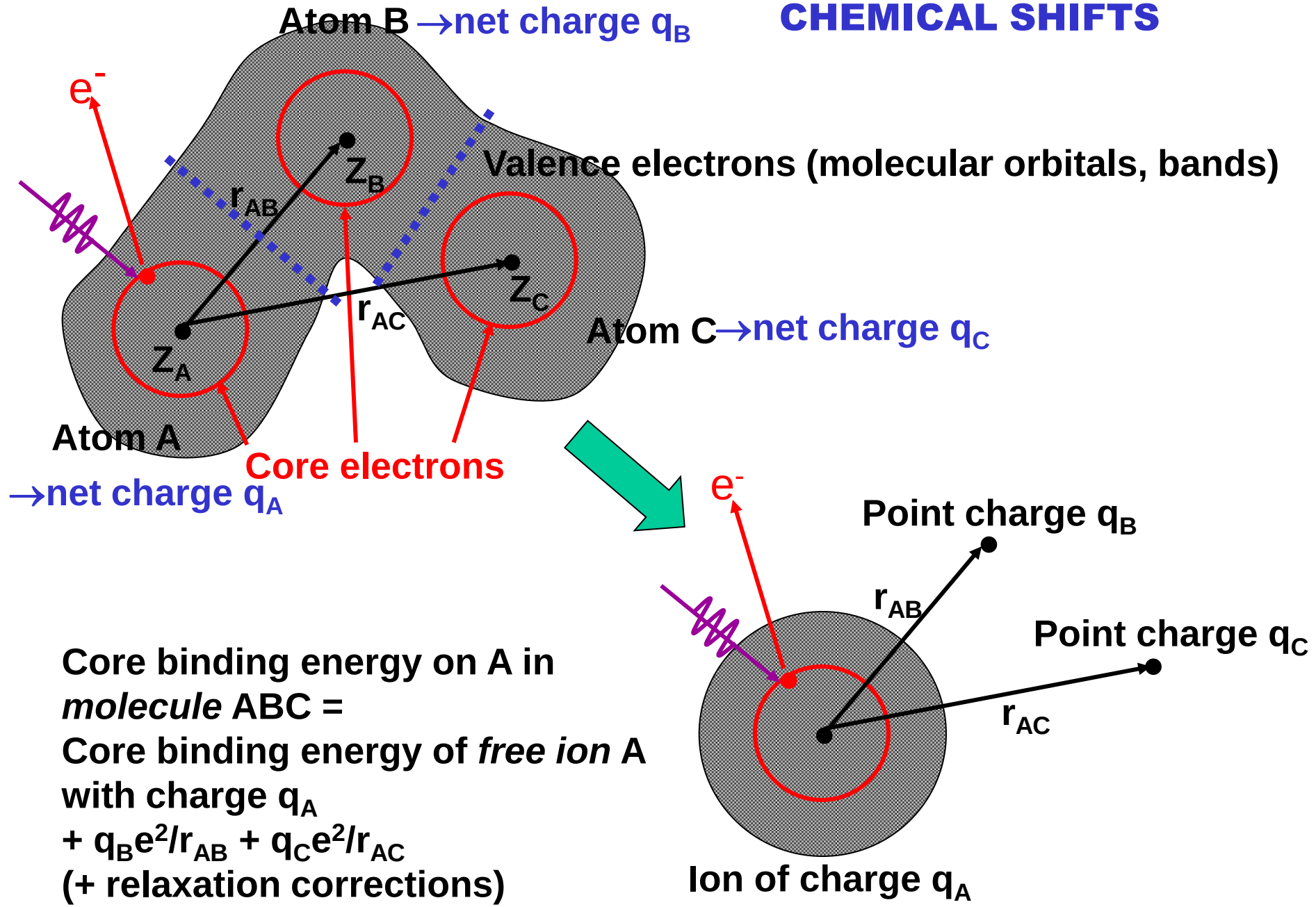

Core binding energy on A in *molecule* ABC =
Core binding energy of *free ion* A with charge q_A
+ $q_B e^2/r_{AB}$ + $q_C e^2/r_{AC}$
(+ relaxation corrections)

FREE-ION (INTRAATOMIC) ASPECTS OF SHIFTS: KOOPMANS' THEOREM & CLASSICAL CHARGED SHELL

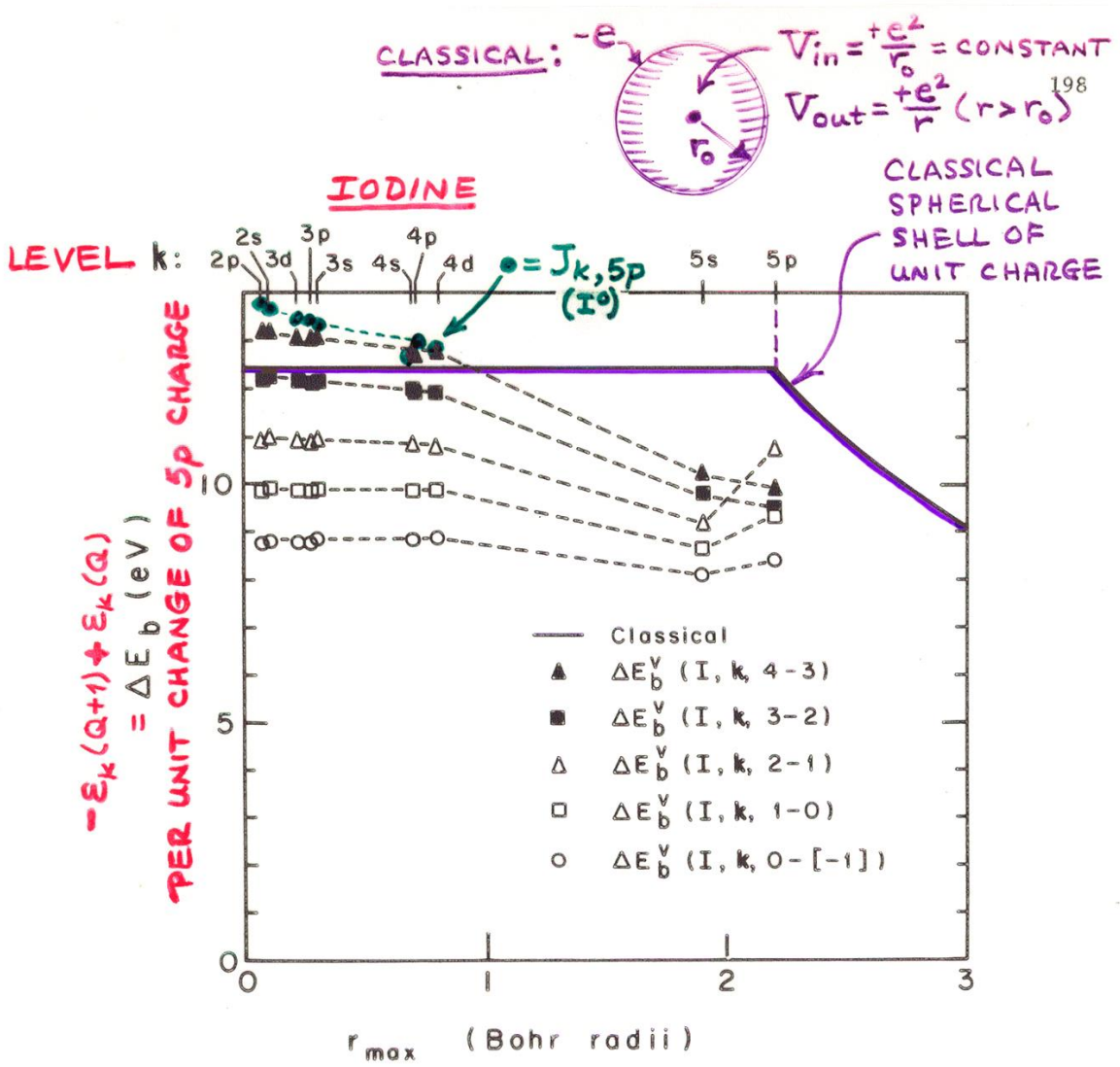

⇒ REMOVAL/ADDITION OF VALENCE e⁻ CHARGE IN BONDING SHIFTS ALL INNER e⁻ E_b's ≈ E_K's BY ~SAME AMOUNT

"Basic Concepts of XPS"
Figure 19

POTENTIAL MODEL CALCULATION OF CARBON CHEMICAL SHIFTS

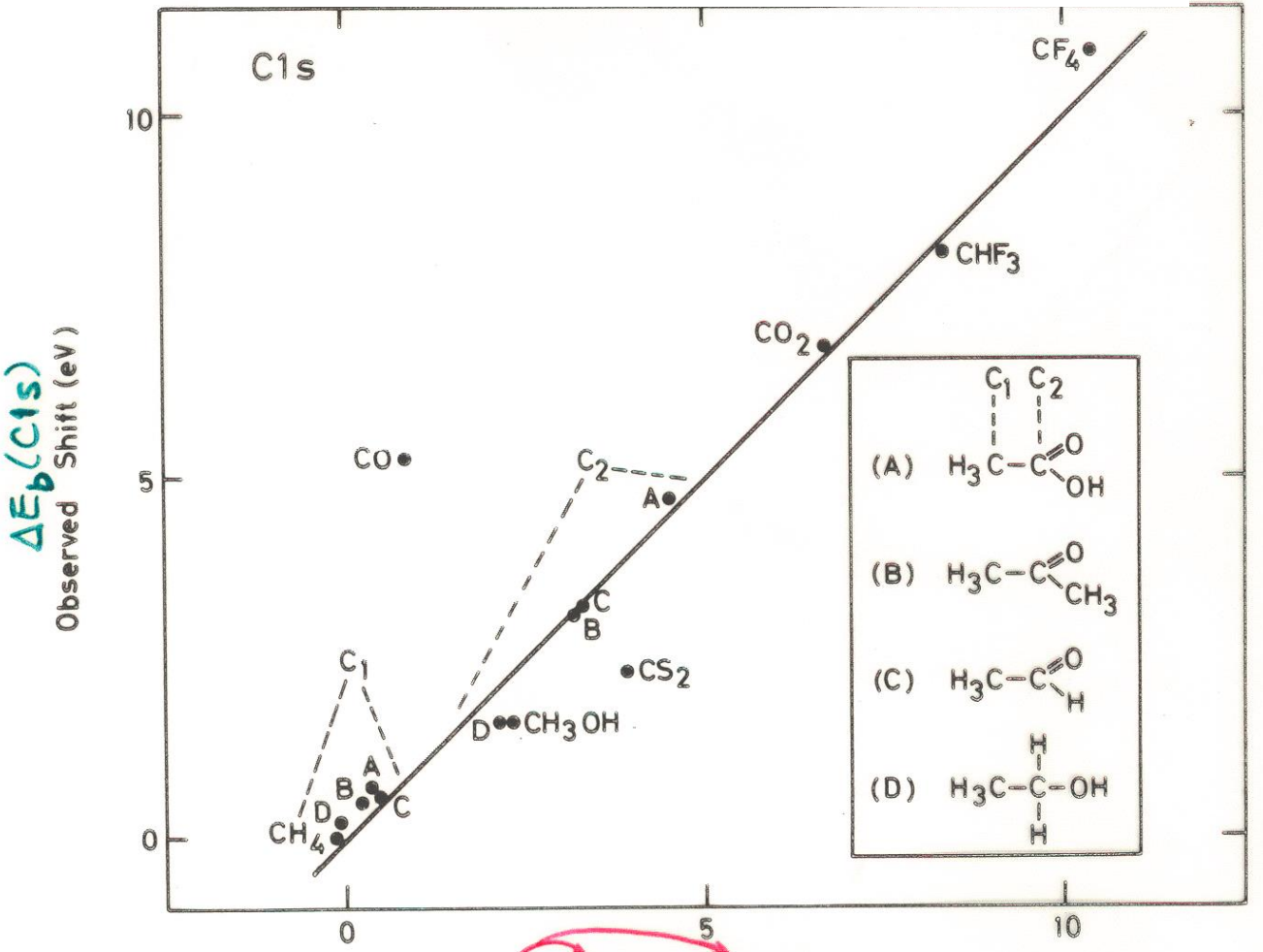

"Basic Concepts of XPS"
Figure 24

Outline—Here to end of quarter

- Core-level chemical shifts: Koopmans', relaxation, the potential model
- Various other final state effects providing information in core-level spectra
- Valence-band spectra: low-energy UPS limit and high-energy XPS limit
- Photoelectron diffraction, extended x-ray absorption fine structure (EXAFS, XAFS)
- Photoelectron spectroscopy at realistic pressures in the multi-Torr range
- Photoelectron microscopy: adding lateral spatial resolution in 2 dimensions

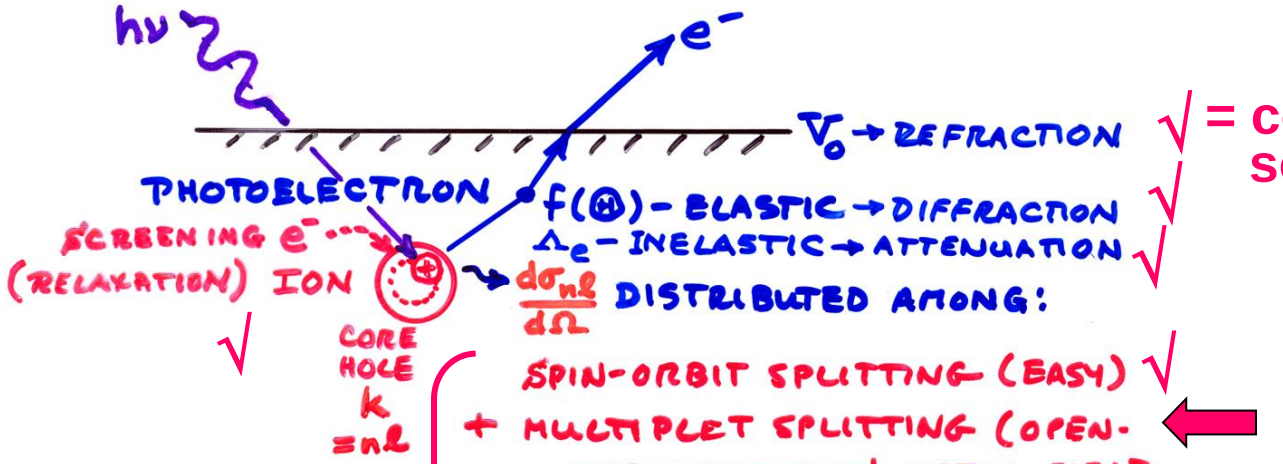

√ = covered so far

ADDITIONAL SOURCES OF STRUCTURE (AND INFORMATION!) IN SPECTRA BEYOND CHEMICAL SHIFTS

REALLY ALL AT ONCE, BUT SUM RULES + THEORY HELP

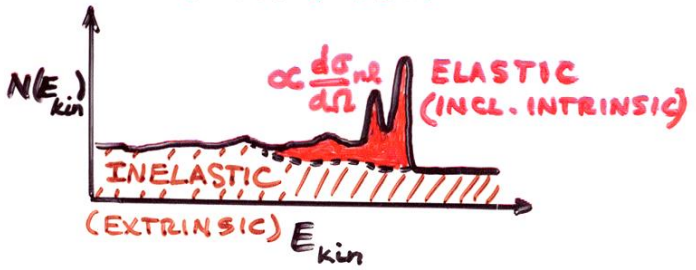

CORE-LEVEL MULTIPLET SPLITTINGS IN Mn COMPOUNDS

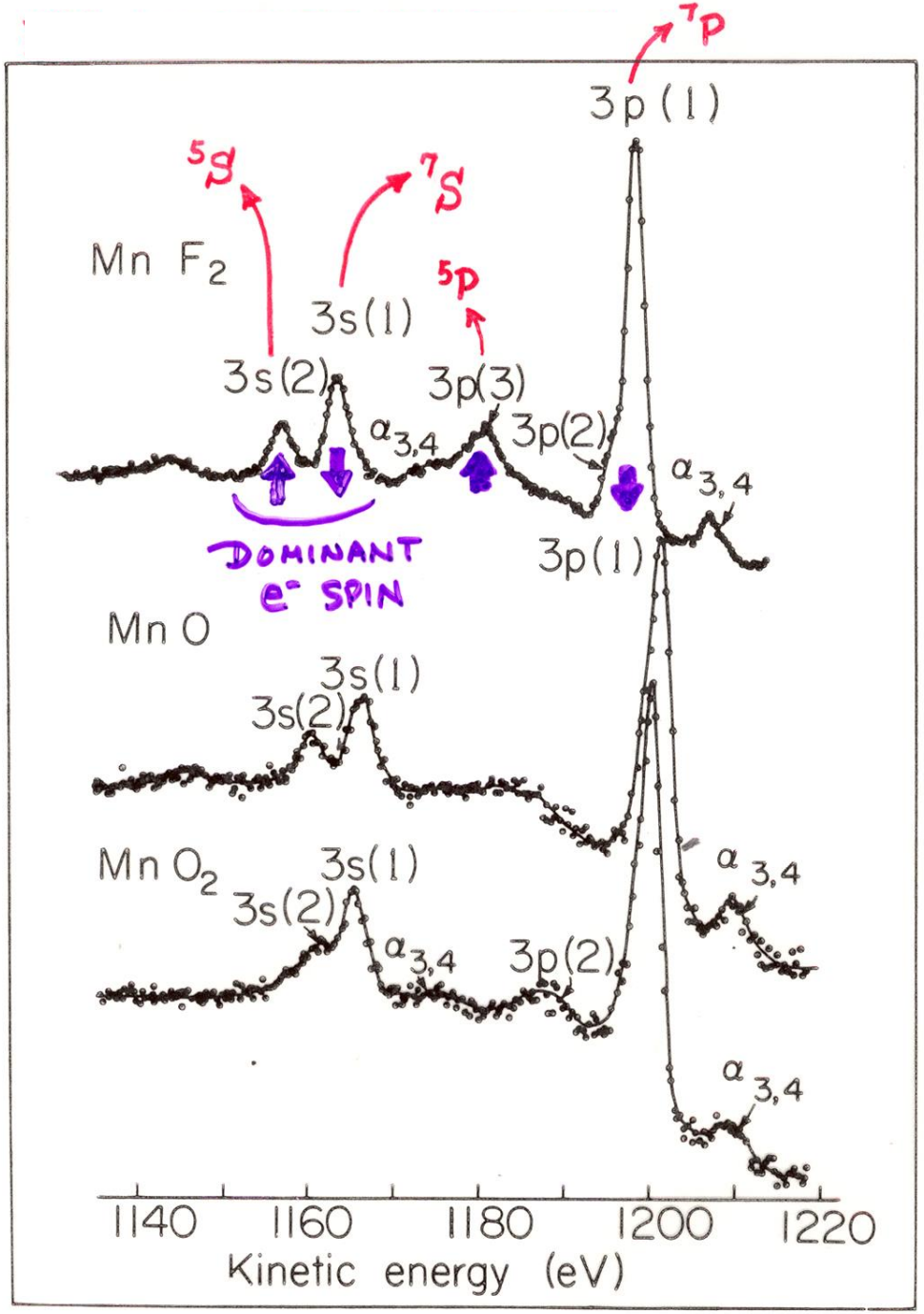

"Basic Concepts of XPS"
Figure 31

ORIGIN OF MULTIPLET SPLITTINGS IN Mn^{2+}: "ONE-ELECTRON" THEORY

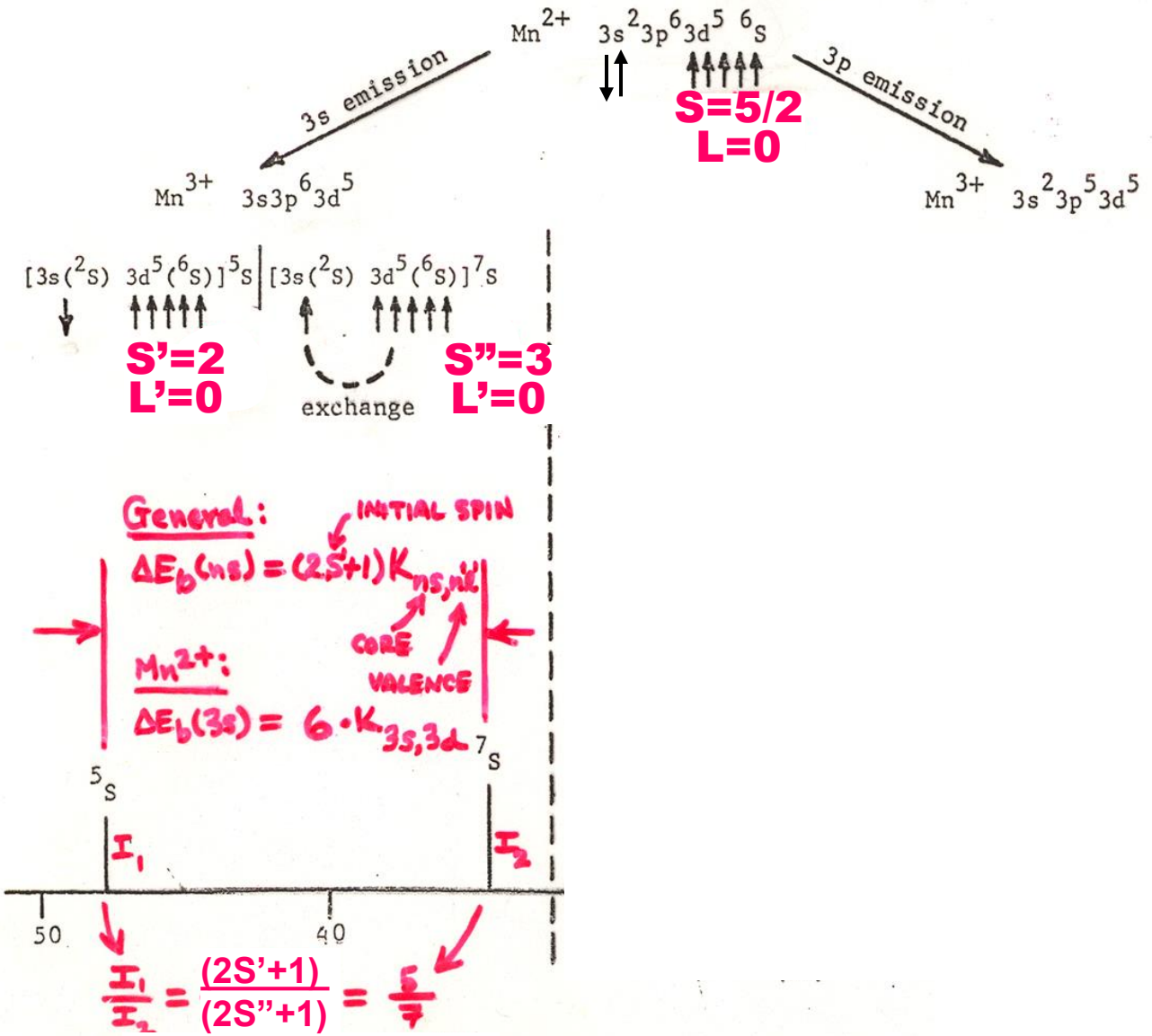

General Mn^{2+}

"Basic Concepts of XPS"
Figure 30

COMPARISON OF GAS-PHASE AND SOLID-STATE SPECTRA

EXPT.: (a), (b), (d), HERMSMEIER ET AL., PHYS. REV. LETT. 61, 2592 (1988) (OUR GROUP)

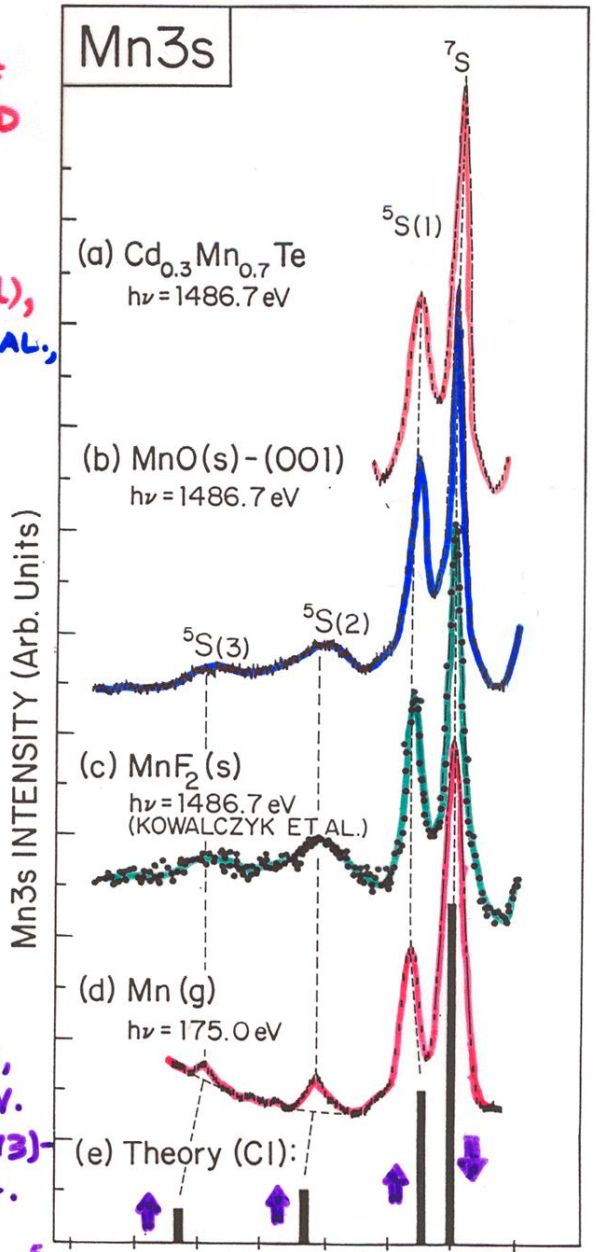

THEORY: BAGUS, FREEMAN, SASAKI, PHYS. REV. LETT. 30, 850 (1973) - ATOMIC CONFIG. INT. IN

$Mn^{3+}...3s^1...3d^5$

+ $Mn^{3+}...3s^2 3p^4 3d^6$

Correlation CI effects: anti-parallel electrons

CI = configuration interaction

"Basic Concepts of XPS" Figure 33

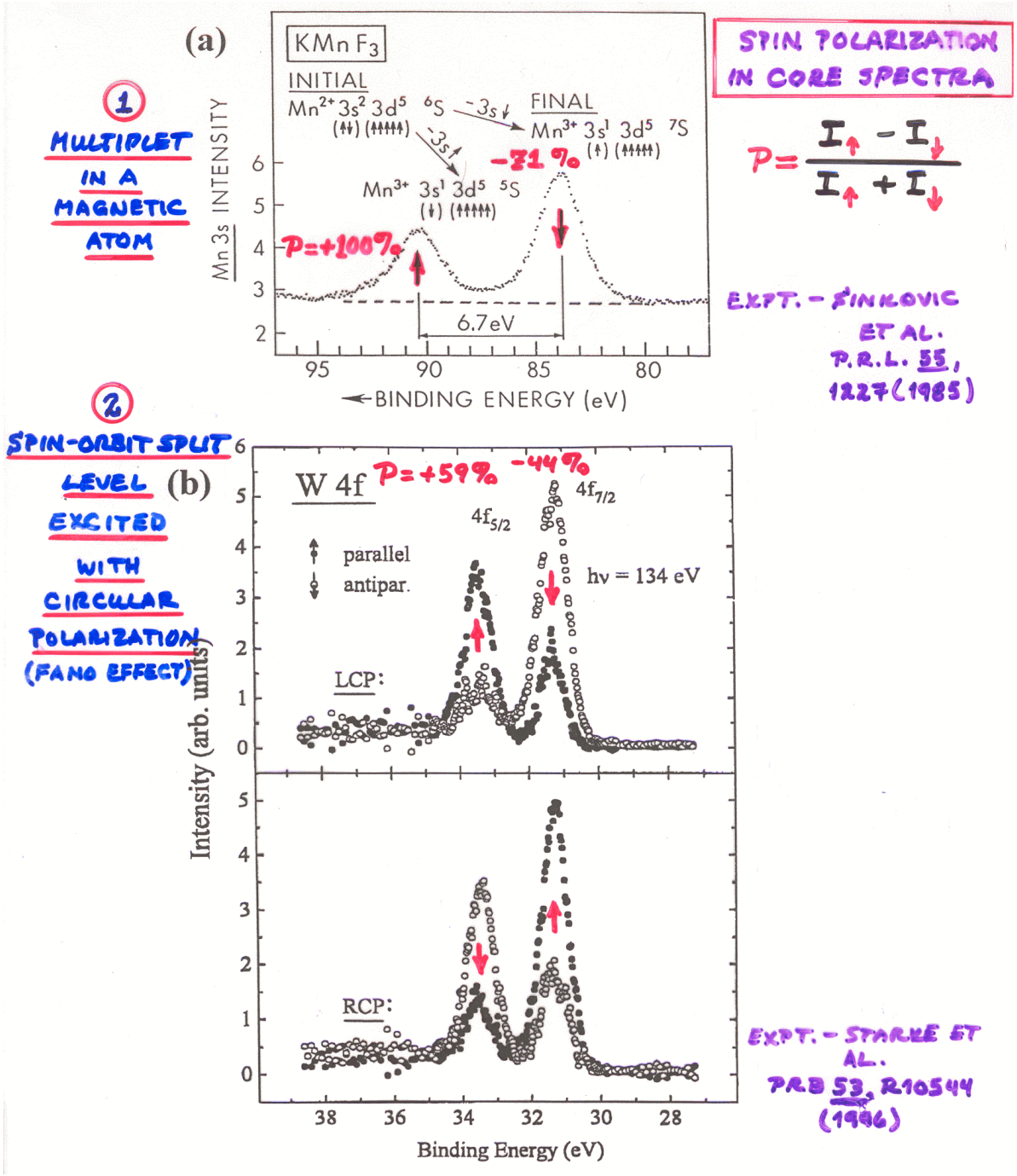

Spin <u>internally</u> referenced to spin of each ion

Spin <u>externally</u> referenced to $\vec{k}_{h\nu}$ and $\vec{M}$ of sample

DIRECT OBSERVATION OF SPIN-SPLIT CORE LEVELS IN A FERROMAGNET

$$\frac{I_\uparrow - I_\downarrow}{I_\uparrow + I_\downarrow}$$

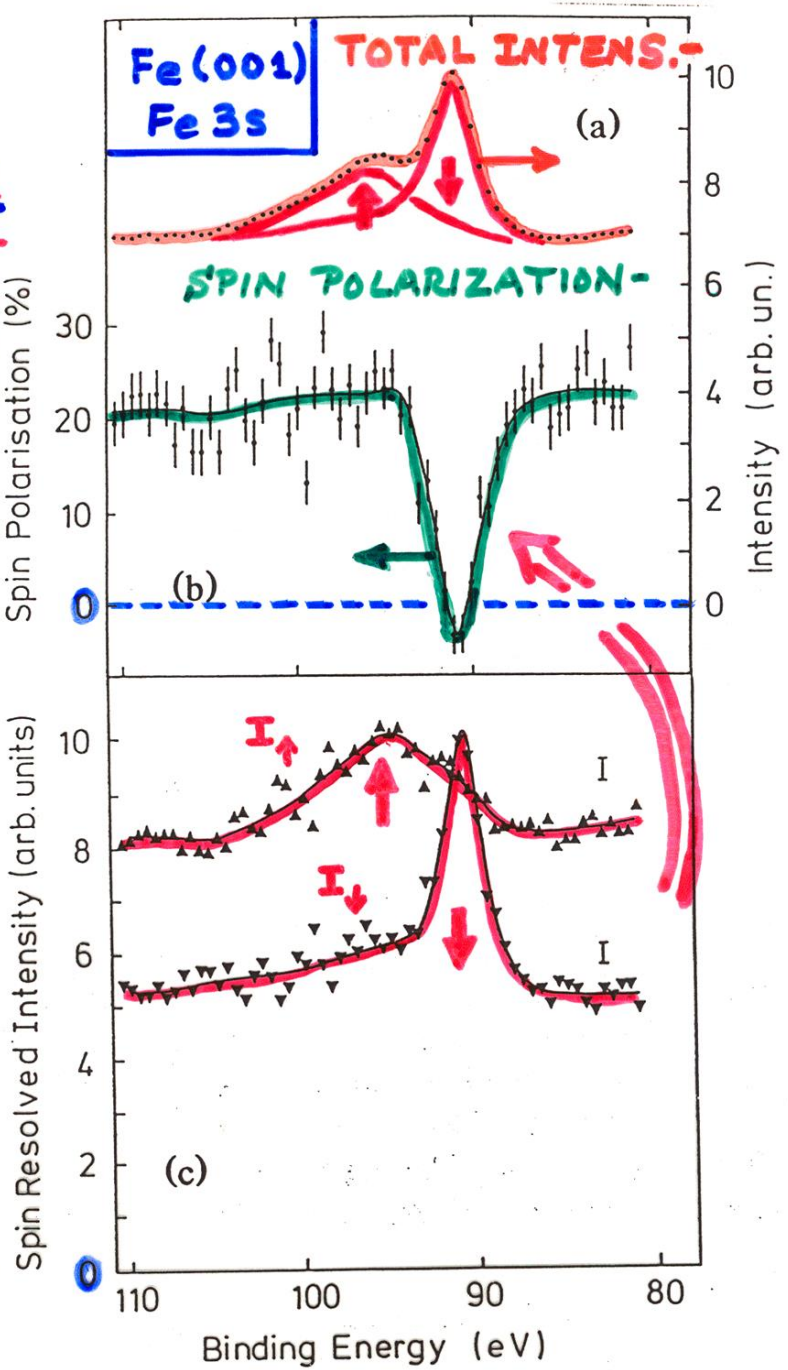

HILLEBRECHT ET AL., PHYS. REV. LETT. 65, 2450 (1990)

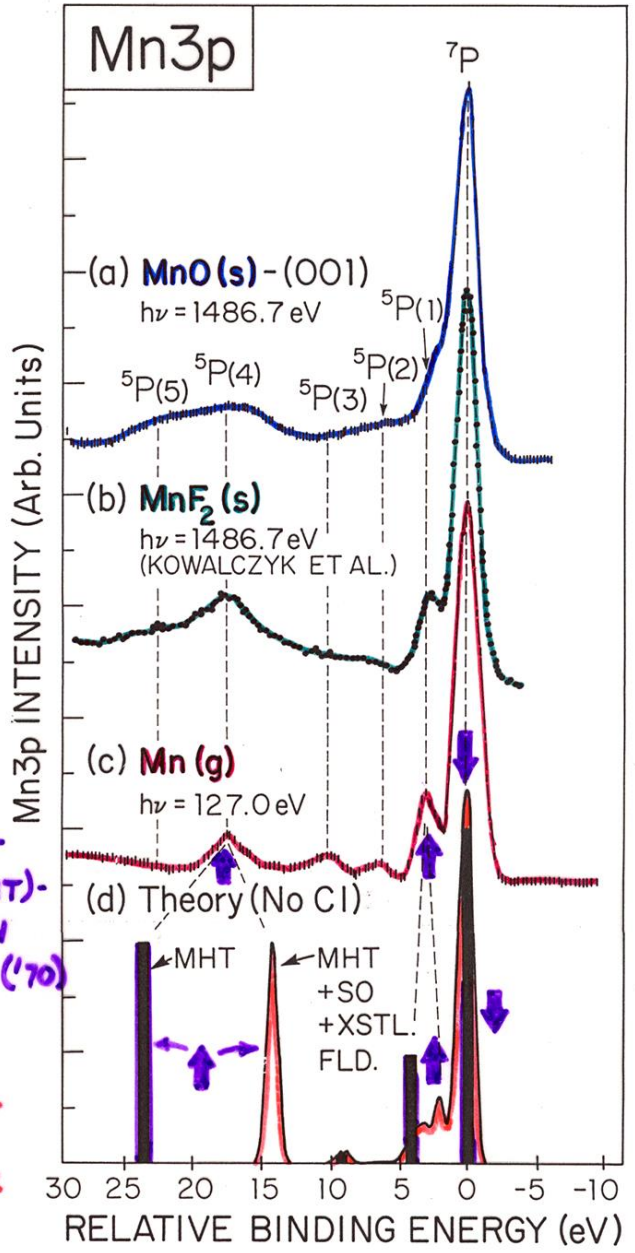

THEORY: NO CI

SIMPLE MULTIPLET HOLE THEORY (MHT) - FADLEY, SHIRLEY PHYS. REV. A2, 1109 ('70)

EMPIRICAL MHT WITH SPIN ORBIT & CRYSTAL FIELD - SUGANO ET AL., J. PHYS. C 15, 2625 (1982)

HERMSMEIER ET AL., P.R.L. 61, 2592 ('88)

MHT = multiplet hole theory with CI
SO = spin-orbit
XSTAL FLD. = crystal field

ORIGIN OF MULTIPLET SPLITTINGS IN Mn^{2+}: "ONE-ELECTRON" THEORY

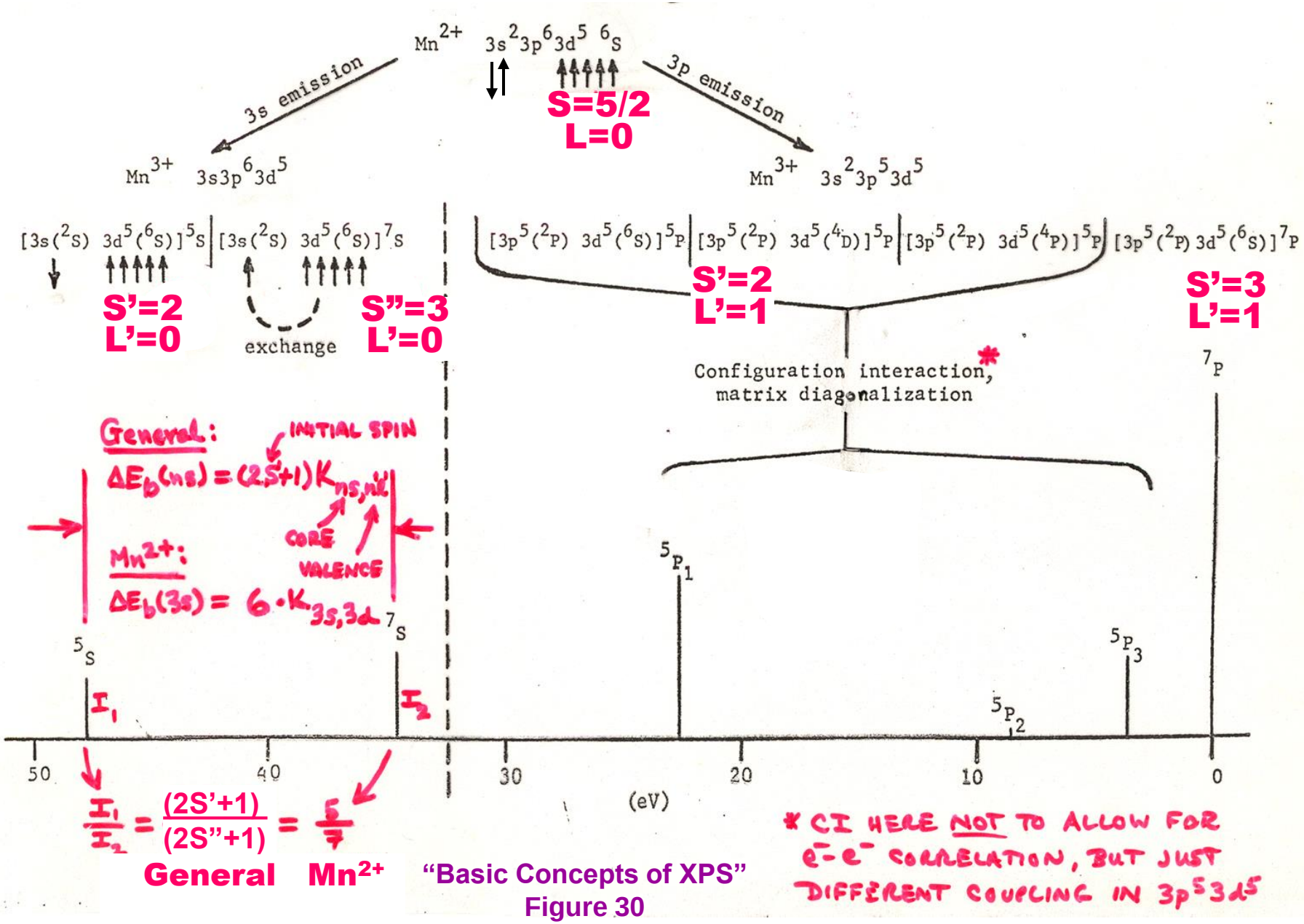

"Basic Concepts of XPS"
Figure 30

ORIGIN OF MULTIPLET SPLITTINGS IN Mn^{2+}: "ONE-ELECTRON" THEORY

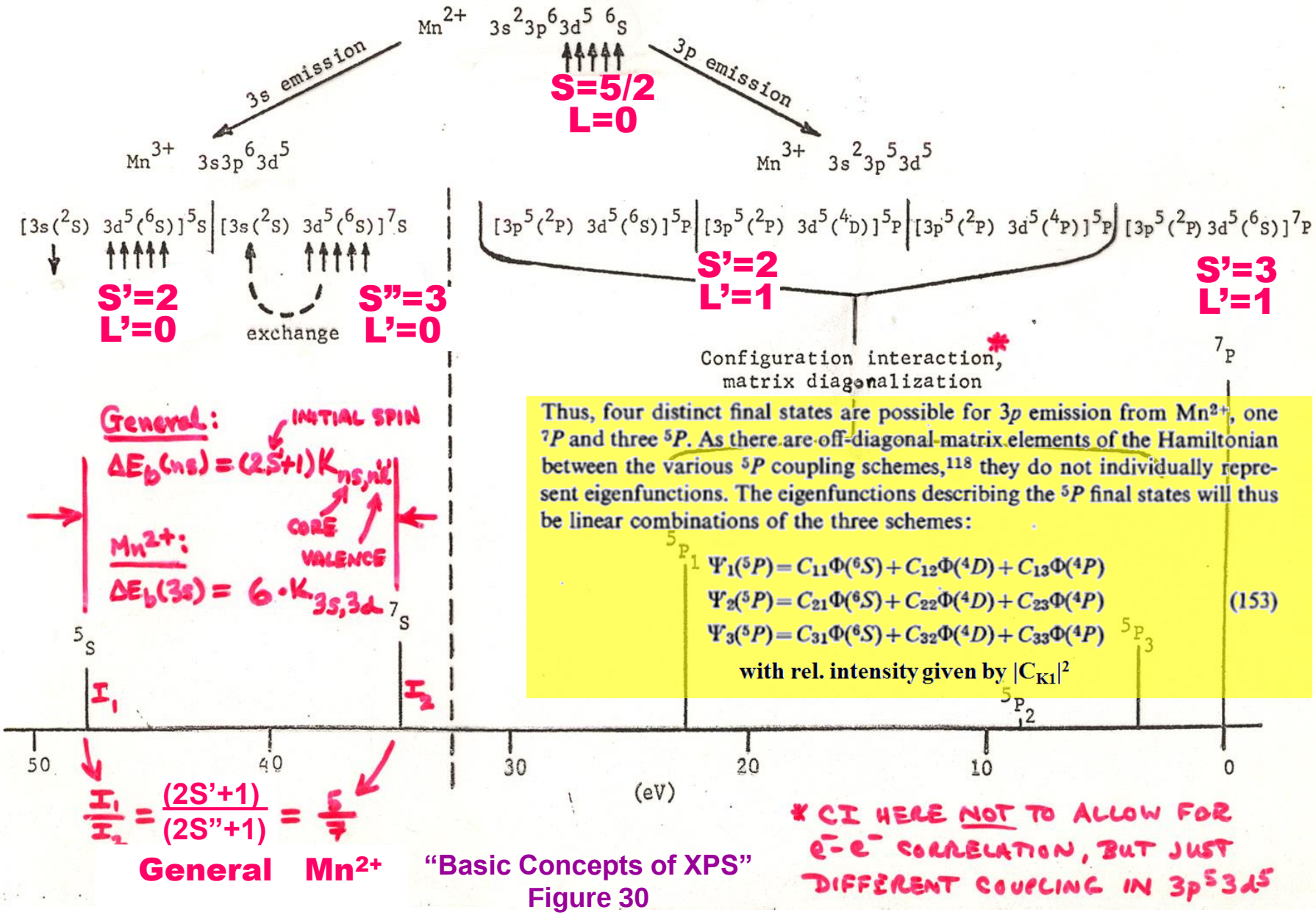

Thus, four distinct final states are possible for $3p$ emission from Mn^{2+}, one ^7P and three ^5P. As there are off-diagonal matrix elements of the Hamiltonian between the various ^5P coupling schemes,[118] they do not individually represent eigenfunctions. The eigenfunctions describing the ^5P final states will thus be linear combinations of the three schemes:

$$\Psi_1(^5P) = C_{11}\Phi(^6S) + C_{12}\Phi(^4D) + C_{13}\Phi(^4P)$$
$$\Psi_2(^5P) = C_{21}\Phi(^6S) + C_{22}\Phi(^4D) + C_{23}\Phi(^4P) \quad (153)$$
$$\Psi_3(^5P) = C_{31}\Phi(^6S) + C_{32}\Phi(^4D) + C_{33}\Phi(^4P)$$

with rel. intensity given by $|C_{K1}|^2$

* CI HERE NOT TO ALLOW FOR e^--e^- CORRELATION, BUT JUST DIFFERENT COUPLING IN $3p^5 3d^5$

"Basic Concepts of XPS"
Figure 30

INTENSITIES IN PHOTOELECTRON SPECTRA:

- GENERAL: FINAL STATE K (k-SUBSHELL + ALL OTHER DESIG.)

$$\text{INT.}_K \propto \left| \hat{e} \cdot \langle \Psi^f_{tot}(N,K) | \sum_{i=1}^{N} \vec{r}_i | \Psi^i_{tot}(N) \rangle \right|^2 \quad \text{(DIPOLE APPROX.)}$$

- BORN-OPPENHEIMER: e^-'s FAST, VIBRATIONS SLOW

$$\text{INT.}_K \propto \underbrace{|\langle \Psi^f_{VIB,v'} | \Psi^i_{VIB,v} \rangle|^2}_{\text{FRANCK-CONDON FACTOR}} \left| \hat{e} \cdot \langle \Psi^f_{e^-}(N,K) | \sum_{i=1}^{N} \vec{r}_i | \Psi^i_{e^-}(N) \rangle \right|^2$$

- SUDDEN APPROXIMATION: $\varphi_K \rightarrow \varphi_f$ = PHOTO e^- (FAST)

$$\left.\begin{array}{l} \varphi_1 \rightarrow \varphi_1' \\ \vdots \\ \varphi_{K-1} \rightarrow \varphi_{K-1}' \\ \varphi_{K+1} \rightarrow \varphi_{K+1}' \\ \vdots \\ \varphi_N \rightarrow \varphi_N' \end{array}\right\} \text{(SLOW)}$$

k HOLE

$$\text{INT.}_K \propto |\langle \Psi^f_{VIB,v'} | \Psi^i_{VIB,v} \rangle|^2 \, |\langle \Psi^f_{e^-}(N-1,K) | \Psi^{\uparrow}_{K}(N-1,K) \rangle|^2$$

k MISSING

$\Phi(3s^1 3p^6 3d^5\ {}^6S)$ from initial state

$$|\hat{e} \cdot \langle \varphi_f | \vec{r} | \varphi_K \rangle|^2$$

SAME SUBSHELL COUPLING + TOTAL L,S → "MONOPOLE"

↳ NORMAL $\frac{d\sigma_K}{d\Omega}$

Differential cross section: $d\sigma/d\Omega_{3s}$

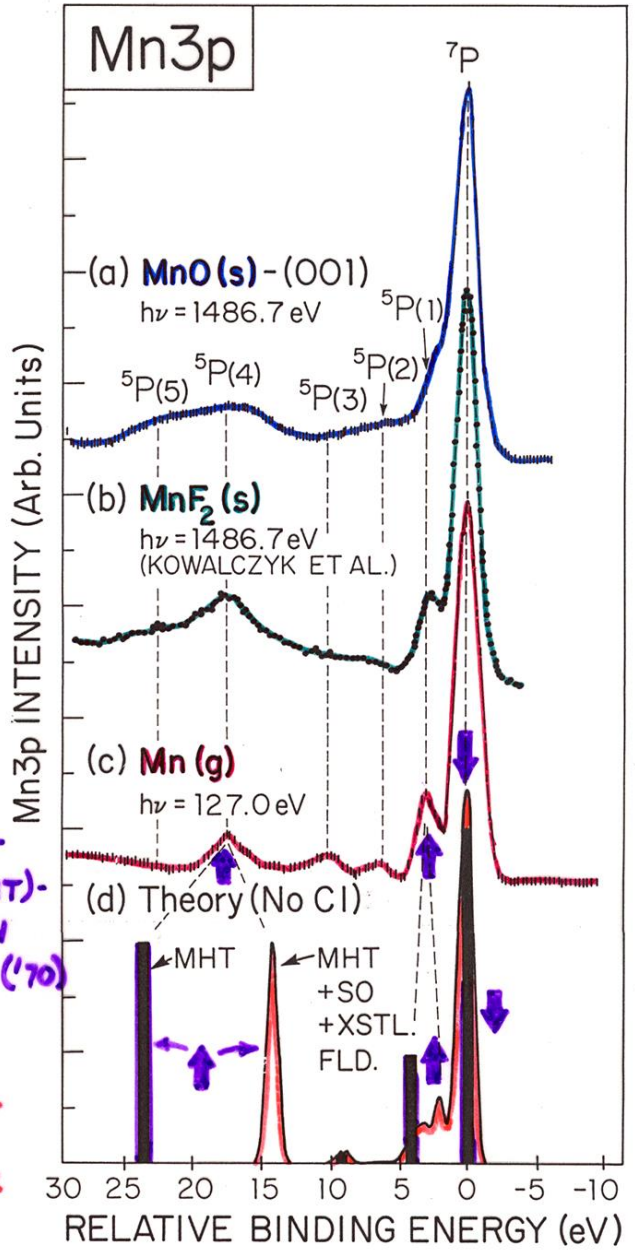

THEORY: NO CI

SIMPLE MULTIPLET HOLE THEORY (MHT) - FADLEY, SHIRLEY PHYS. REV. A2, 1109 ('70)

EMPIRICAL MHT WITH SPIN ORBIT & CRYSTAL FIELD - SUGANO ET AL., J. PHYS. C 15, 2625 (1982)

HERMSMEIER ET AL., P.R.L. 61, 2592 ('88)

MHT = multiplet hole theory with CI
SO = spin-orbit
XSTAL FLD. = crystal field

MORE COMPLEX MULTIPLETS FOR L > 0 WITH SPIN-ORBIT COUPLING:

Mn 2p emission from MnF_2:

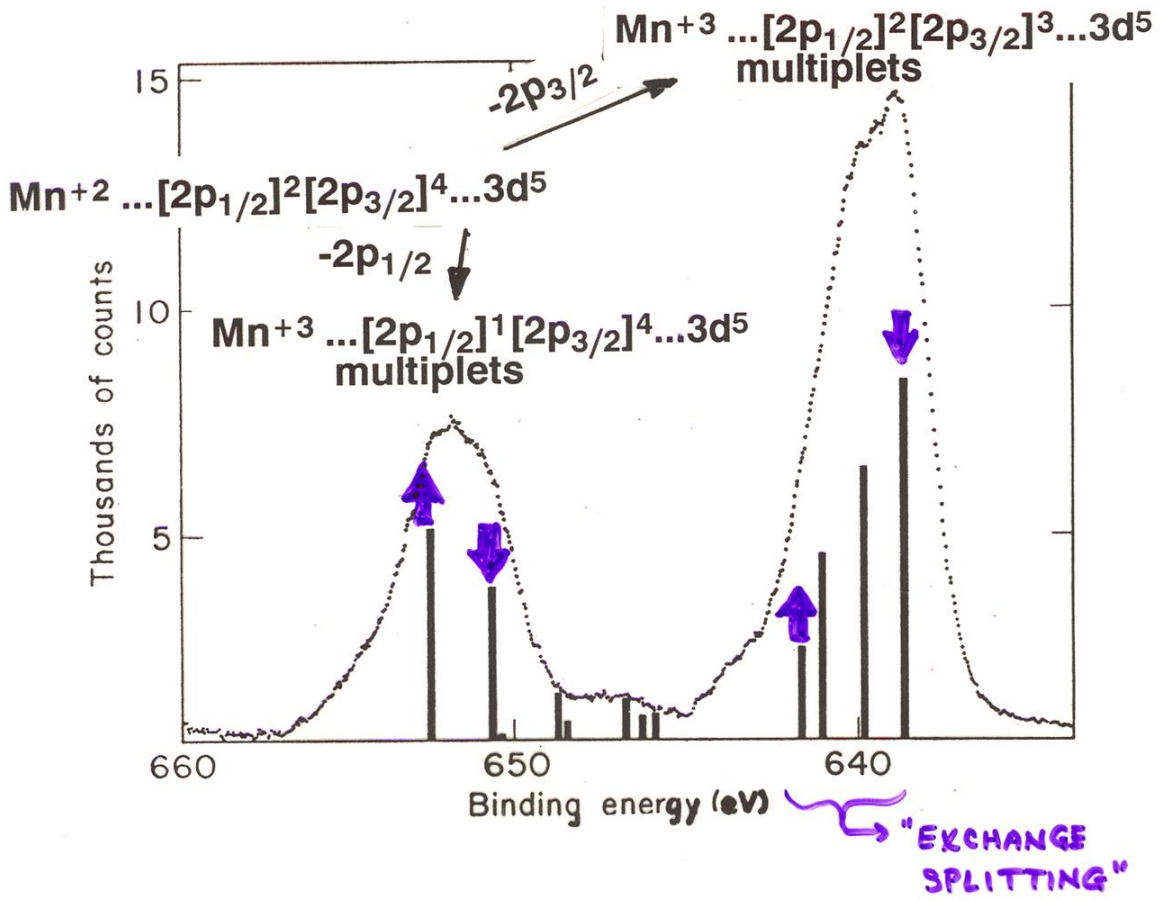

Expt.--Kowalczyk et al., Phys. Rev. B11, 1721 (1975)

Theory--Gupta and Sen, Phys. Rev. B10, 71 (1974)

Park et al., Phys. Rev. B37, 10867 (1988)

FILLING OF THE MOLECULAR ELECTRONIC STATES OF DIATOMIC NO AND O_2

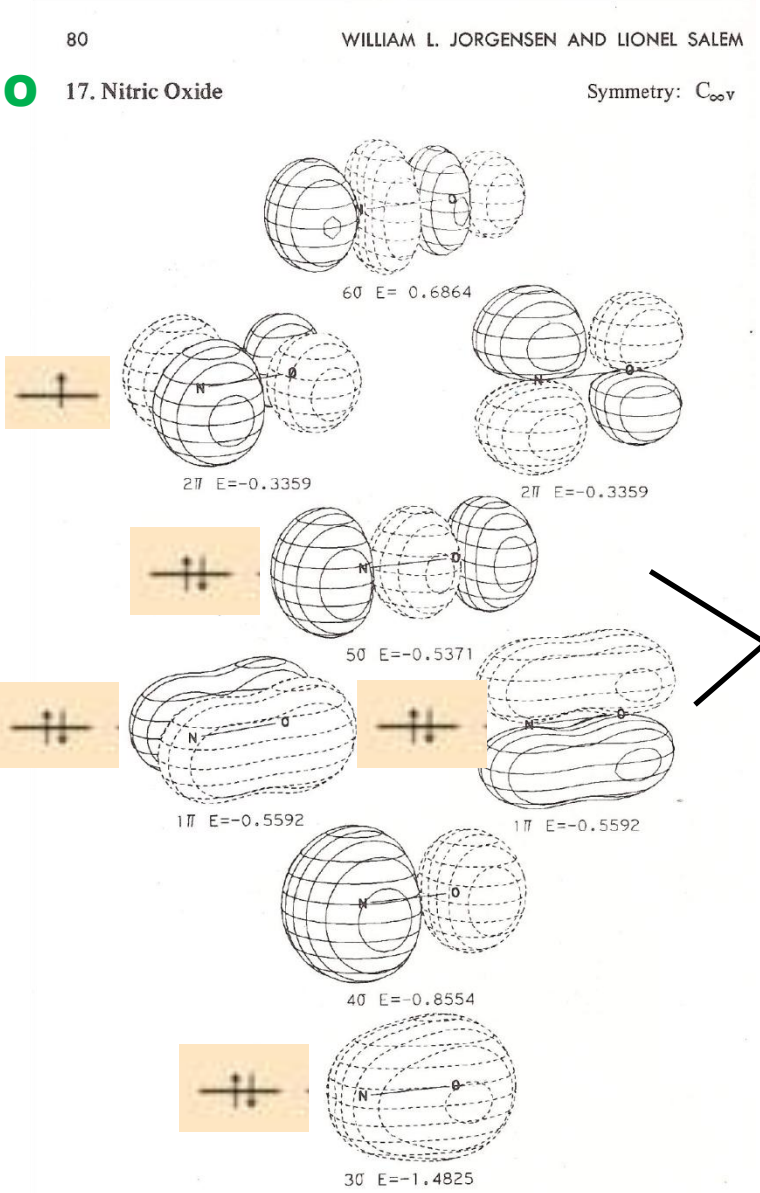

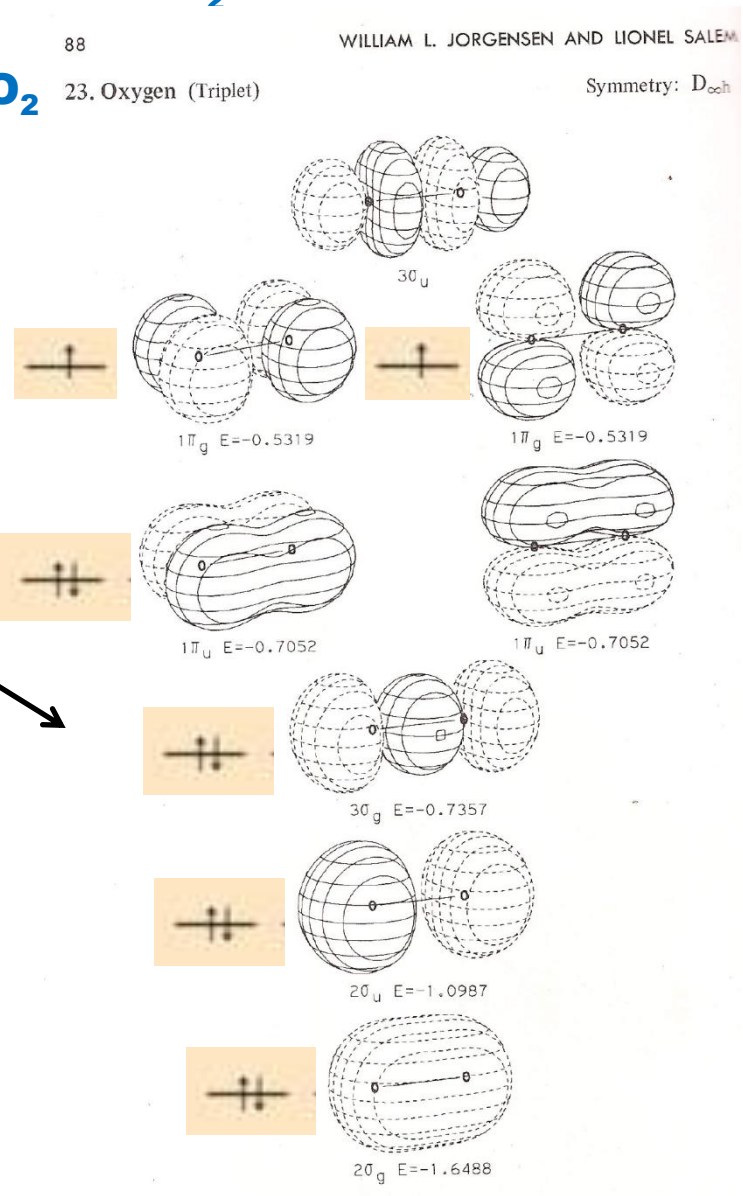

1s core levels

FILLING OF THE MOLECULAR ELECTRONIC STATES OF HOMONUCLEAR DIATOMIC MOLECULES & NO

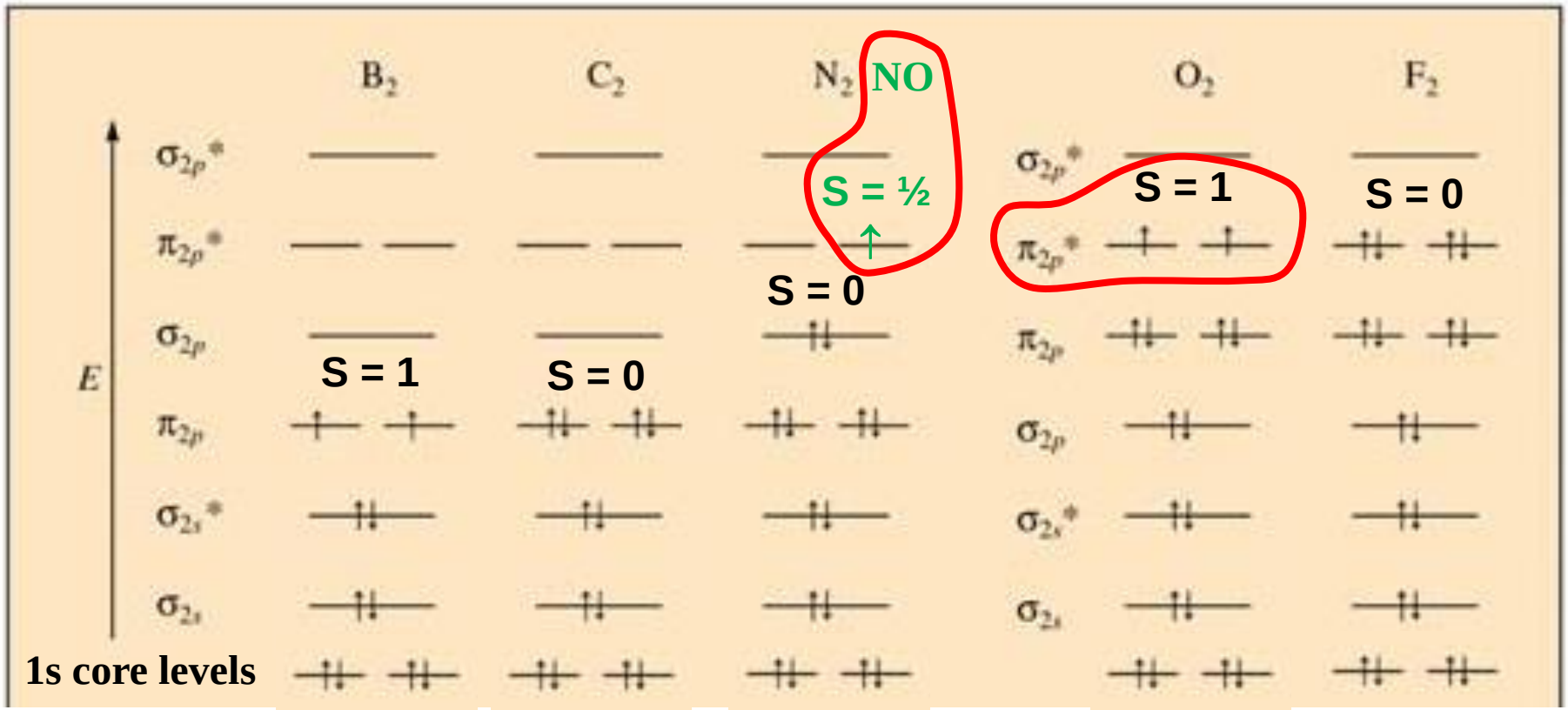

Multiplet splitting $\propto K_{1s,\pi 2p^*}$

MULTIPLETS IN FREE MOLECULES

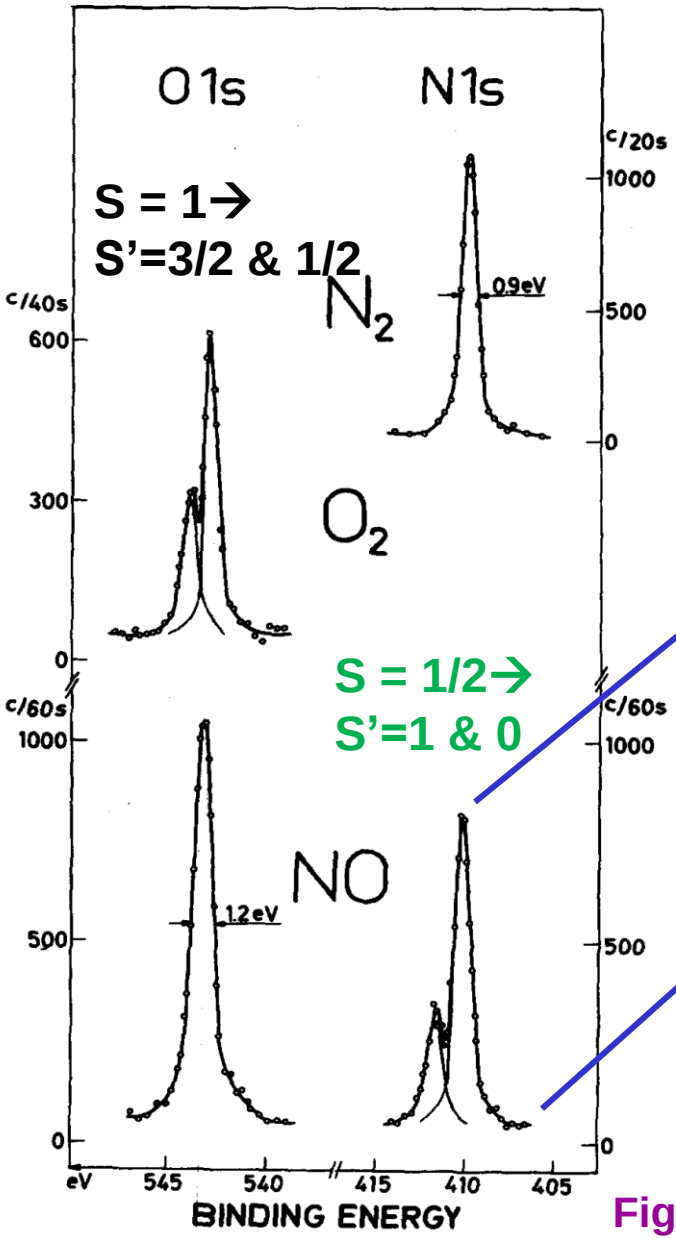

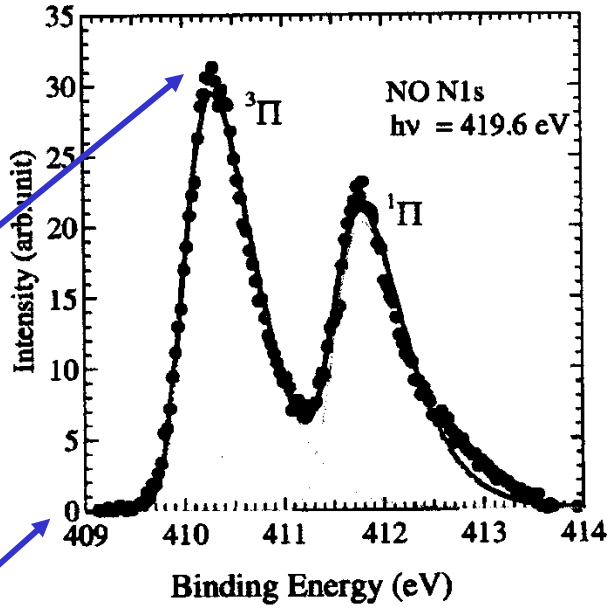

Hosaka et al., J. Phys. B 36, 4617 (2003), and earlier theory from Bagus and Schaefer, J. Chem. Phys. 55, 1474 (1971)

Fig. 34
Basic Concepts of XPS

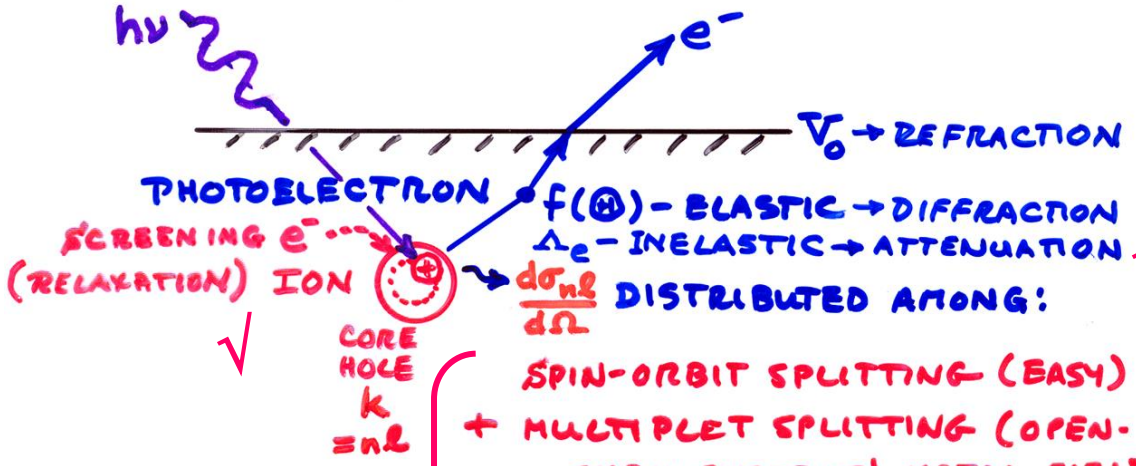

√ = covered so far

ADDITIONAL SOURCES OF STRUCTURE (AND INFORMATION!) IN SPECTRA BEYOND CHEMICAL SHIFTS

- SPIN-ORBIT SPLITTING (EASY) √
- \+ MULTIPLET SPLITTING (OPEN-SHELL SYSTEMS), XSTAL FIELD √
- \+ CORRELATION / CONFIGURATION INTERACTION √
- \+ SHAKE-UP/SHAKE-OFF/e^--HOLE
- \+ SCREENING / NON-SCREENING: CONFIGURATION INTERACTION
- \+ VIBRATIONAL EXCITATIONS
- \+ RESONANT PHOTOEMISSION ($h\nu \approx E_{b,n'l'}$) √

REALLY ALL AT ONCE, BUT SUM RULES + THEORY HELP

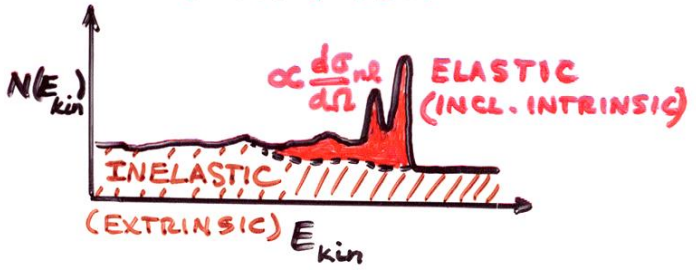

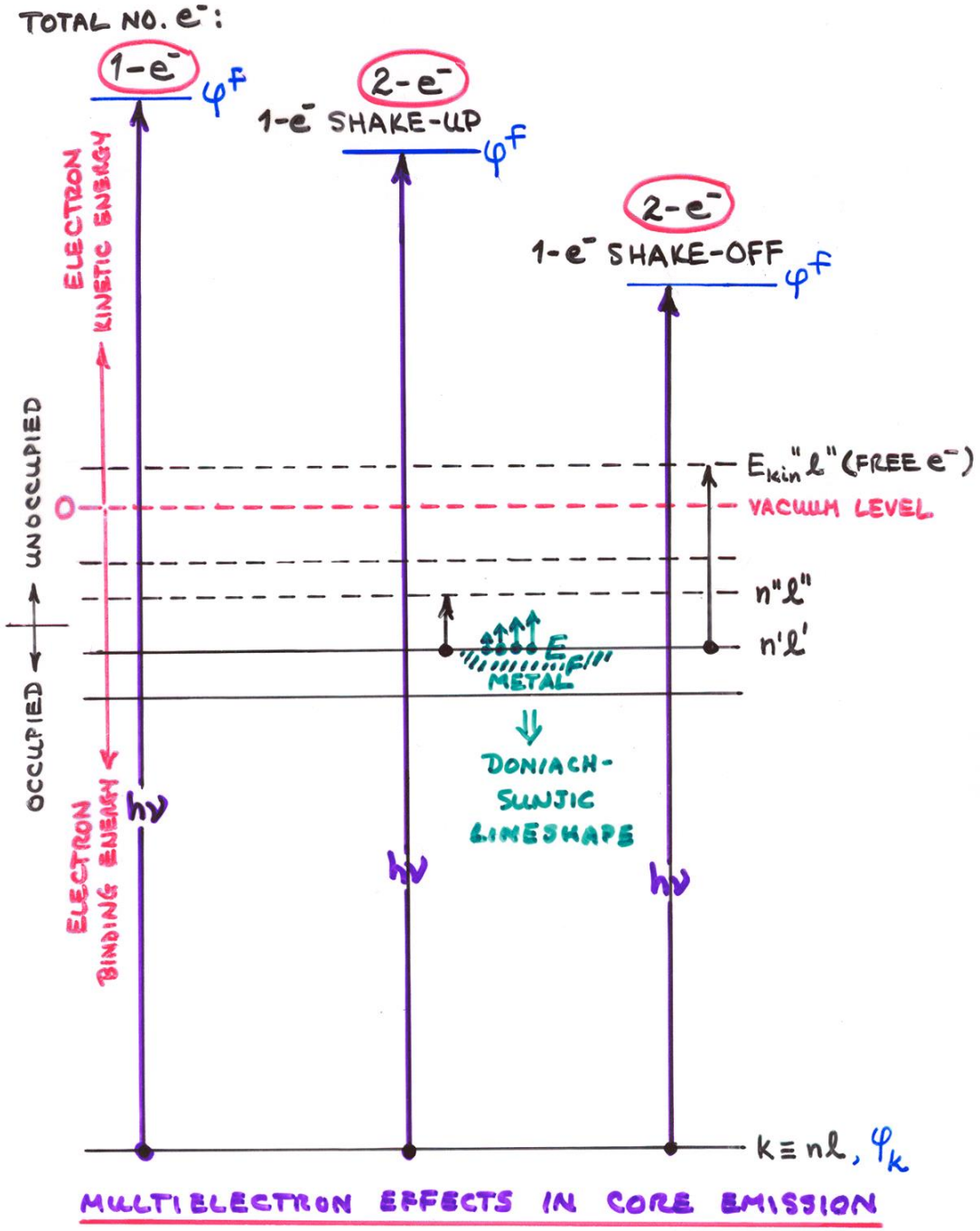

MULTIELECTRON EFFECTS IN CORE EMISSION

INTENSITIES IN PHOTOELECTRON SPECTRA:

- GENERAL: FINAL STATE K (k-SUBSHELL + ALL OTHER DESIG.)

$$\text{INT.}_K \propto \left| \hat{e} \cdot \langle \Psi^f_{tot}(N,K) | \sum_{i=1}^{N} \vec{r}_i | \Psi^i(N) \rangle \right|^2 \quad \text{(DIPOLE APPROX.}$$

- BORN-OPPENHEIMER: e⁻'s FAST, VIBRATIONS SLOW

$$\text{INT.}_K \propto \underbrace{\left| \langle \Psi^f_{VIB,v'} | \Psi^i_{VIB,v} \rangle \right|^2}_{\text{FRANCK-CONDON FACTOR}} \left| \hat{e} \cdot \langle \Psi^f_{e^-}(N,K) | \sum_{i=1}^{N} \vec{r}_i | \Psi^i_{e^-}(N) \rangle \right|^2$$

- SUDDEN APPROXIMATION: $\Psi_K \rightarrow \Psi_f$ = PHOTO e⁻ (FAST)

$$\left.\begin{array}{l} \varphi_1 \rightarrow \varphi_1' \\ \vdots \\ \varphi_{K-1} \rightarrow \varphi_{K-1}' \\ \varphi_{K+1} \rightarrow \varphi_{K+1}' \\ \vdots \\ \varphi_N \rightarrow \varphi_N' \end{array}\right\} \text{(SLOW)} \qquad \text{k HOLE} \rightarrow$$

S_0^2 in EXAFS (LATER)

$$\text{INT.}_K \propto \left| \langle \Psi^f_{VIB,v'} | \Psi^i_{VIB,v} \rangle \right|^2 \left| \langle \underbrace{\Psi^f_{e^-}(N-1,K) | \Psi^i_K(N-1,K)}_{\text{k MISSING}} \rangle \right|^2$$

$$\left| \hat{e} \cdot \langle \varphi_f | \vec{r} | \varphi_K \rangle \right|^2$$

SAME SUBSHELL COUPLING + TOTAL L,S → "MONOPOLE"

↳ NORMAL $\frac{d\sigma_K}{d\Omega}$

- SLATER DETS. FOR $\Psi^f_{e^-} = \det(\varphi_1' \varphi_2' \cdots \varphi_{K-1}' \varphi_{K+1}' \cdots \varphi_N')$

$$\Psi_K = \det(\varphi_1 \varphi_2 \cdots \varphi_{K-1} \varphi_{K+1} \cdots \varphi_N)$$

$$\text{INT.}_K \propto \left| \langle \Psi^f_{VIB,v'} | \Psi^i_{VIB,v} \rangle \right|^2 \left| \langle \varphi_1' | \varphi_1 \rangle \right|^2 \left| \langle \varphi_2' | \varphi_2 \rangle \right|^2 \cdots$$

$$\left| \langle \varphi_{K-1}' | \varphi_{K-1} \rangle \right|^2 \left| \langle \varphi_{K+1}' | \varphi_{K+1} \rangle \right|^2 \cdots \left| \langle \varphi_N' | \varphi_N \rangle \right|^2 .$$

$$\left| \hat{e} \cdot \langle \varphi_f | \vec{r} | \varphi_K \rangle \right|^2$$

1e- DIPOLE → $d\sigma/d\Omega$

(N-1)e⁻ SHAKE-UP/ SHAKE-OFF → "MONOPOLE"

- PLUS DIFFRACTION EFFECTS IN φ_f ESCAPE

NEON 1s SHAKE-UP / SHAKE-OFF:

$Ne\ 1s^2 2s^2 2p^6\ {}^1S \xrightarrow{-e^-} Ne^+\ 1s^1 2s^2 2p^6\ {}^2S$

1-e^- SHAKE-UP: $Ne^+\ 1s^1 2s^2 2p^5\ np^1\ (n = 3,4,5,\dots)\ {}^2S$ / $Ne^+\ 1s^1 2s^1 2p^6\ ns^1\ (n = 3,\dots)\ {}^2S$

2-e^- SHAKE-UP: $Ne^+\ 1s^1 2s^2 2p^4 3p^2\ {}^2S$

2p SHAKE-OFF: $Ne^+\ 1s^1 2s^2 2p^5, E_{kin}\ "p"\ {}^2S$

"Basic Concepts of XPS"
Figure 36

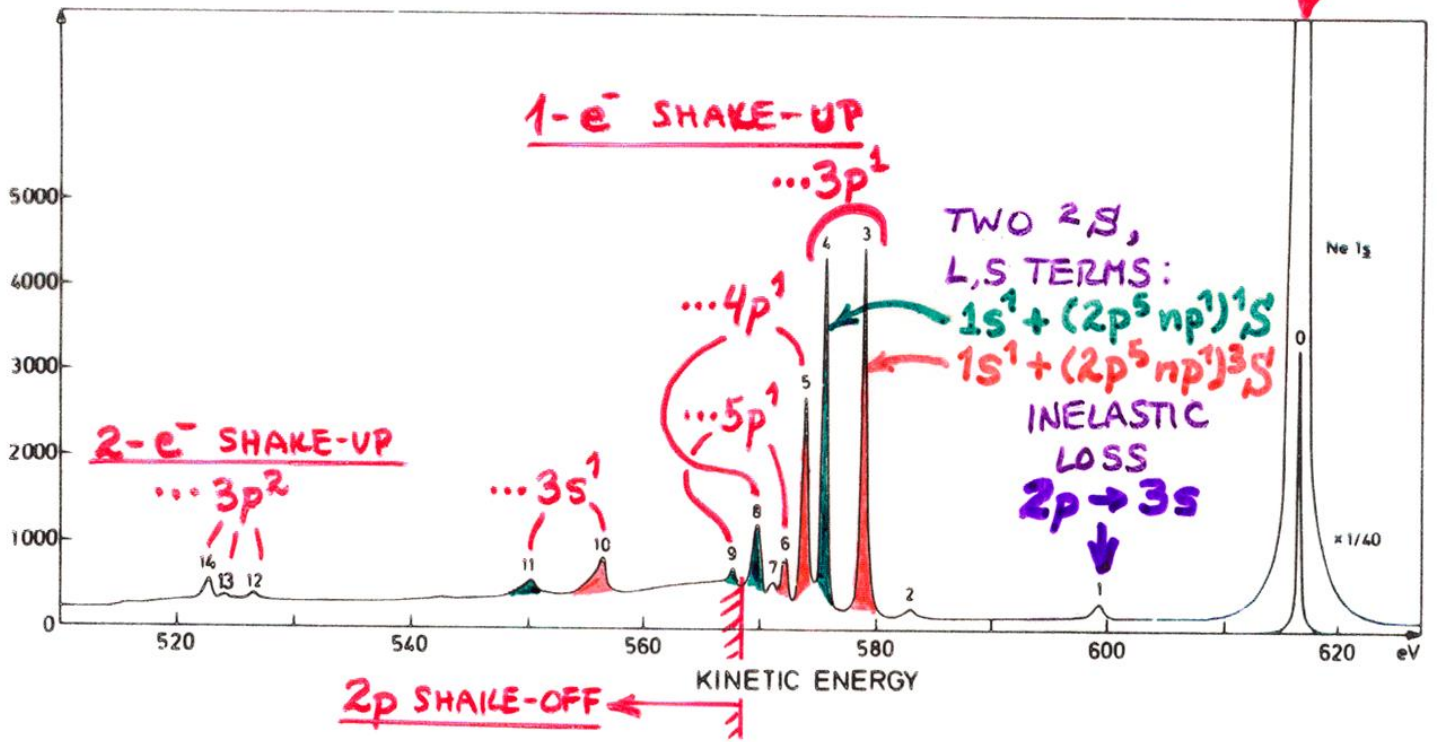

OVERALL: ~12% SHAKE-UP + 16% SHAKE-OFF ≈ 28% OF EVENTS

Many electron effects and satellites in x-ray emission

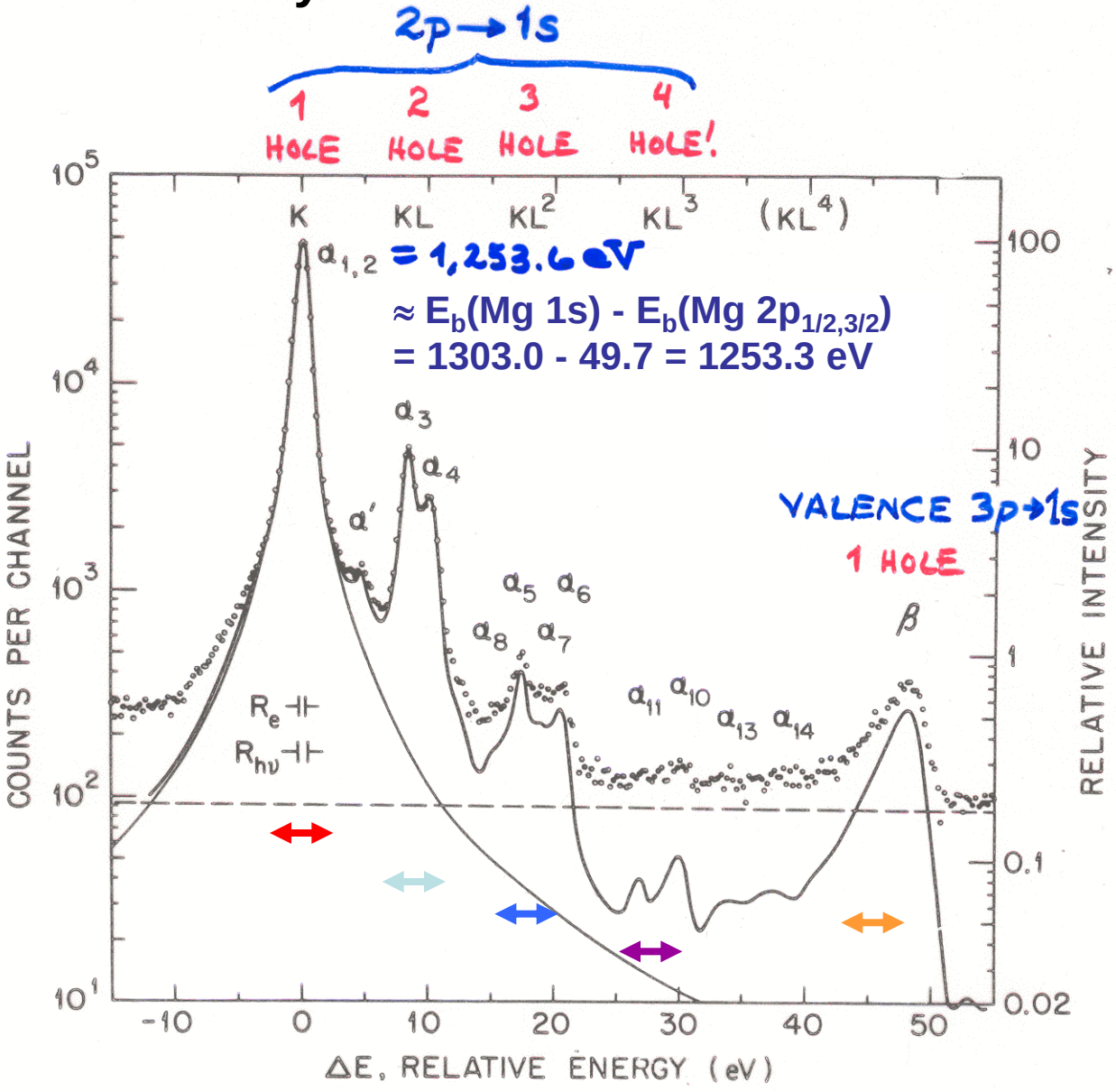

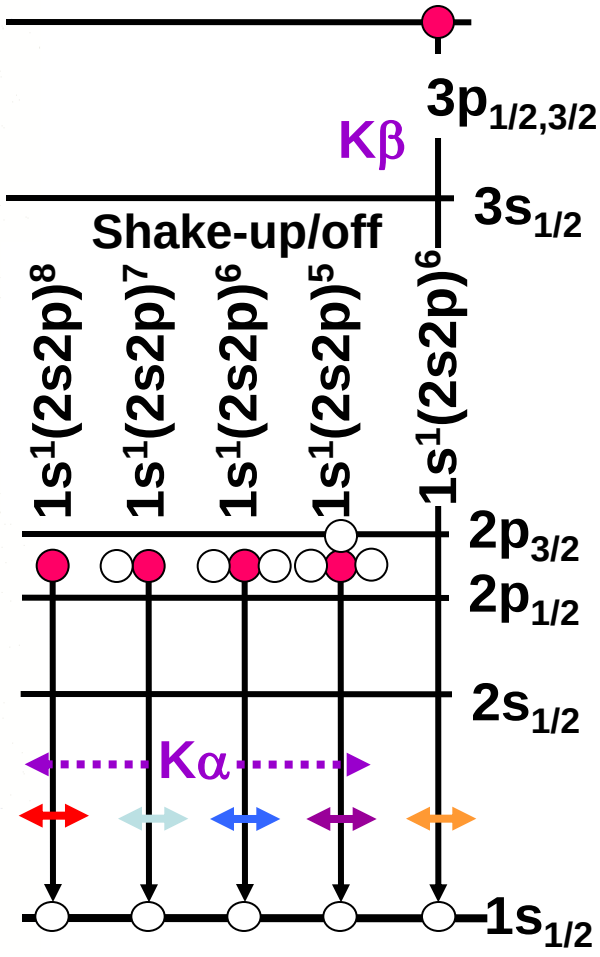

Mg K series of x-rays:
atomic no. = 12
Fluorescence Yield ≈ 0.03

"Basic Concepts of XPS"
Figure 2

Ethane: C 1s NEXAFS, with shakeup also

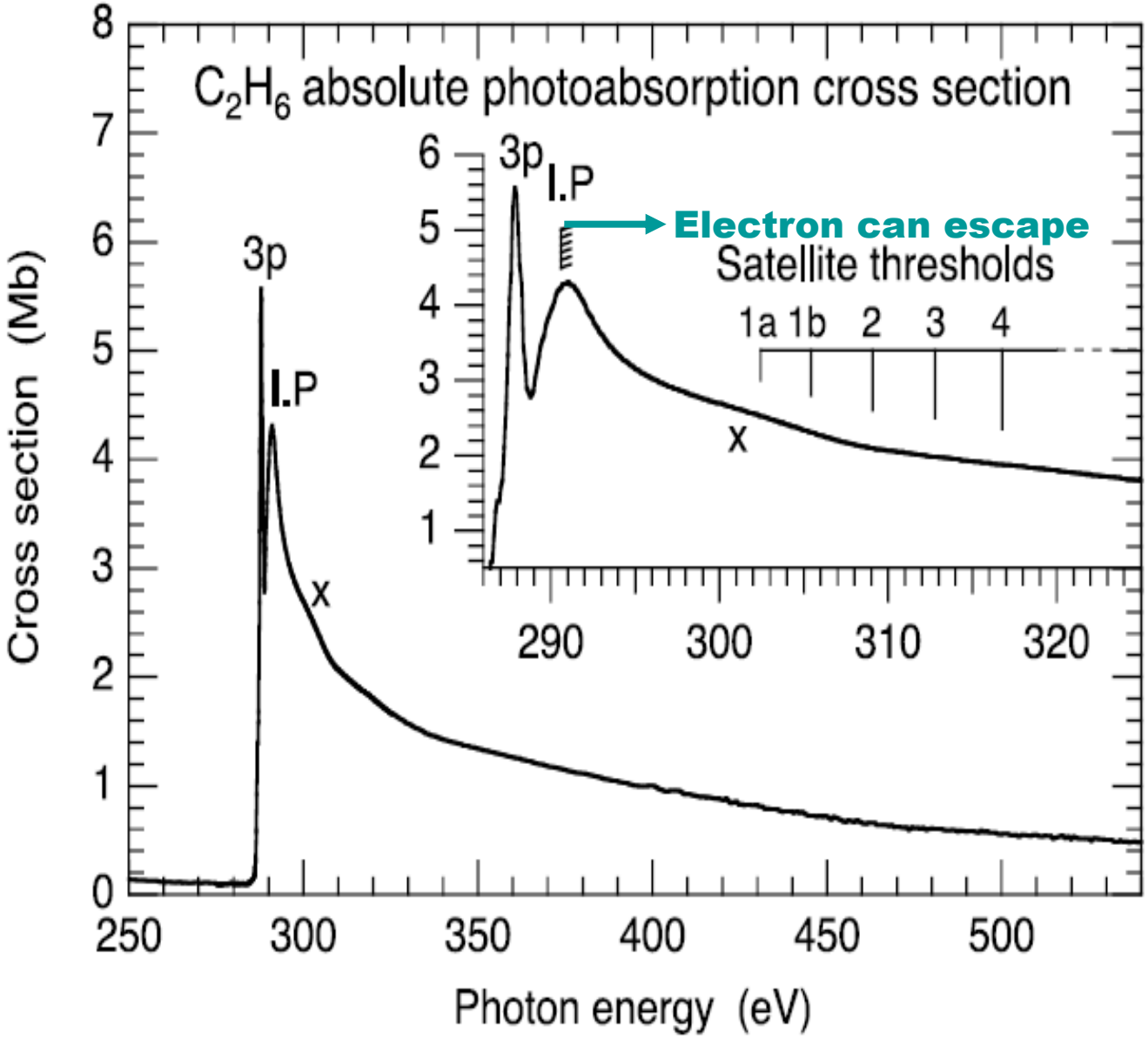

Rennie et al., J. Phys. B: At. Mol. Opt. Phys. 32 (1999) 2691

Ethane-
C 1s photoemission:
"Conjugate shake-up"
C 1s→unoccupied MO +occupied MO to free electron

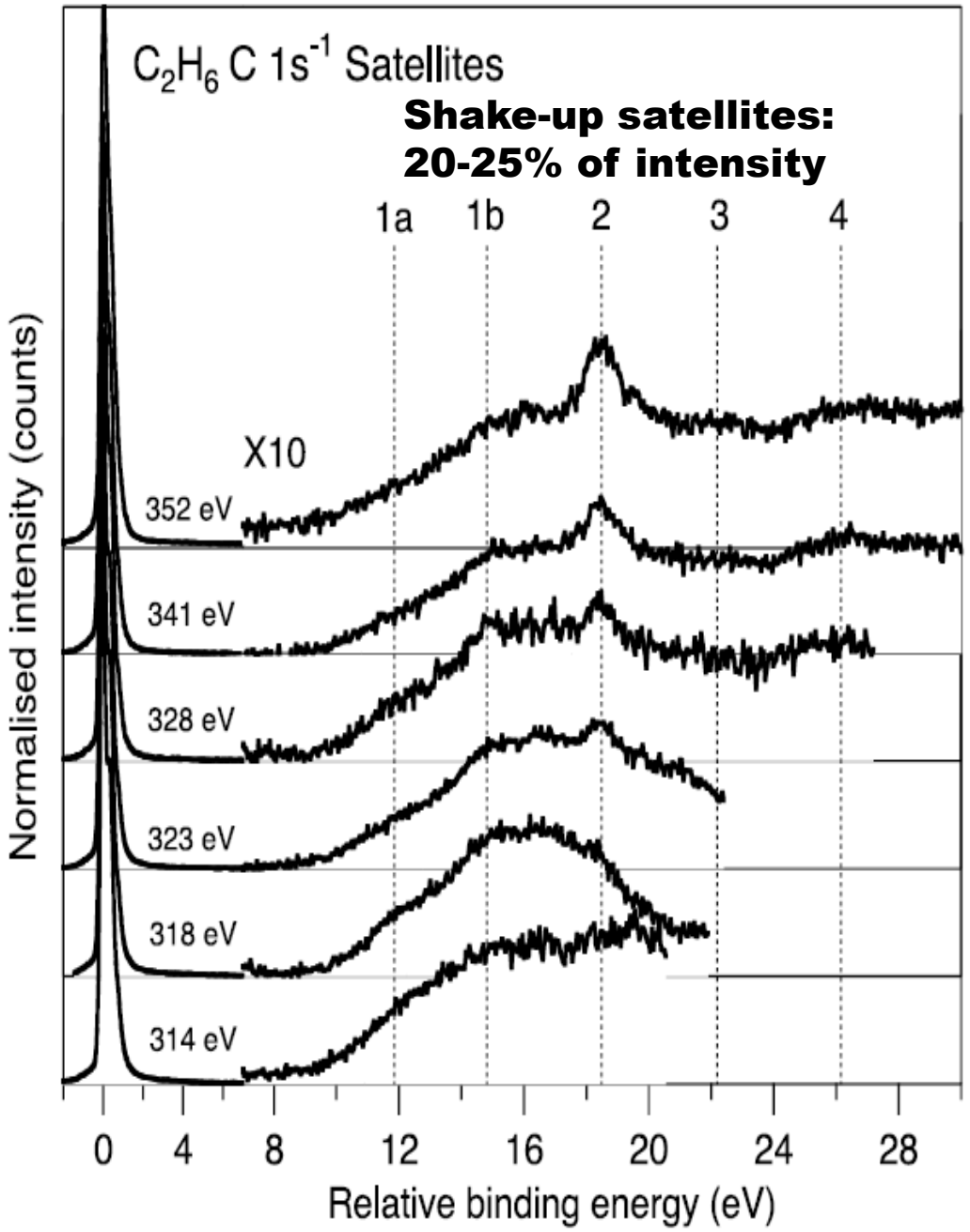

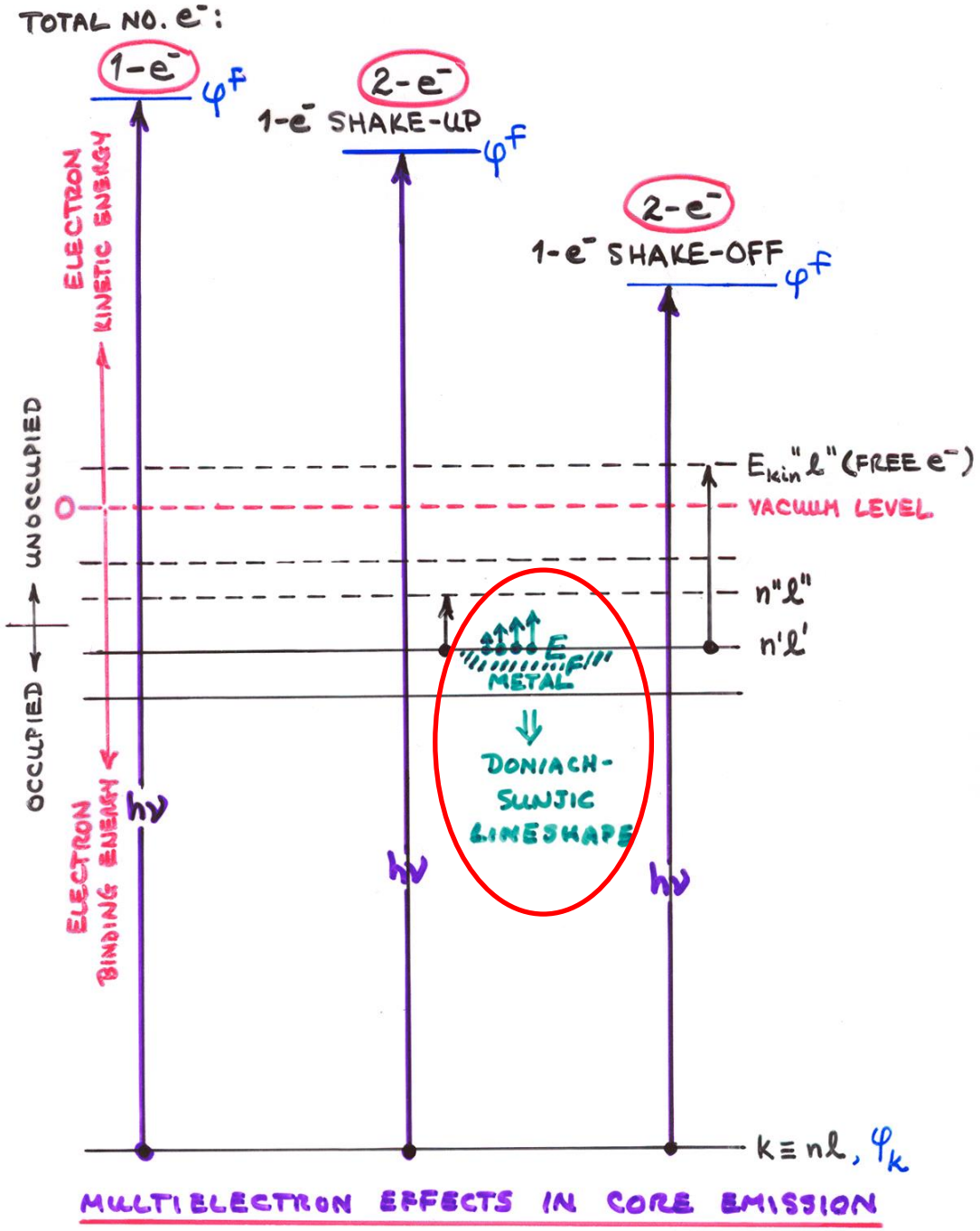

MULTIELECTRON EFFECTS IN CORE EMISSION

BAND THEORY—D.O.S:

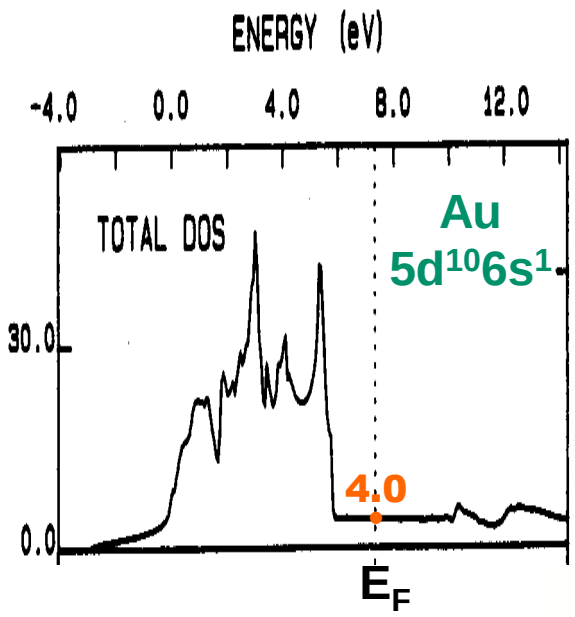

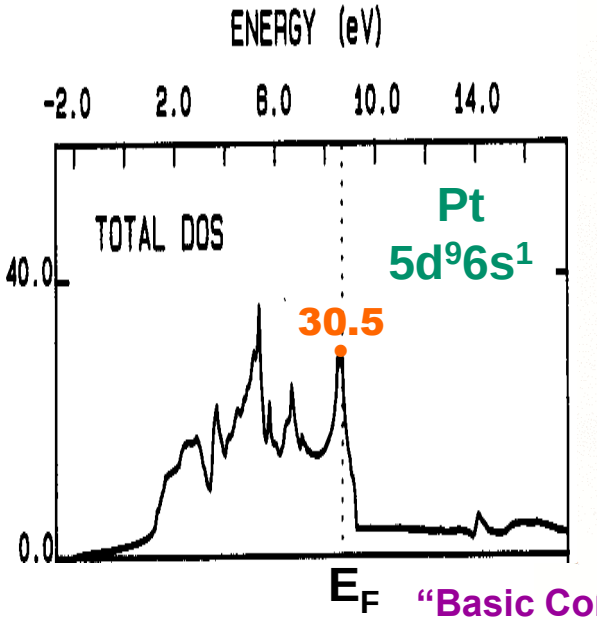

SHAKE-UP IN METALS— ∝ D.O.S AT E_F:

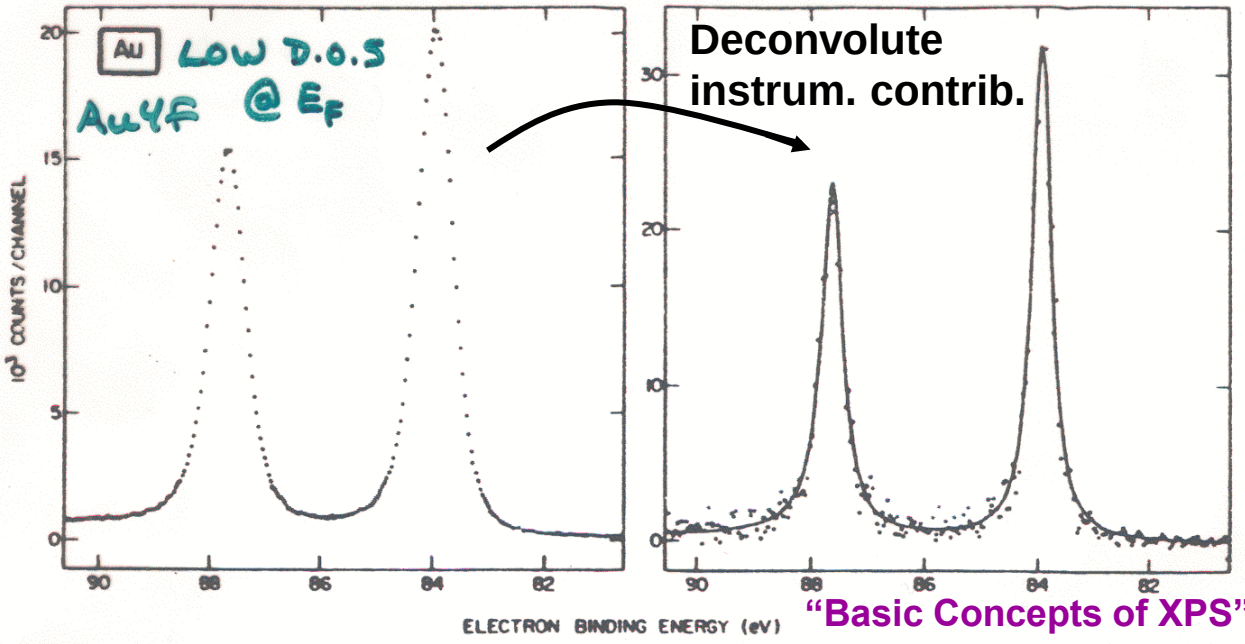

"Basic Concepts of XPS" Figure 10

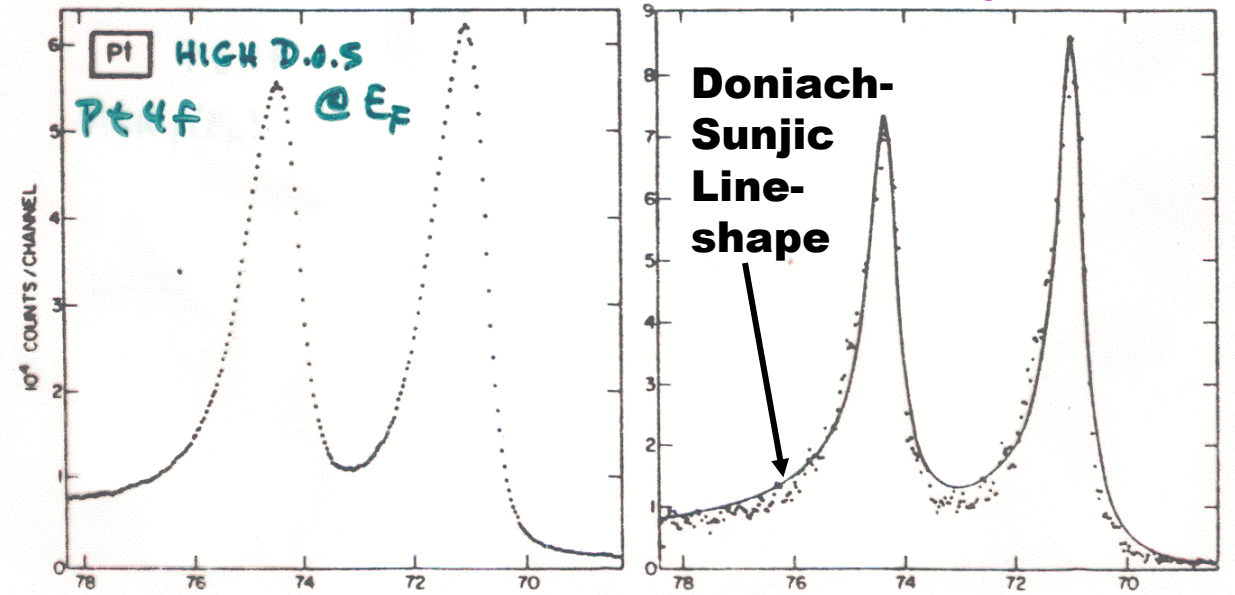

"Basic Concepts of XPS", Figure 37

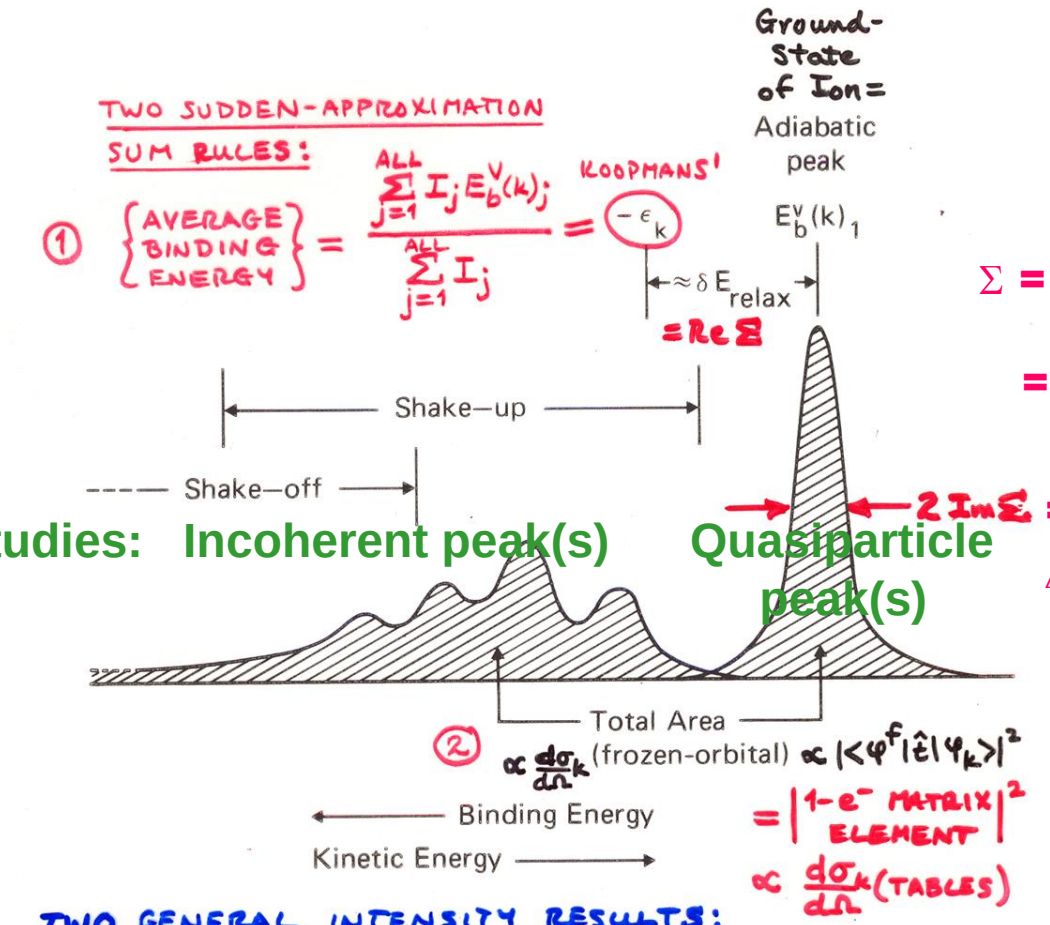

Figure 8 -- Schematic illustration of a photoelectron spectrum involving shake-up and shake-off satellites. The weighted average of all binding energies yields the Koopmans' Theorem binding energy $-\epsilon_k$ (sum rule (77)), and the sum of all intensities is proportional to a frozen-orbital cross section σ_k (sum rule (78)). The adiabatic peak corresponds to formation of the ground-state of the ion ($E_b(k)_1 \equiv E_b(K=1)$).

Σ = many-body "self energy"
= ReΣ + iImΣ

$\Delta E \times \tau_{lifetime} \approx \hbar/2$

S_0^2 in EXAFS (LATER)

② (TOTAL SHAKE-UP + SHAKE-OFF) $= 1 - |\langle \Psi^f(N-1,1) | \Psi_R(N-1) \rangle|^2$
$\approx$ 15-25 % FOR ATOMS/MOLEC.

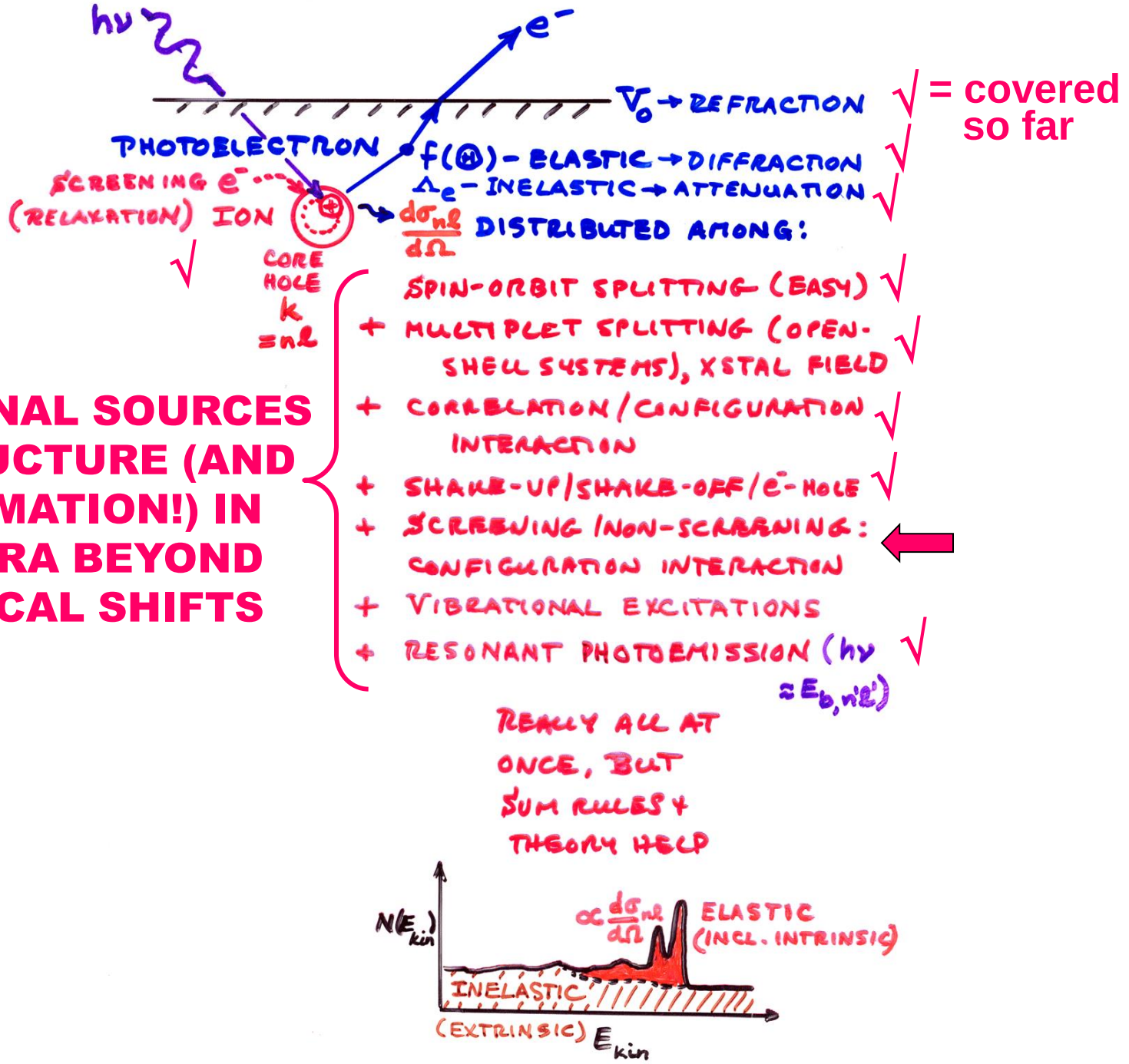

√ = covered so far

ADDITIONAL SOURCES OF STRUCTURE (AND INFORMATION!) IN SPECTRA BEYOND CHEMICAL SHIFTS

SATELLITES & CHARGE-TRANSFER SCREENING

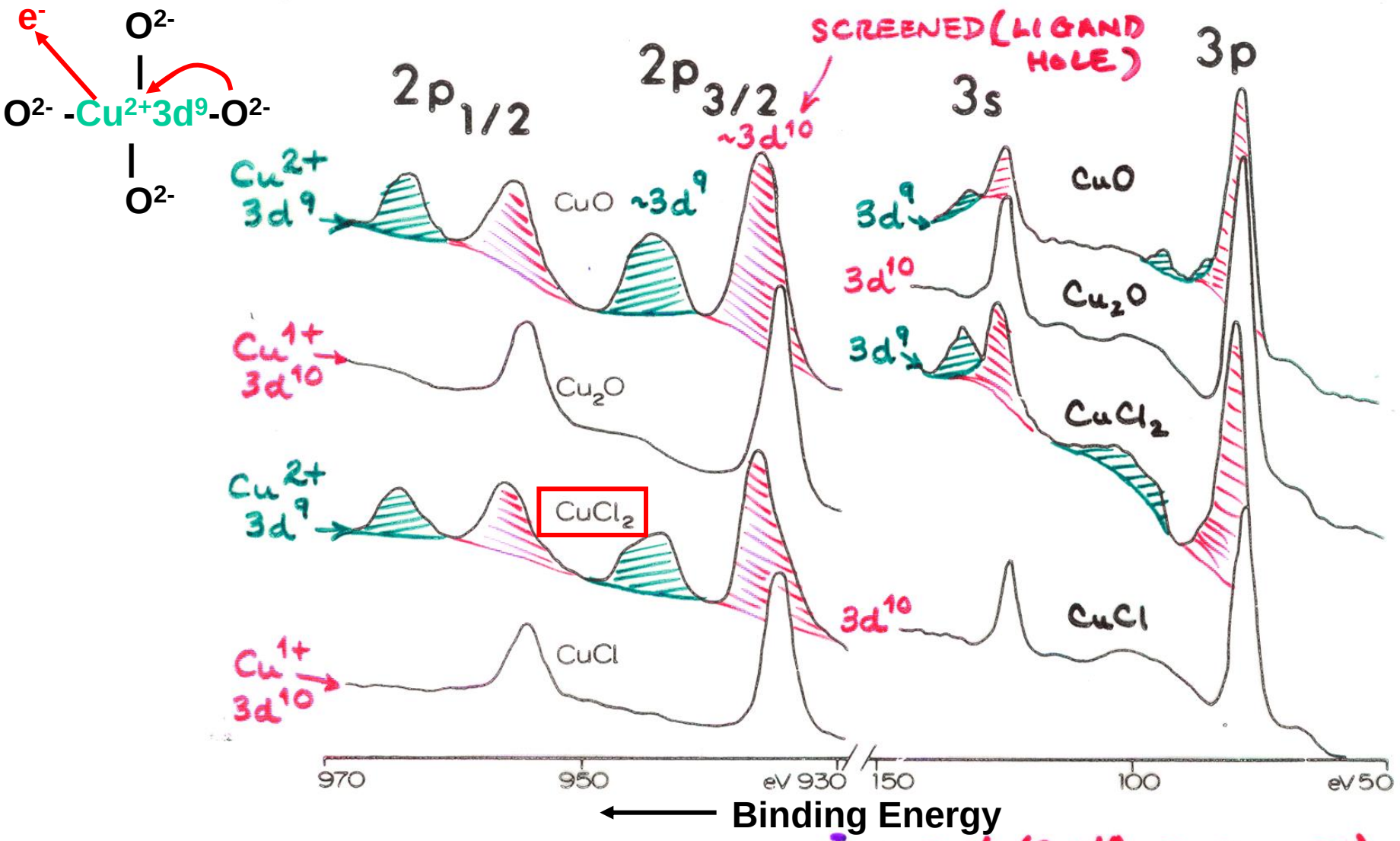

ACTUAL FINAL STATE $\Psi \approx C_1\Phi_1$ (3d10 - SCREENED)
$+ C_2\Phi_2$ (3d9 - UNSCREENED)

"Basic Concepts of XPS"
Figure 38

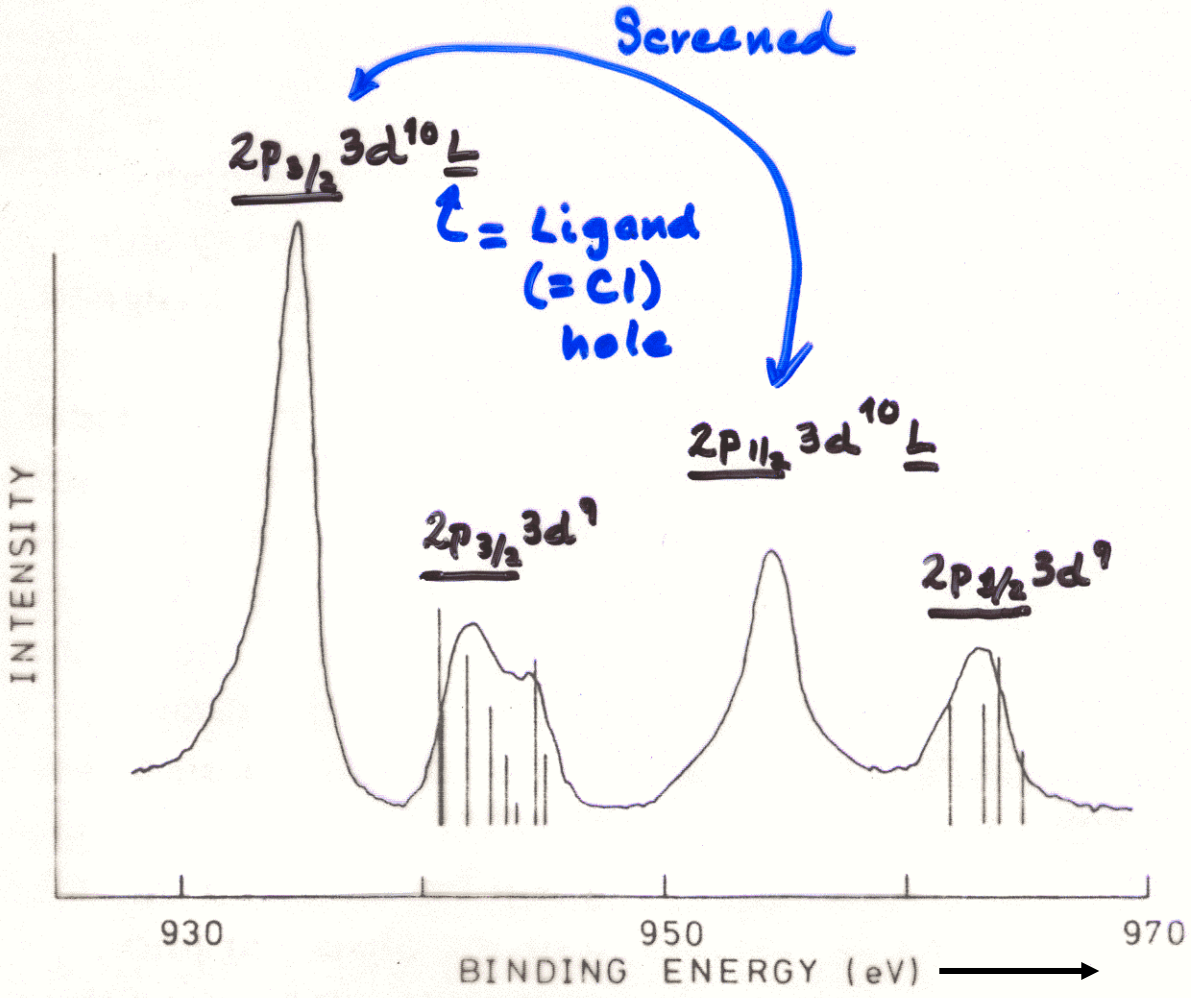

FIG. 2. The Cu $2p$ spectrum of $CuCl_2$ together with the expected multiplet splittings, represented by bars, for the $\underline{2p}3d^9$ level as calculated and discussed in the text.

VAN DER LAAN ET AL., PHYS. REV. B 23, 4369 (1981)

Screening depends on Ionicity/covalency→ satellite intensities can be used to measure interaction parameters

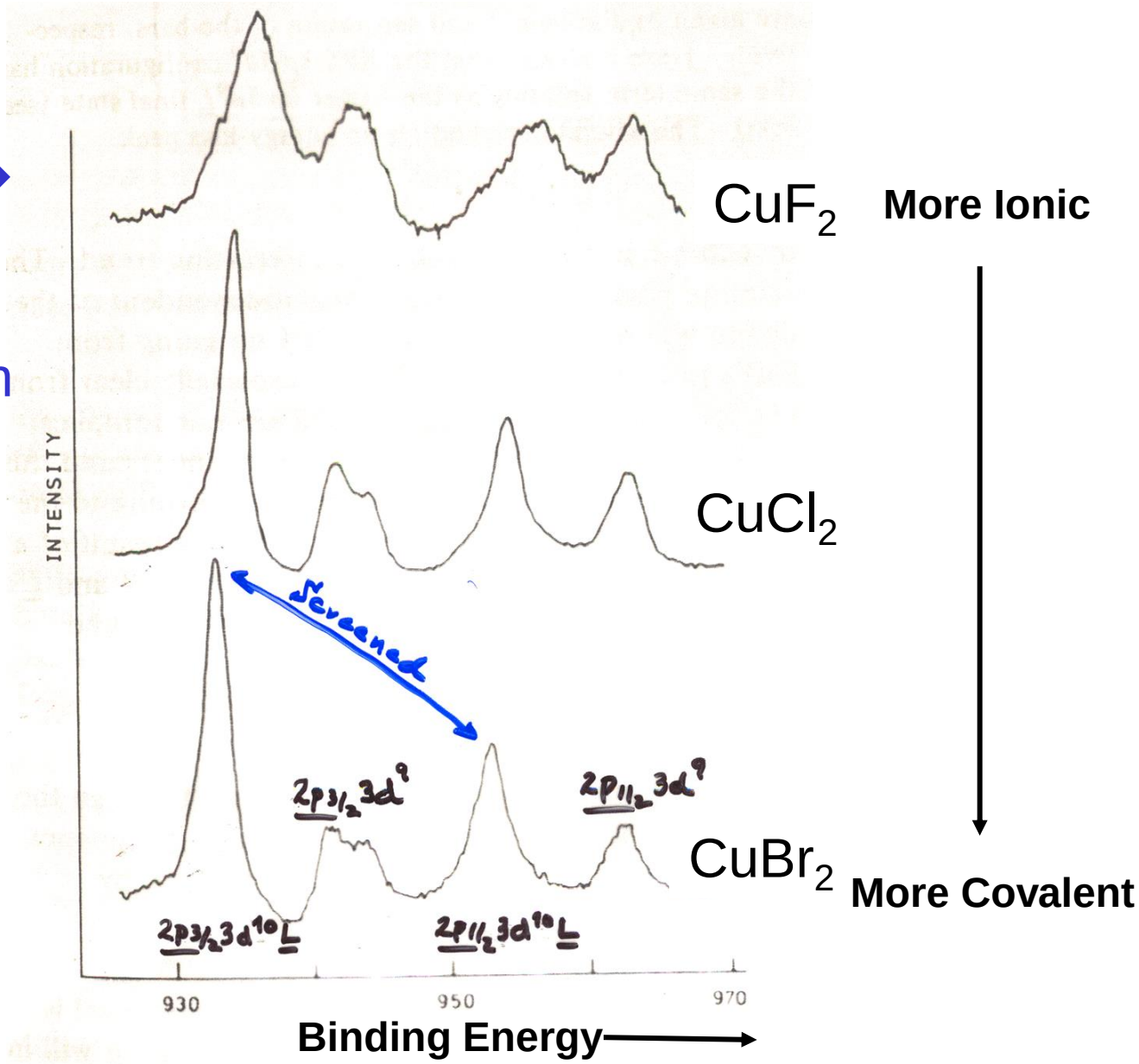

FIG. 1. Cu 2*p* photoelectron spectra of Cu dihalides. The lines leading to a final state with a ligand hole ($\underline{L}$) show a chemical shift.

Screening depends on Ionicity/covalency→ satellite intensities and energy spacings can be used to measure interaction parameters

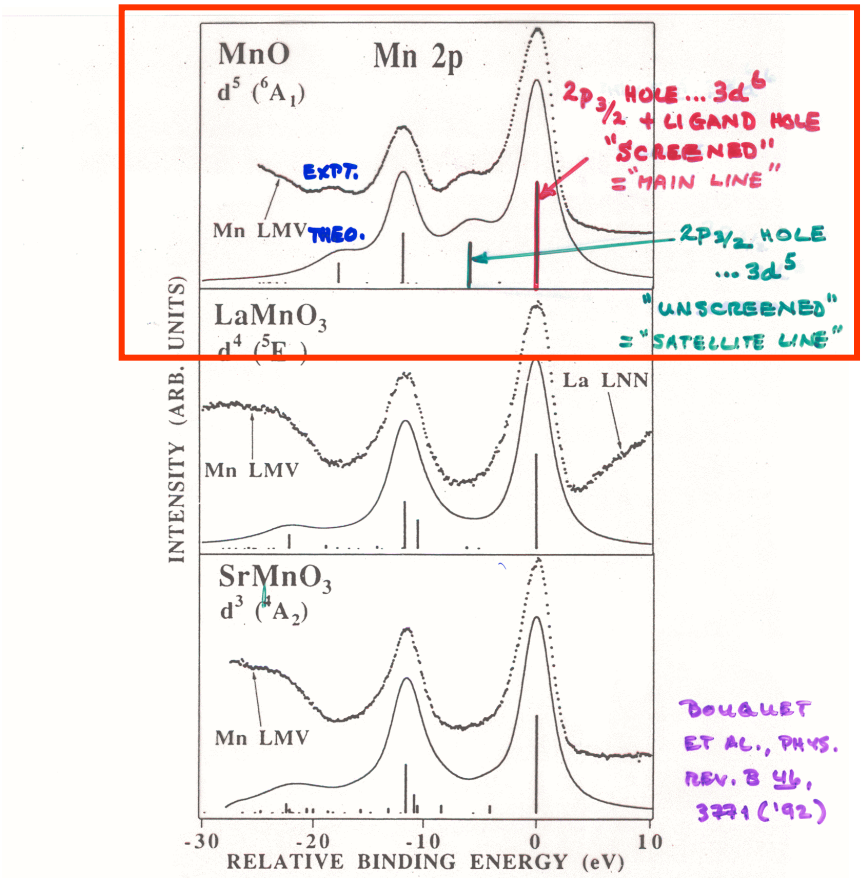

FIG. 1. Theoretical $2p$ core-level XPS spectra (solid line) compared with experimental data (dots) after background subtraction for Mn cations with varying valence. Emission due to the Mn *LMV* Auger peak is observed on the high-binding-energy side of the $2p_{1/2}$ spin-orbit peak, partially obscuring the $2p_{1/2}$ satellite structure.

The Hubbard model-mixing a localized on-site picture and a delocalized band picture (optional)

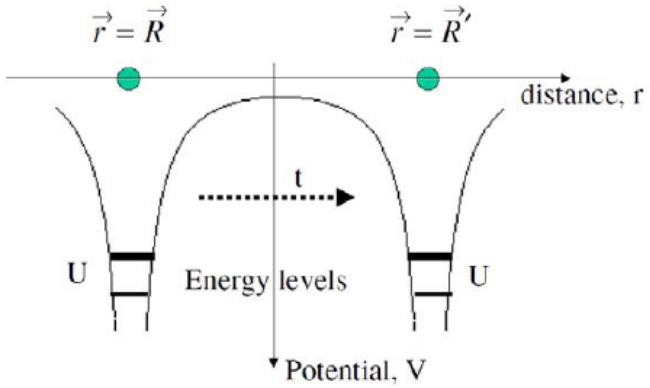

See problem 5 in Chapter 32 of Ashcroft and Mermin, "Solid State Physics", which this paper goes through in nice detail:

B Alvarez-Fernández and J A Blanco

Eur. J. Phys. **23** (2002) 11–16

+243A download at website

$$H = h_1 + h_2 + V_{12} \qquad (1)$$

= U below

where h_1 and h_2 are one-electron Hamiltonians and V_{12} is the Coulomb repulsion potential between the two electrons when they are found to be on the same atom. In order to solve the problem we shall use the following procedure. First we consider a hydrogen molecule in which an atom at $\vec{R}$ is described in the spatial representation by a single orbital electronic level $|\vec{R}\rangle$. When there is no electron on the atom $|\vec{R}, 0\rangle_{\text{vacuum}}$, i.e. an empty level, the energy is zero, if there is one electron of either spin in the level $|\vec{R}, \uparrow\rangle_{\text{up}}$ or $|\vec{R}, \downarrow\rangle_{\text{down}}$ its energy is E_0, and if there are two electrons of opposite spins in the level $|\vec{R}, \uparrow\downarrow\rangle_{\text{singlet}}$ the energy is $2E_0 + U$. The last additional positive energy U represents the intra-atomic Coulomb repulsion between the two localized electrons. = $\mathbf{J_{1s,1s}}$. The amplitude for tunnelling is represented by the off-diagonal term in the one-electron Hamiltonian

bonding =

$$\langle \vec{R}|h|\vec{R}'\rangle = \langle \vec{R}'|h|\vec{R}\rangle = -t \qquad (2)$$

The same U and t used in the de Groot multiplet program (to come later)

T =

The Hubbard model-mixing a localized on-site picture and a delocalized band picture (continued)

Ground-state Hubbard energy:

$$E_{\text{Hubbard}} = 2E_0 + \tfrac{1}{2}U - \sqrt{4t^2 + \tfrac{1}{4}U^2}.$$

And wave function:

$$\Phi_{\text{Hubbard}} = \frac{1}{\sqrt{2}}\Phi_0 + \left(\sqrt{1 + \left(\frac{U}{4t}\right)^2} - \frac{U}{4t}\right)\frac{1}{2}(\Phi_1 + \Phi_2)$$

With $\Phi_0 = \frac{1}{\sqrt{2}}[|\vec{R}\rangle|\vec{R}'\rangle + |\vec{R}'\rangle|\vec{R}\rangle]$

$\Phi_1 = |\vec{R}\rangle|\vec{R}\rangle$

$\Phi_2 = |\vec{R}'\rangle|\vec{R}'\rangle$

Electrons on different protons

Electrons on the same proton

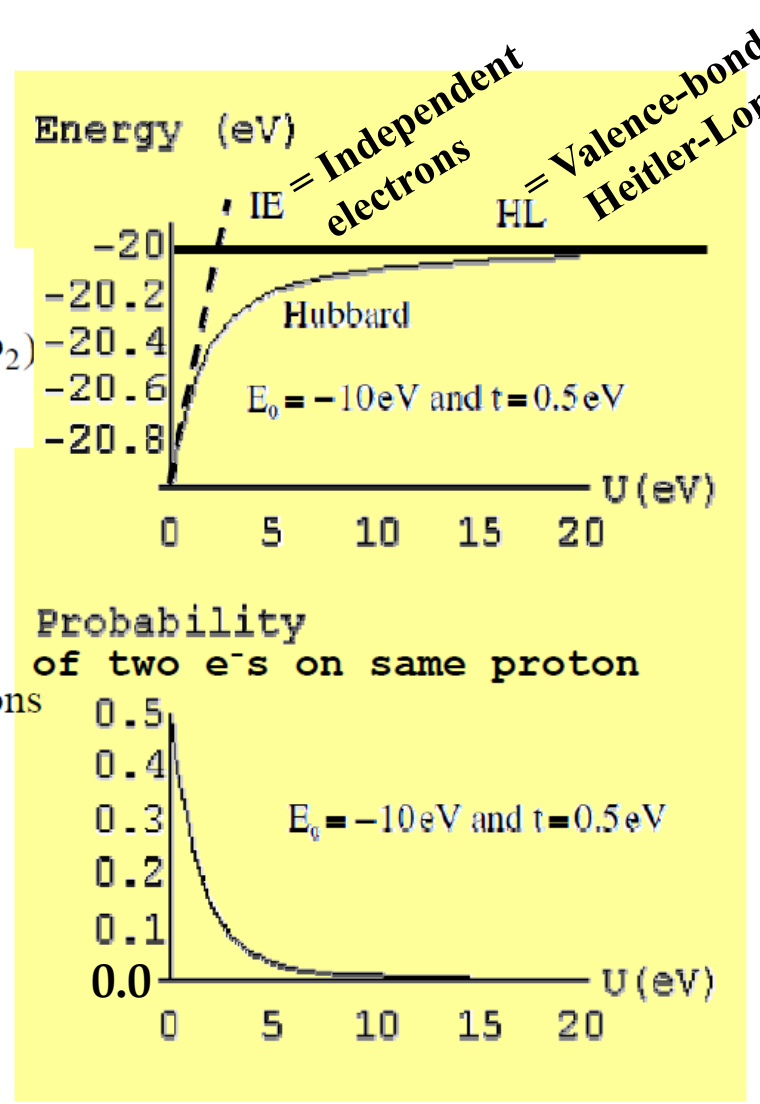

Localized configuration interaction approach to spectrum simulation: Anderson impurity model (AIM, SIAM) for PS, XAS, XES

(SUGANO, LARSSON ~> SAWATZKY, VAN DER LAAN, FUJIMORI, OH, ET AL.)

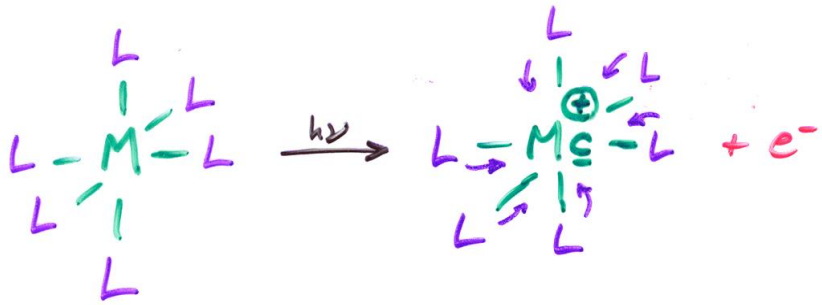

$\underline{c}$ = CORE HOLE ON METAL

$\underline{L}$ = VALENCE (τ) HOLE ON LIGAND

$$\psi_i = a_0|d^n\rangle + \sum_m a_m|d^{(n+m)}\underline{L}^m\rangle$$

$$\psi_f = b_0|\underline{c}d^n\rangle + \sum_m b_m|\underline{c}d^{(n+m)}\underline{L}^m\rangle$$

WITH INTERACTIONS OF:

$10Dq$ = CRYSTAL FIELD (OFTEN NEGLECTED)

Δ = LIGAND-TO-METAL CHARGE TRANSF. ENERGY
= $E(d^{n+1}\underline{L}) - E(d^n)$

$U_{dd} = U$ = d-d COULOMB REPULSION ENERGY
= $E(d^{n-1}) + E(d^{n+1}) - 2E(d^n) \approx J_{dd}$

T = LIGAND p-TO-METAL d HYBRIDIZATION
= $\langle d_\alpha|\hat{H}|p_\alpha\rangle$ (α = SAME SYMMETRY)

$U_{pd} \equiv U_{cd} = Q$ = CORE-HOLE-TO-d INTERACTION: $\langle \underline{c}|\hat{H}|d\rangle \approx J_{cd}$ = coulomb integral

Good discussion of model: Bocquet & Fujimori, J. Elect. Spect. & Rel. Phen. 82, 87 (1996)

$$\rho(e_k) = \sum_f |\langle \Psi_f|c|\Psi_g\rangle|^2 \delta(h\nu - e_k - E_f)$$

By now: Book by de Groot and Kotani (@website) and the CTM4XAS program for calculating this for some cases:
http://www.anorg.chem.uu.nl/CTM4XAS/index.html

WITH INTENSITIES FROM SUDDEN APPROX.

AS:

$$I(E_{kin}) \propto \sum_{f,k} |\langle \psi_f(N-1,k)|\psi_R(N-1,k)\rangle|^2 \cdot \delta(h\nu - E_f - E_{kin})$$

($\underline{c}$ = CORE HOLE)

WHERE: $\psi_R(N-1,k) = \psi_i$ (N WITH k HOLE = $\underline{c}$)

From Bocquet & Fujimori, J. Elect.Spect. & Rel. Phen. 82, 87 (1996):

The electronic structures of transition-metal (TM) compounds, particularly the 3d TM halides, oxides and chalcogenides, have long provided intriguing problems for physicists and chemists. These compounds are highly correlated electron systems where the essential physics can be described in terms of a few interaction strengths, namely the on-site d–d coloumbic repulsion energy U, the ligand-to-metal charge-transfer energy Δ, and the ligand p–metal d hybridization strength T. Core-level X-ray photoemission spectroscopy (XPS) is a useful probe of the valence electronic structures of TM compounds, and has been successfully used in recent years to extract parame values for these interaction strengths [1–5]. In

From CTM manual:

C: Charge Transfer Parameters

- **Delta:** This is the charge transfer parameter Δ, which gives the energy difference between the (centers of the) $3d^N$ and $3d^{N+1}\underline{L}$ configurations. The effective value of Δ (Δ_{eff}) is affected by the multiplet and crystal field effects on each configuration. In the next version, the value of Δ_{eff} will be given in a parameter-output file.
- **Udd:** This is the value of the Hubbard U.
- **Upd:** This is the core hole potential. In case of XAS spectra, only the difference between U_{pd} and U_{dd} is important.
- **Hopping T:** The hopping parameters are given for the 4 symmetries in tetragonal symmetry A_1, B_1, E and B_2. A_1 (z^2) and B1 (x^2-y^2) are part of the e_g-orbitals and E (xz, yz) and B_2 (xy) are part of the t_{2g} orbitals. In Oh symmetry the values of A_1=B_1 and E=B_2. (This is not yet automatic in the test-version).

Originated in the Hubbard Model: Ashcroft and Mermin, pp. 689-691, article at website, and (downloadable) book by de Groot and Kotani

E.g.—Crystal field in Mn^{3+} & Mn^{2+} with negative octahedral ligands

High-spin*/Low-spin*

Mn^{2+} $3d^5$ | **Mn^{3+} $3d^4$**

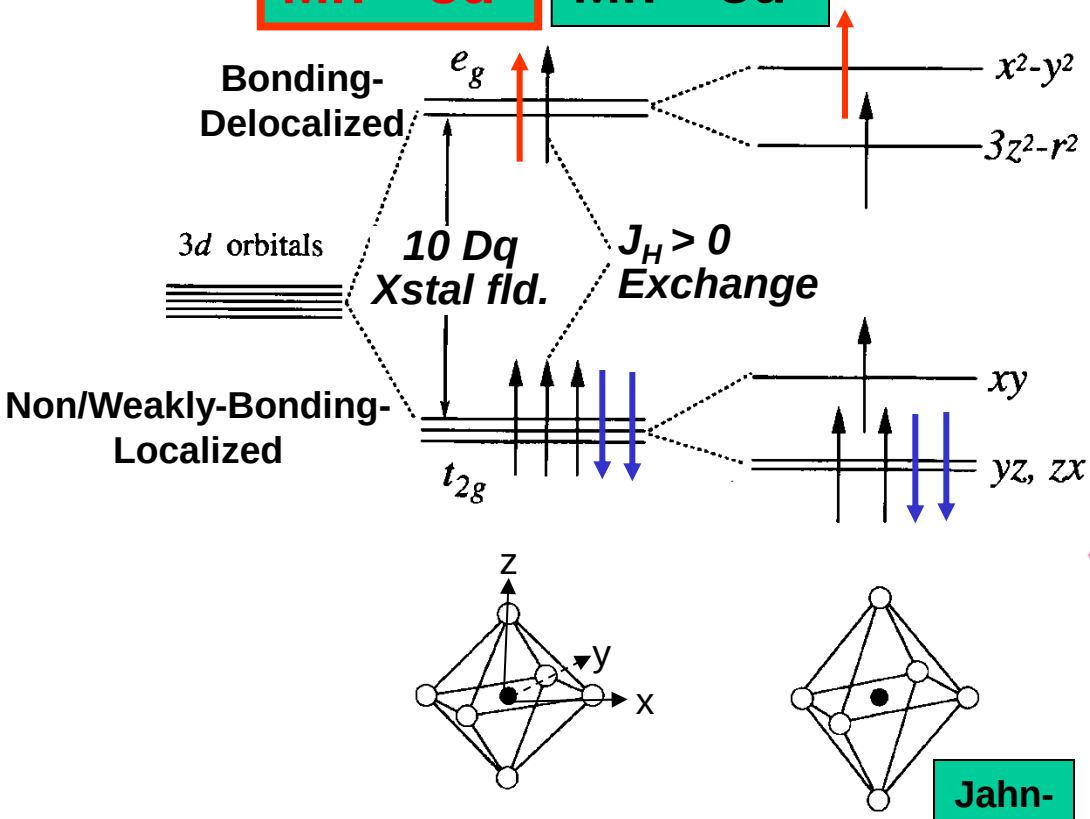

Jahn-Teller

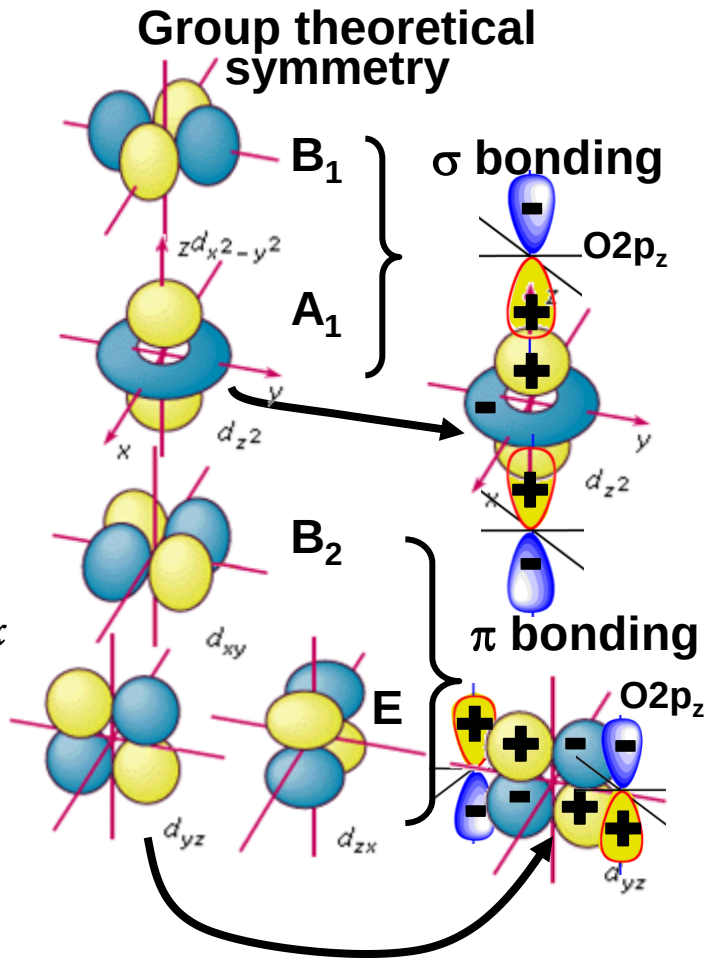

High-spin*: 10Dq << J_H

Low-spin*: 10Dq >> J_H

J_H calculated from atomic exchange integrals: $K_{3d,3d}$

Calculating all these effects in XPS, XAS, XES, RIXS
The CTM4XAS Program

http://www.anorg.chem.uu.nl/CTM4XAS/

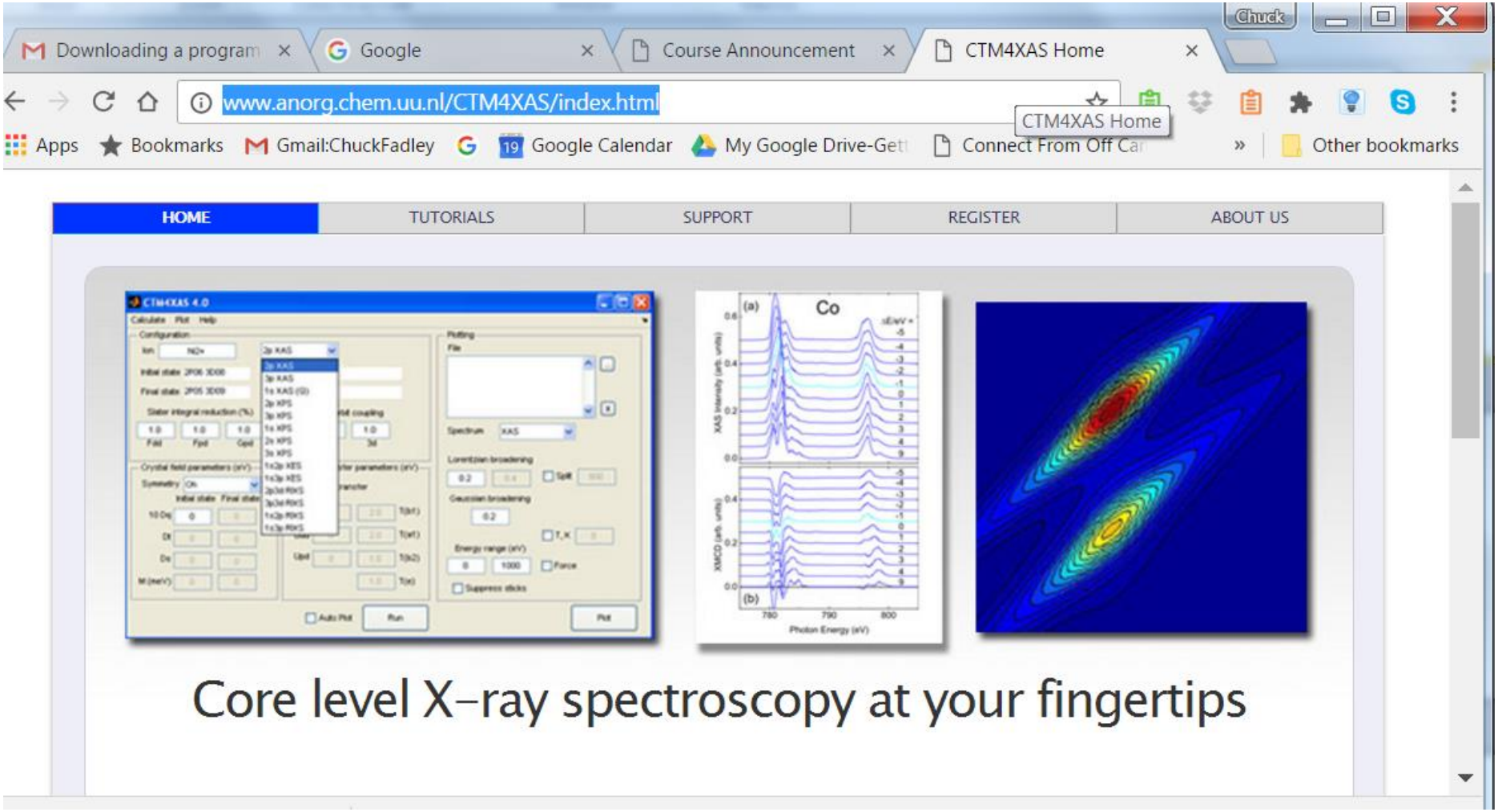

Register and follow download and install sequence

If you get a truncated GUI like this:

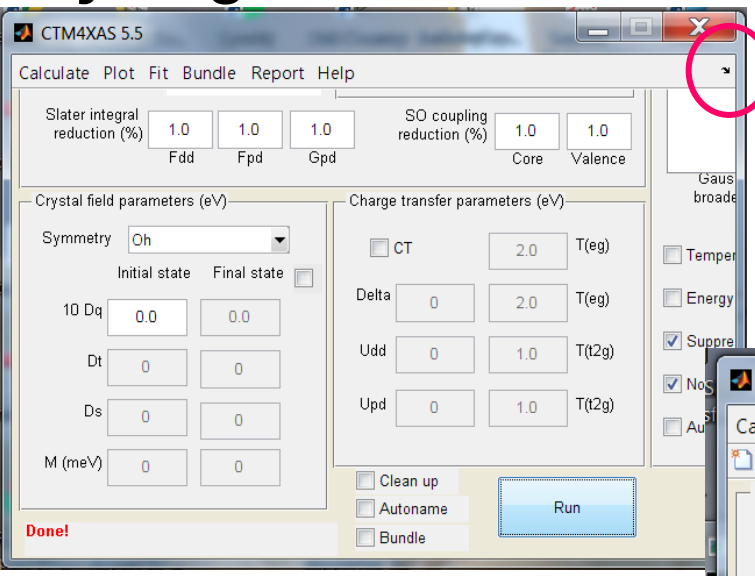

Click on this little arrow

And then you get something expandable to:

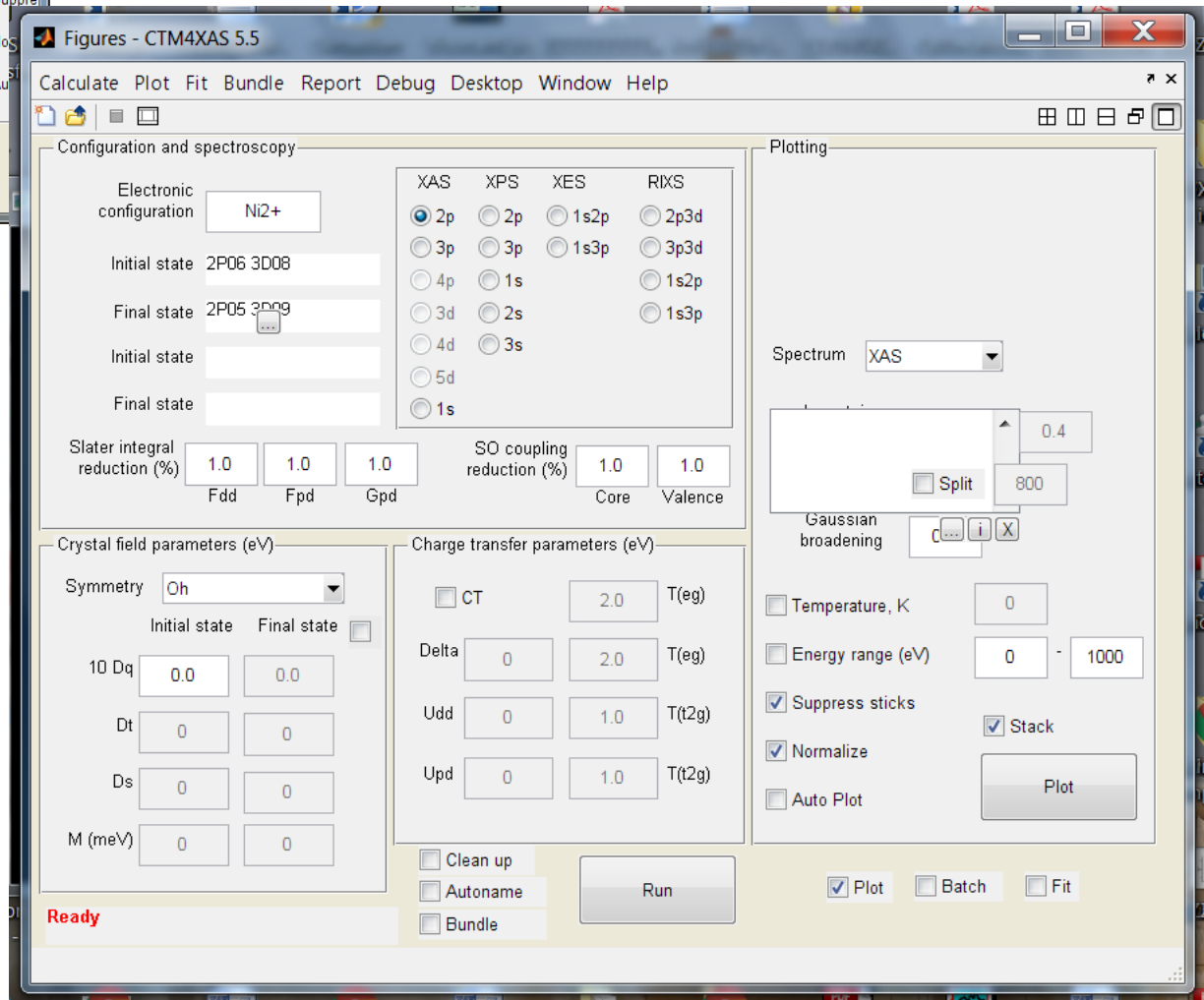

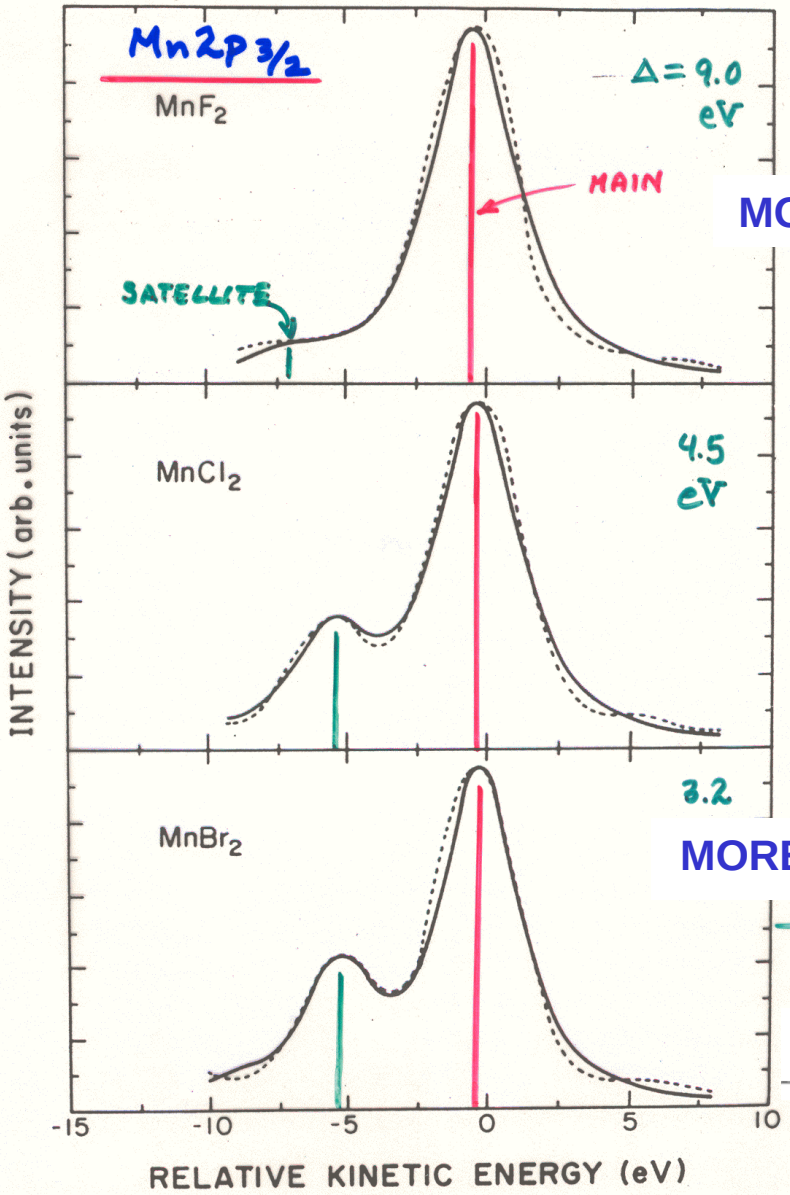

MORE IONIC

MORE COVALENT

DECREASING Δ

Park et al.
Phys. Rev. B
37, 10867 (1988)

Core hole-d attraction
U_{pd} =
U_{cd} =

Compound	Δ (eV)	U (eV)	T (eV)	Q (eV)	$\langle n_d \rangle$
MnF_2	9.0	3.2	1.5	4.5	5.12
$MnCl_2$	4.5	3.2	1.5	4.5	5.32
$MnBr_2$	3.2	3.2	1.4	4.5	5.41

FIG. 6. Fits of the cluster model results with the experimental $2p_{3/2}$ spectra of the manganese dihalides. The parameters used are listed in Table II. A Lorentzian broadening is 2.6–3.0 eV, and a Gaussian broadening of 1.2 eV (FWHM) was used.

MnO as a typical example-XAS

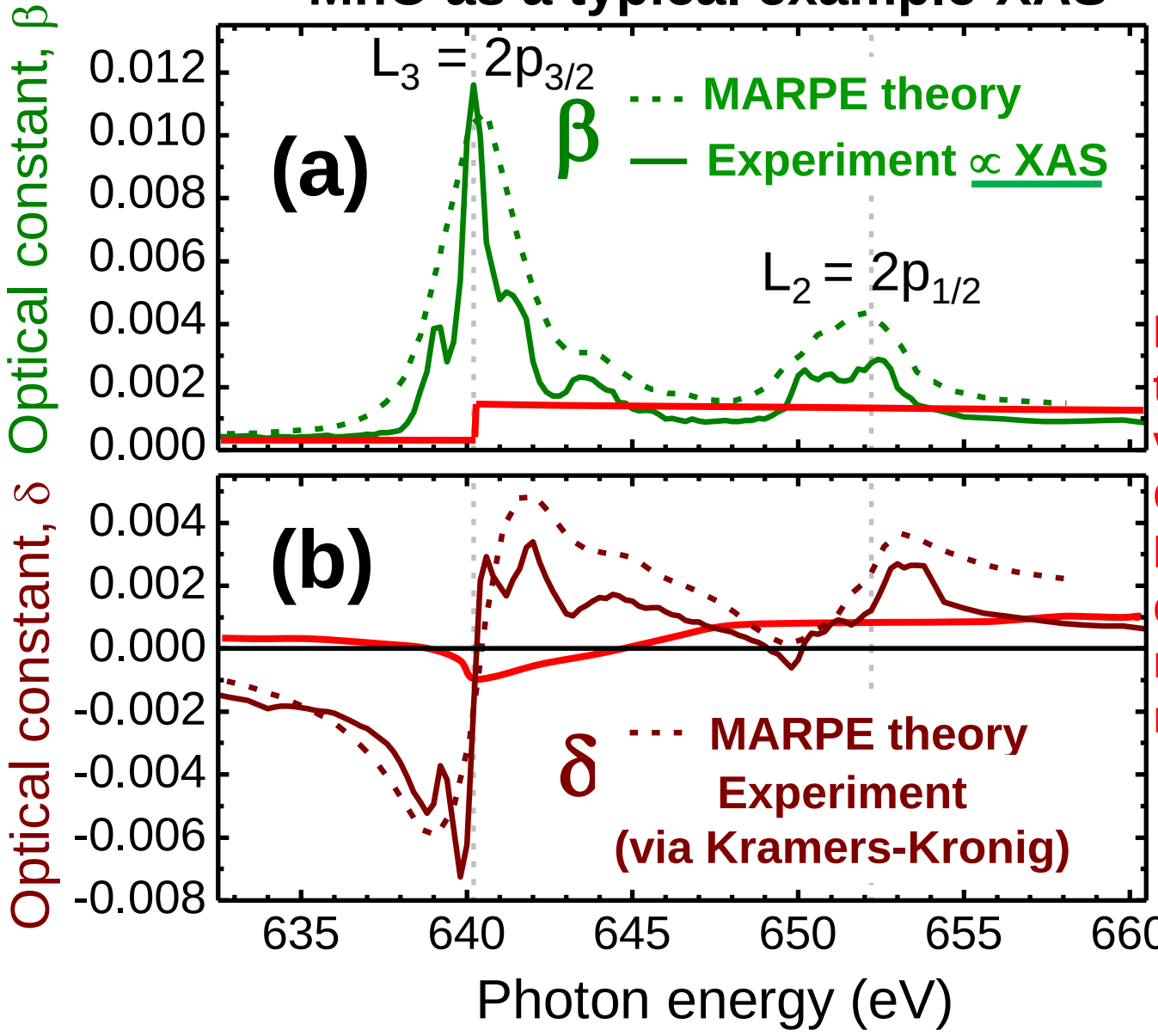

From tabulated values: CXRO, Much different near resonances!

Kay et al., Phys. Rev. B 63, 115119 (2001)

MnO (NaCl structure)

Mn octahedral

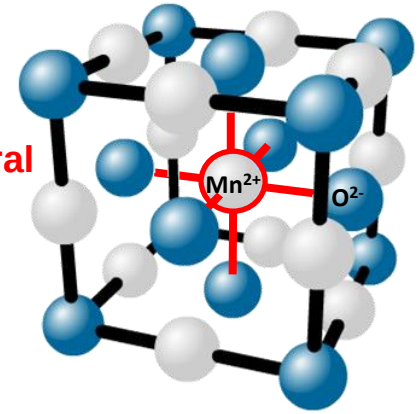

XPS satellites-MnO

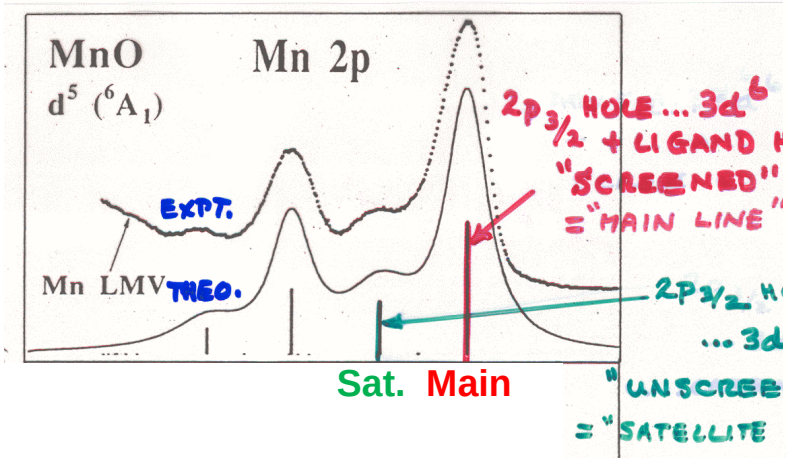

ANALYSIS VIA ANDERSON IMPURITY MODEL

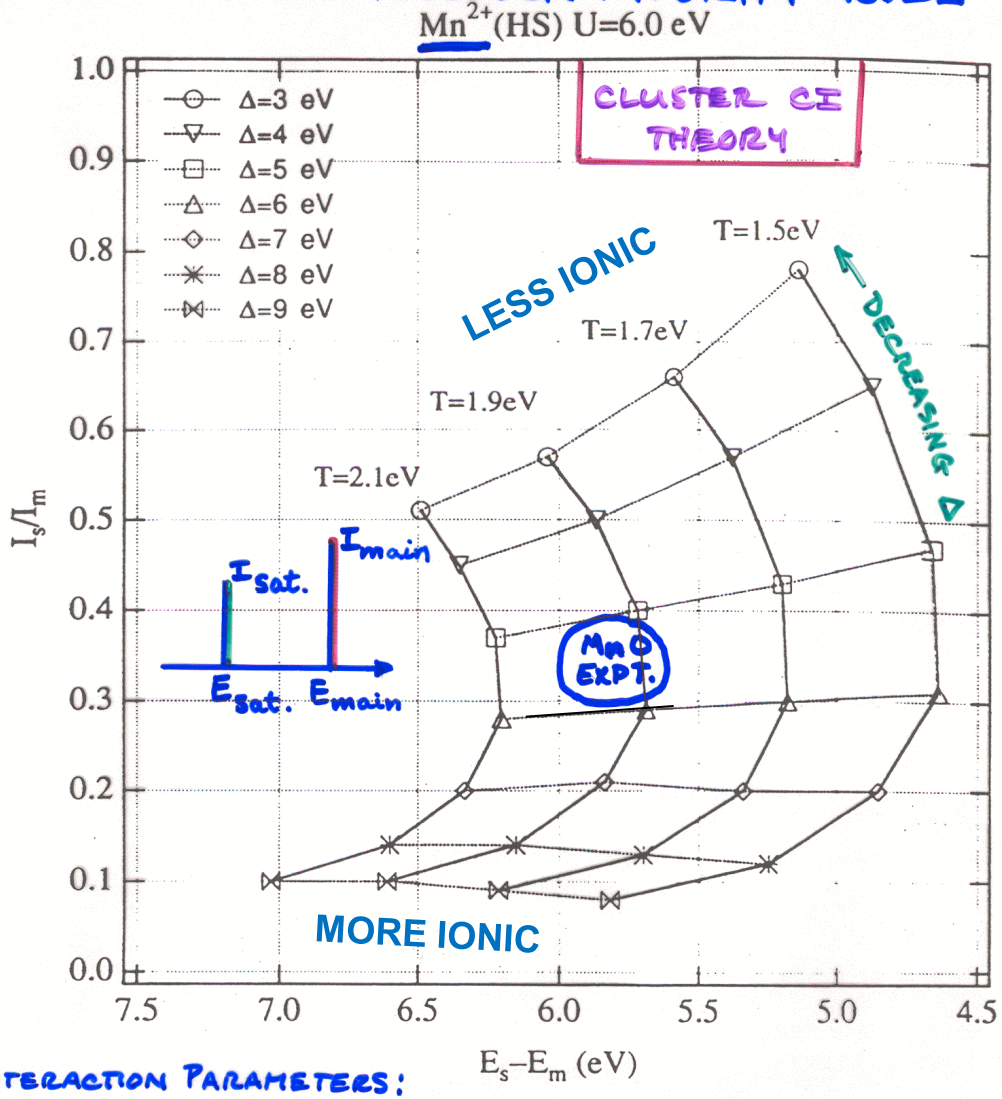

INTERACTION PARAMETERS:

U = 3d-3d COULOMB REPULSION ENERGY

Δ = LIGAND-TO-METAL CHARGE TRANSFER ENERGY

T = LIGAND p – METAL 3d HYBRIDIZATION ENERGY

Q = CORE HOLE-3d COULOMB

BOURNET ET AL., J. EL. SP. 62, 87 (199

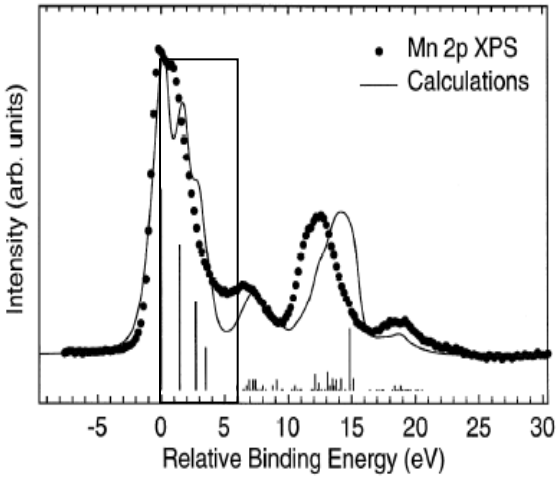

More recent data:
Phys. Rev. B 63, 115119 (2001)
In problem set

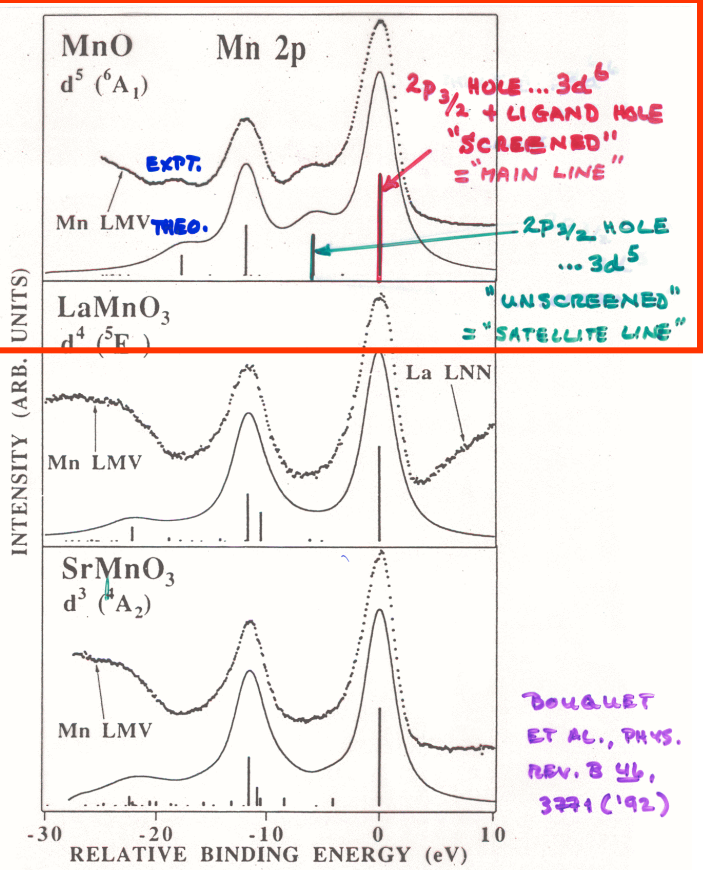

FIG. 1. Theoretical $2p$ core-level XPS spectra (solid line) compared with experimental data (dots) after background subtraction for Mn cations with varying valence. Emission due to the Mn *LMV* Auger peak is observed on the high-binding-energy side of the $2p_{1/2}$ spin-orbit peak, partially obscuring the $2p_{1/2}$ satellite structure.

For octahedral coord.:

$$T_\sigma = \sqrt{3}(pd\sigma),\ T_\pi = 2(pd\pi)$$

$$T_\sigma / T_\pi \propto (pd\sigma)/(pd\pi) \approx -2.2$$

Compound	d^n	Valence	Δ	U	$(pd\sigma)$	Δ_{eff}	U_{eff}	Main peak	Satellite peak	Ref.
$SrMnO_3$	d^3	4+	2.0	7.8	−1.5	−0.2	7.1	$d^4\underline{L}$	$d^4\underline{L}$	This work
$LaMnO_3$	d^4	3+	4.5	7.5	−1.8	1.8	6.8	$d^5\underline{L}$	$d^6\underline{L}^2$	This work
MnO	d^5	2+	6.5	7.0	−1.1	8.8	11.6	$d^6\underline{L}$	d^5	This work
			7.0	7.5	−0.9					3

From later paper and Brief Manual 6.5 6.0 -1.99/√3 = -1.1 U/(Q = core hole attraction) = 0.7-1.0, a best fit no. is 0.83.

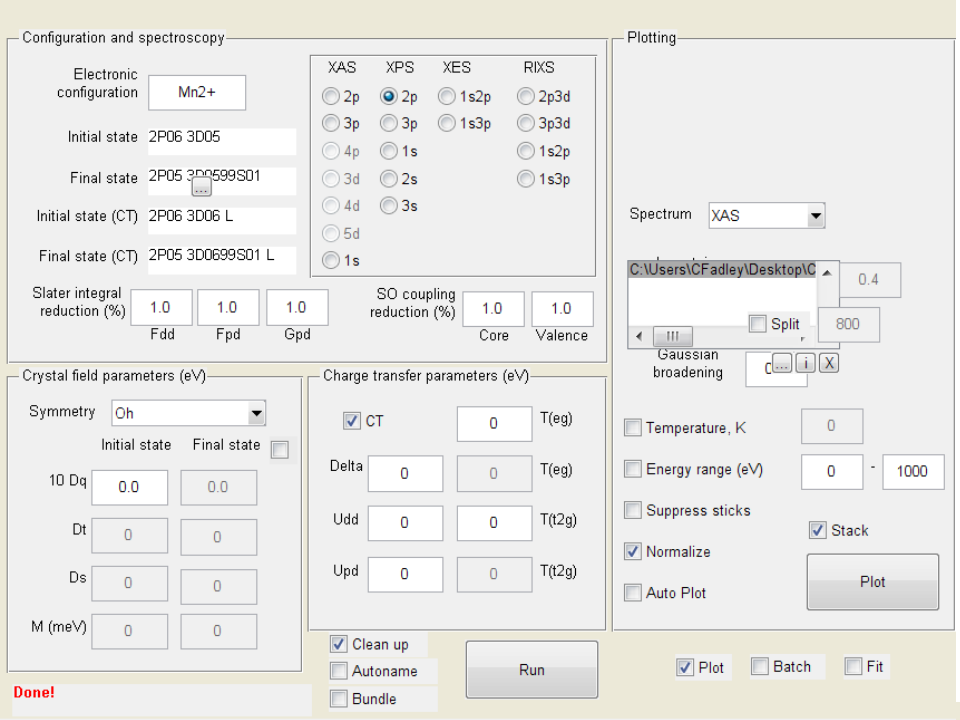

Free atom

MnO

Much more info. and several examples in the *Brief Manual for CTM4XAS20 charge-transfer multiplet simulation program*, downloadable from website

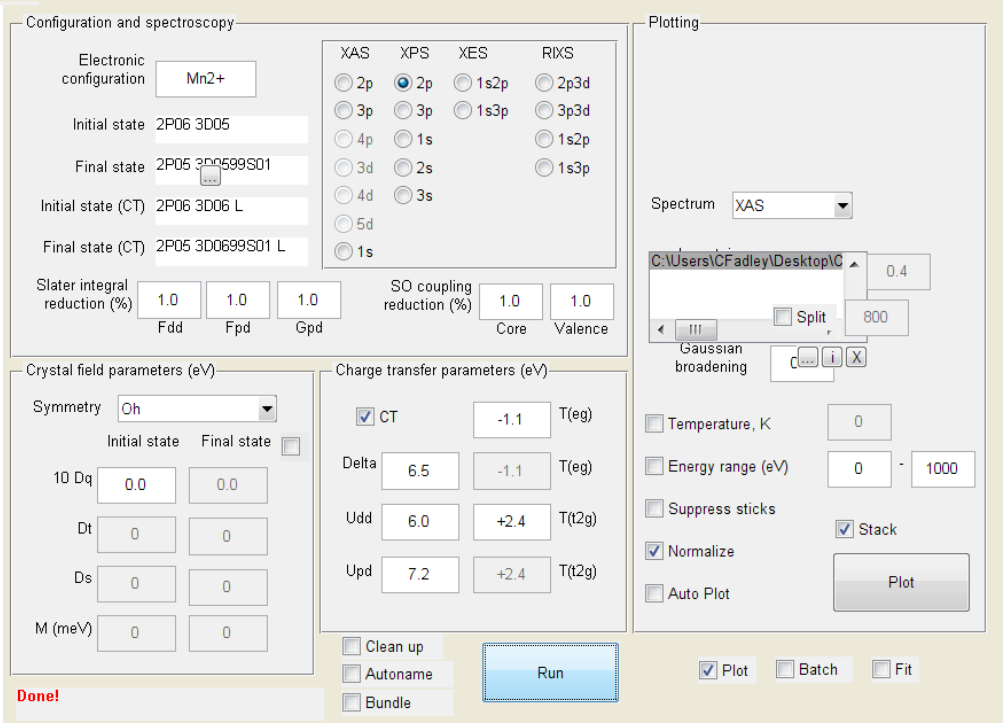

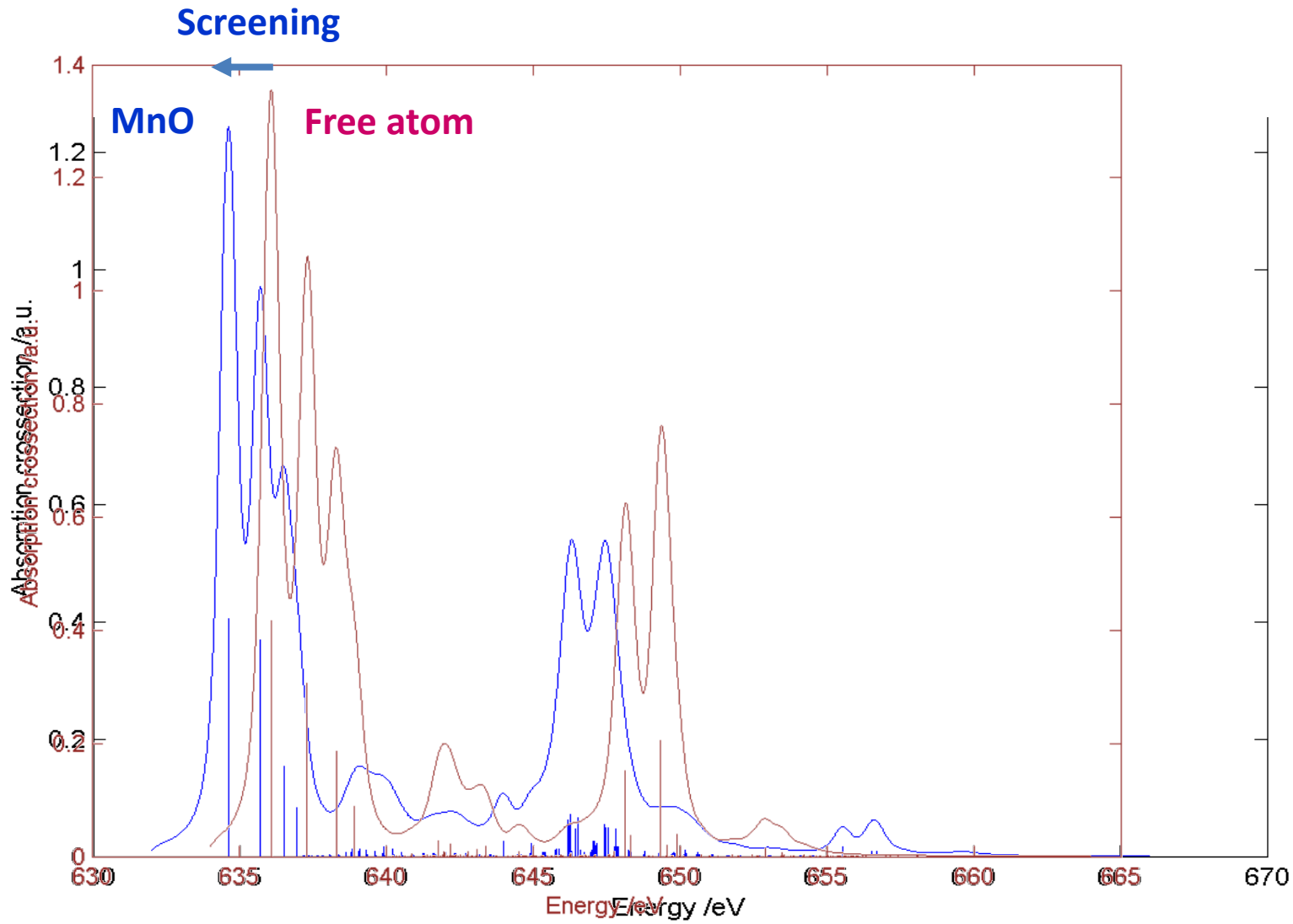
Screening
MnO
Free atom
Absorption cross section /a.u.
Energy /eV
1.4
1.2
1
0.8
0.6
0.4
0.2
0
630
635
640
645
650
655
660
665
670

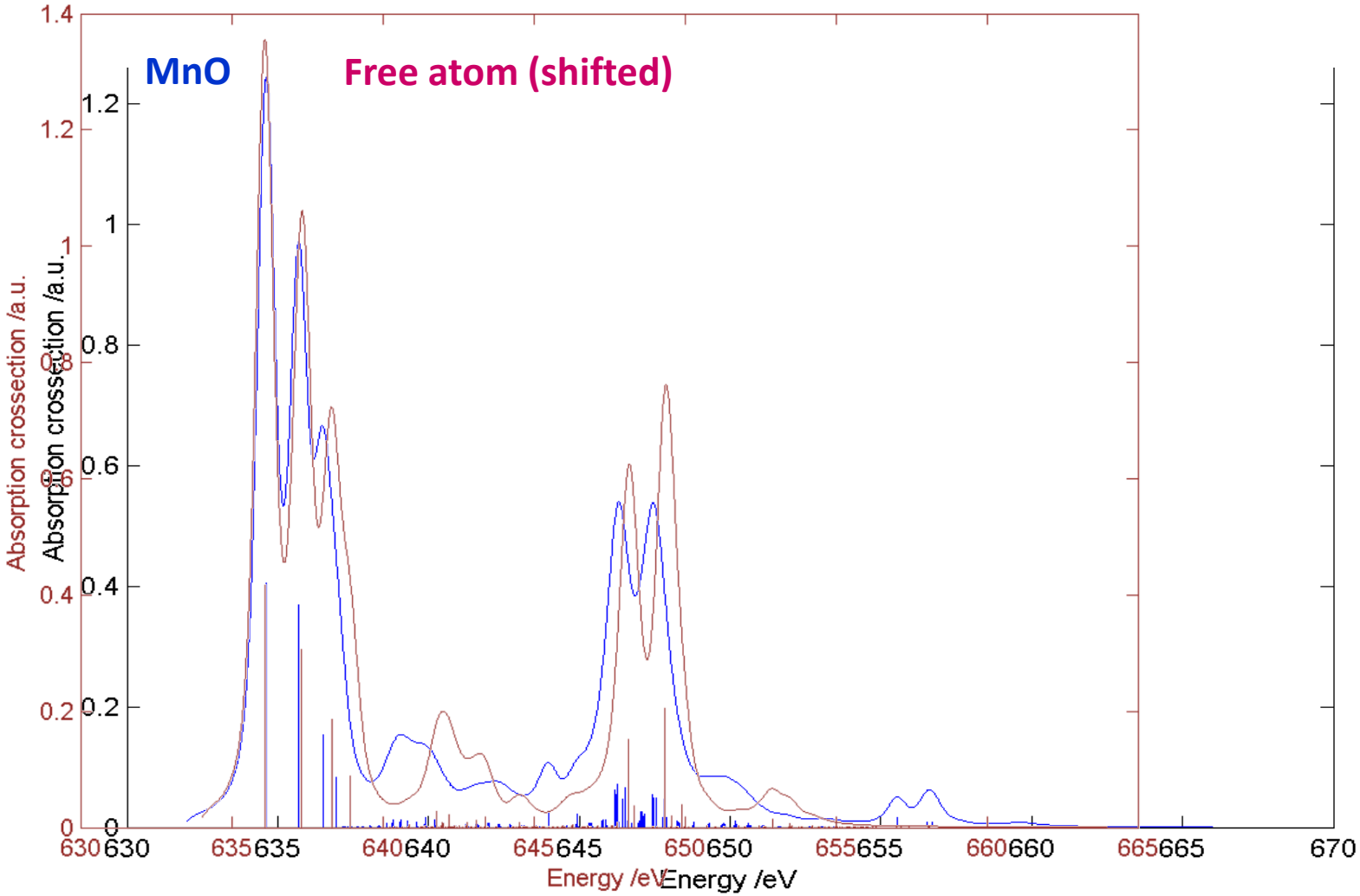
MnO
Free atom (shifted)
Absorption crossection /a.u.
Energy /eV
1.4
1.2
1
0.8
0.6
0.4
0.2
0
630
635
640
645
650
655
660
665
670

The same thing happens in open d-shell metals, but more complicated to simulate!

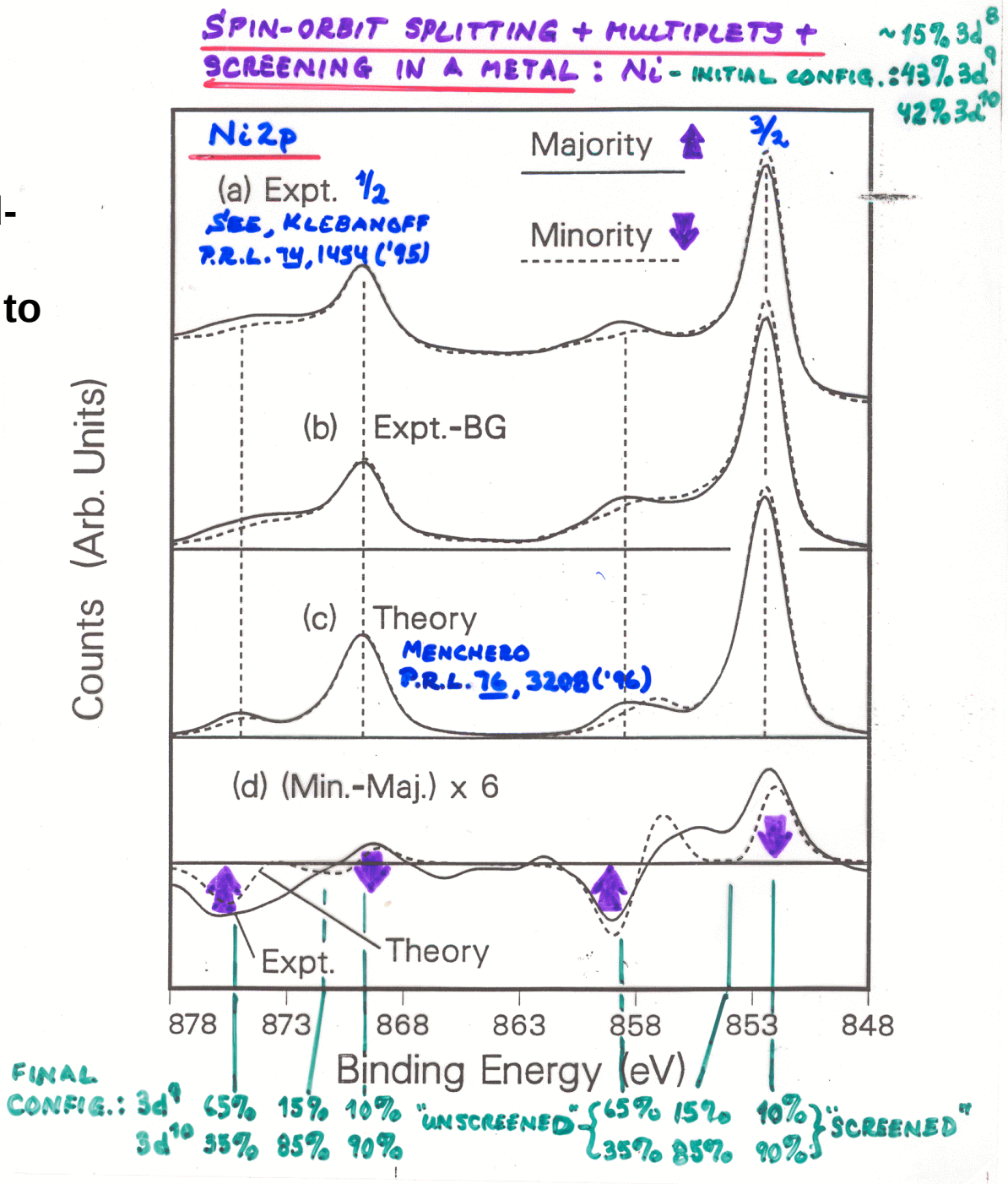

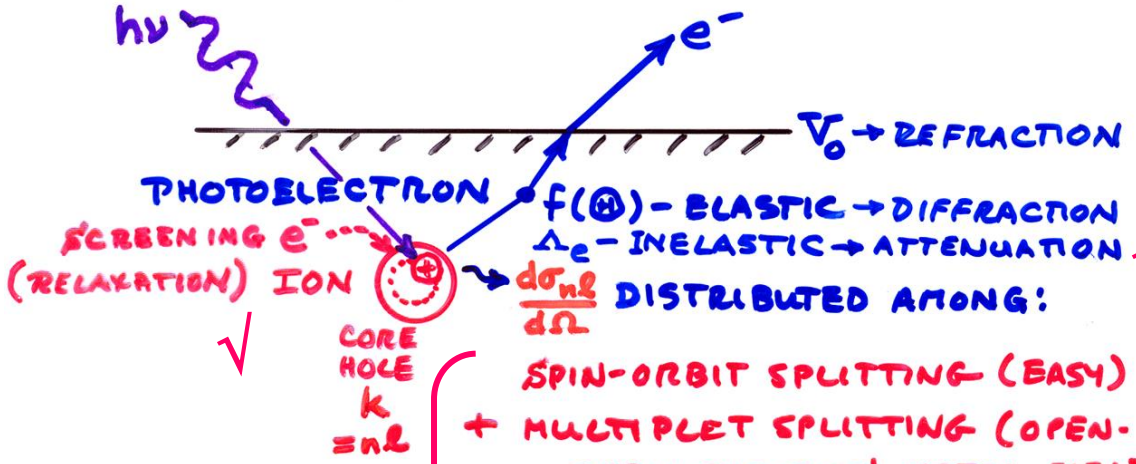

√ = covered so far

ADDITIONAL SOURCES OF STRUCTURE (AND INFORMATION!) IN SPECTRA BEYOND CHEMICAL SHIFTS

- SPIN-ORBIT SPLITTING (EASY) √
- \+ MULTIPLET SPLITTING (OPEN-SHELL SYSTEMS), XSTAL FIELD √
- \+ CORRELATION / CONFIGURATION INTERACTION √
- \+ SHAKE-UP/SHAKE-OFF/e^--HOLE √
- \+ SCREENING/NON-SCREENING: CONFIGURATION INTERACTION √
- \+ VIBRATIONAL EXCITATIONS √ Review
- \+ RESONANT PHOTOEMISSION ($h\nu \approx E_{b,n'l'}$) √

REALLY ALL AT ONCE, BUT SUM RULES + THEORY HELP

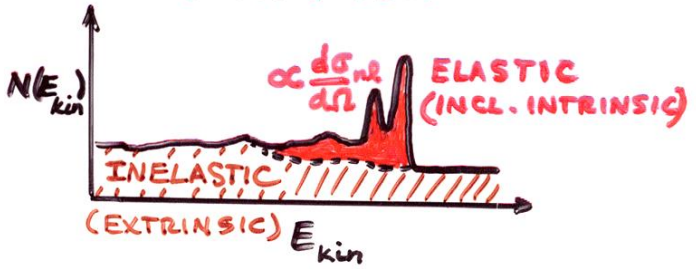

INTENSITIES IN PHOTOELECTRON SPECTRA:

- GENERAL: FINAL STATE K (k-SUBSHELL + ALL OTHER DESIG.)

$$\text{INT.}_K \propto \left| \hat{e} \cdot \langle \Psi^f_{tot}(N,K) | \sum_{i=1}^{N} \vec{r}_i | \Psi^i(N) \rangle \right|^2 \quad \text{(DIPOLE APPROX.}$$

- BORN-OPPENHEIMER: e^-'s FAST, VIBRATIONS SLOW

$$\text{INT.}_K \propto \underbrace{\left| \langle \psi^f_{VIB,v'} | \psi^i_{VIB,v} \rangle \right|^2}_{\text{FRANCK-CONDON FACTOR}} \left| \hat{e} \cdot \langle \Psi^f_{e^-}(N,K) | \sum_{i=1}^{N} \vec{r}_i | \psi^i_{e^-}(N) \rangle \right|^2$$

- SUDDEN APPROXIMATION: $\psi_K \rightarrow \psi_f$ = PHOTOe^- (FAST)

$$\left.\begin{array}{l} \psi_1 \rightarrow \psi_1' \\ \vdots \\ \psi_{K-1} \rightarrow \psi_{K-1}' \\ \psi_{K+1} \rightarrow \psi_{K+1}' \\ \vdots \\ \psi_N \rightarrow \psi_N' \end{array}\right\} \text{(SLOW)} \qquad K \text{ HOLE} \rightarrow$$

$$\text{INT.}_K \propto \left| \langle \psi^f_{VIB,v'} | \psi^i_{VIB,v} \rangle \right|^2 \underbrace{\left| \langle \psi^f_{e^-}(N-1,K) | \psi^{\dagger}_K(N-1,K) \rangle \right|^2}_{K \text{ MISSING}} \left| \hat{e} \cdot \langle \psi_f | \vec{r} | \psi_K \rangle \right|^2$$

SAME SUBSHELL COUPLING + TOTAL L,S → "MONOPOLE"

↳ NORMAL $\frac{d\sigma_K}{d\Omega}$

- SLATER DETS. FOR $\Psi^f_{e^-} = \det(\psi_1' \psi_2' \cdots \psi_{K-1}' \psi_{K+1}' \cdots \psi_N')$

$$\Psi_K = \det(\psi_1 \psi_2 \cdots \psi_{K-1} \psi_{K+1} \cdots \psi_N)$$

$$\text{INT.}_K \propto \left| \langle \psi^f_{VIB,v'} | \psi^i_{VIB,v} \rangle \right|^2 \left| \langle \psi_1' | \psi_1 \rangle \right|^2 \left| \langle \psi_2' | \psi_2 \rangle \right|^2 \cdots$$
$$\left| \langle \psi_{K-1}' | \psi_{K-1} \rangle \right|^2 \left| \langle \psi_{K+1}' | \psi_{K+1} \rangle \right|^2 \cdots \left| \langle \psi_N' | \psi_N \rangle \right|^2 \cdot \left| \hat{e} \cdot \langle \psi_f | \vec{r} | \psi_K \rangle \right|^2$$

1e- DIPOLE → $d\sigma/d\Omega$

$(N-1)e^-$ SHAKE-UP/ SHAKE-OFF → "MONOPOLE"

- PLUS DIFFRACTION EFFECTS IN ψ_f ESCAPE

VIBRATIONAL STRUCTURE IN VALENCE-LEVEL (MO) SPECTRA

Diatomic A-B example

(Also applies to core-level emission if equilibrium distance changes on forming core hole)

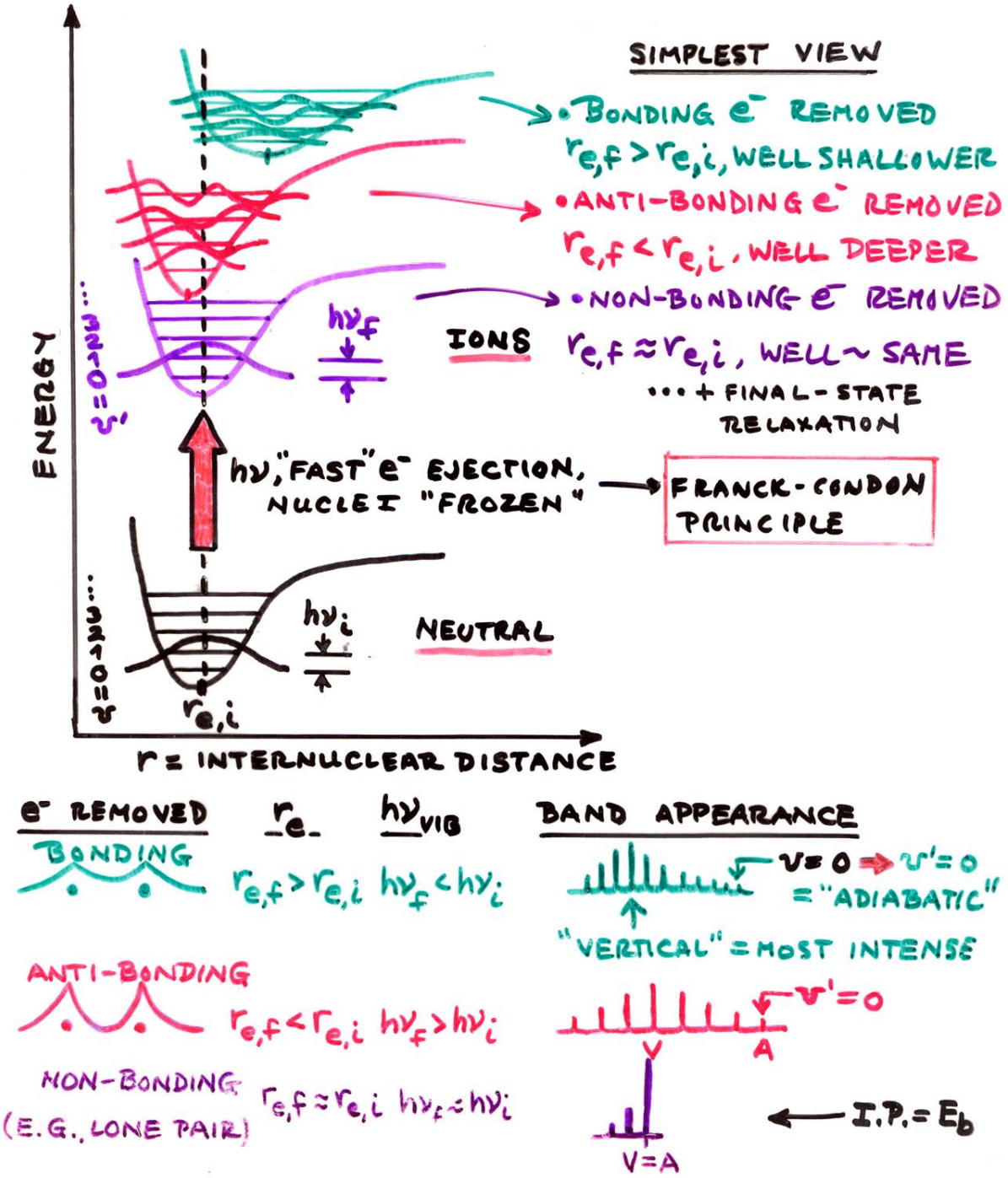

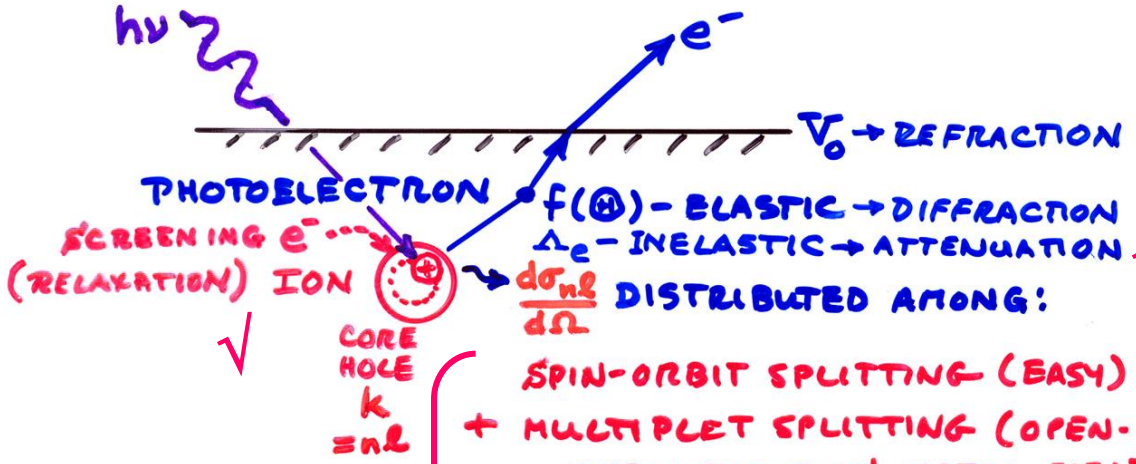

√ = covered so far

ADDITIONAL SOURCES OF STRUCTURE (AND INFORMATION!) IN SPECTRA BEYOND CHEMICAL SHIFTS

- SPIN-ORBIT SPLITTING (EASY) √
- \+ MULTIPLET SPLITTING (OPEN-SHELL SYSTEMS), XSTAL FIELD √
- \+ CORRELATION / CONFIGURATION INTERACTION √
- \+ SHAKE-UP/SHAKE-OFF/e^--HOLE √
- \+ SCREENING / NON-SCREENING: CONFIGURATION INTERACTION √
- \+ VIBRATIONAL EXCITATIONS √
- \+ RESONANT PHOTOEMISSION ($h\nu \approx E_{b,n'l'}$) √

REALLY ALL AT ONCE, BUT SUM RULES + THEORY HELP

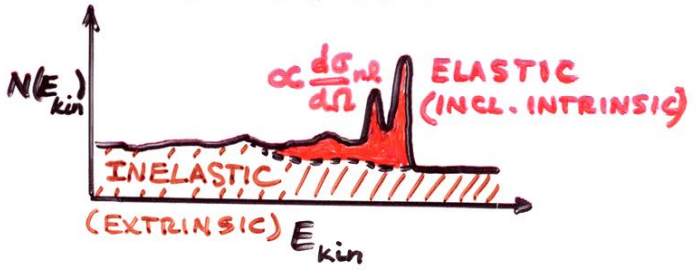

Outline—Here to end of quarter

- Core-level chemical shifts: Koopmans', relaxation, the potential model
- Various other final state effects providing information in core-level spectra
- Photoelectron diffraction, extended x-ray absorption fine structure (EXAFS, XAFS)
- Photoelectron spectroscopy at realistic pressures in the multi-Torr range
- Photoelectron microscopy: adding lateral spatial resolution in 2 dimensions
- Valence-band spectra: low-energy UPS limit and high-energy XPS limit

CALCULATION OF PHOTOELECTRON INTENSITIES—THE 3-STEP MODEL

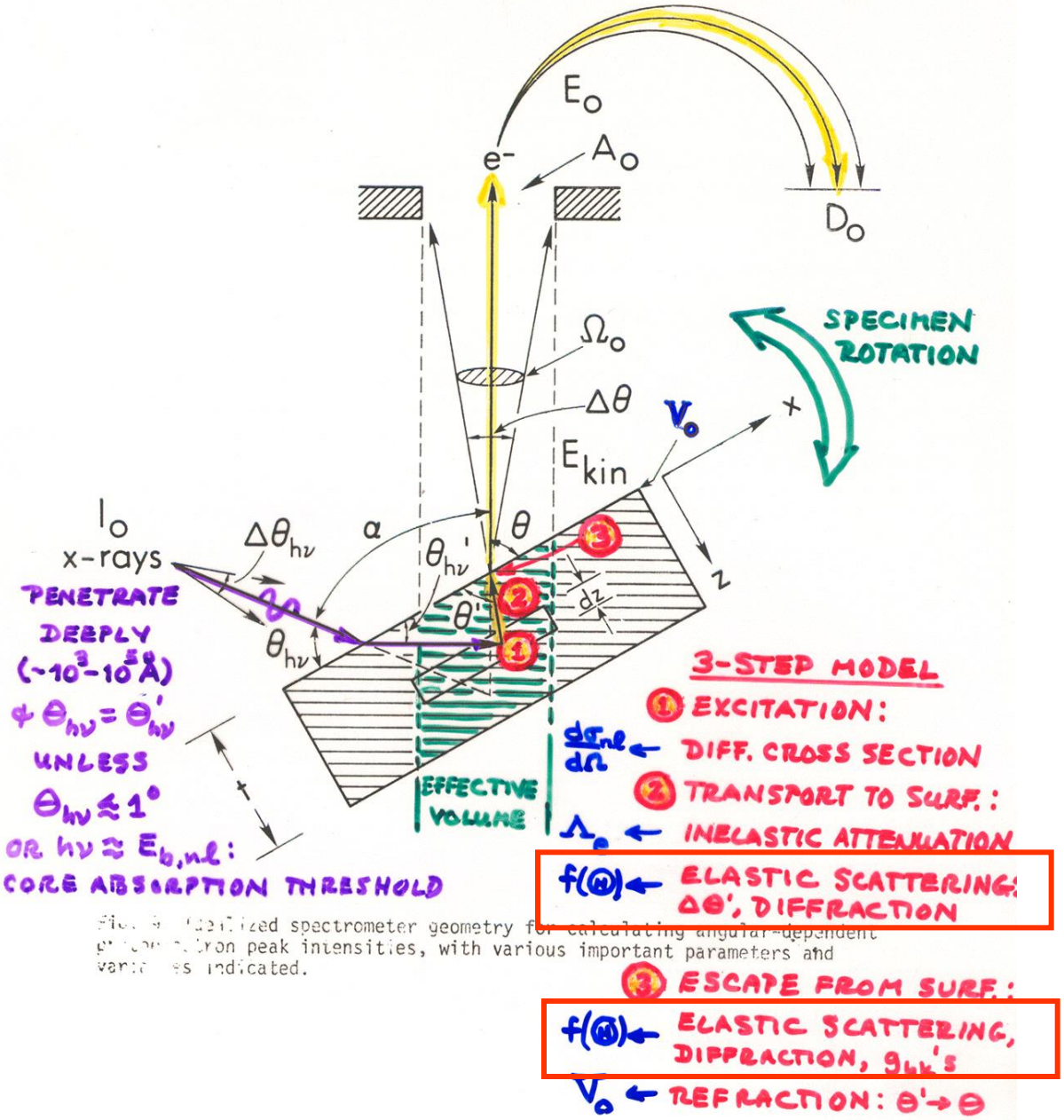

Fig. 4. Idealized spectrometer geometry for calculating angular-dependent photoelectron peak intensities, with various important parameters and variables indicated.

Photoelectron diffraction: A Simple Picture

FORWARD SCATT. = "OTH ORDER" → Bond & Low-Index Directions

HIGHER ORDERS → Bond Lengths & Atomic Positions

→Holographic fringes

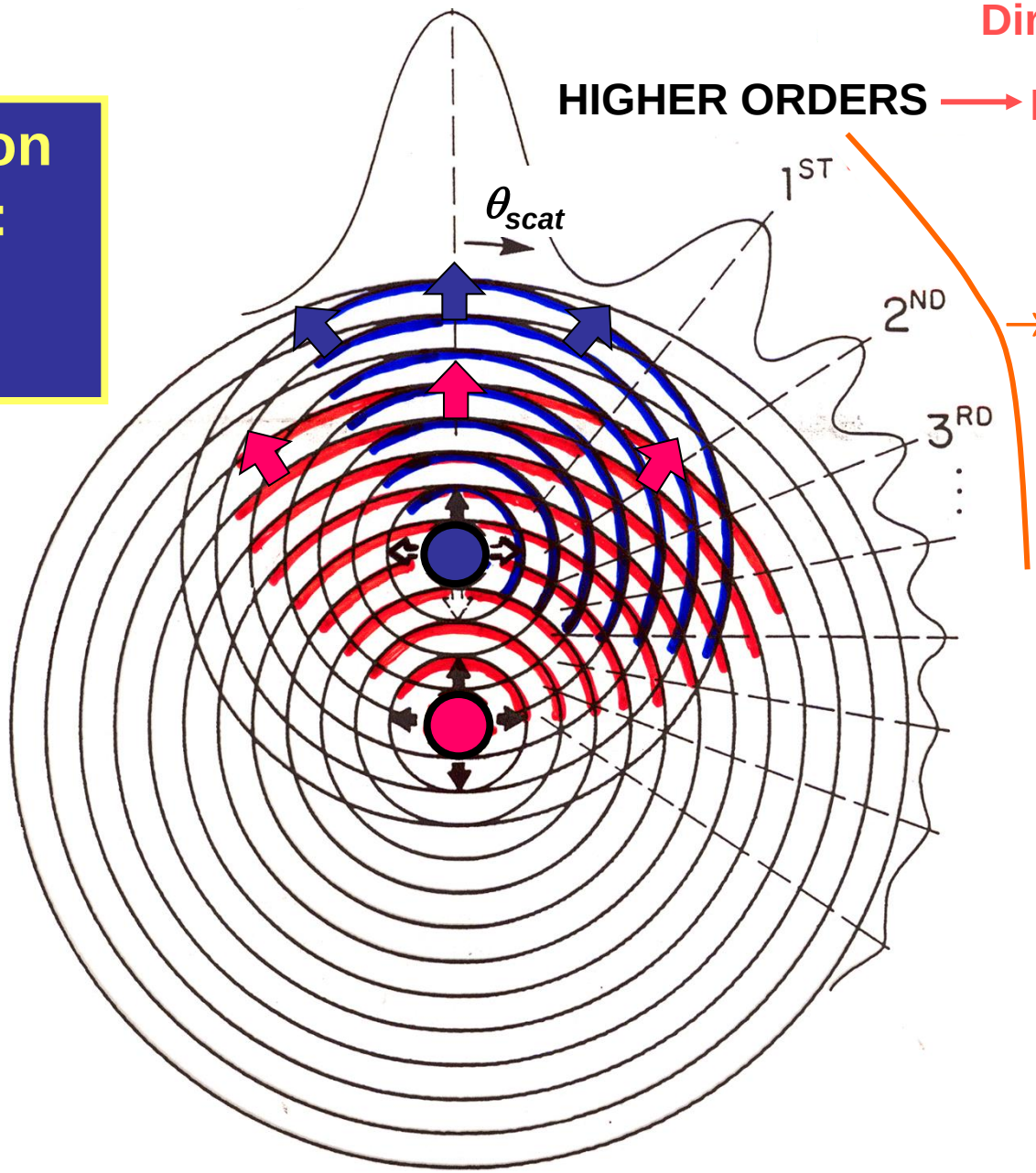

PHOTOELECTRON DIFFRACTION AND HOLOGRAPHY

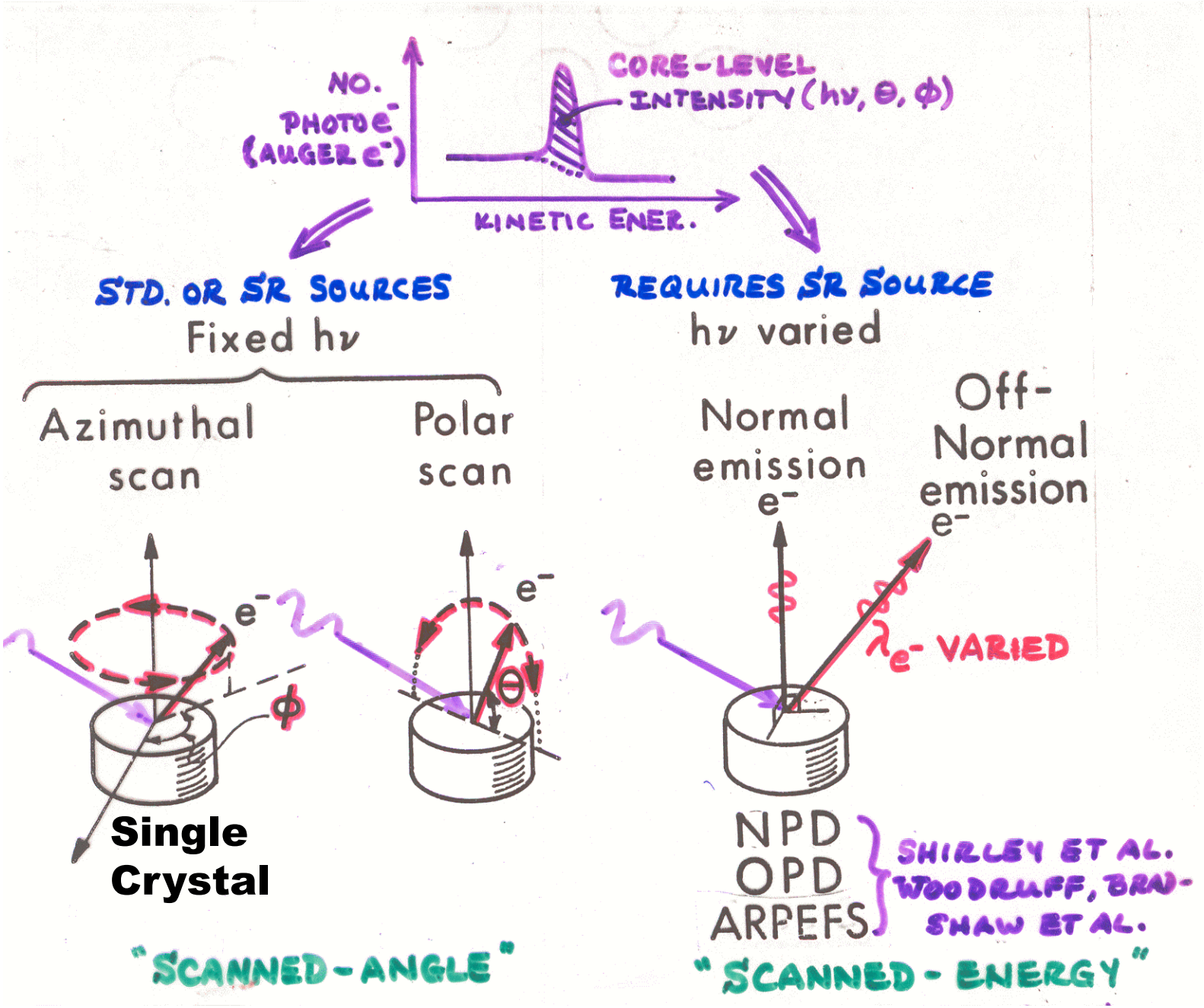

Scanned-angle photoelectron diffraction: Ge(111)

Ge 3d emission from Ge(111)
At 1458 eV

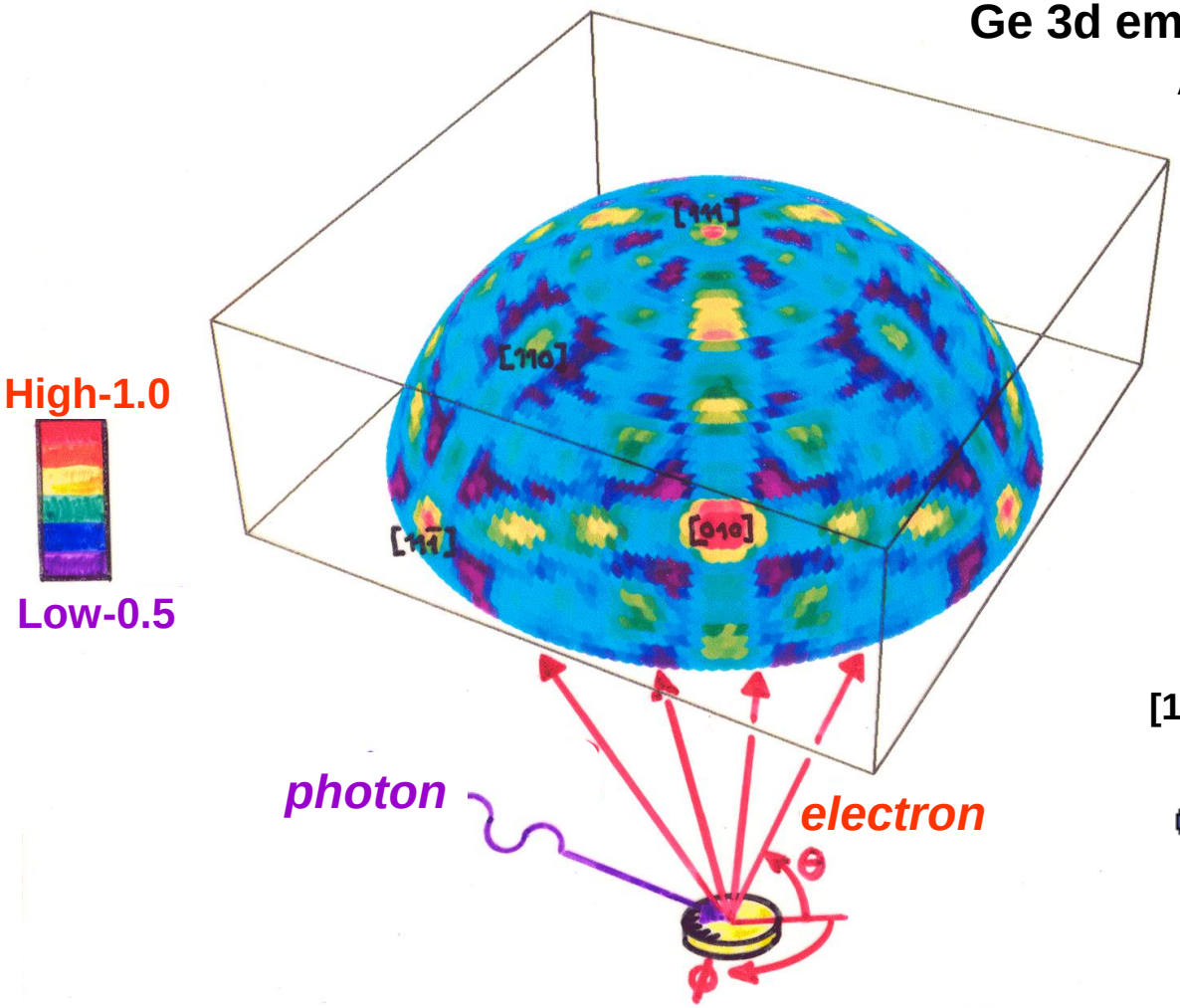

The inside view

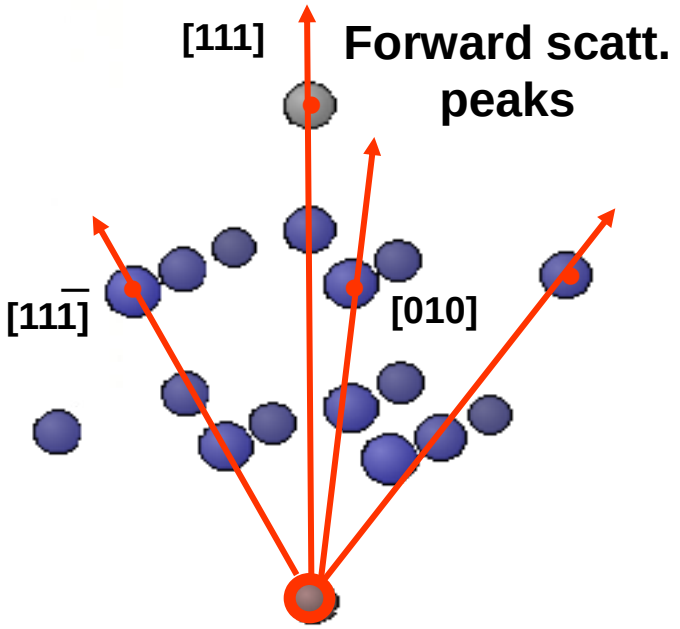

Tran et al.
Surf. Sci.
281, 270 (1993)

Photoelectron Intensities From Different Surfaces
(Stereographic Projection)

Ni(001):Ni 2p at 636 eV

fcc
(001)

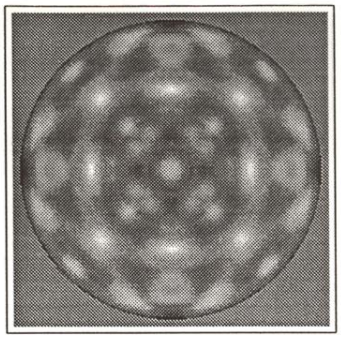

THEVUTHASAN ET AL.

Ru(0001):Ru 3d at 1206 eV

hcp
(0001)

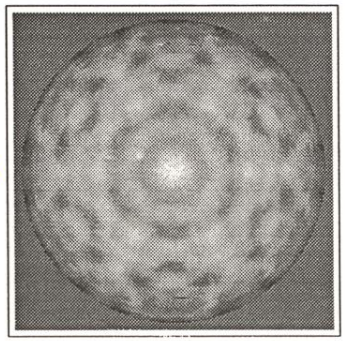

THEVUTHASAN ET AL.

HOPG: Graphite (0001): C 1s at 946 eV

textured

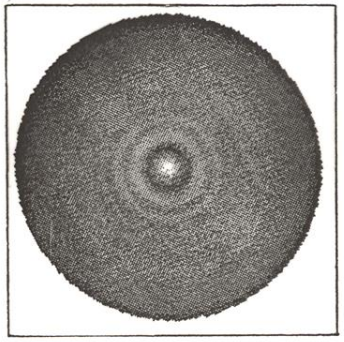

OSTERWALDER ET AL.

Fingerprint identification of short-range atomic structure and symmetry

SCANNED-ENERGY PHOTOELECTRON DIFF.

$(\sqrt{3}\times\sqrt{3})$ AL ON Si(111)

* 41 diffraction curves χ taken from Al 2p
* $\theta = 0 \sim 70°$, $\varphi = 0 \sim 60°$

} ~1100 DATA POINTS

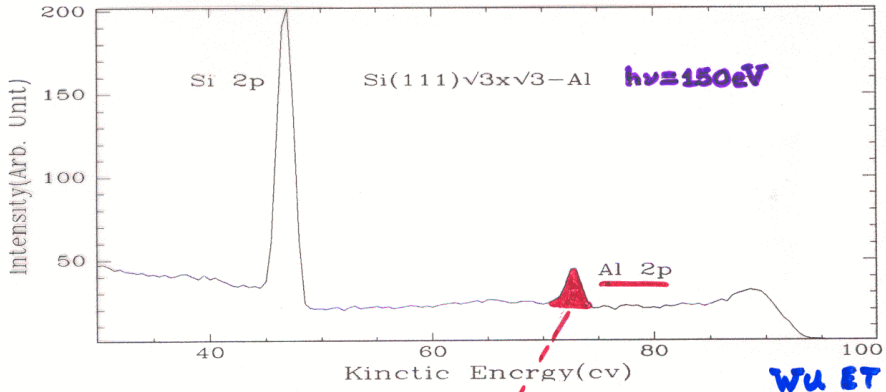

WU ET AL.,
P.R.L. 71, 251('93)
P.R.B 51, 14549('95)

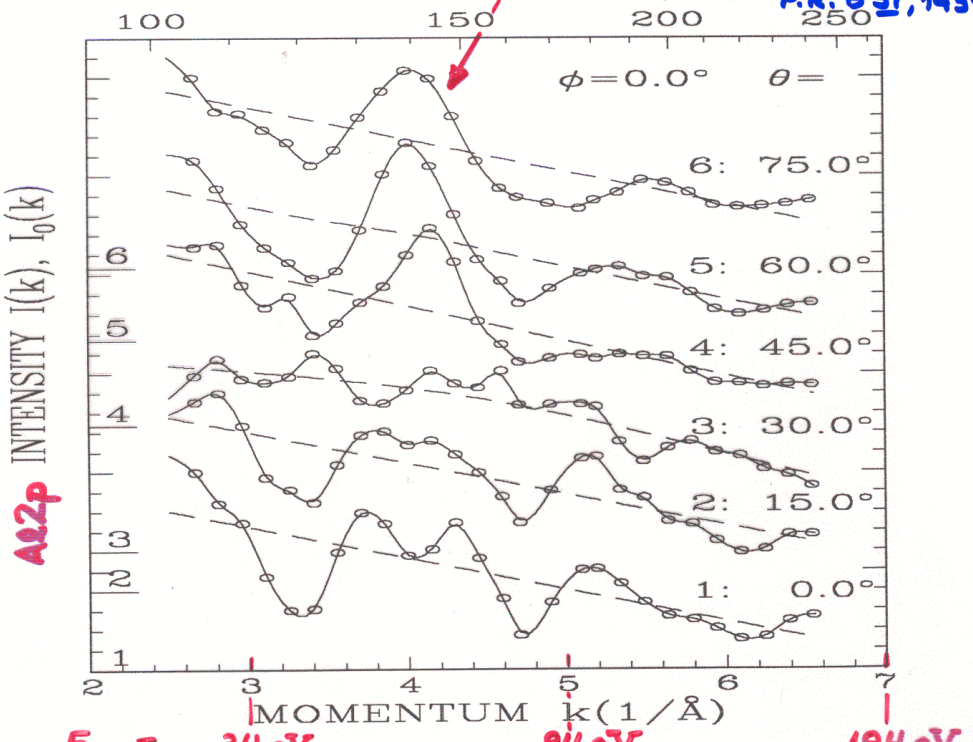

EFFECTS OF ELASTIC SCATTERING ON ANGULAR DISTRIBUTIONS: SINGLE-CRYSTAL SAMPLE→→ *PHOTOELECTRON DIFFRACTION And PHOTOELECTRON HOLOGRAPHY*

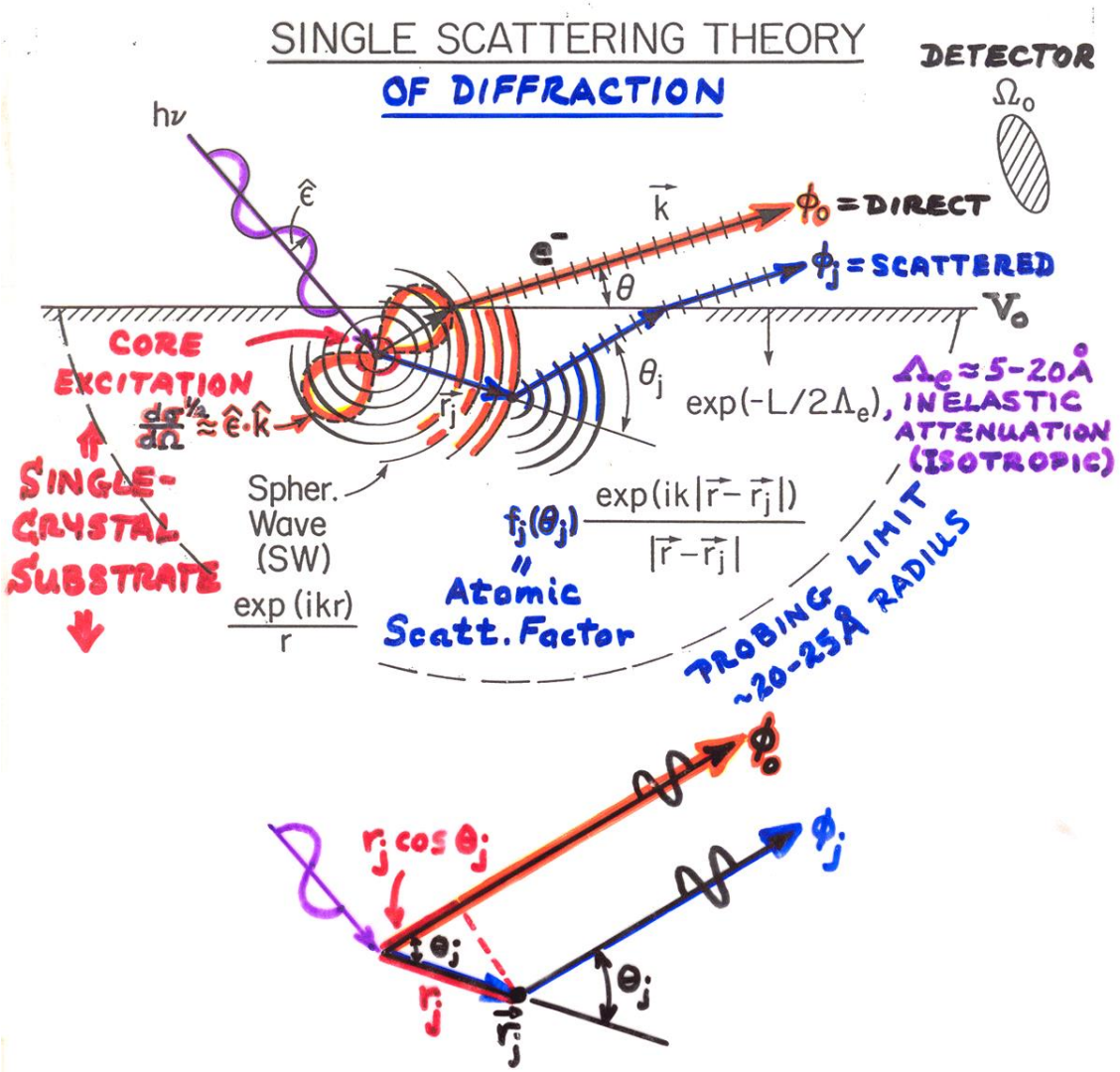

⇒ ALL BOND DISTANCE INFORMATION IN:

PATH LENGTH DIFFERENCE = $r_j(1-\cos\theta_j)$

∴ PHASE DIFFERENCE = $kr_j(1-\cos\theta_j)$

$= kr_j - \vec{k}\cdot\vec{r}_j$

Photoelectron diffraction: Simple single-scattering theory for s-subshell emission

SINGLE SCATTERING THEORY

(Orders, Fadley, P.R.B 27, 781('83))

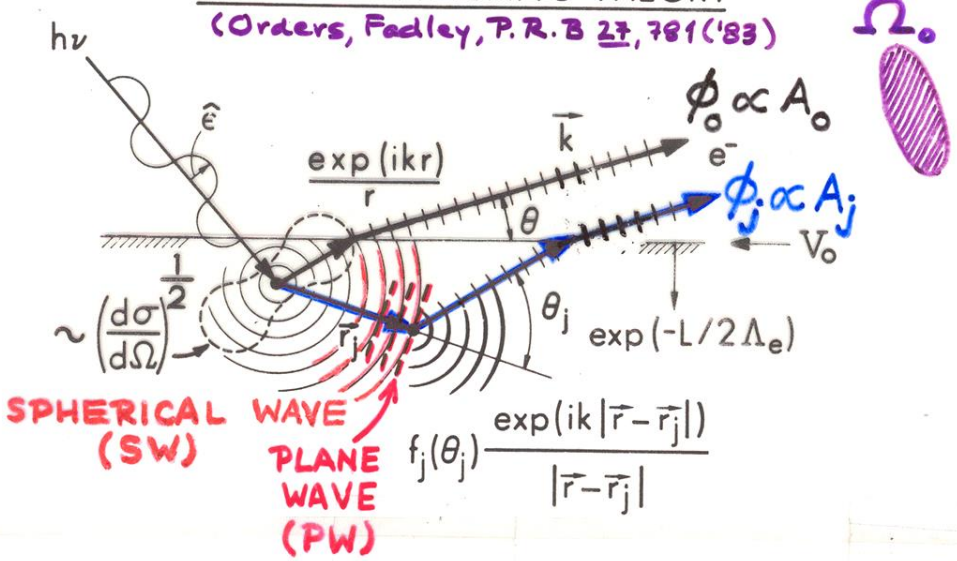

$$\chi(E \text{ or } \vec{k}) \propto \sum_{j\,(\text{CLUSTER})} \frac{F_j(k)}{F_0} \cos\left[\underbrace{kr_j(1-\cos\theta_j)}_{\text{PATH LENGTH DIFFERENCE (P.L.D.)}} + \underbrace{\Psi_j(\theta_j,k)}_{\text{SCATTERING PHASE SHIFT}}\right]$$

Ω_0

$$F_j(k) = (\hat{\varepsilon}\cdot\hat{r}_j)\frac{|f_j(\theta_j,k)|}{r_j} W_j(\theta_j,k) \exp(-L_j/2\Lambda_e)$$

ELASTIC e⁻–ATOM SCATTERING; DEBYE-WALLER; INELASTIC e⁻–e⁻ SCATTERING

= amplitude of scattered wave

$$F_0 = (\hat{\varepsilon}\cdot\hat{k})\exp(-L_0/2\Lambda_e)$$

= amplitude of direct wave

∴ FOURIER TRANSFORM OF $\chi(k) \Rightarrow$ PEAKS AT ~ P.L.D. $= r_j(1-\cos\theta_j)$

FROM SINGLE-SCATTERING THEORY:

(E.G., P.R.B 22, 6085 ('80); P.R.B 27, 781 ('83))

$$I(\vec{k}) \propto \left|\phi_0 + \sum_j \phi_j\right|^2, \quad \sum_j \text{ ON FINITE CLUSTER},$$

$$\propto |\phi_0|^2 + \sum_j (\phi_0^* \phi_j + \phi_0 \phi_j^*) + \sum_j \sum_{j'} \phi_j^* \phi_{j'}$$

IF $\phi_j \phi_{j'}^*$ SMALL W.R.T $\phi_0^* \phi_j + \phi_0 \phi_j^*$, A NECESSARY CONDITION FOR SIMPLE HOLOGRAPHY:

$$I(\vec{k}) \propto \underbrace{F_0^2}_{\| \; I_0} + 2F_0 \sum_j |F_j(\theta_j)| \cos\left[\underbrace{kr_j(1-\cos\theta_j)}_{\text{PATH LENGTH DIFFERENCE}} + \underbrace{\psi_j(\theta_j, k)}_{\text{SCATTERING PHASE}}\right]$$

$$\chi(\vec{k}) = \frac{I(\vec{k}) - I_0}{I_0^{1/2}} \propto \left\{\sum_j |F_j(\theta_j)| \cos\left[kr_j(1-\cos\theta_j) + \psi_j(\theta_j, k)\right]\right\}$$

WITH: $F_0 = (\hat{\varepsilon}\cdot\hat{k}) \exp(-L_0/2\Lambda_e)$

$= \text{amplitude of direct wave} = I_0^{1/2}$

$$|F_j(\theta_j)| = (\hat{\varepsilon}\cdot\hat{r}_j)\frac{|f_j(\theta_j)|}{r_j} W_j(\theta_j) \exp(-L_j/2\Lambda_e)$$

$= \text{amplitude of scattered wave}$

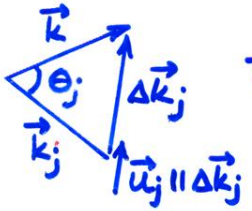

$$W_j = \exp(-\Delta k_j^2 \overline{u_j^2})$$

$$= \exp(-2k^2(1-\cos\theta_j)\overline{u_j^2})$$

LIKE EXAFS/SEXAFS, BUT THERE:

- ADD CENTRAL ATOM PHASE SHIFT δ_1
- $\psi_j \Rightarrow \pi$ FOR ALL SCATTERERS
- cos $\Rightarrow$ sin IN ANGLE INTEGRATION
- $\hat{\varepsilon}\cdot\hat{r}_j/r_j \Rightarrow \hat{\varepsilon}\cdot\hat{r}_j/r_j^2$ IN OUT/BACK PATHS

CALCULATION OF e^--ATOM SCATTERING FACTORS:

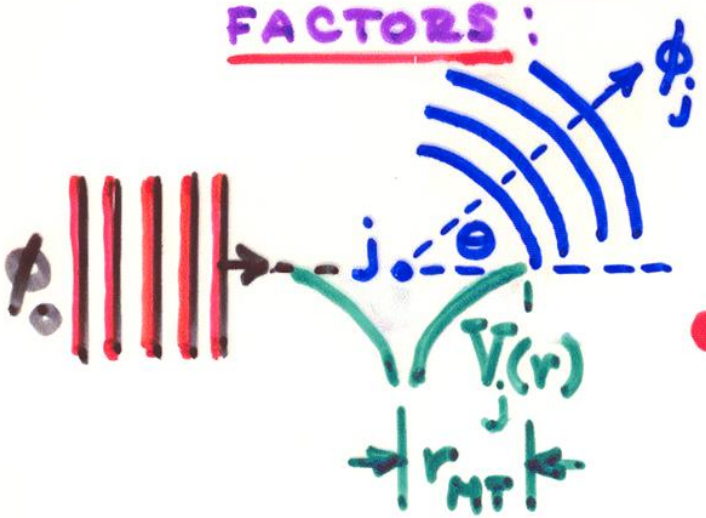

PLANE-WAVE SCATTERING: PARTIAL-WAVE METHOD†

PHASE SHIFT

$$f_j^{PW}(\theta) = \frac{1}{k} \sum_{\ell=0}^{\ell_{max}} (2\ell+1) e^{i\delta_\ell} \sin\delta_\ell \, P_\ell(\cos\theta)$$

$$\ell_{max} \lesssim k r_{MT}$$

† ANY TEXTBOOK ON SCATTERING

$$L_{max} = r_{MT} \times p = \hbar k r_{MT} \approx \hbar \ell_{max}$$

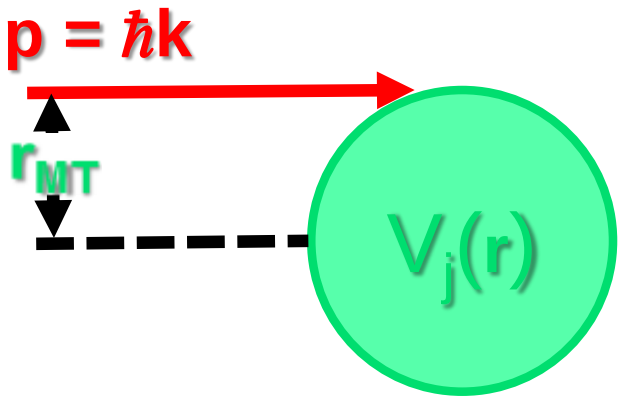

ENERGY DEPENDENCE OF ELECTRON ELASTIC SCATTERING

$f(\theta) = |f(\theta)| e^{i\Psi(\theta)}$

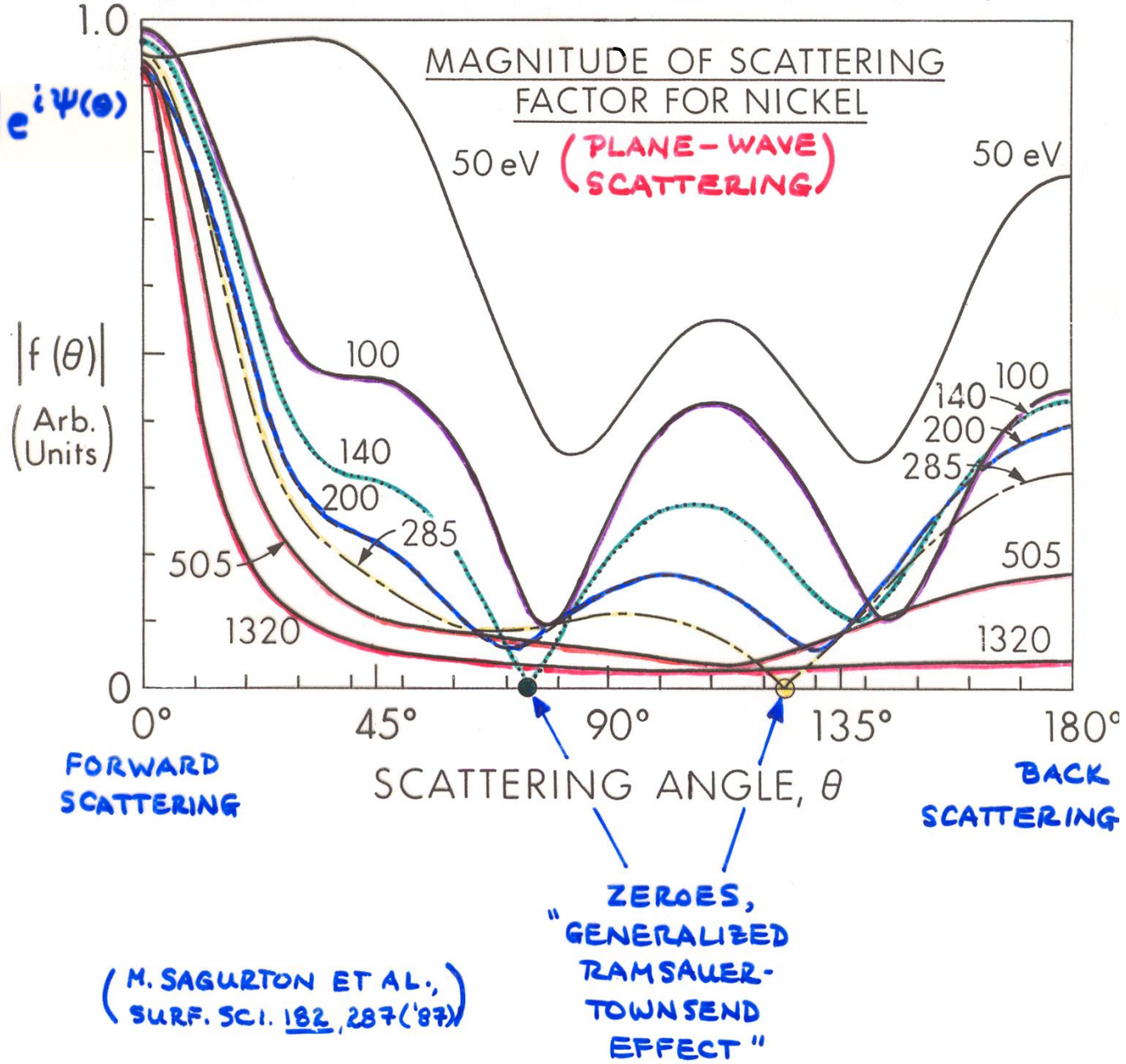

ENERGY DEPENDENCE OF ELECTRON ELASTIC SCATTERING

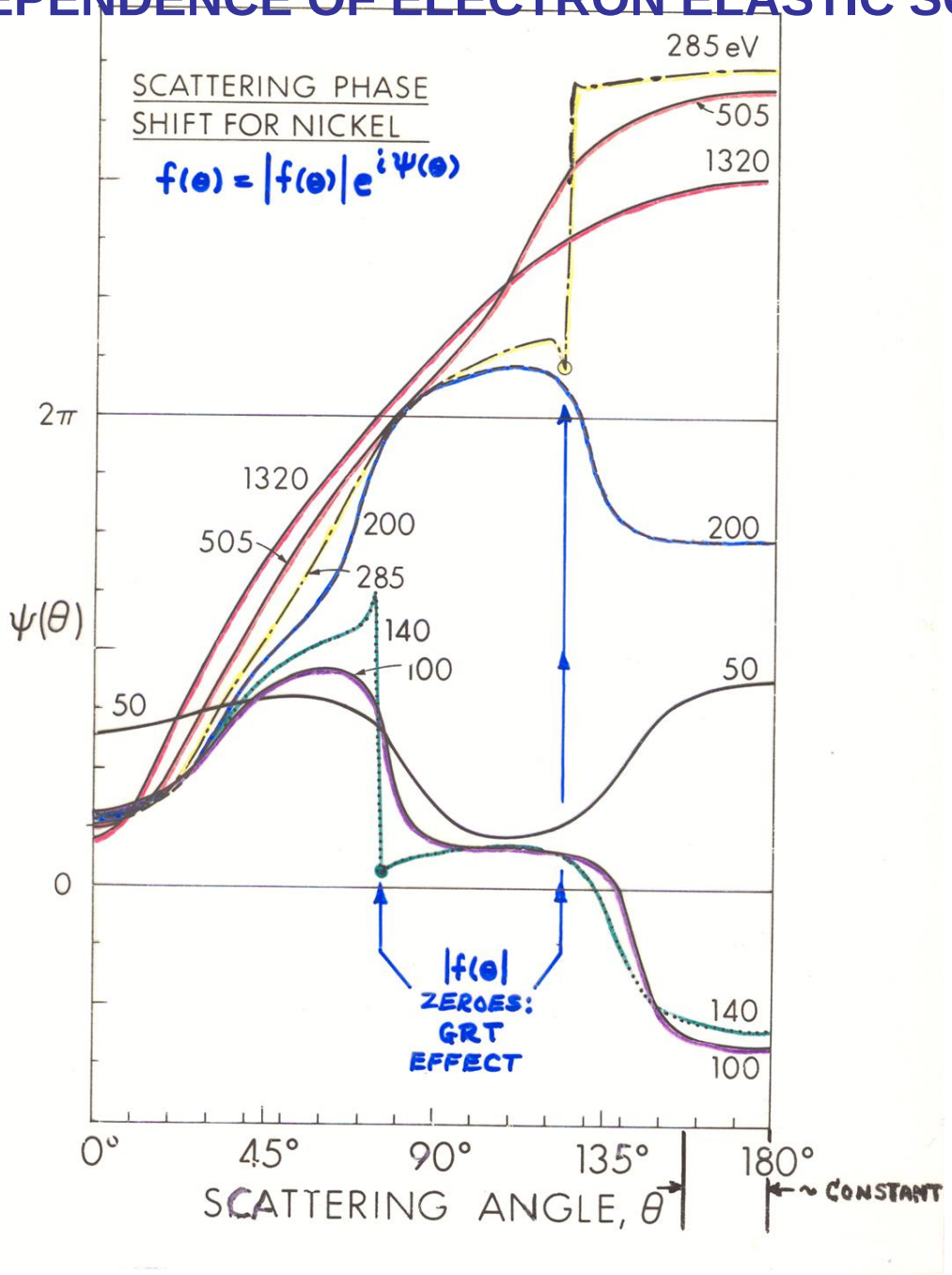

Vibrational effects on diffraction: The Debye Waller factor

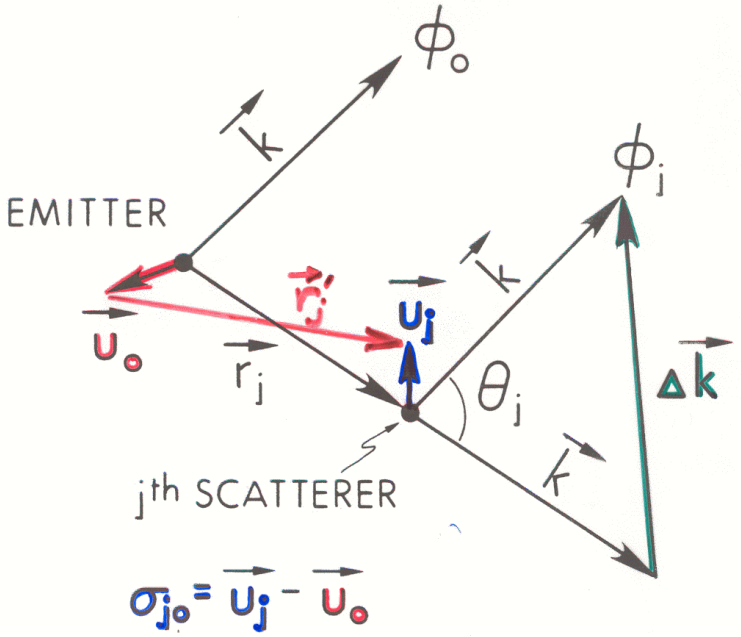

- DW FACTOR $= e^{-\frac{1}{2}\overline{(\Delta\vec{k}\cdot\vec{\sigma}_{jo})^2}} = e^{-\frac{1}{2}\Delta k^2 \overline{\sigma_{jo,II}^2}}$
- $\vec{u}_j, \vec{u}_o$ UNCORRELATED:

  $DW = e^{-\frac{1}{2}\overline{(\Delta\vec{k}\cdot\vec{u}_j)^2}}\, e^{-\frac{1}{2}\overline{(\Delta\vec{k}\cdot\vec{u}_o)^2}}$
- $\vec{u}_j \approx \vec{u}_o$ IN DISTRIBUTION:

  $DW = e^{-\overline{(\Delta\vec{k}\cdot\vec{u}_j)^2}}$
- $\vec{u}_j$ ISOTROPIC:

  $DW = e^{-\Delta k^2 \overline{u_j^2}} = e^{-2k^2(1-\cos\theta_j)\overline{u_j^2}}$ ← USUAL LEVEL

DECREASING ACCURACY

+ CORRELATED?

No effect in forward scattering: $\Delta\vec{k} = 0$

Maximum effect in backward scattering

Table 1 Debye temperature and thermal conductivity[a]

Li	Be											B	C	N	O	F	Ne
344	1440												2230				75
0.85	2.00											0.27	1.29				
Na	Mg											Al	Si	P	S	Cl	Ar
158	400	Low temperature limit of θ, in Kelvin										428	645				92
1.41	1.56	Thermal conductivity at 300 K, in W $cm^{-1}K^{-1}$										2.37	1.48				
K	Ca	Sc	Ti	V	Cr	Mn	Fe	Co	Ni	Cu	Zn	Ga	Ge	As	Se	Br	Kr
91	230	360.	420	380	630	410	470	445	450	343	327	320	374	282	90		72
1.02		0.16	0.22	0.31	0.94	0.08	0.80	1.00	0.91	4.01	1.16	0.41	0.60	0.50	0.02		
Rb	Sr	Y	Zr	Nb	Mo	Tc	Ru	Rh	Pd	Ag	Cd	In	Sn $_w$	Sb	Te	I	Xe
56	147	280	291	275	450		600	480	274	225	209	108	200	211	153		64
0.58		0.17	0.23	0.54	1.38	0.51	1.17	1.50	0.72	4.29	0.97	0.82	0.67	0.24	0.02		
Cs	Ba	La β	Hf	Ta	W	Re	Os	Ir	Pt	Au	Hg	Tl	Pb	Bi	Po	At	Rn
38	110	142	252	240	400	430	500	420	240	165	71.9	78.5	105	119			
0.36		0.14	0.23	0.58	1.74	0.48	0.88	1.47	0.72	3.17		0.46	0.35	0.08			
Fr	Ra	Ac															

Ce	Pr	Nd	Pm	Sm	Eu	Gd	Tb	Dy	Ho	Er	Tm	Yb	Lu
						200		210				120	210
0.11	0.12	0.16		0.13		0.11	0.11	0.11	0.16	0.14	0.17	0.35	0.16

Th	Pa	U	Np	Pu	Am	Cm	Bk	Cf	Es	Fm	Md	No	Lr
163		207											
0.54		0.28	0.06	0.07									

[a] Most of the θ values were supplied by N. Pearlman; references are given the *A.I.P. Handbook*, 3rd ed; the thermal conductivity values are from R. W. Powell and Y. S. Touloukian, Science **181**, 999 (1973).

Determining the orientation of an adsorbed molecule from photoelectron diffraction at about 1 keV energy

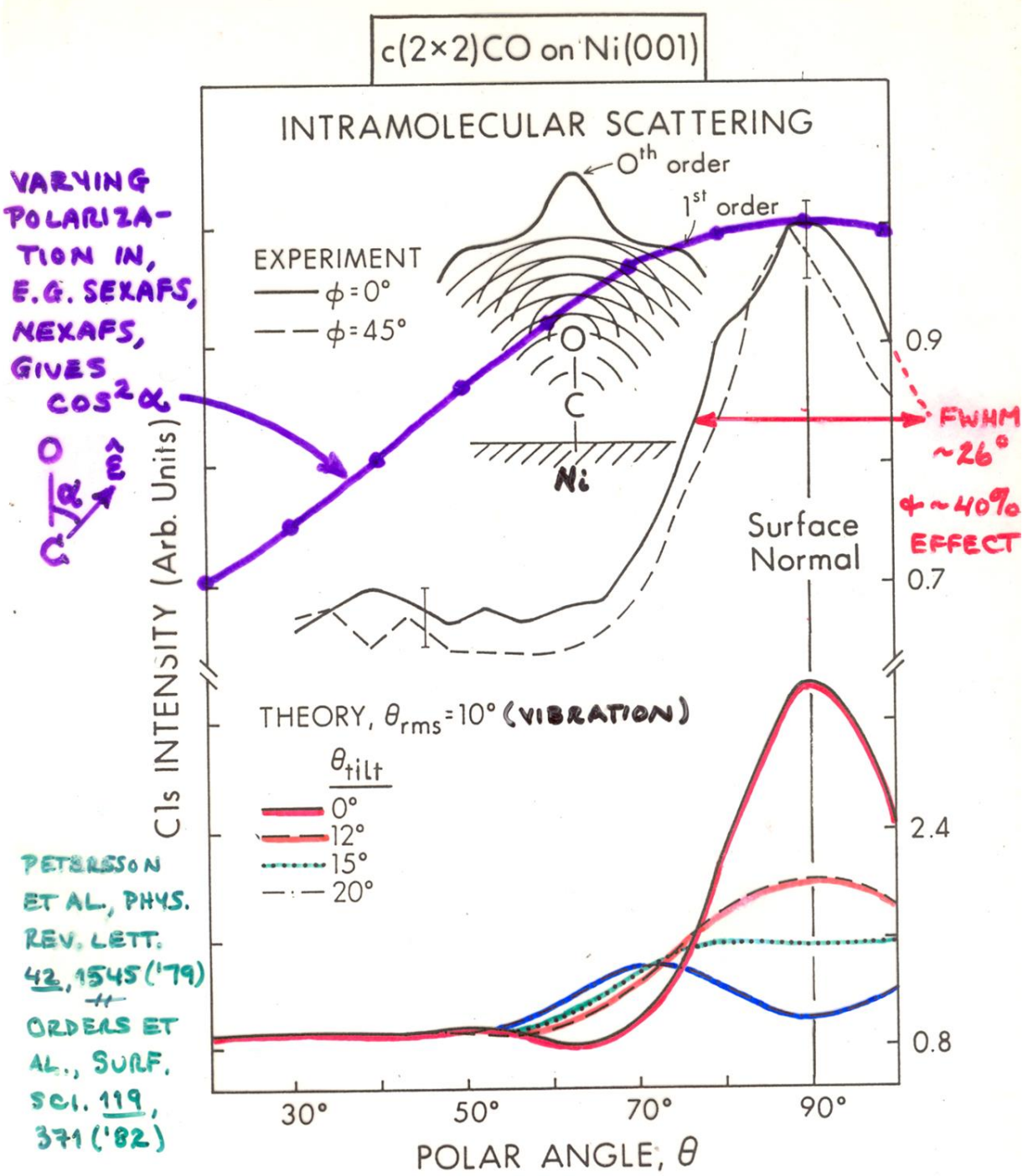

TEMPERATURE-DEPENDENT ADSORBATE ORIENTATION

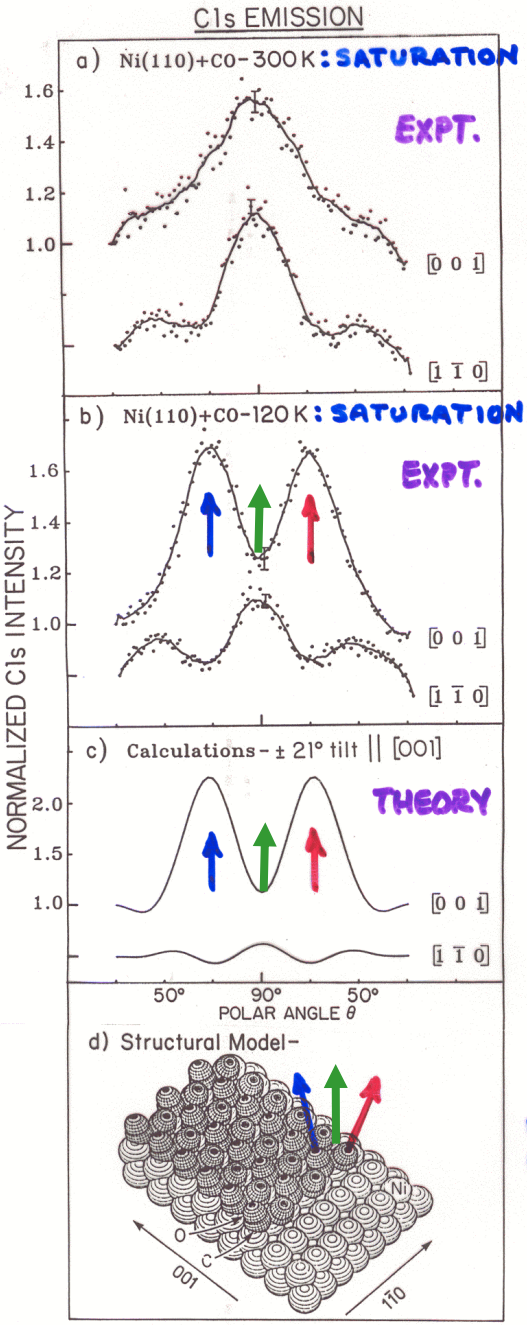

WESNER, BONZEL
COENEN, P.R.L.
60, 1045 ('88)

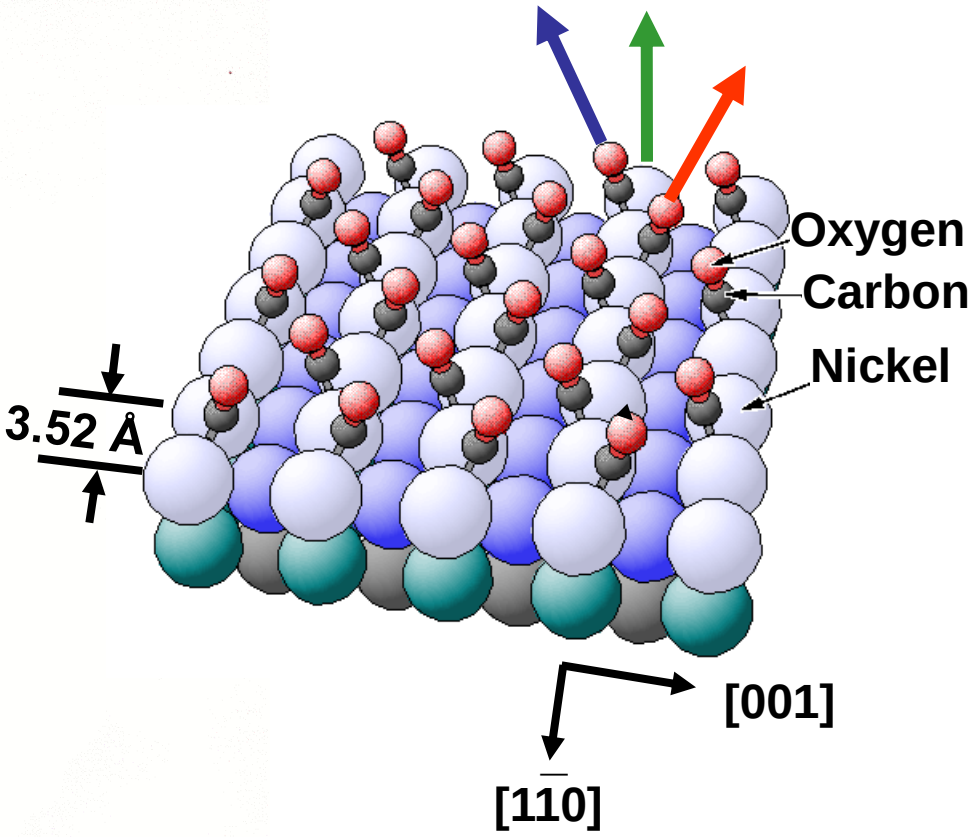

ORIENTATION OF A HIGHLY TILTED MOLEC. ON SURFACE

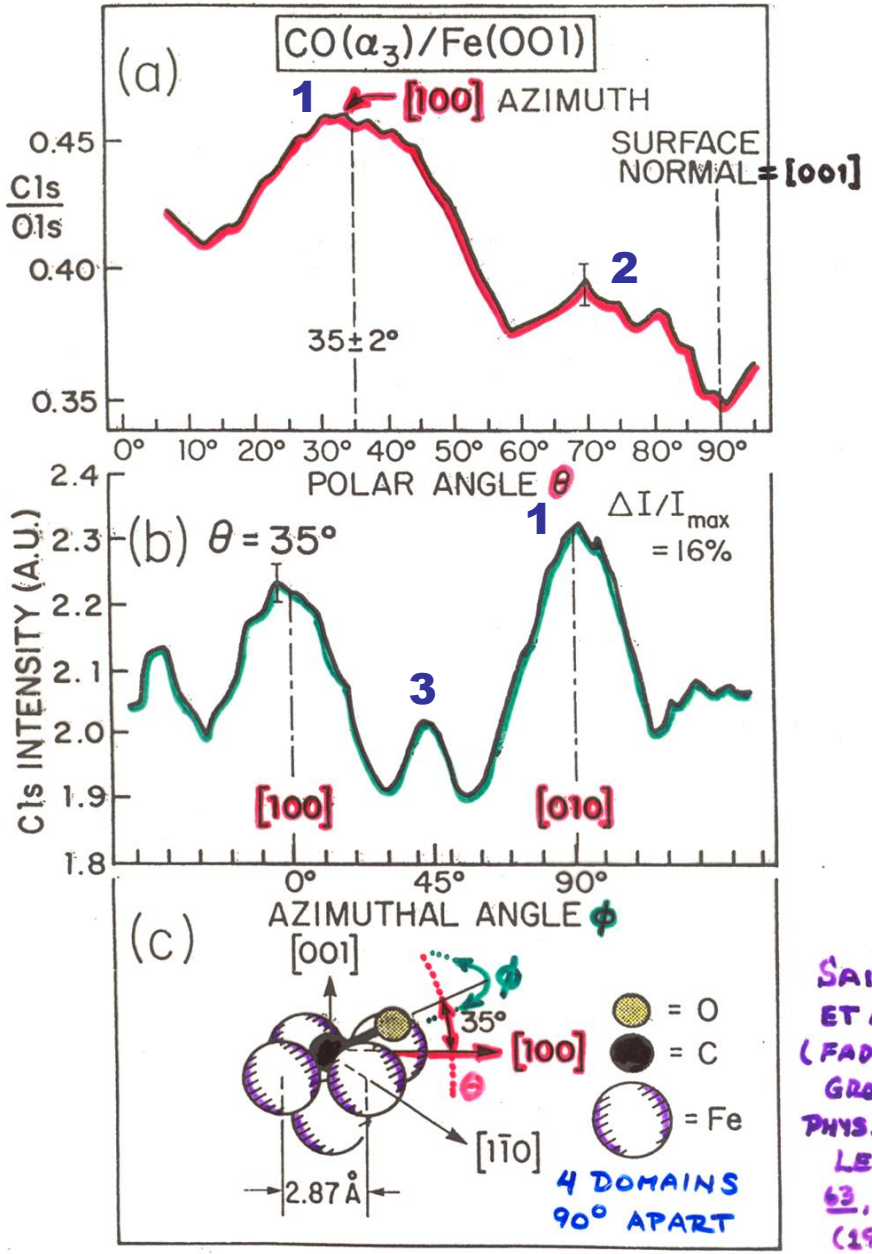

SAIKI ET AL. (FADLEY GROUP) PHYS. REV. LETT. 53, 283 (1984)

CALCULATED 2π INTENSITY

$CO(\alpha_3)/Fe(001)$

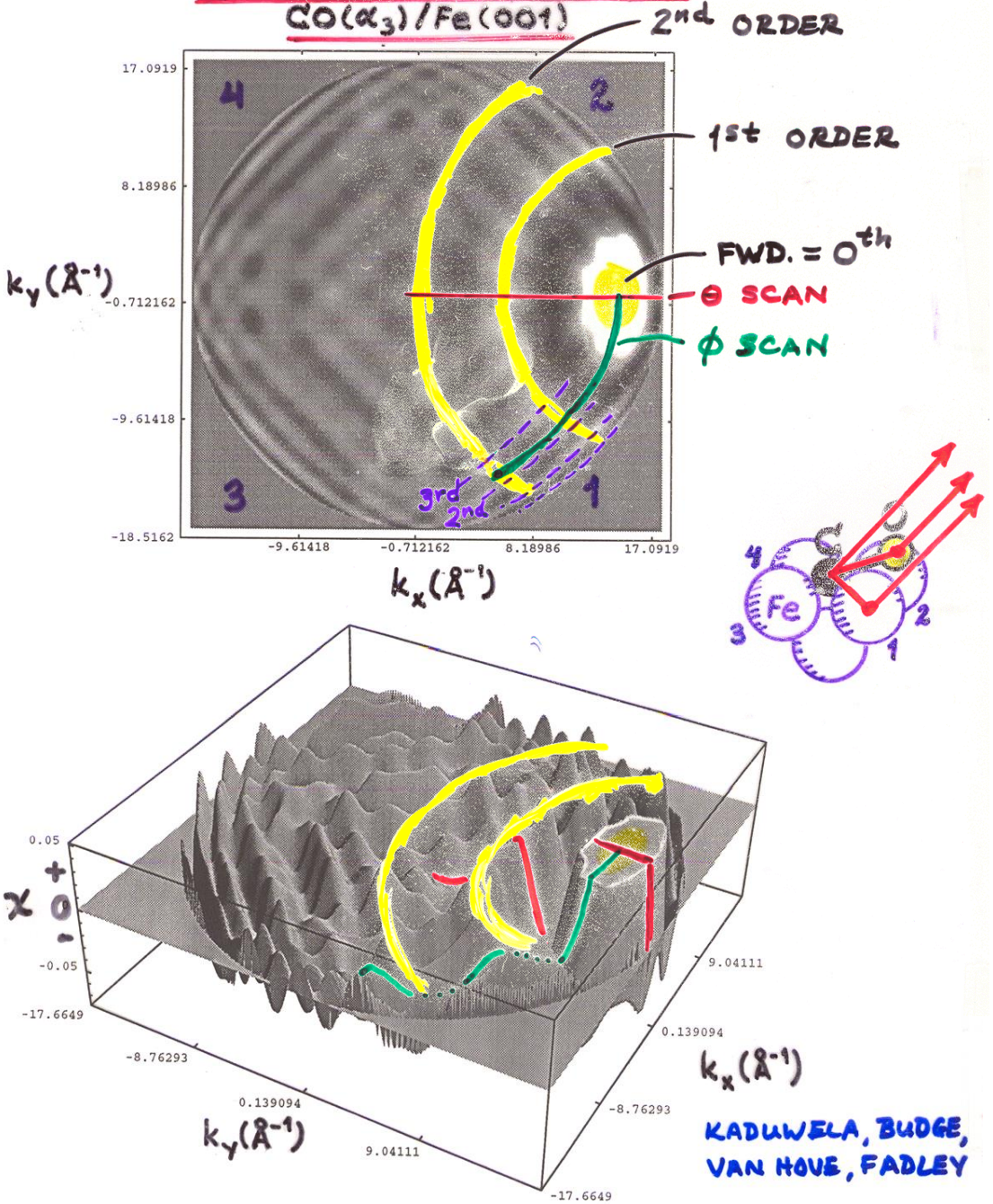

KADUWELA, BUDGE, VAN HOVE, FADLEY

Online calculation of photoelectron diffraction patterns:

EDAC output for CO/Fe(001)

Click on the figure to download data.

http://garciadeabajos-group.icfo.es/widgets/edac/index.html

Oxygen 1st order diff. ring

7 atoms:

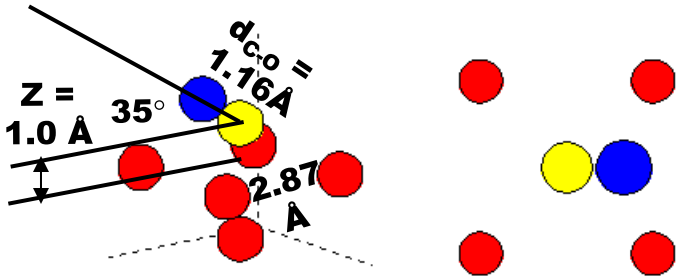

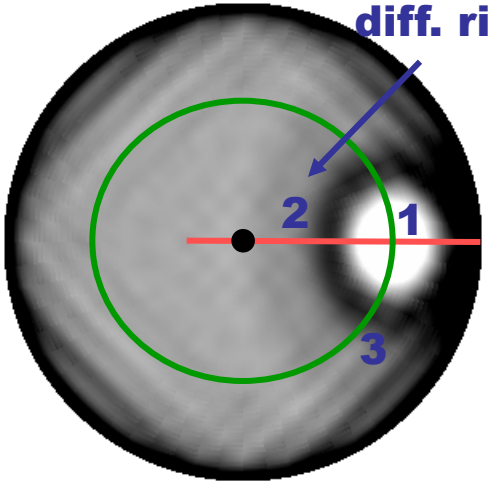

Left: representation of the cluster rocking around a line parallel to the z direction and passing by the **emitter (yellow atom)**. The dashed lines stand for the xyz axes. **Right:** top view of the cluster, where the x/y direction (not plotted) runs along the horizontal/vertical screen direction. Different atomic species have been assigned the colors O, Fe.

Polar scan of photoemission intensity (logarithmic scale). White/black regions correspond to high/low intensity. The orientation is the same as in the top-view of the cluster. The distance to the center of the figure is proportional to the polar angle θ. The polar angle range is (0.0, 89.0) (in degrees).

Parameters used in the calculation:

N=7 atoms
Iteration order=4
l_{max}=25
V_0=10.5 eV
Photoelecton energy=1202 eV
p-polarized light
z_0=1.435 Å
Recursion iteration method

X 4 domains rotated by 90°

User friendly web-based program for PD calculations by Javier Garcia de Abajo, DIPC, Donostia-San Sebastian, Spain

Electron Diffraction in Atomic Clusters

for Core Level Photoelectron Diffraction Simulations

Created by F. Javier García de Abajo (CSIC and DIPC, San Sebastian, Spain)
in collaboration with M. A. Van Hove and C. S. Fadley (LBNL, Berkeley, and UCD, Davis, California)

This site allows performing on-line photoelectron diffraction calculations. Multiple scattering (MS) of the photoelectron is carried out for a cluster representing a solid or molecule. Select the corresponding parameters and click on the "Calculate" button below to perform the actual calculation and to produce a plot of the calculated data (a separate window pops out to display it). A numerical data table can be downloaded by clicking on the resulting plot. Click on the different parameter names in blue to see fuller explanations. Click on the "Preview Cluster" button to display the currently selected atomic cluster (but without performing a MS calculation) or the button "Download Cluster" to download the currently selected cluster. Notice that the scattering phase shifts and excitation radial matrix elements are calculated internally for each cluster configuration, so that the user does not have to provide them. Please, read the terms of use and the restrictions on input parameters before using this site for the first time.

Terms and conditions of use

Terms of use Restrictions on input parameters Password: ********

A password is only necessary for large computation times (click here for more details). Leave it blank otherwise.

Title (optional): CO/Fe(001)

Cluster definition

The cluster and the list of emitters are defined by a list of commands with the following format (click here or on the items of this list for further details):

atom symbol *x y z* layer symbol *x y z a b* α_1 α_2

surface symbol *x y z a* type emitter *x y z*

Fill in the text box with these commands according to the cluster specifications that you need. Some examples are provided by clicking here (you may cut and paste them to this page and modify them further).

```
atom O 0.95 0 1.66
atom C 0 0 1.0
surface Fe 1.435 1.435 0 2.87 bcc100
emitter 0 0 1.0
end
```

The cluster consists of a maximum of 7 atoms. (Warning: a finite number of atoms generally introduces symmetry breaking.)

The size of the cluster is determined by the distance d_{max} = 10 Å and the reference point x_0 = 0 Å, y_0 = 0 Å, z_0 = 0 Å.

See cluster shape for more details.

Plot cluster on output? (•) Yes ( ) No

Cluster shape: (•) Parabolic ( ) Spherical

Preview Cluster* Download Cluster*

Geometry of beam and analyzer

Incoming beam parameters (see figure)

Polar angle θ_i = 0 degrees

Azimuthal angle φ_i = 0 degrees

Polarization:
(•) p-polarization
( ) s-polarization
( ) RCP
( ) LCP

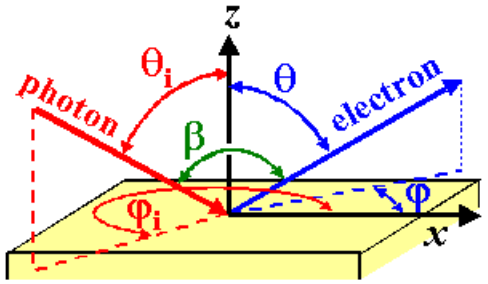

Schematic representation of the geometry

Mobility of cluster beam, and sample (click here for details):
(•) Only the sample moves with constant β = 90 degrees
( ) Only the analyzer moves
( ) Both the sample and the analyzer move

Energy and angle scanning parameters (see figure above)

The following entries will select the range of photoelectron energies and angles of emission.

Energy scans for a given emission angle can be chosen by selecting more than one energy of emission and only one polar angle and one azimuthal angle (the value of each angle is then taken as the lower limit of the selected angular range, and the value of the upper limits are disregarded). In this case, the output is a 1D plot with the photoelectron intensity as a function of photoelectron energy.

Electron energy range: 1 equally-spaced value(s) of the electron energy from 1202 eV to 1202 eV

Polar angle: 50 equally-spaced value(s) of the polar angle θ from 0 degrees to 89 degrees

Azimuthal angle: 61 equally-spaced value(s) of the azimuthal angle φ from 0 degrees to 360 degrees

Type of 2D angular representation: ○ Linear scale ◉ Logarithmic scale

Type of azimuthal of polar angular representation: ◉ Cartesian ○ Polar

Photoelectron detector half-width acceptance angle = 0 degrees. The photoelectron intensities are angle-averaged over a cone with half aperture given by this parameter.

Multiple scattering parameters

Internal code parameters

Maximum orbital quantum number l_{max} = 25

Scattering order = 4

Iteration method: ○ Jacobi (regular MS) ◉ Recursion

Additional solid parameters

Inner potential V_0 = 12.4 eV

8.1 eV from band struct. + work function = 4.3 eV = 12.4 eV

Electronic edge z_0 = 1.435 Å

Inelastic mean free path: either choose a fixed value = 17.8 Å

or (if that last entry is <0) use the TPP-2M formula

with parameters ρ = 8.91 g/cm^3, N_v = 10, E_p = 35.45 eV, and E_g = 0 eV

Temperature (K) = 300 and Debye emperature (K) = 450

Table 4 Density and atomic concentration

The data are given at atmospheric pressure and room temperature, or at the stated temperature in deg K. (Crystal modifications as for Table 3.)

Atomic radius
= r_{MT}
= 0.5 n-n dist.

Average surface density = $\rho_S = (\rho_V)^{2/3}$

H 4K 0.088																	He 2K 0.205 (at 37 atm)
Li 78K 0.542 4.700 3.023	Be 1.82 12.1 2.22											B 2.47 13.0 -	C 3.516 17.6 1.54	N 20K 1.03	O	F 1.44	Ne 4K 1.51 4.36 3.16
Na 5K 1.013 2.652 3.659	Mg 1.74 4.30 3.20	← Density in g cm^{-3} (10^3kg m^{-3}) →										Al 2.70 6.02 2.86	Si 2.33 5.00 2.35	P	S	Cl 93K 2.03 2.02	Ar 4K 1.77 2.66 3.76
		← Concentration in 10^{22} cm^{-3} (10^{28} m^{-3}) →															
		← Nearest-neighbor distance, in Å (10^{-10}m) →															
K 5K 0.910 1.402 4.525	Ca 1.53 2.30 3.95	Sc 2.99 4.27 3.25	Ti 4.51 5.66 2.89	V 6.09 7.22 2.62	Cr 7.19 8.33 2.50	Mn 7.47 8.18 2.24	Fe 7.87 8.50 2.48	Co 8.9 8.97 2.50	Ni 8.91 9.14 2.49	Cu 8.93 8.45 2.56	Zn 7.13 6.55 2.66	Ga 5.91 5.10 2.44	Ge 5.32 4.42 2.45	As 5.77 4.65 3.16	Se 4.81 3.67 2.32	Br 123K 4.05 2.36	Kr 4K 3.09 2.17 4.00
Rb 5K 1.629 1.148 4.837	Sr 2.58 1.78 4.30	Y 4.48 3.02 3.55	Zr 6.51 4.29 3.17	Nb 8.58 5.56 2.86	Mo 10.22 6.42 2.72	Tc 11.50 7.04 2.71	Ru 12.36 7.36 2.65	Rh 12.42 7.26 2.69	Pd 12.00 6.80 2.75	Ag 10.50 5.85 2.89	Cd 8.65 4.64 2.98	In 7.29 3.83 3.25	Sn 5.76 2.91 2.81	Sb 6.69 3.31 2.91	Te 6.25 2.94 2.86	I 4.95 2.36 3.54	Xe 4K 3.78 1.64 4.34
Cs 5K 1.997 0.905 5.235	Ba 3.59 1.60 4.35	La 6.17 2.70 3.73	Hf 13.20 4.52 3.13	Ta 16.66 5.55 2.86	W 19.25 6.30 2.74	Re 21.03 6.80 2.74	Os 22.58 7.14 2.68	Ir 22.55 7.06 2.71	Pt 21.47 6.62 2.77	Au 19.28 5.90 2.88	Hg 227 14.26 4.26 3.01	Tl 11.87 3.50 3.46	Pb 11.34 3.30 3.50	Bi 9.80 2.82 3.07	Po 9.31 2.67 3.34	At — 	Rn —
Fr — 	Ra — 	Ac 10.07 2.66 3.76															

Ce 6.77 2.91 3.65	Pr 6.78 2.92 3.63	Nd 7.00 2.93 3.66	Pm — 	Sm 7.54 3.03 3.59	Eu 5.25 2.04 3.96	Gd 7.89 3.02 3.58	Tb 8.27 3.22 3.52	Dy 8.53 3.17 3.51	Ho 8.80 3.22 3.49	Er 9.04 3.26 3.47	Tm 9.32 3.32 3.54	Yb 6.97 3.02 3.88	Lu 9.84 3.39 3.43
Th 11.72 3.04 3.60	Pa 15.37 4.01 3.21	U 19.05 4.80 2.75	Np 20.45 5.20 2.62	Pu 19.81 4.26 3.1	Am 11.87 2.96 3.61	Cm — 	Bk — 	Cf — 	Es — 	Fm — 	Md — 	No — 	Lr —

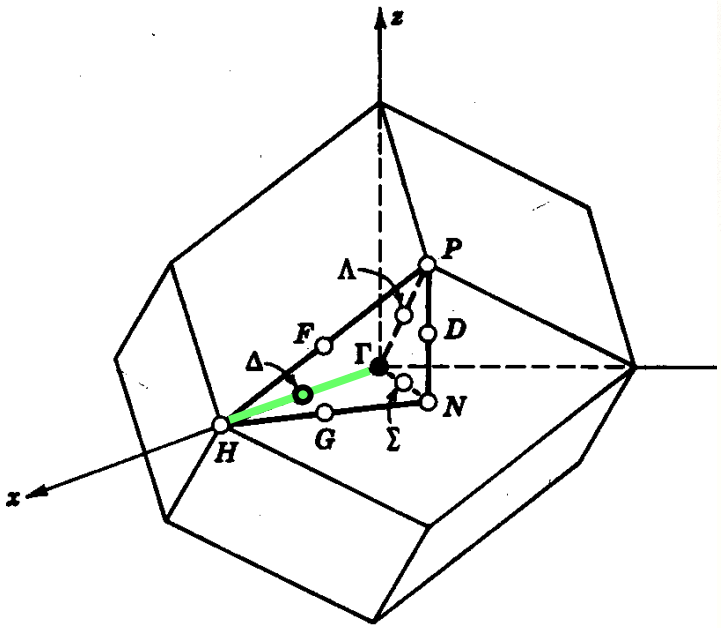

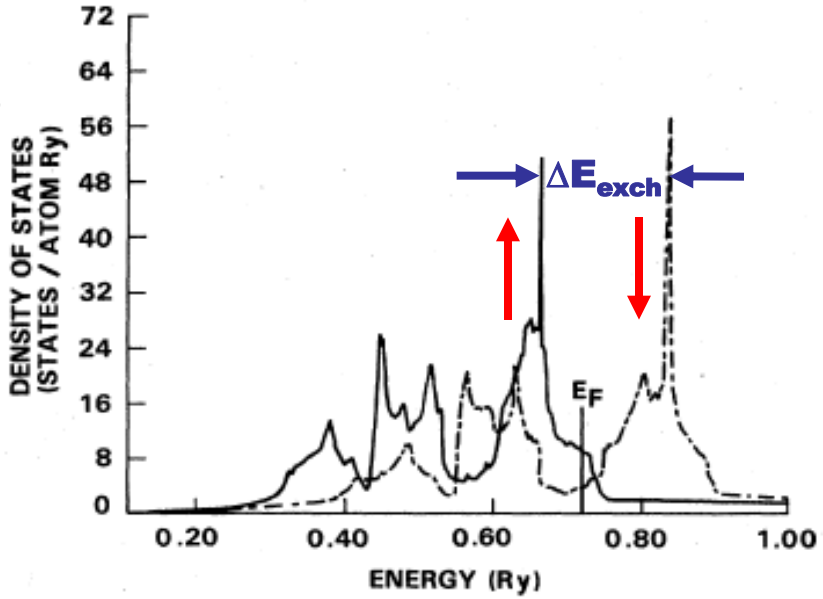

FIG. 4. Density of states at the equilibrium lattice constant of Fe for majority- (solid line) and minority- (broken line) spin states.

Hathaway et al., Phys. Rev. B 31, 7603 ('85)

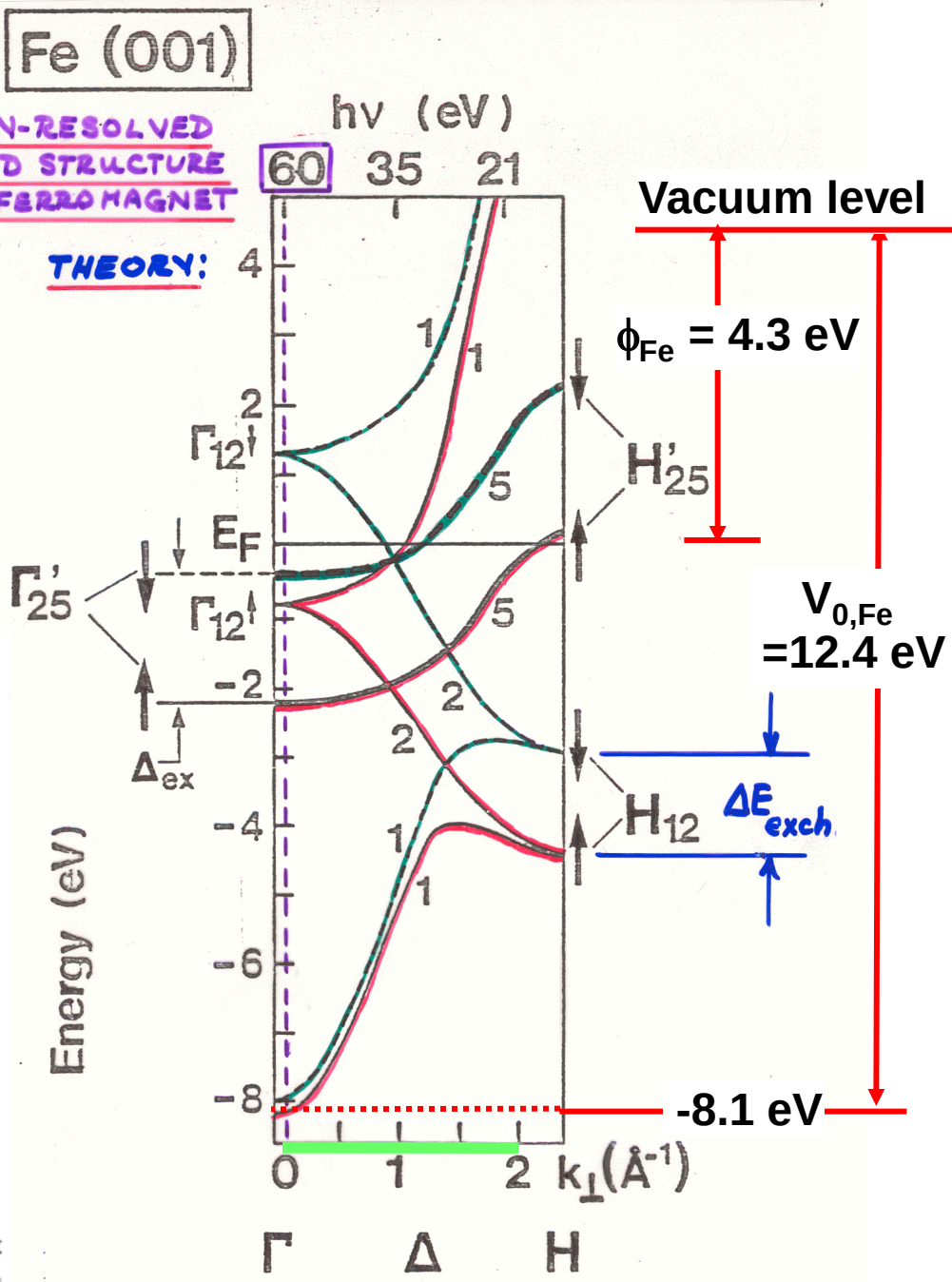

Initial core-state quantum numbers

Radial matrix elements:

- (•) Automatic: core level (e.g. 1s, 2s, 2p, etc.) = [1s]
- ( ) Manual: l_0=[0], R_{l0+1}=[1.0], δ_{l0+1}=[0.0], R_{l0-1}=[0.0], δ_{l0-1}=[0.0]

[Calculate*] [Download Input File**] [Reset***]

COMPUTATION TIME: the CPU time needed for the calculation using the default cluster and input parameters (use Reset to recover default input) is 1.24 seconds on a Pentium III @ 733 MHz. This gives a time scale to estimate the computation time for other input parameters, keeping in mind that it scales like $\sim (n_{scat} - 1)\, N^2\, (l_{max}+1)^3$, where N is the number of atoms in the cluster and n_{scat} is the scattering order. For reference, the default values are N=48, l_{max}=6, and n_{scat}=2, for which the above number is $7.9\ 10^5$.

IMPORTANT: READ THESE LINES BEFORE RUNNING THE CODE FOR THE FIRST TIME.

***The results will be plotted on a separate window.**

****The input file can be used to run the code locally, for which a copy of the code is needed. This can be obtained from F. Javier García de Abajo. An online version of the input-file manual is also available here.**

*****Reset all input values (including cluster specification) to the original settings.**

For comments/questions/suggestions, please contact F. Javier García de Abajo at jga@sw.ehu.es

CO/Fe(001)—Effect of CO height z above first Fe plane

2 atoms: $Z = \infty$

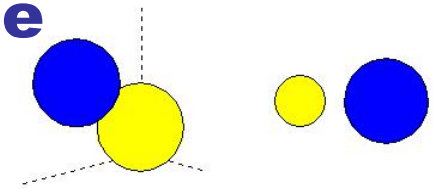

7 atoms:

1.0 Å

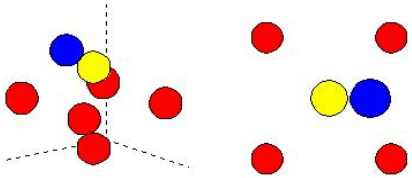

0.5 Å

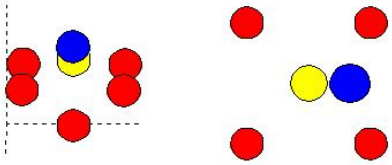

0.0 Å

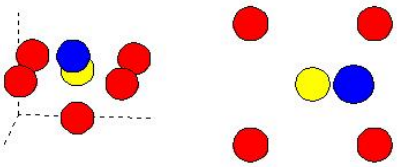

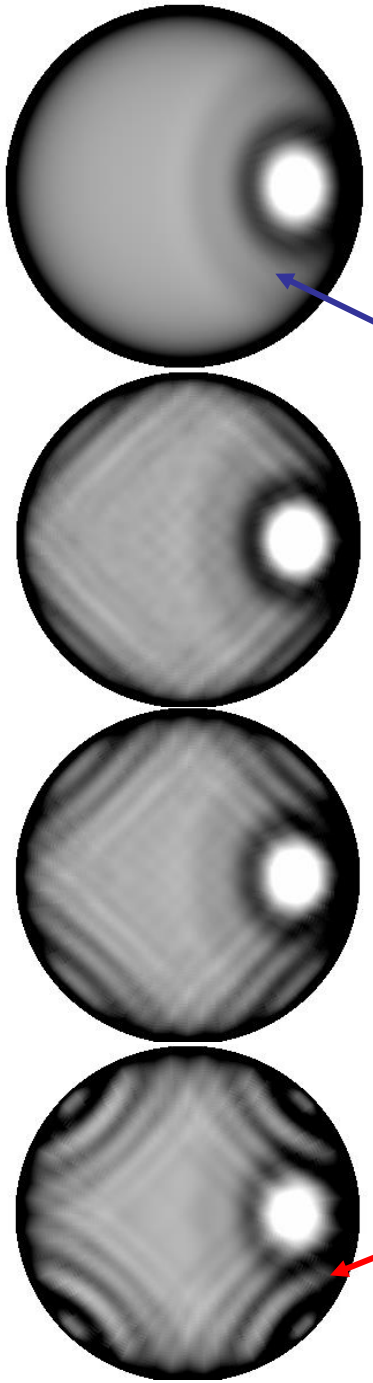

CO/Fe(001)—Effect of CO bond dist.

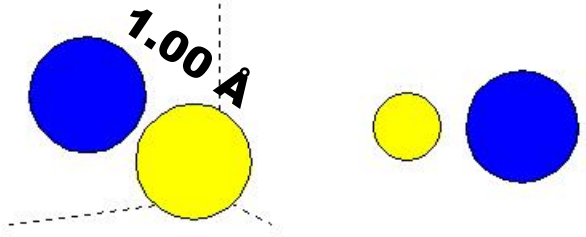

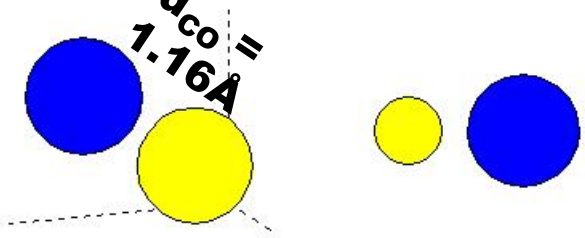

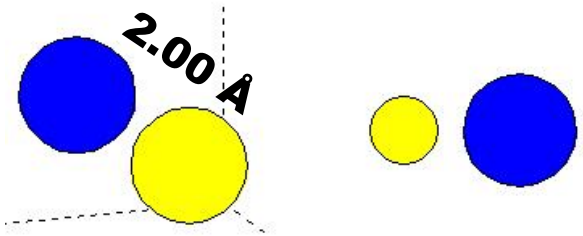

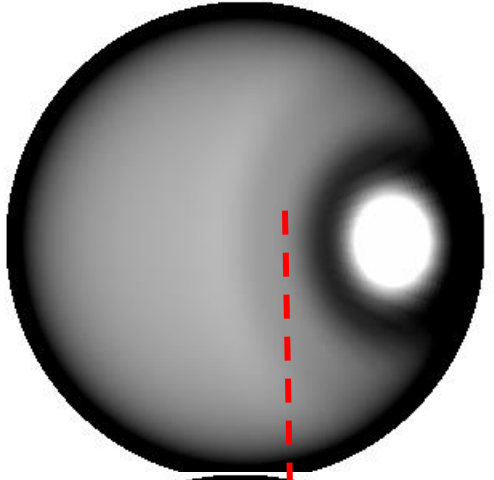

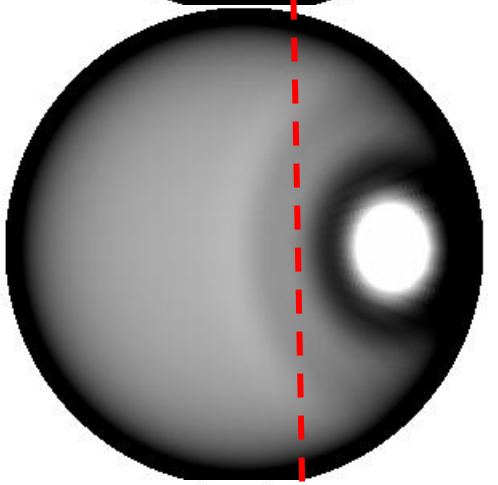

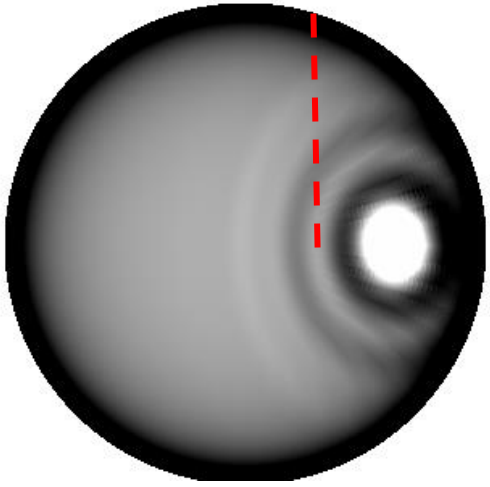

CO/Fe(001)—Effect of CO height z above first Fe plane

2 atoms: $Z = \infty$

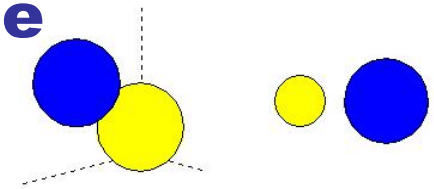

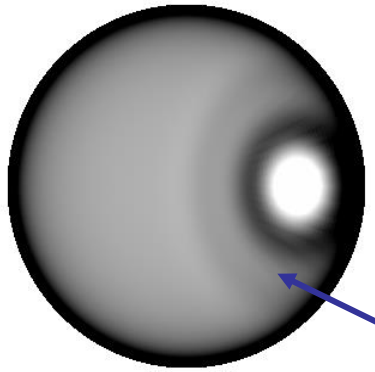

Oxygen-
1st order
diff. ring

7 atoms: 1.0 Å

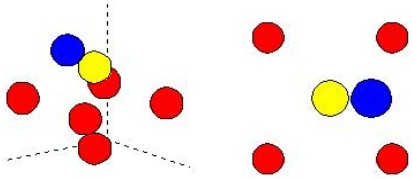

0.5 Å

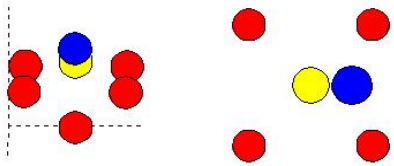

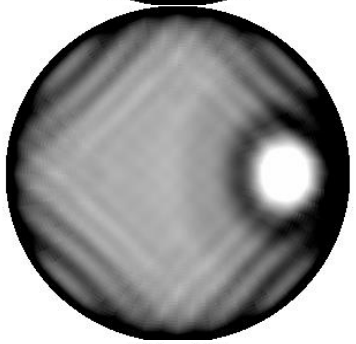

0.0 Å

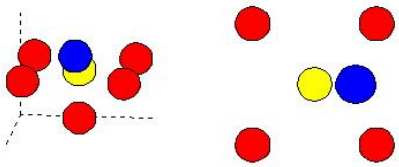

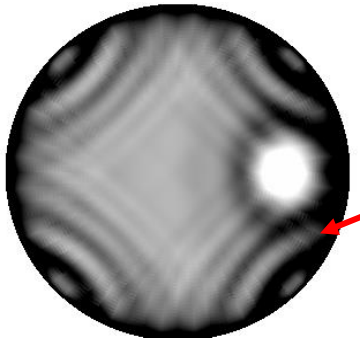

Iron-
1st order
diff. ring

CO/Fe(001)—Effect of CO bond dist.

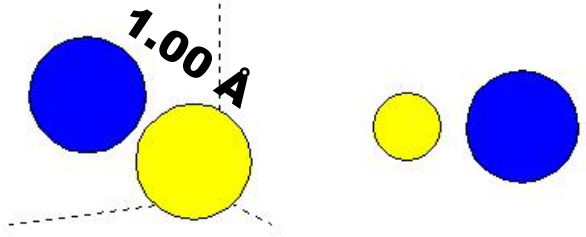

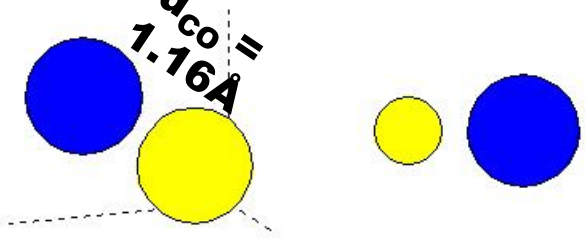

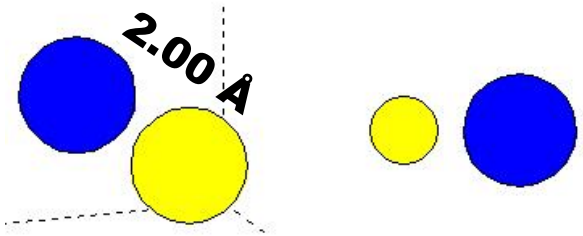

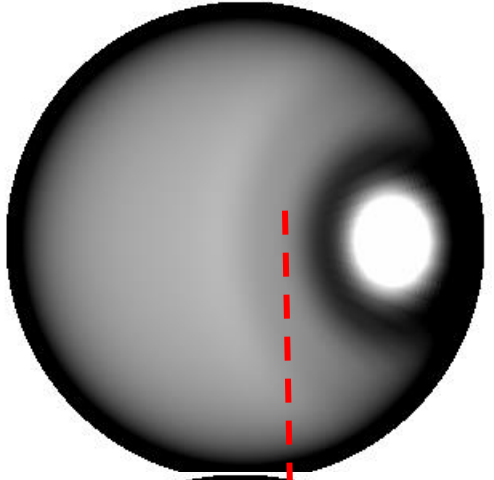

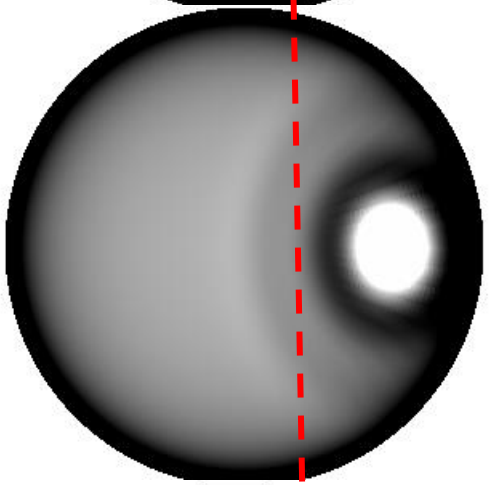

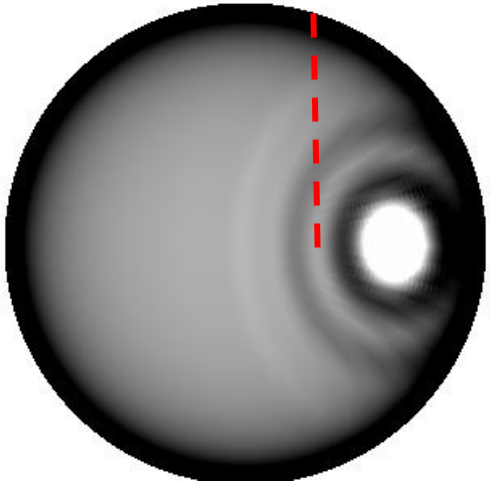

CO/Fe(001)—Effect of cluster size

19 atoms:

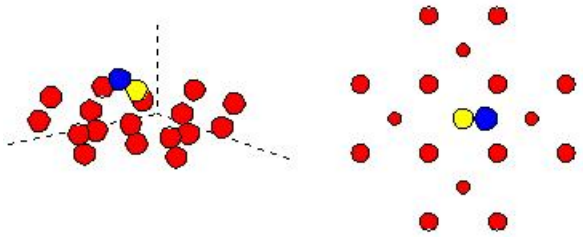

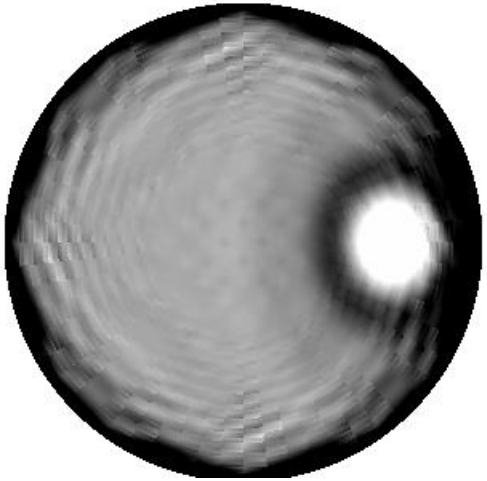

31 atoms:

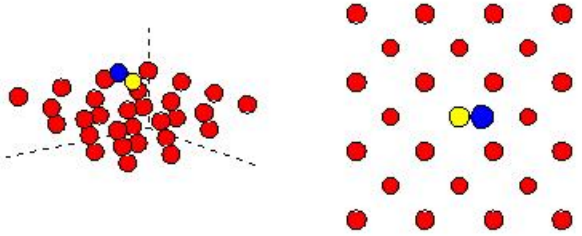

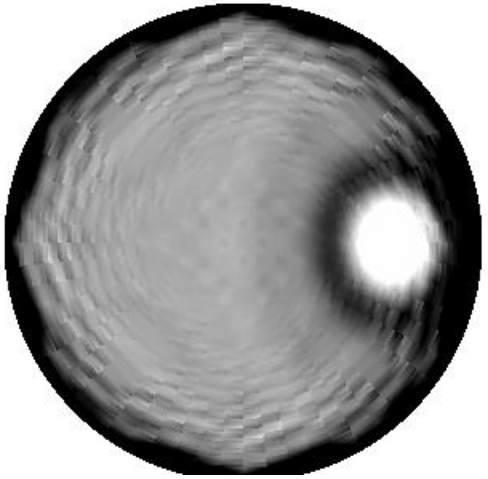

19 ≈ 31, AND SO “CONVERGED” AT 19 OR LESS

CO/Fe(001)—Effect of scattering order

Single scattering:

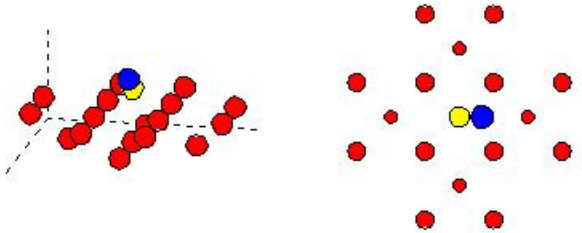

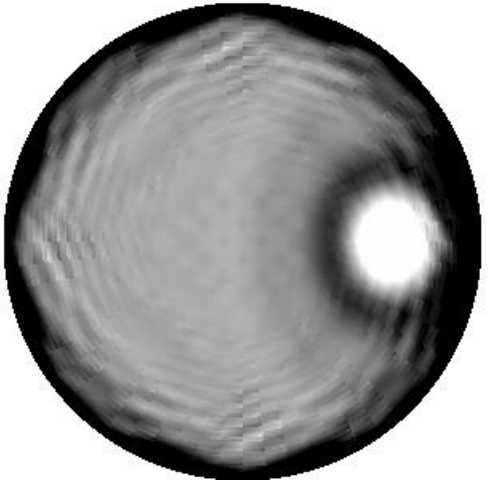

Fourth order scattering:

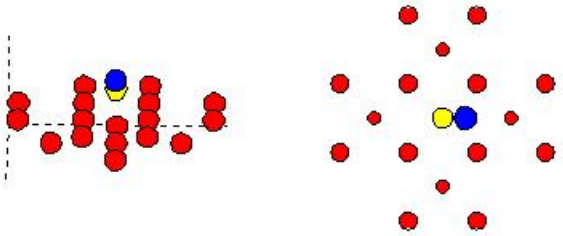

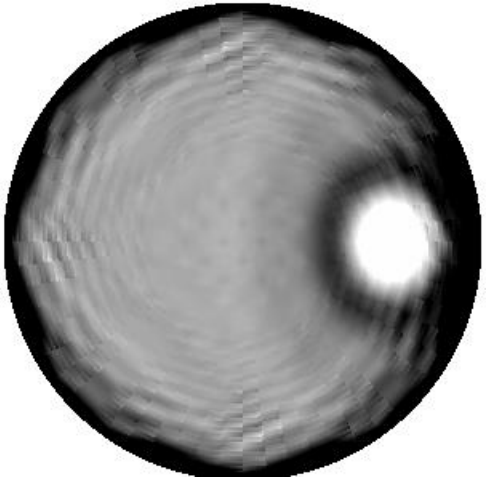

APPROX. CONVERGED AT SINGLE—FOR THIS PARTICULAR PROBLEM ONLY!

4-atom Fe nearest-neighbor chain along [110]—Effect of scattering order

Generally need multiple scattering for deeper-layer emitters

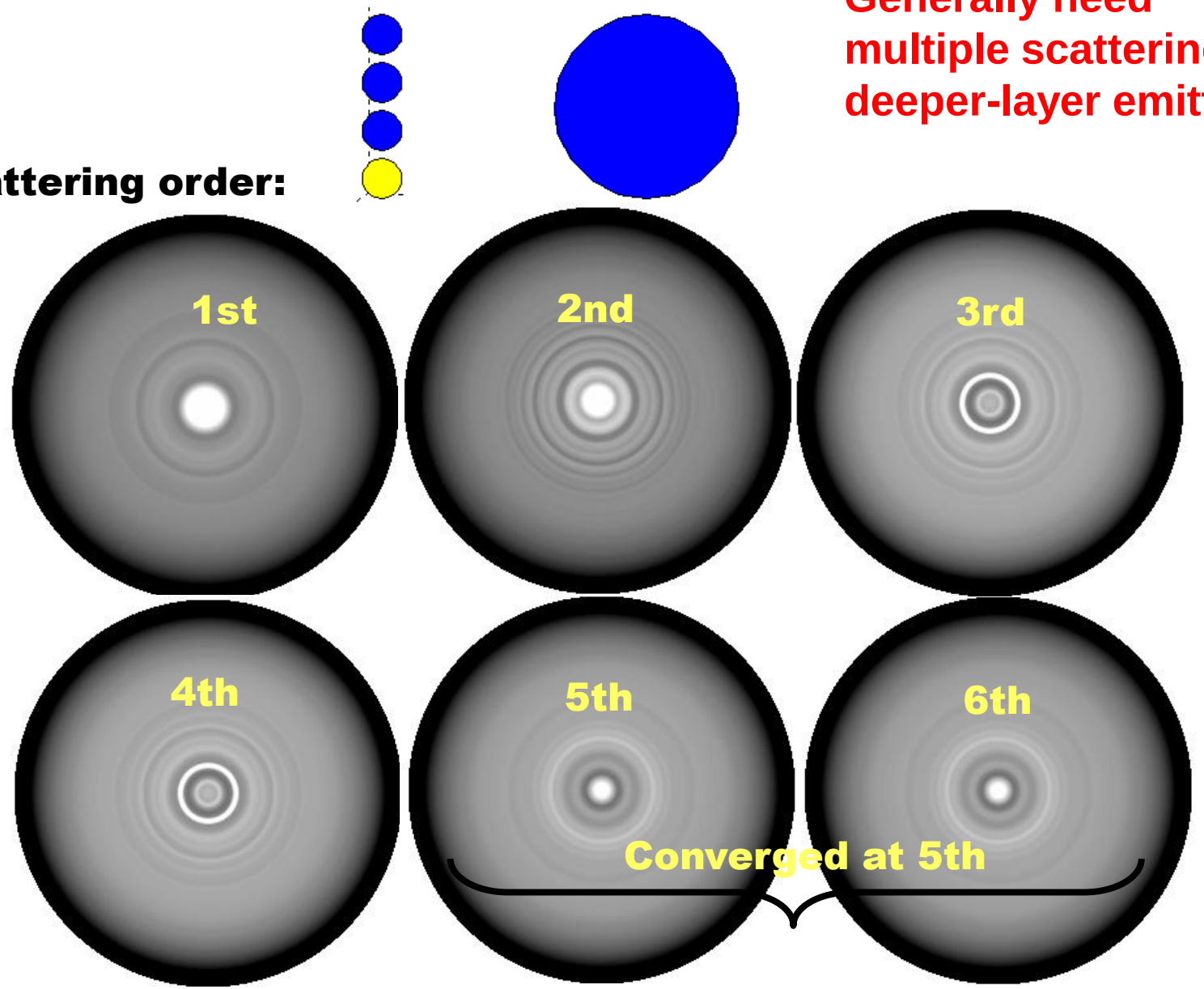

Multiple scattering along atomic chains: Cu nearest-neighbor chains along [110]—Effect of scattering order

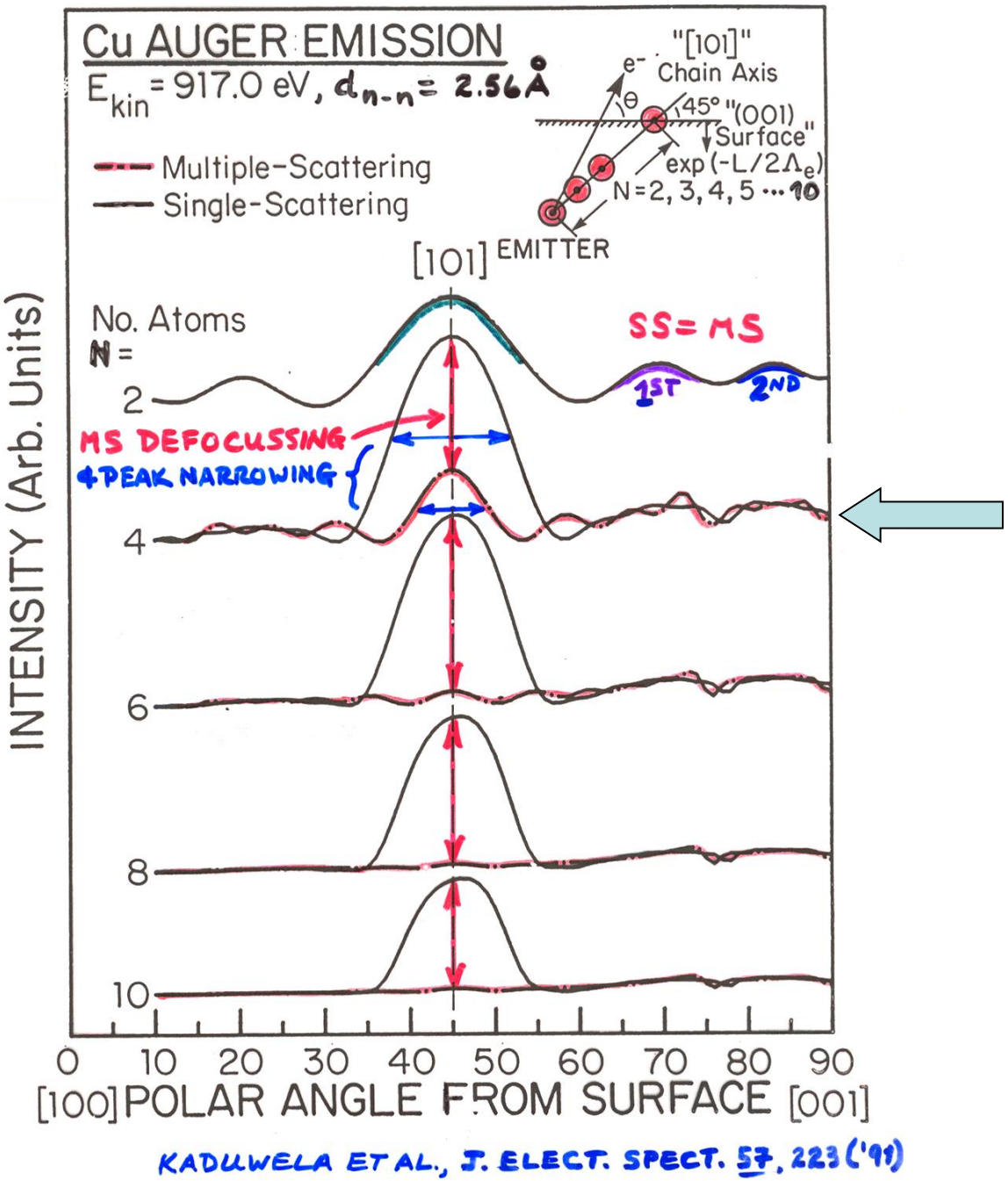

Plus cf. Figs. 6 and 7 in C.F., "The Study of Surface Structures by Photoelectron Diffraction and Auger Electron Diffraction"

Effect of varying the polarization?: C 1s emission from CO

E_{kin} = 200 eV

Linear p polarization:

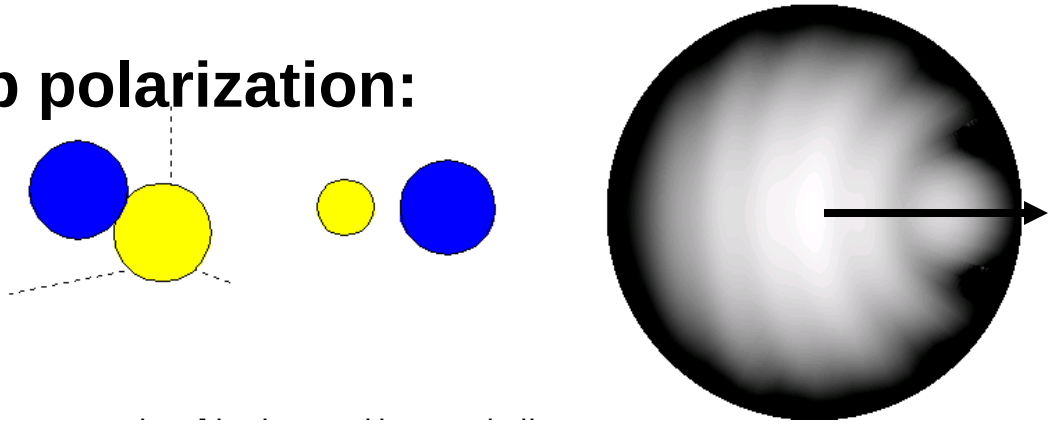

Right circular polarization:

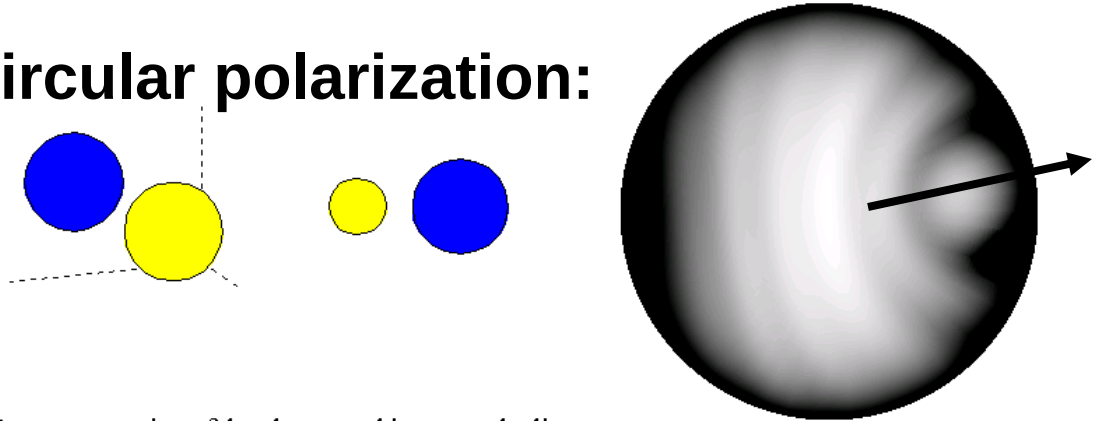

Left circular polarization:

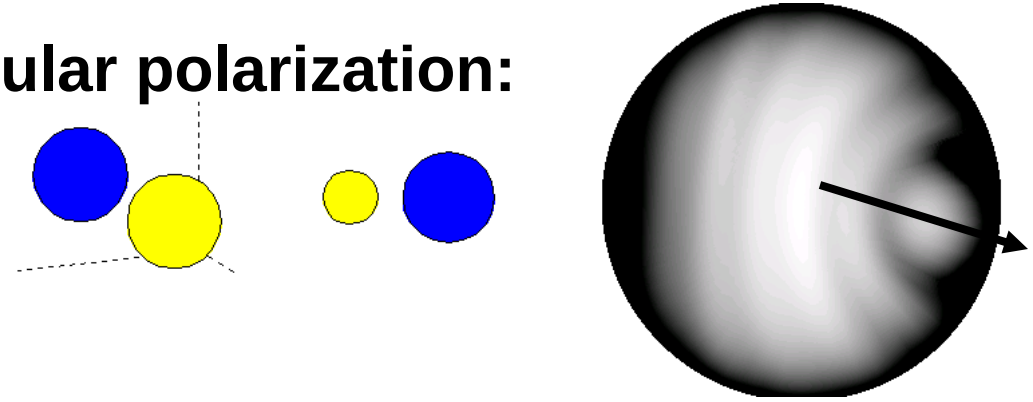

Circular dichroism in angular distributions (CDAD)

CIRCULAR DICHROISM IN PHOTOELECTRON ANGULAR DISTRIBUTIONS (CDAD)

non-magnetic dichroism effects due to photoelectron diffraction

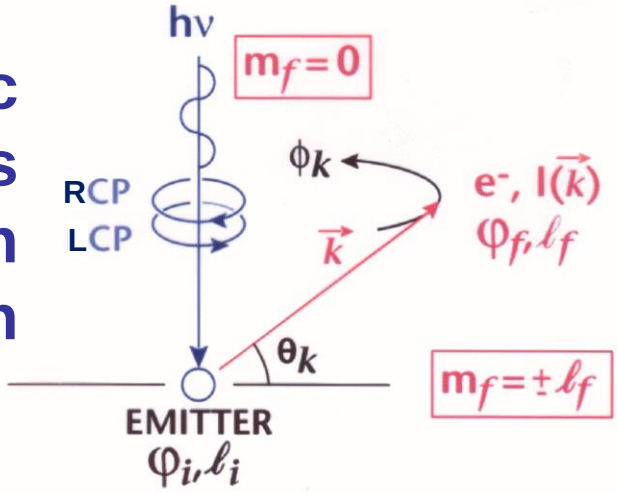

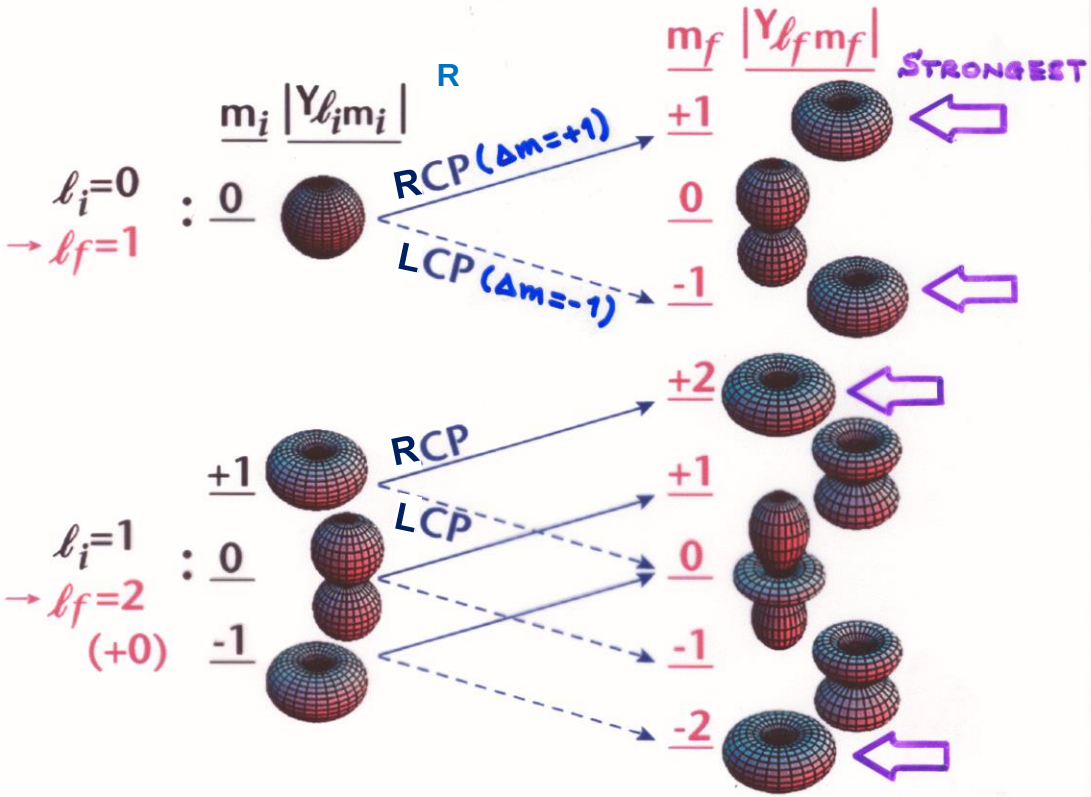

CIRCULAR DICHROISM IN PHOTOELECTRON DIFFRACTION

CONSTANT-PHASE SURFACE OF:

$$\psi_{\text{PHOTOE}^-}(r,\theta,\phi) \propto \frac{e^{ikr}}{r} \Theta_{lm} e^{i m_f \phi}$$

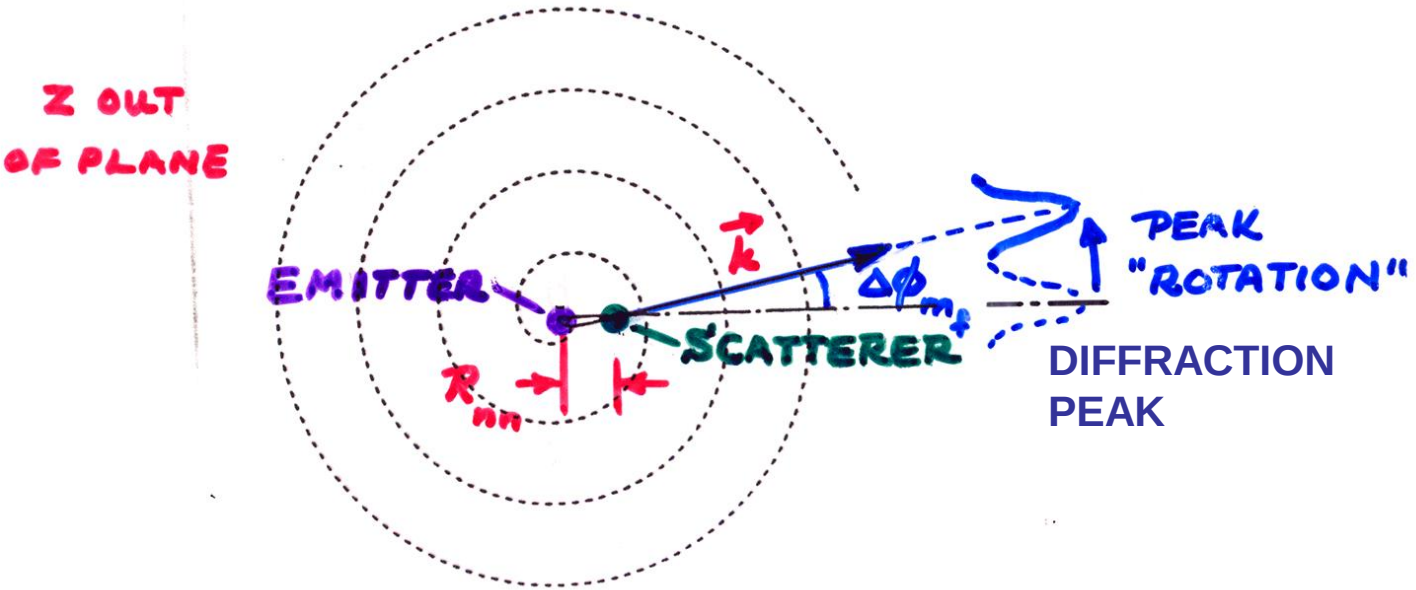

$$\Delta\phi_{m_f} = \frac{\bar{m}_f}{R_{nn,\parallel} k_{\parallel}}$$

Phase accumulation To a scatterer at R_{nn}

$$\bar{m}_f \approx m_{f,\max}$$

DAIMON ET AL.
JPN. J. APPL. PHYS.
32, L1480 ('93)

CIRCULAR DICHROISM - NON-MAGNETIC SYSTEMS

Si2p -- 250eV = E_{kin}

EXPERIMENT

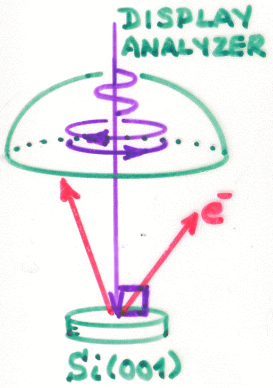

(a) LCP (b) RCP

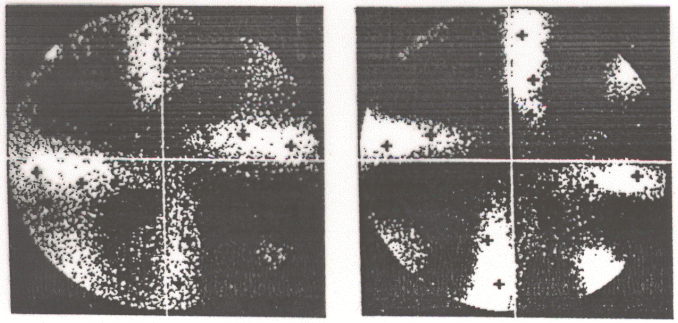

DAIMON ET AL.
JPN. J. APPL. PHYS.
32, L1480 ('93)

THEORY

(c) LCP (d) RCP

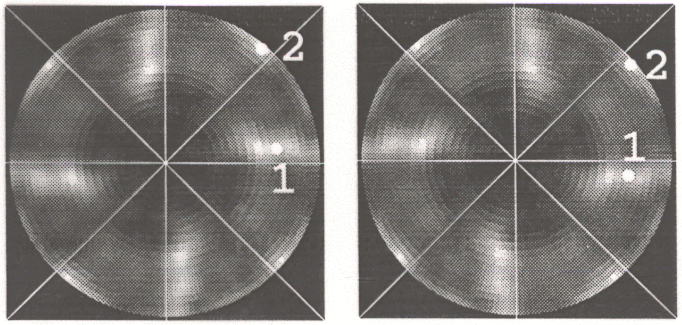

KADUWELA ET AL.
P. R. B 50, 6203 ('94)

(e) UNPOLARIZED

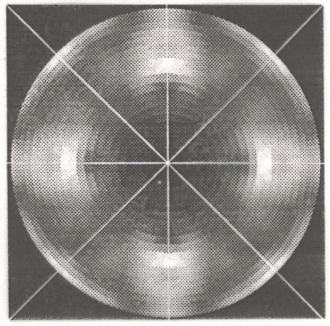

INTENSITIES IN PHOTOELECTRON SPECTRA:

- GENERAL: FINAL STATE K (k-SUBSHELL + ALL OTHER DESIG.)

$$\text{INT.}_K \propto \left| \hat{e} \cdot \langle \Psi^f_{tot}(N,K) | \sum_{i=1}^{N} \vec{r}_i | \Psi^i(N) \rangle \right|^2 \quad \text{(DIPOLE APPROX.}$$

- BORN-OPPENHEIMER: e^-'s FAST, VIBRATIONS SLOW

$$\text{INT.}_K \propto \underbrace{|\langle \psi^f_{VIB,v'} | \psi^i_{VIB,v} \rangle|^2}_{\text{FRANCK-CONDON FACTOR}} \left| \hat{e} \cdot \langle \Psi^f_{e^-}(N,K) | \sum_{i=1}^{N} \vec{r}_i | \psi^i_{e^-}(N) \rangle \right|^2$$

- SUDDEN APPROXIMATION: $\psi_K \rightarrow \psi_f$ = PHOTOe^- (FAST)

k HOLE → $\psi_1 \rightarrow \psi_1'$, $\psi_{k-1} \rightarrow \psi_{k-1}'$, $\psi_{k+1} \rightarrow \psi_{k+1}'$, $\psi_N \rightarrow \psi_N'$ (SLOW)

$$\text{INT.}_K \propto |\langle \psi^f_{VIB,v'} | \psi^i_{VIB,v} \rangle|^2 \underbrace{|\langle \Psi^f_{e^-}(N-1,K) | \Psi_K(N-1,K) \rangle|^2}_{\text{k MISSING}}$$

$$|\hat{e} \cdot \langle \psi_f | \vec{r} | \psi_K \rangle|^2$$

↳ NORMAL $\frac{d\sigma_K}{d\Omega}$

SAME SUBSHELL COUPLING + TOTAL L,S → "MONOPOLE"

- SLATER DETS. FOR $\Psi^f_{e^-} = \det(\psi_1' \psi_2' \cdots \psi_{k-1}' \psi_{k+1}' \cdots \psi_N')$

$$\Psi_K = \det(\psi_1 \psi_2 \cdots \psi_{k-1} \psi_{k+1} \cdots \psi_N)$$

$$\text{INT.}_K \propto |\langle \psi^f_{VIB,v'} | \psi^i_{VIB,v} \rangle|^2 |\langle \psi_1' | \psi_1 \rangle|^2 |\langle \psi_2' | \psi_2 \rangle|^2 \cdots$$
$$|\langle \psi_{k-1}' | \psi_{k-1} \rangle|^2 |\langle \psi_{k+1}' | \psi_{k+1} \rangle|^2 \cdots |\langle \psi_N' | \psi_N \rangle|^2 .$$

(N-1)e^- SHAKE-UP/ SHAKE-OFF → "MONOPOLE"

spin-orbit + 1e- DIPOLE → $d\sigma/d\Omega$ $\quad |\hat{e} \cdot \langle \psi_f | \vec{r} | \psi_K \rangle|^2$

- PLUS DIFFRACTION EFFECTS IN ψ_f ESCAPE

"Basic Concepts of XPS"
Chapter 3.D.

Photoelectron spin polarization from spin-orbit coupling and circularly-polarized radiation—The Fano Effect

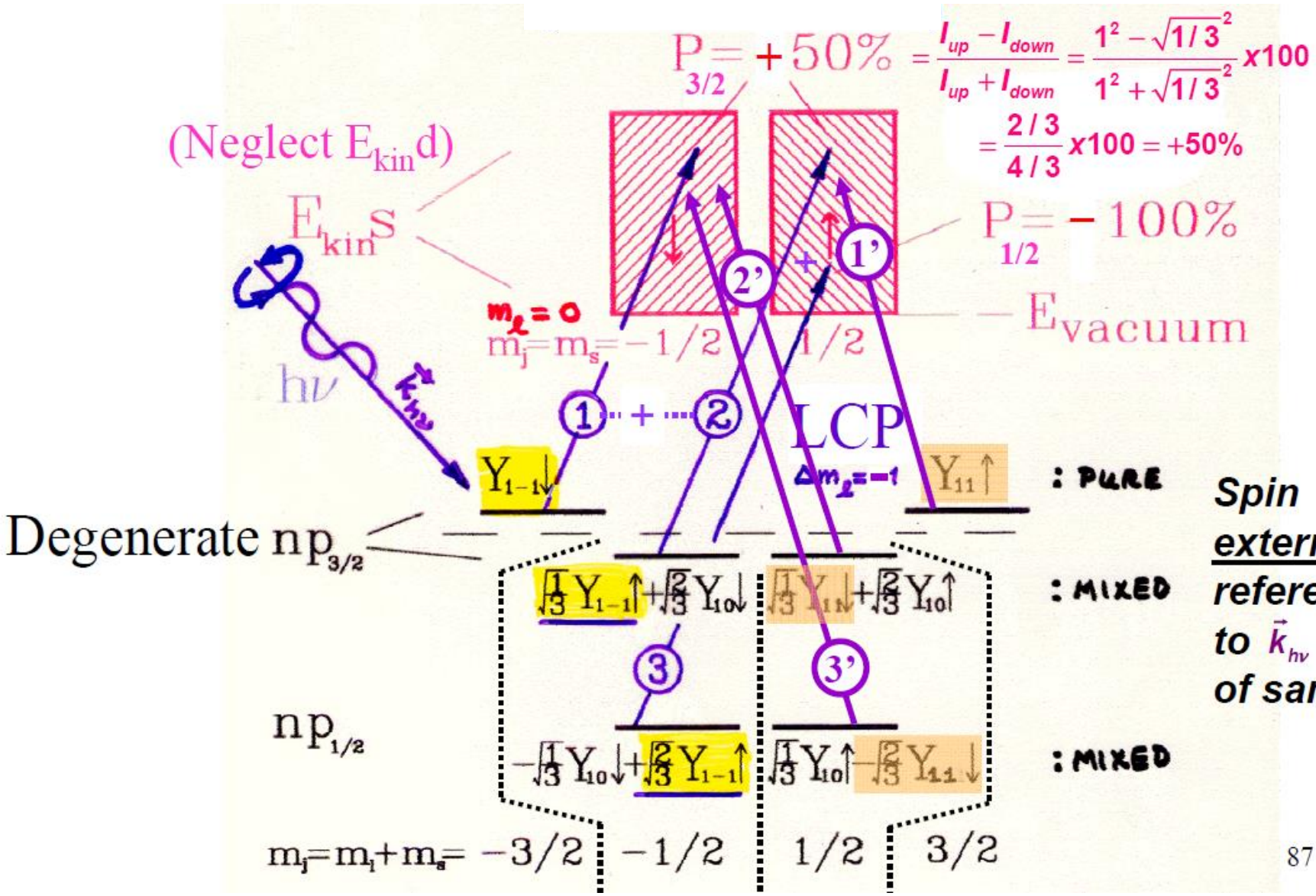

Spin ***externally*** *referenced to* $\vec{k}_{h\nu}$ *and* $\vec{M}$ *of sample*

More Realistic Theory: Single Atom

Free Fe $2p_{1/2}$

THEORY (s+d)

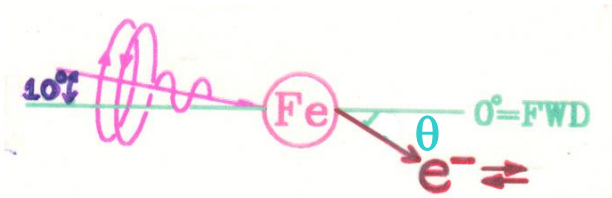

E_{kin} = 145 eV

LCP

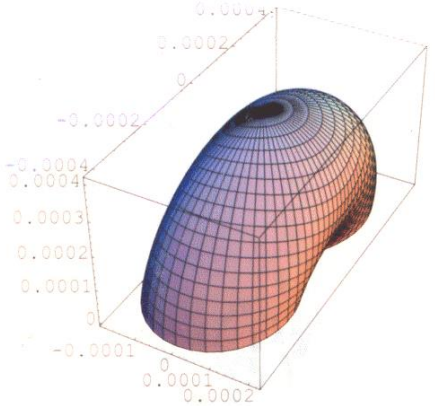

RCP

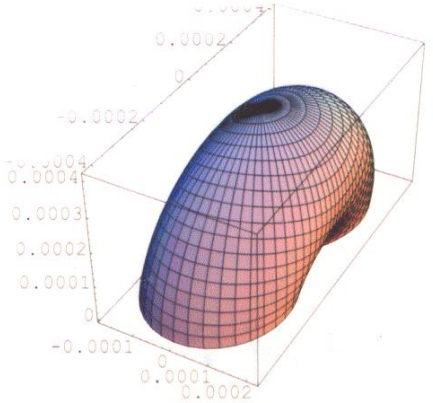

%CDAD

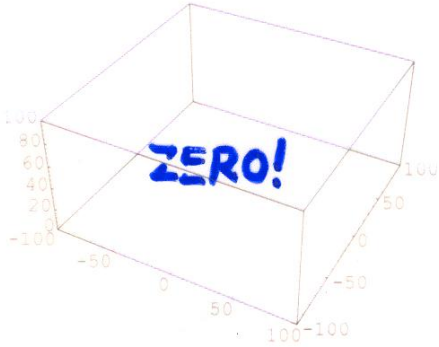

Spin Pol. (LCP)

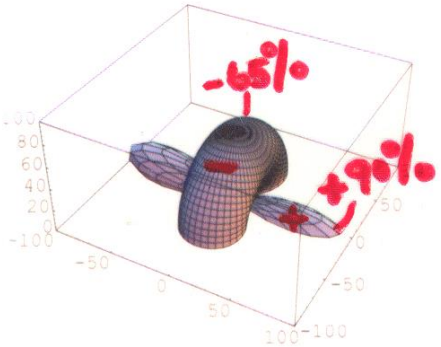

$$\%CDAD = \frac{RCP - LCP}{RCP + LCP} \times 100 \qquad \%P = \frac{LCP(\uparrow) - LCP(\downarrow)}{LCP(\uparrow) + LCP(\downarrow)} \times 100$$

= CIRCULAR DICHROISM IN ANGULAR DISTRIBUTION

A. Kaduwela, unpublished

More Realistic Theory: Ferromagnetic Cluster

Fe $2p_{1/2}$ Ferromagnetic Cluster

THEORY (s + d) – ADDS PHOTOELECTRON DIFFRACTION

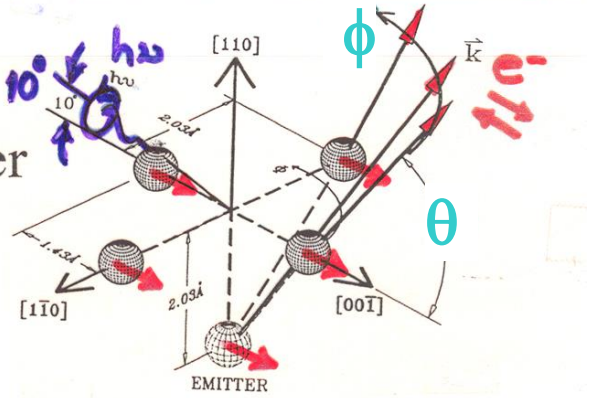

LCP RCP

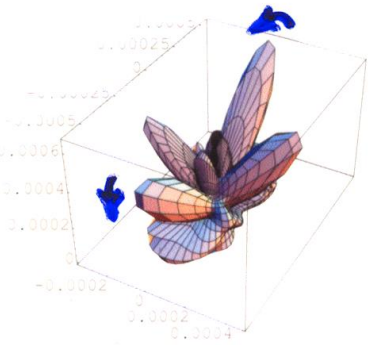

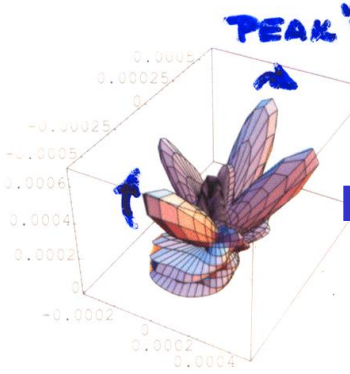

PEAK "ROTATIONS" (ALA DAIMON ET AL.)

%CDAD Spin Pol. (LCP)

"Circular Dichroism In Angular Distributions" (CDAD)-more later

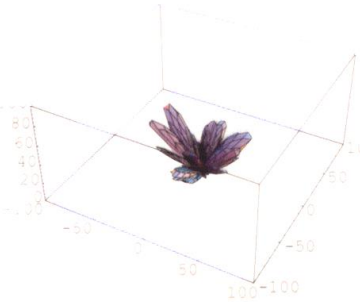

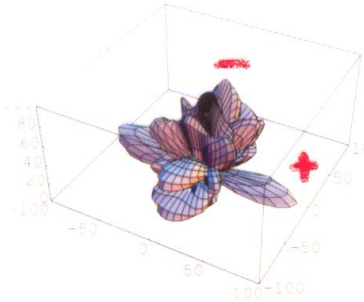

$$\%CDAD = \frac{RCP - LCP}{RCP + LCP} \times 100 \qquad \%P = \frac{LCP(\uparrow) - LCP(\downarrow)}{LCP(\uparrow) + LCP(\downarrow)} \times 100$$

A. Kaduwela, unpublished

Photoelectron diffraction from W(110) interface atoms beneath an Fe overlayer

Photoelectron diffraction: some case studies

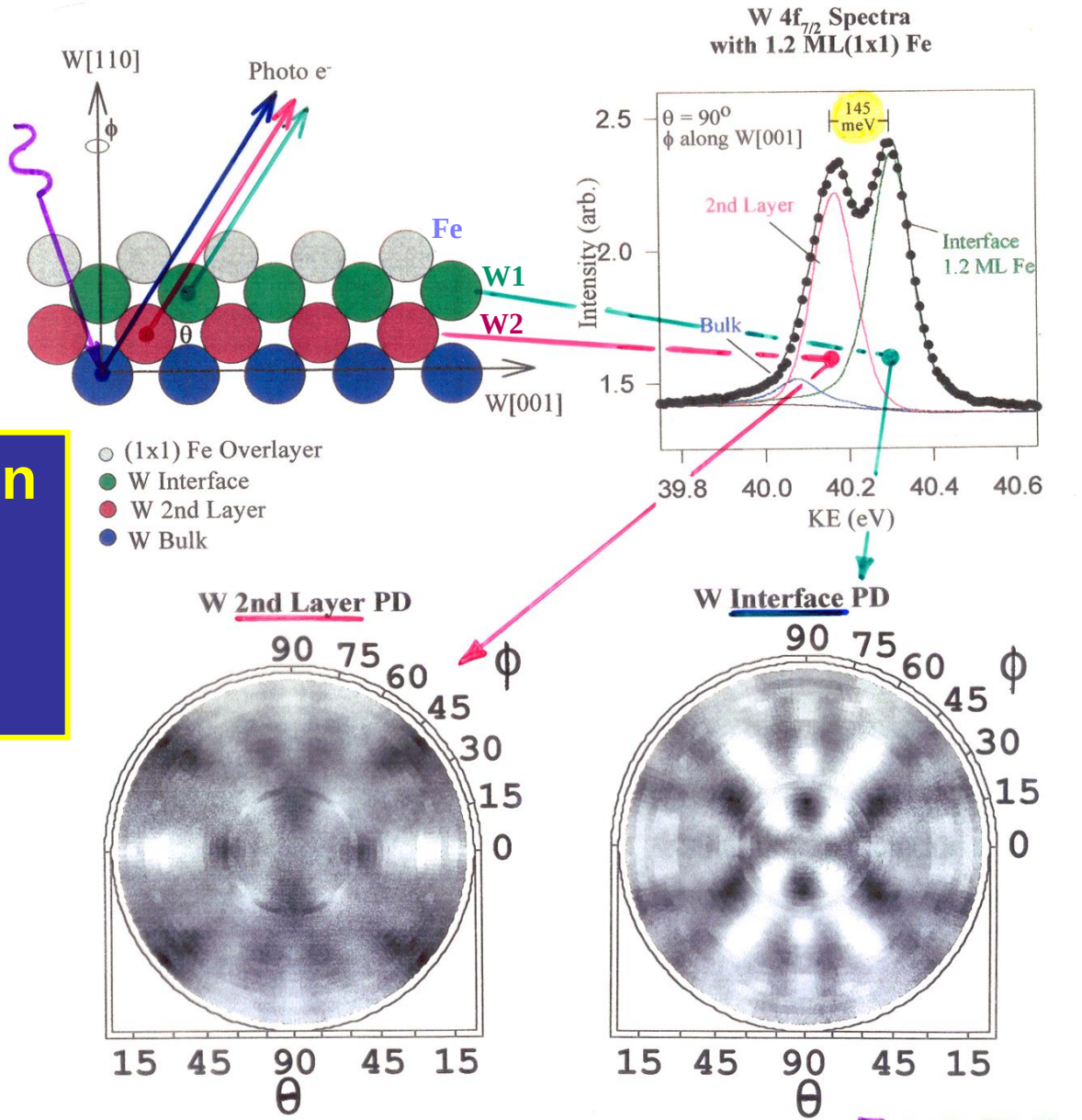

Fe on W(110): Determination of structure by expt./theory comparison

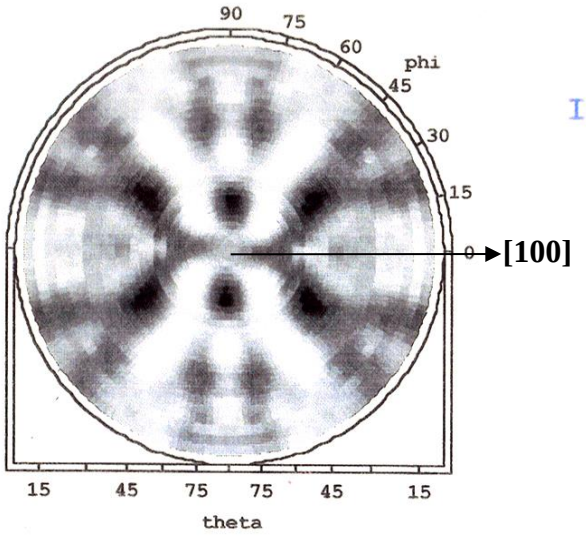

W $4f_{7/2}$
Interface Diffraction

Experiment

$h\upsilon$ = 70 eV
E_{kin} = 40 eV

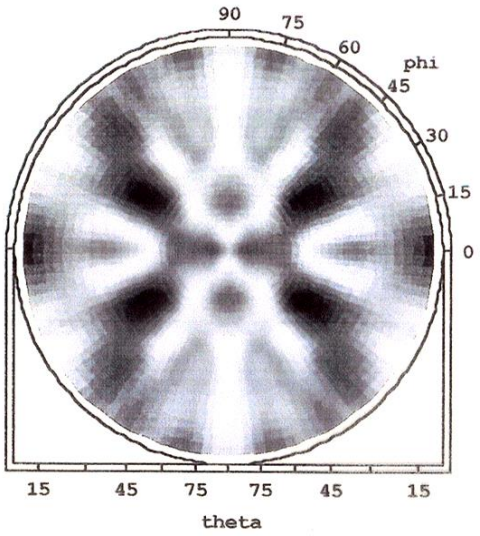

W $4f_{7/2}$
Interface Diffraction

Multiple Scattering
Theory
(110 atom cluster)

E_{kin} = 40 eV
Z_{Fe} = 2.165 Å

(Bridge Site)

↳ ~ CONTINUES BULK W STRUCTURE

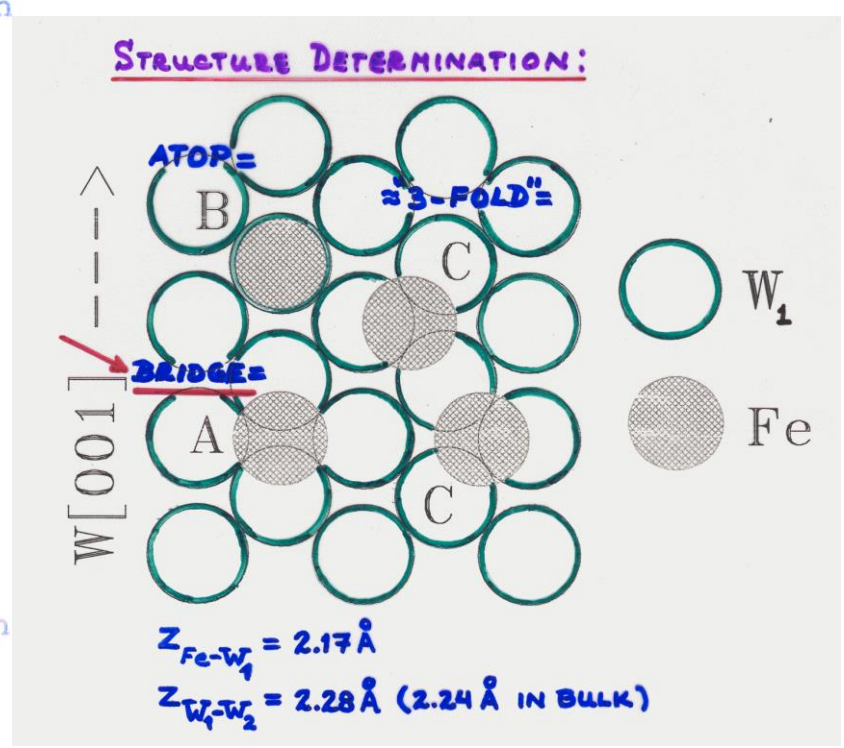

Looking into the silicon dioxide layer with photoelectron spectroscopy

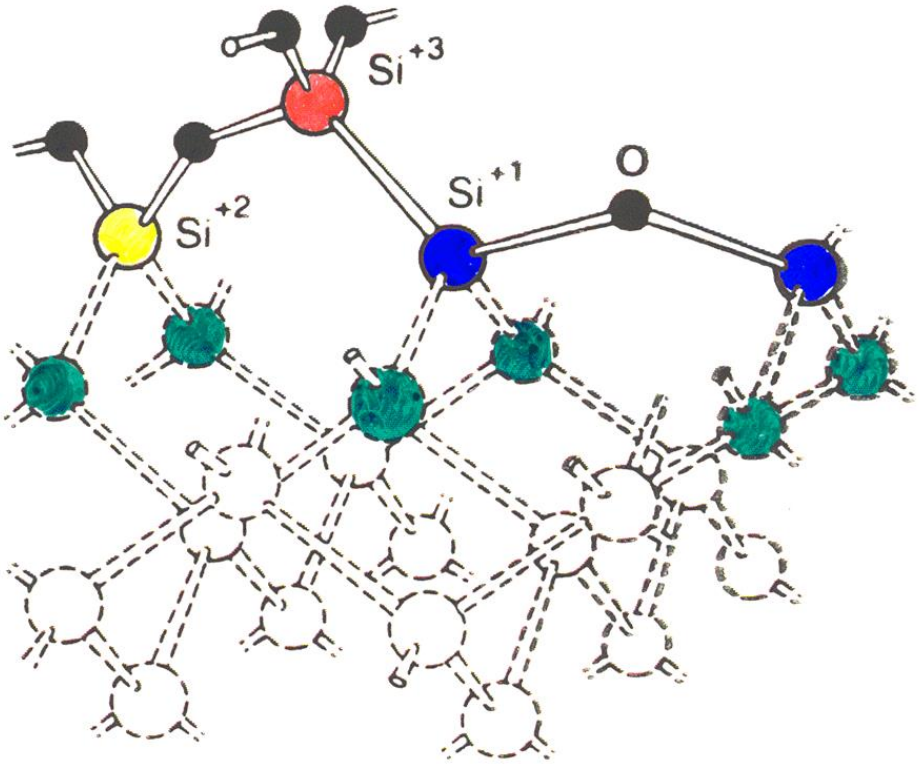

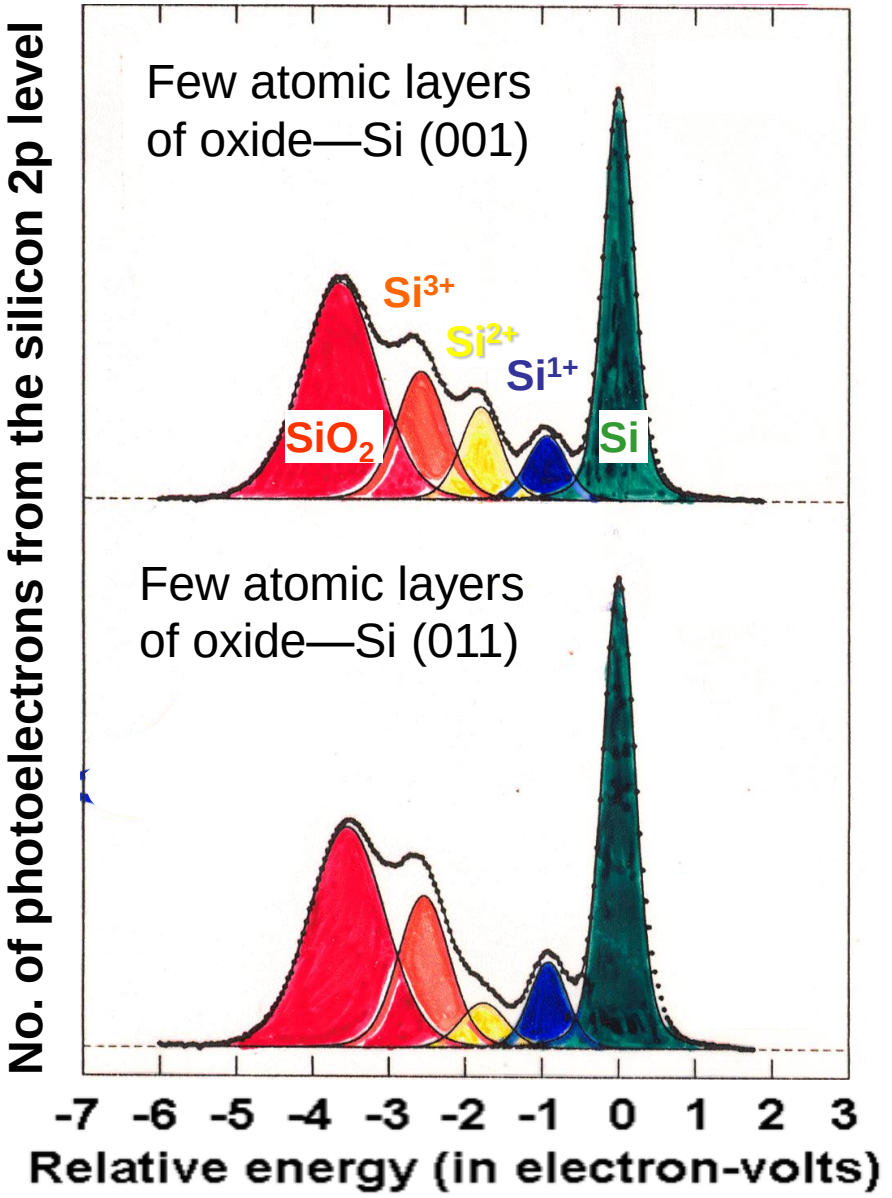

Case study: Interface structure of SiO_x/SiO_2

(Westphal et al.)

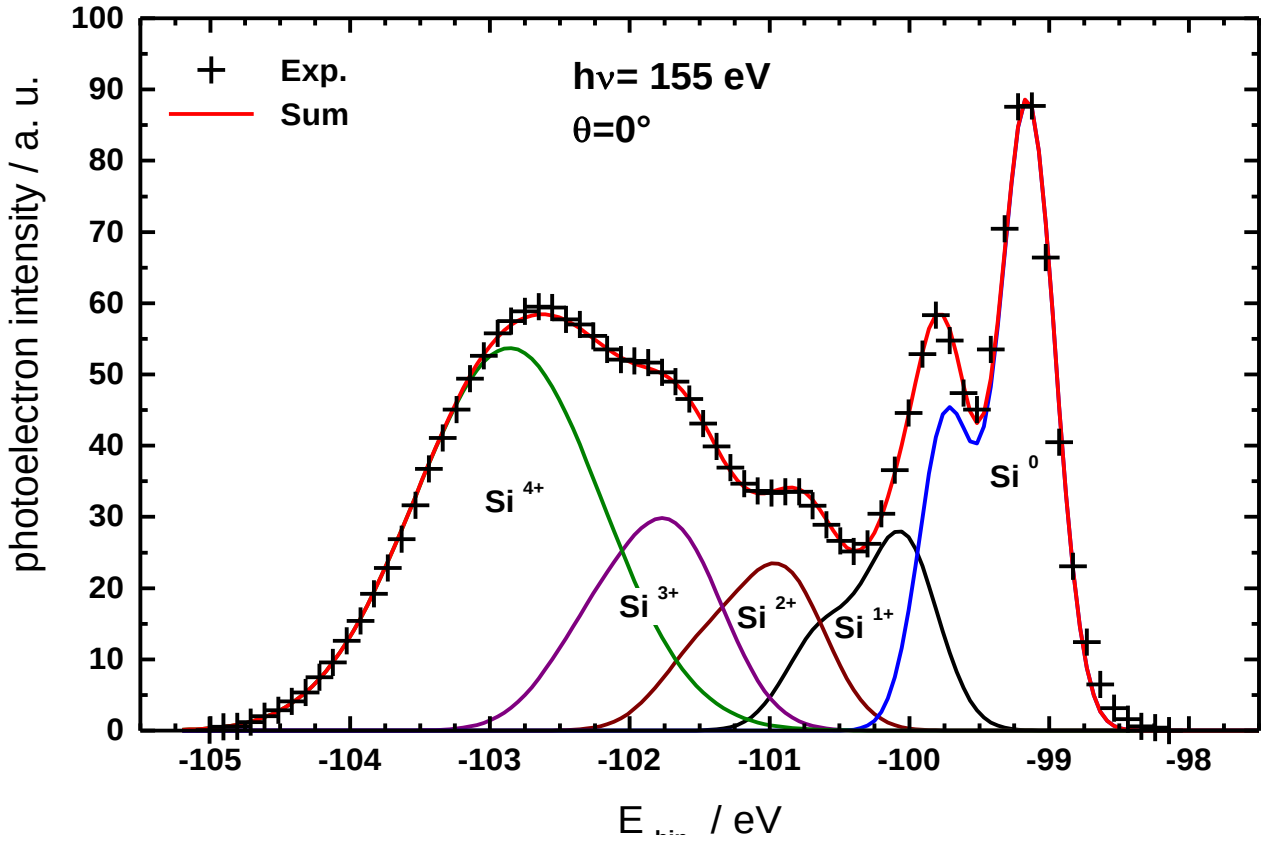

Spin-orbit-splitting	0.58 eV
Si^0 width	0.48 eV
Si^{1+} shift / width	0.9 / 0.59 eV
Si^{2+} shift / width	1.74 / 0.72 eV
Si^{3+} shift / width	2.46 / 0.84 eV
Si^{4+} shift / width	3.54 / 1.42 eV

F.J. Himpsel et al, Phys. Rev. B 38 (1988) 6084

S. Dreiner et al. (Westphal group), Phys. Rev. Lett. 86, 4068 (2001)

Experimental diffraction patterns for SiO_2/Si(100)

3000 L

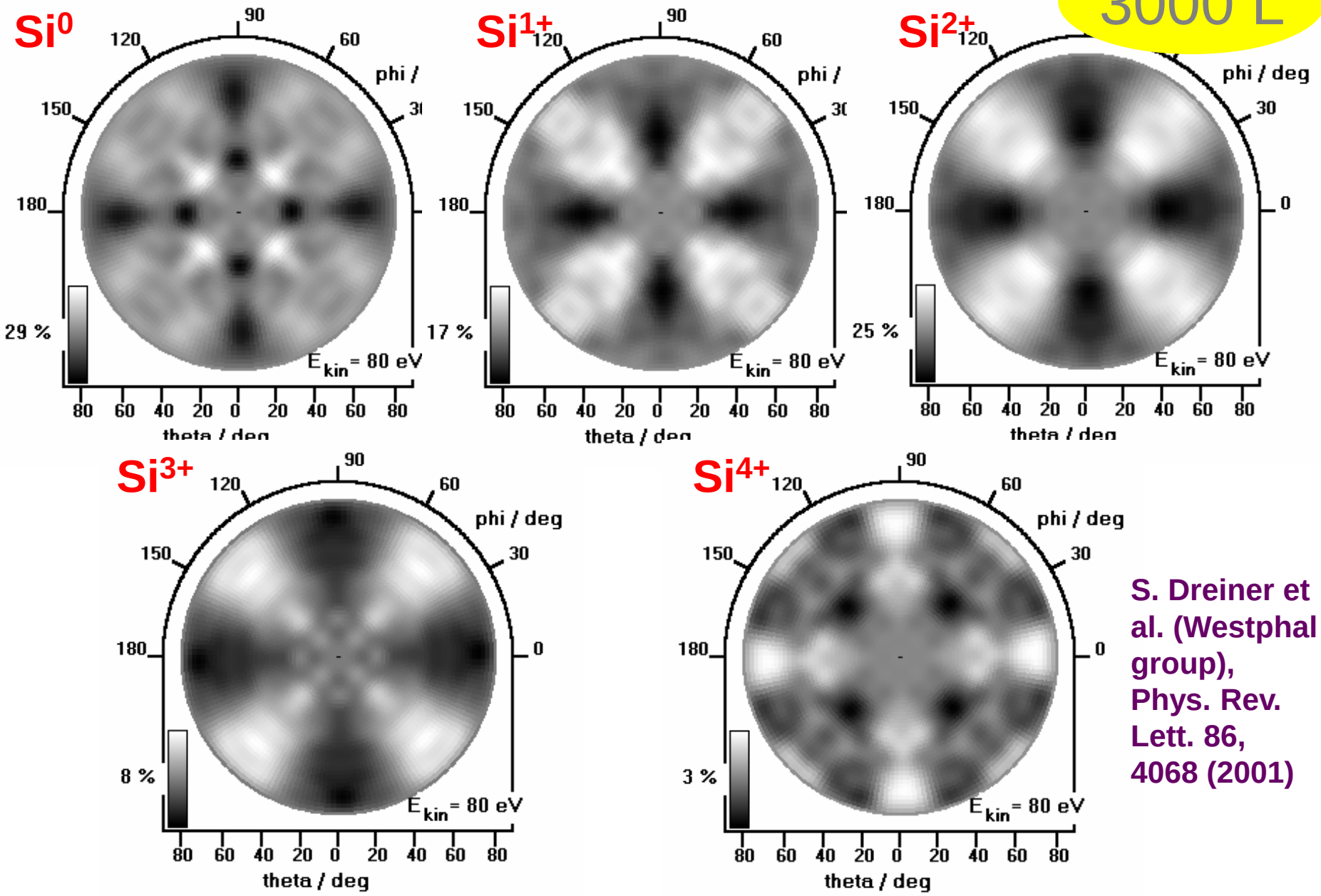

S. Dreiner et al. (Westphal group), Phys. Rev. Lett. 86, 4068 (2001)

simulation results by R-factor analysis, SiO_2/Si(100)

Expt.

Si^{4+}

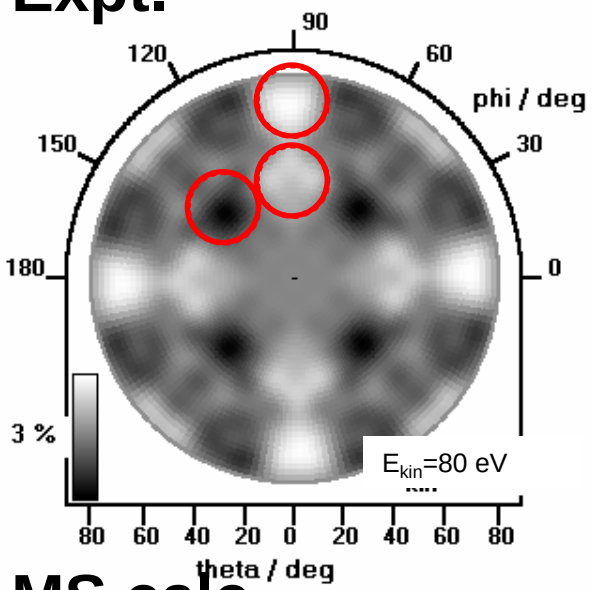

Si^{2+}

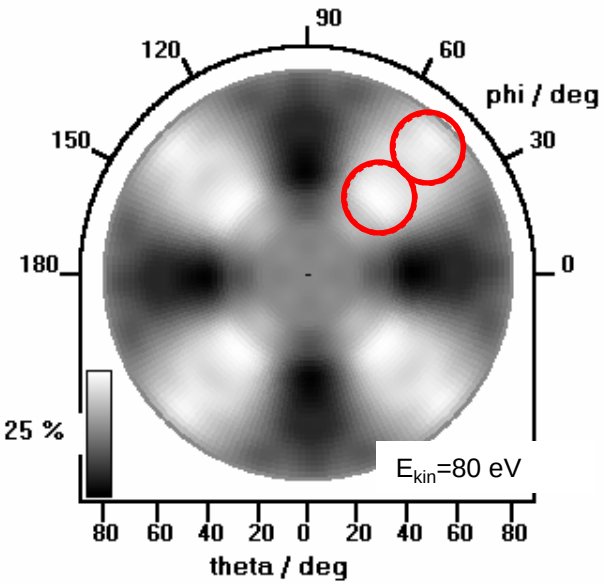

MS calc.

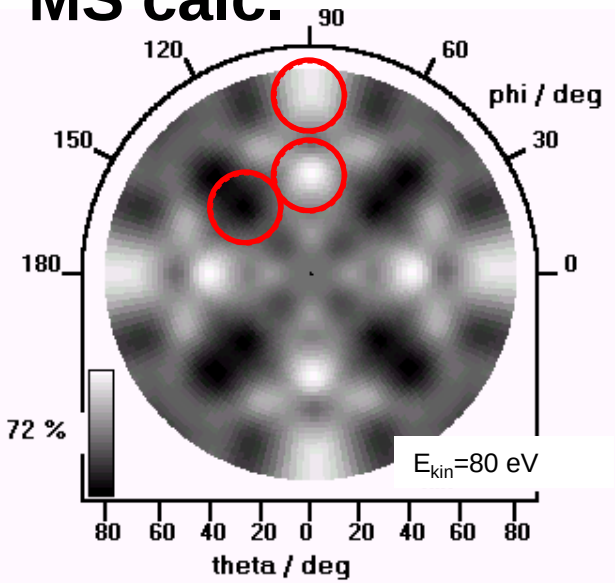

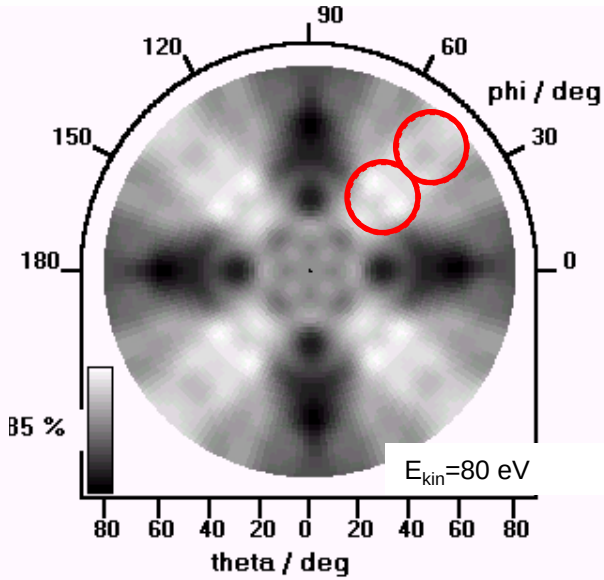

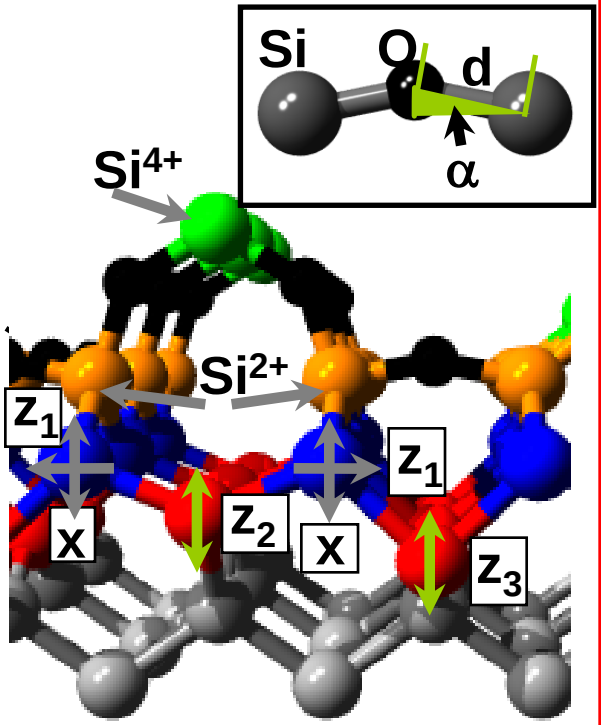

XPD pattern: Fingerprint of molecular orientation

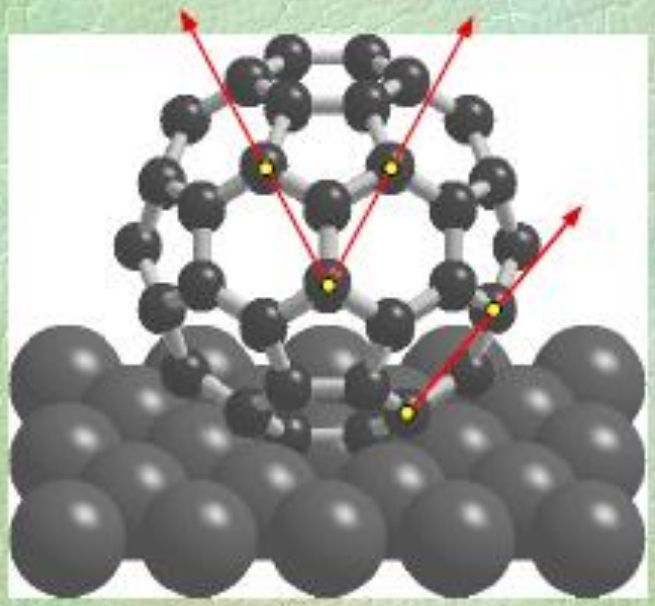

C_{60} scattering situation

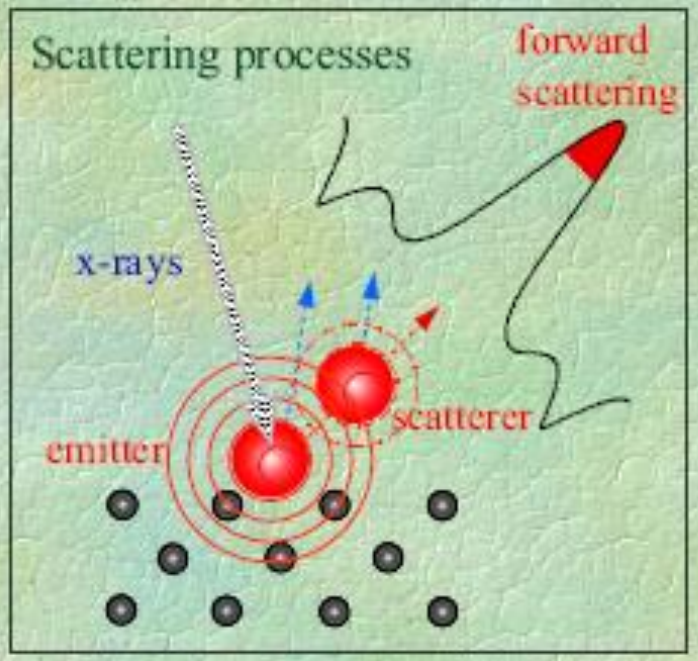

Single scattering cluster (SSC) calculation for C_{60} on 6-ring

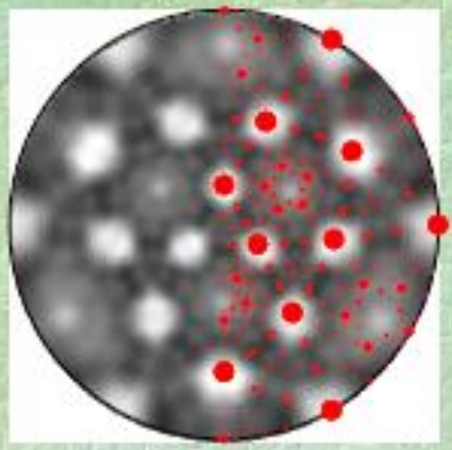

Projections of interatomic (C-C) directions

J. Osterwalder, R. Fasel, et al., PRL 76, 4733 ('96)

Some Complementary Surface Structure Probes

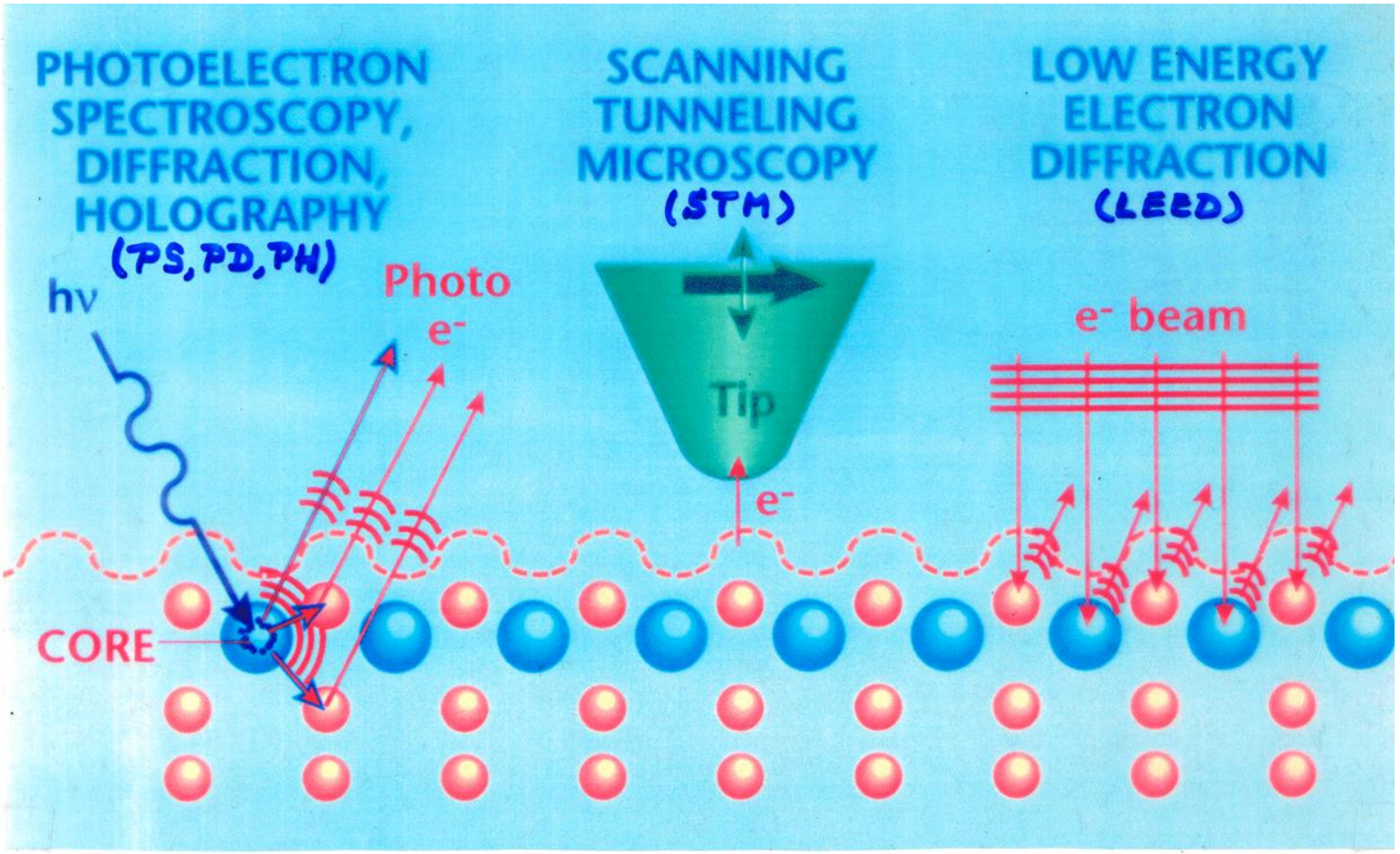

-Type of order:	Short (< 10Å)	Short, long and disorder	Long (> 100Å)
-Atom & site specific:	Yes	No	No
-Sensing depth:	5-40Å	Mostly surface D.O.S.	5-20Å
-Lateral resolution:	1 mm^2 to $(300Å)^2$	Single atom	1 mm^2 to 1 $micron^2$

Case study: 1 ML of FeO on Pt(111): A combined LEED, STM, XPD study

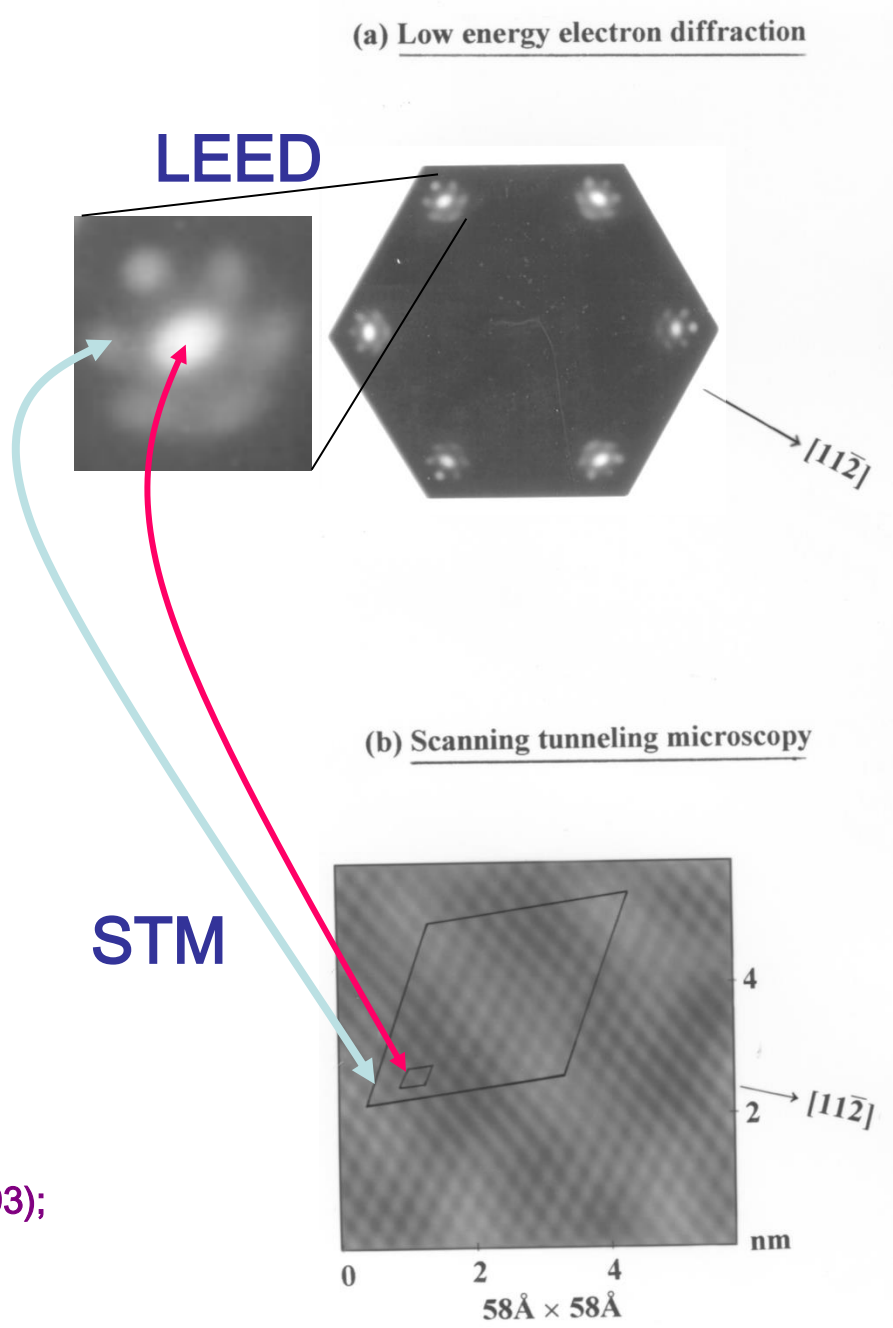

Galloway et al., Surf. Sci. 198, 127 ('93);
J. Vac. Sci. Tech. A12, 2302 ('94).
Y.J. Kim et al.,
Phys. Rev. B 55, R 13448 ('97);
Surf. Sci. 416, 68 ('98)

1 ML of FeO on Pt(111): Structural model from LEED and STM

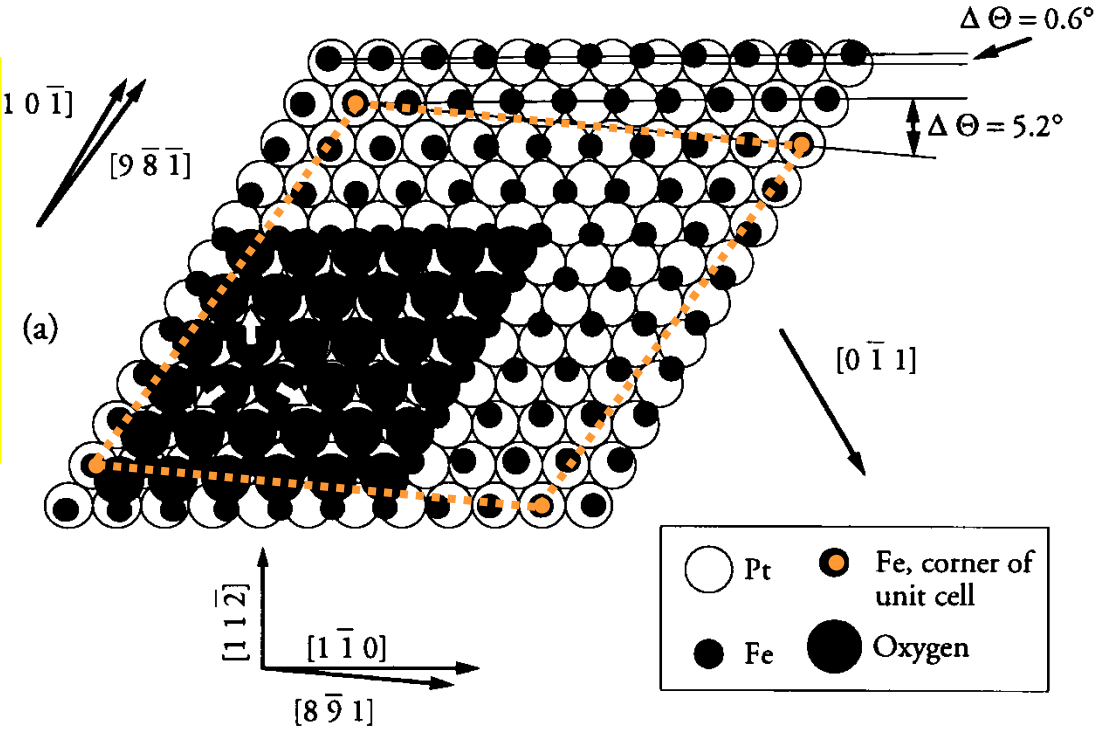

Remaining Questions:

- -Is Fe or O on top?
- -Fe-O interlayer spacing?
- -Fe-O orientation?

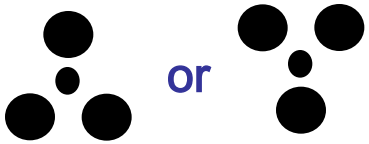

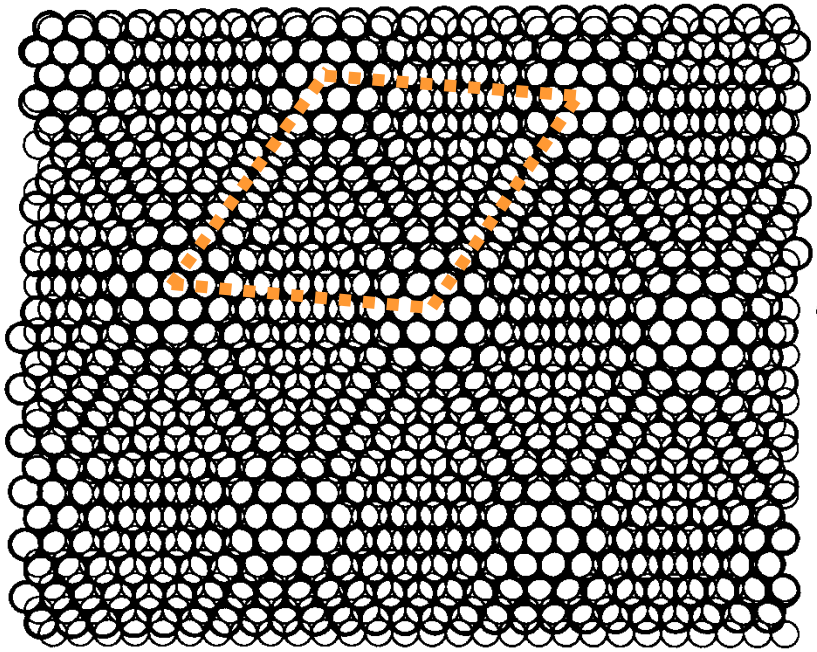

Superlattice or Moiré structure

Galloway et al., Surf. Sci. 198, 127 ('93); J. Vac. Sci. Tech. A12, 2302 ('94).

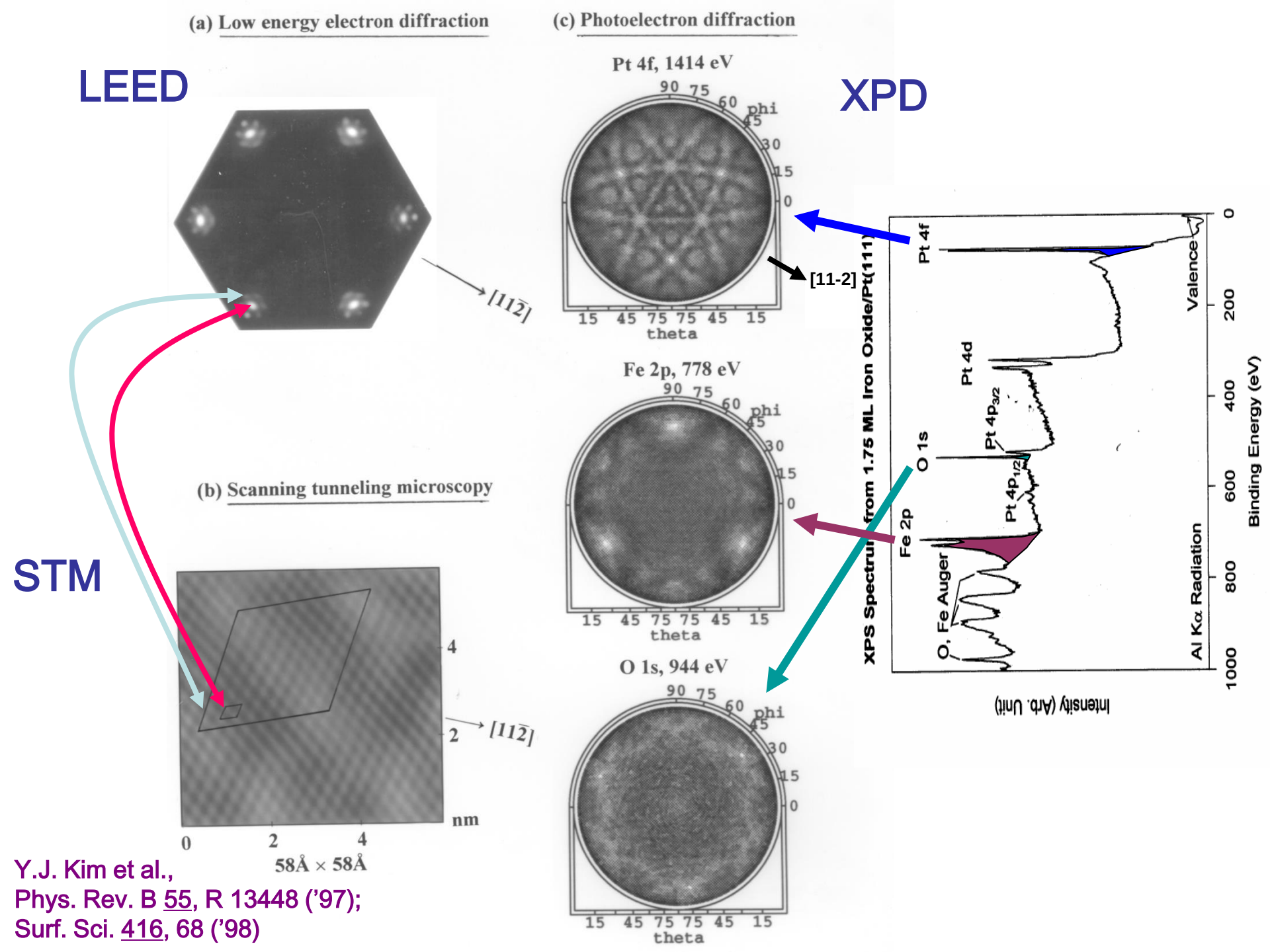

Y.J. Kim et al.,
Phys. Rev. B 55, R 13448 ('97);
Surf. Sci. 416, 68 ('98)

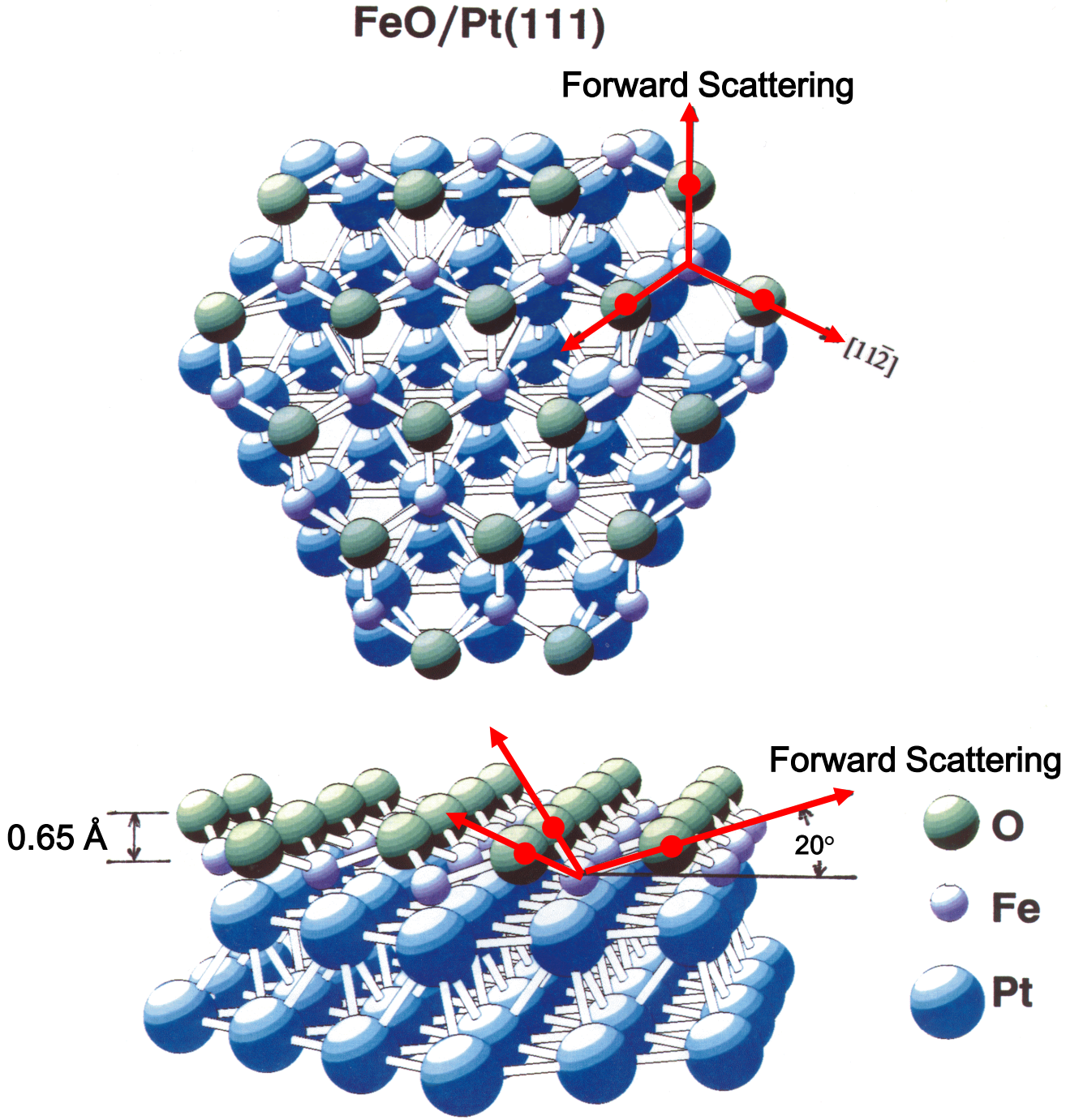
FeO/Pt(111)
Forward Scattering
[11$\bar{2}$]
Forward Scattering
0.65 Å
20°
O
Fe
Pt

X-ray Photoelectron Diffraction: Fe 2p from 1ML FeO on Pt(111)

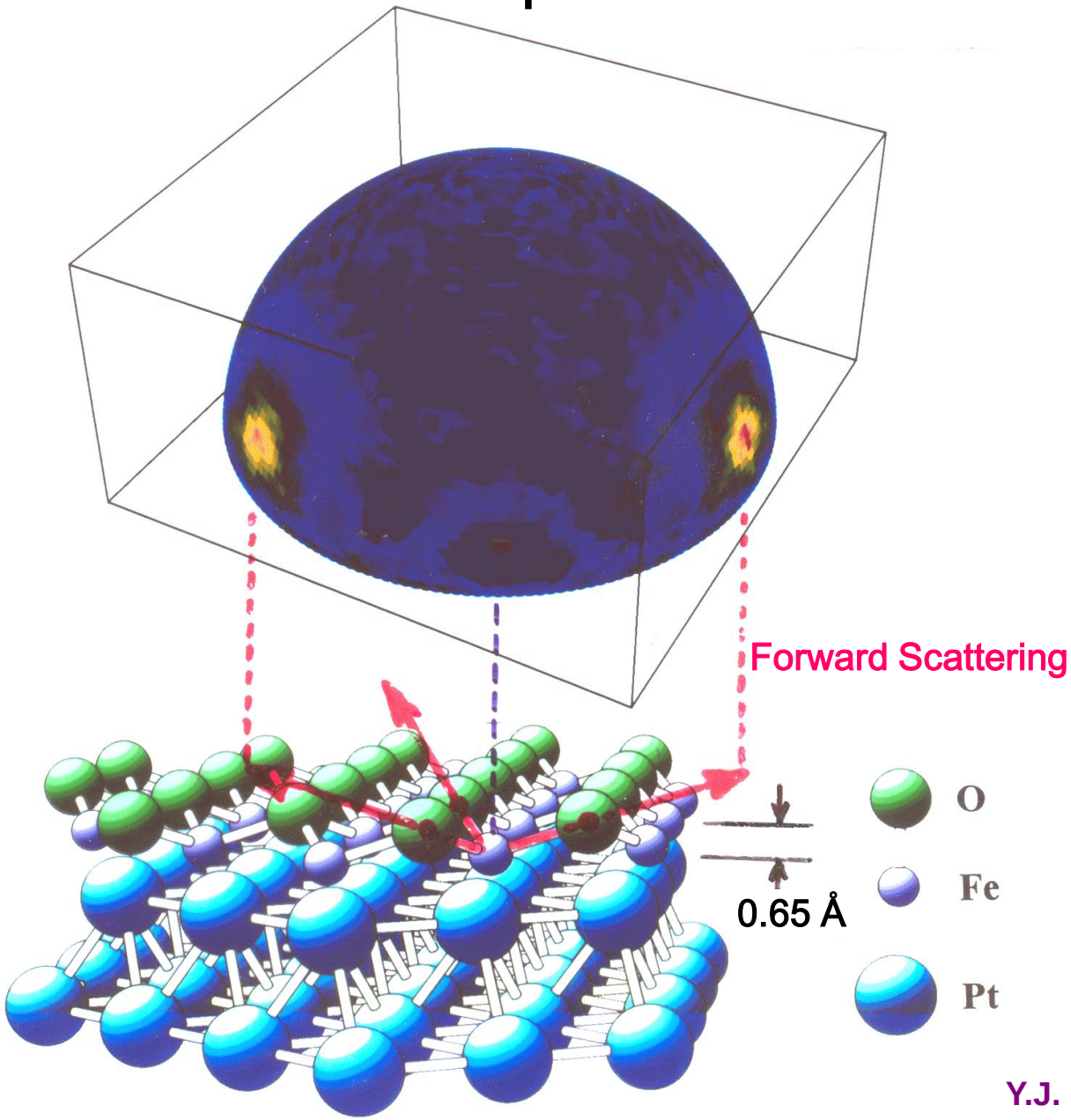

Y.J. Kim et al.
Phys. Rev. B 55, R 13448 ('97)

Permits selecting favored domain of growth—2nd layer Pt effect

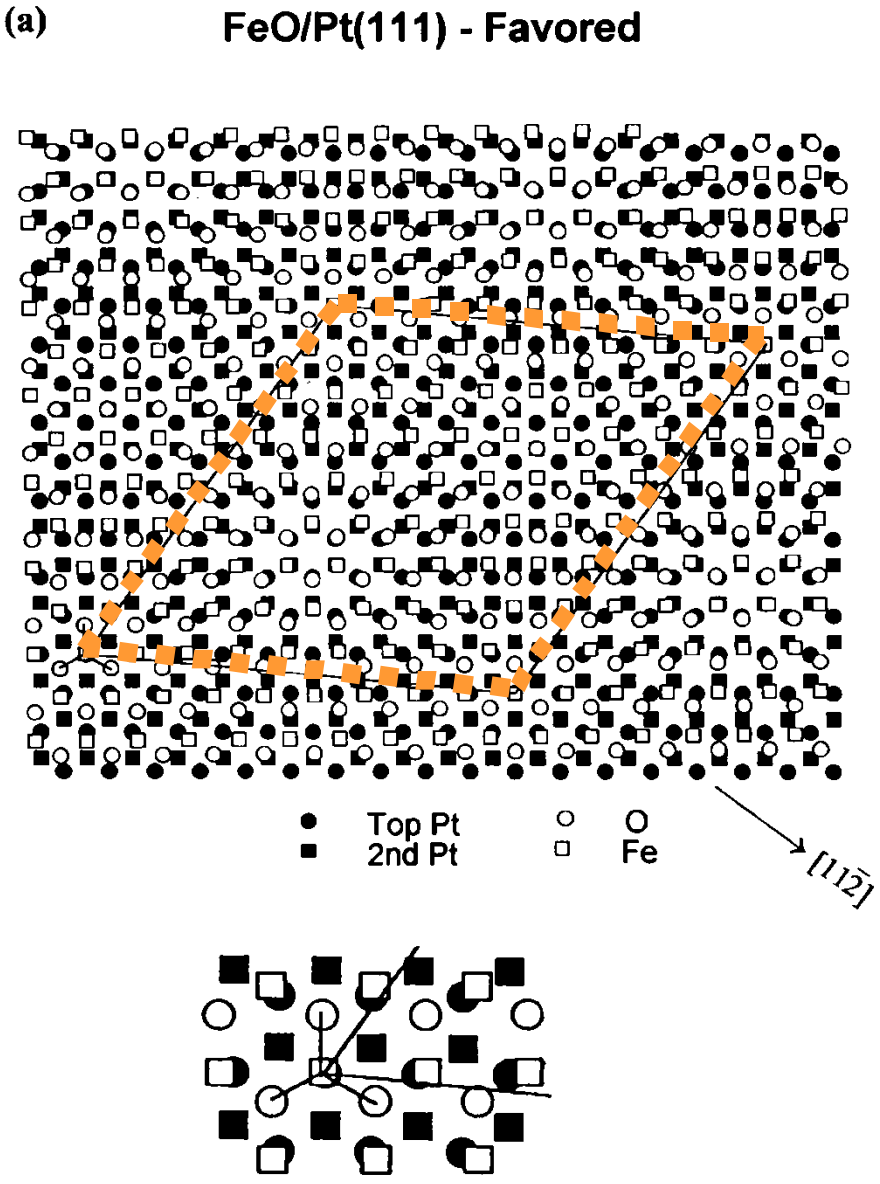

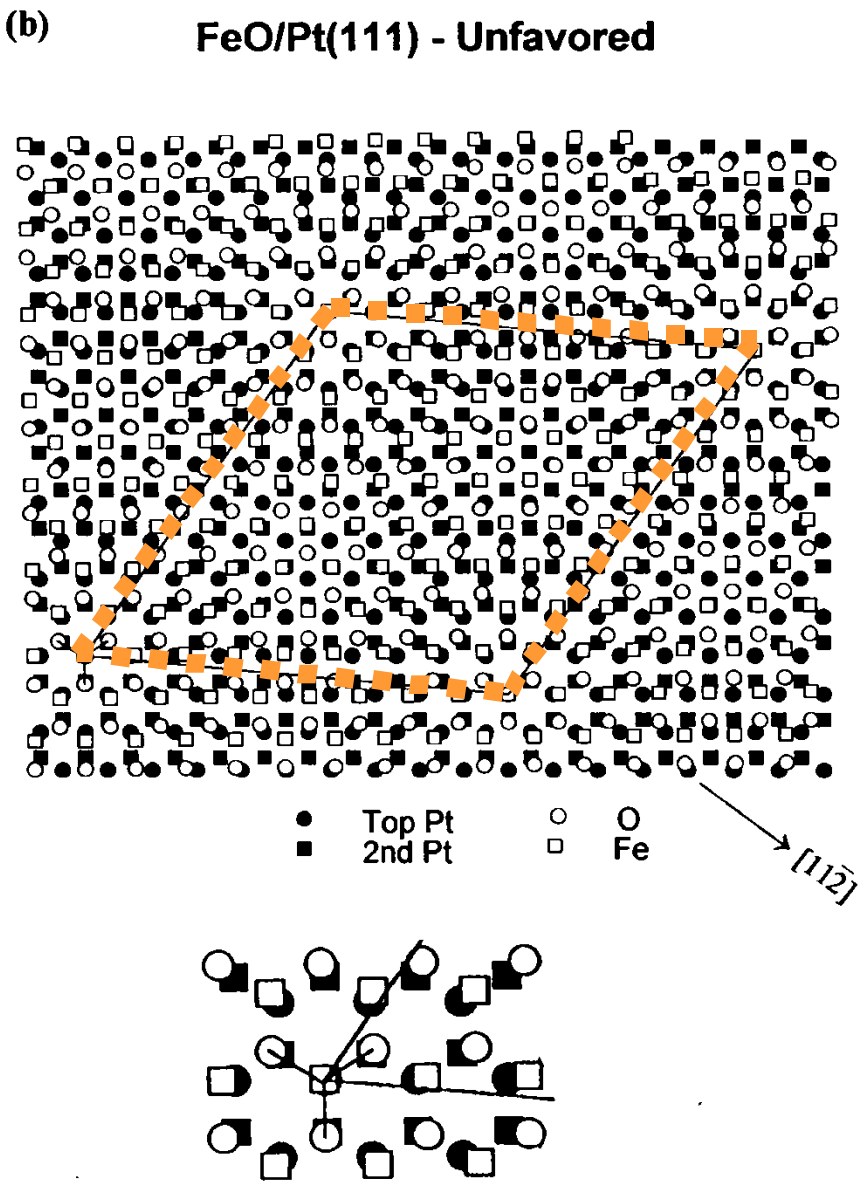

Core-Level photoelectron diffraction: Short-range (cluster) vs long-range (Kikuchi) pictures

Lower energies
up to ~1 keV
(e.g. EDAC program)

Higher energies
Above ~1 keV

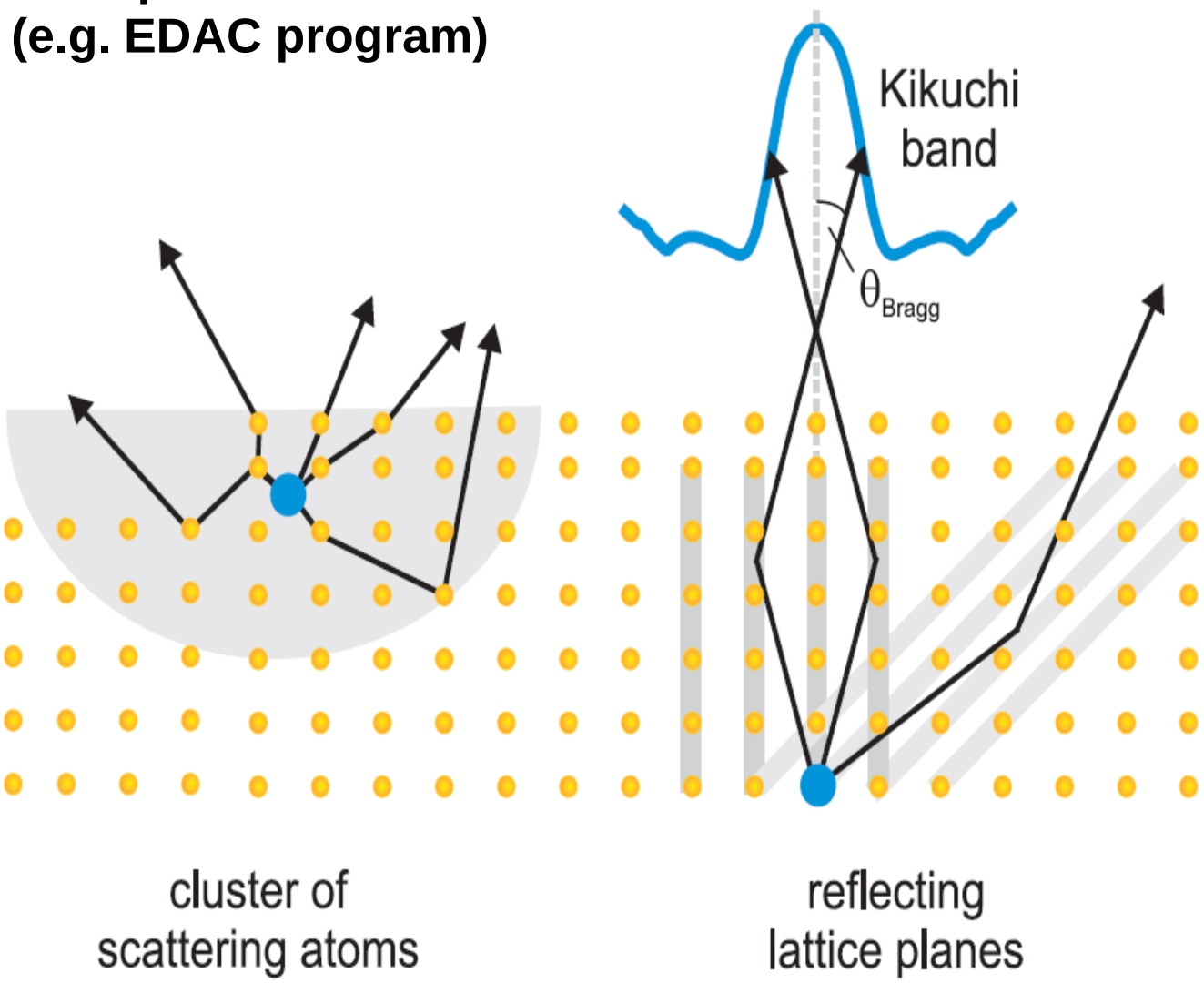

Core-Level photoelectron diffraction at higher energies: "bulk" Bragg reflection→ Kikuchi bands

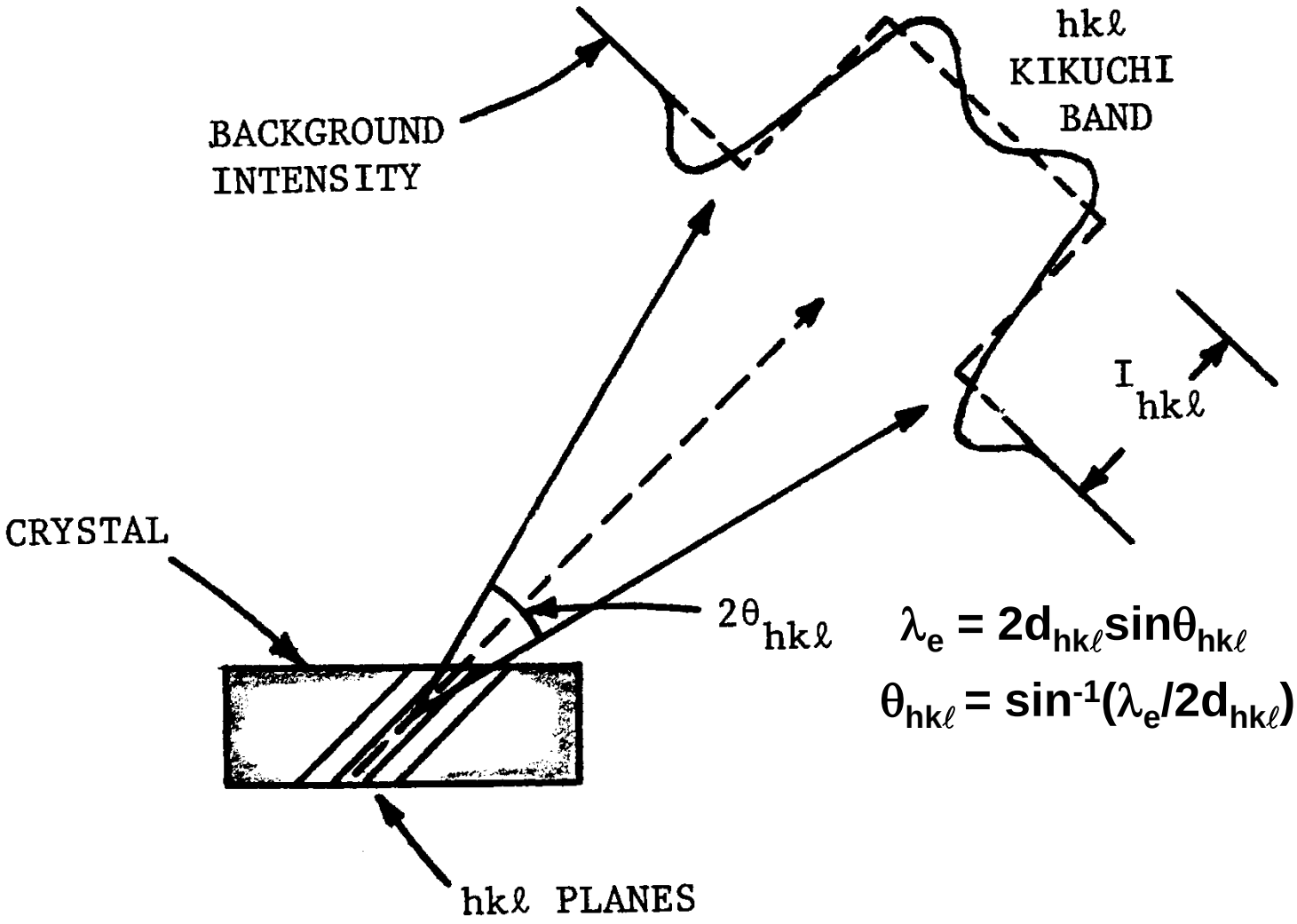

$\lambda_e = 2d_{hk\ell}\sin\theta_{hk\ell}$

$\theta_{hk\ell} = \sin^{-1}(\lambda_e/2d_{hk\ell})$

X-ray Photoelectron Diffraction from Diamond Lattice (111) Surfaces

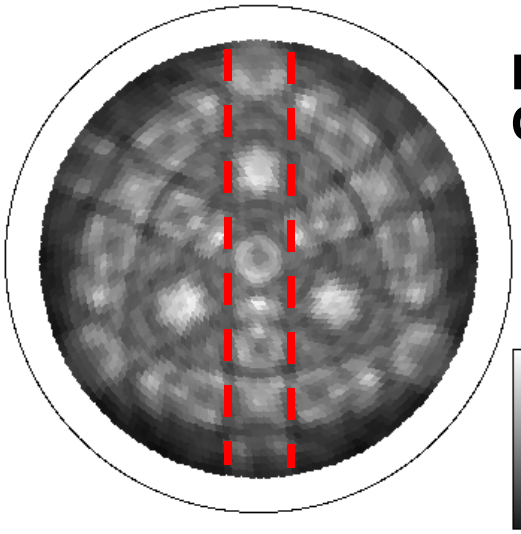

Lattice Constants

3.57Å

C 1s (964eV) from diamond(111)

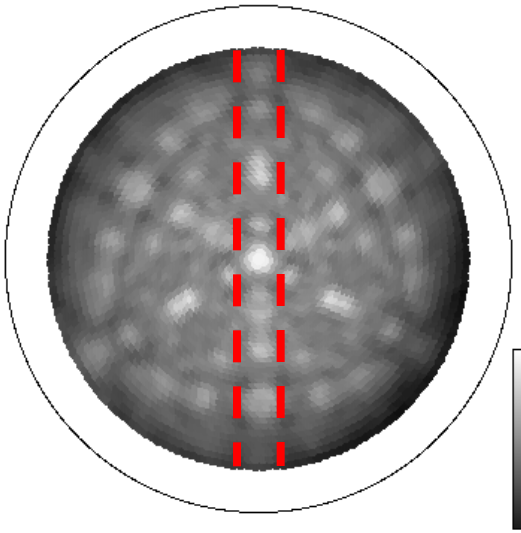

5.43Å

Si 2p (1154eV) from Si(111)

The widths of Kikuchi bands scale inversely with interplanar spacing:

$$\lambda_e = 2d_{hk\ell}\sin\theta_{hk\ell}$$

$$\theta_{hk\ell} = \sin^{-1}(\lambda_e/2d_{hk\ell})$$

J. Osterwalder, R. Fasel, A. Stuck, P. Aebi, L. Schlapbach, JESRP 68, 1 (1994)

Core-Level photoelectron diffraction at higher energies: Expt. compared to Kikuchi and Cluster theories

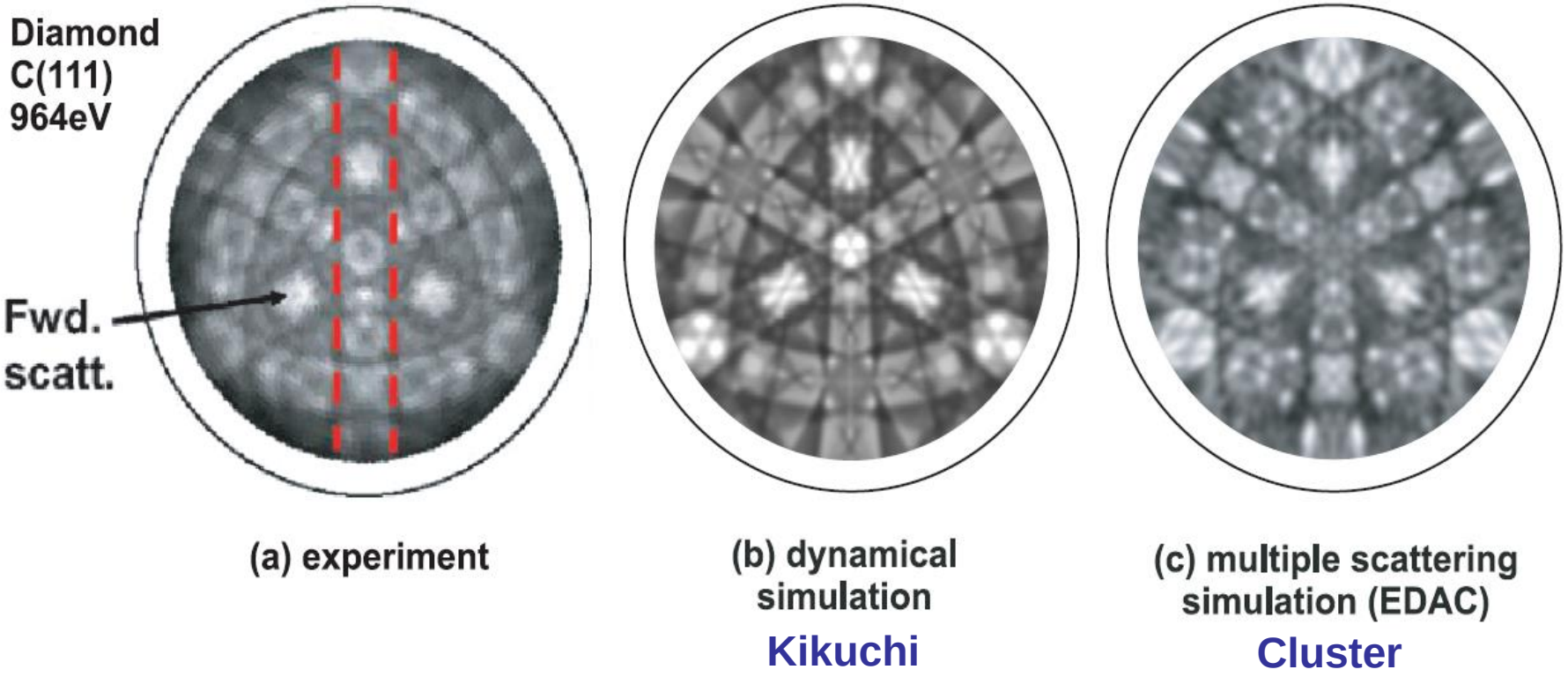

Winkelmann, Fadley, Garcia de Abajo, New Journal of Physics 10 (2008) 113002

Scanned-energy photoelectron diffraction—an alternative approach (Shirley, Woodruff/ Bradshaw, Lapeyre, Chiang et al.)

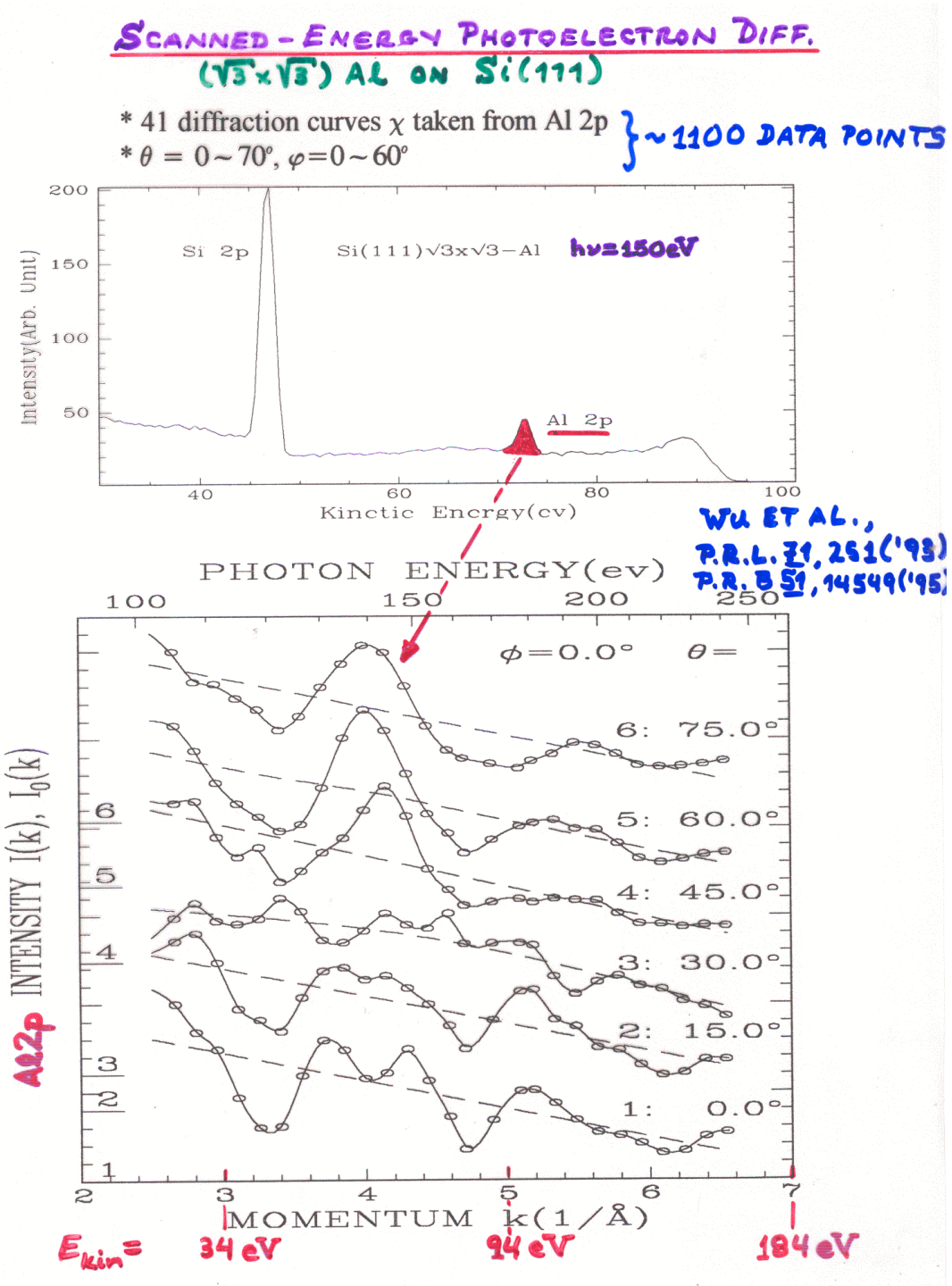

Photoelectron diffraction: Simple single-scattering theory for s-subshell emission

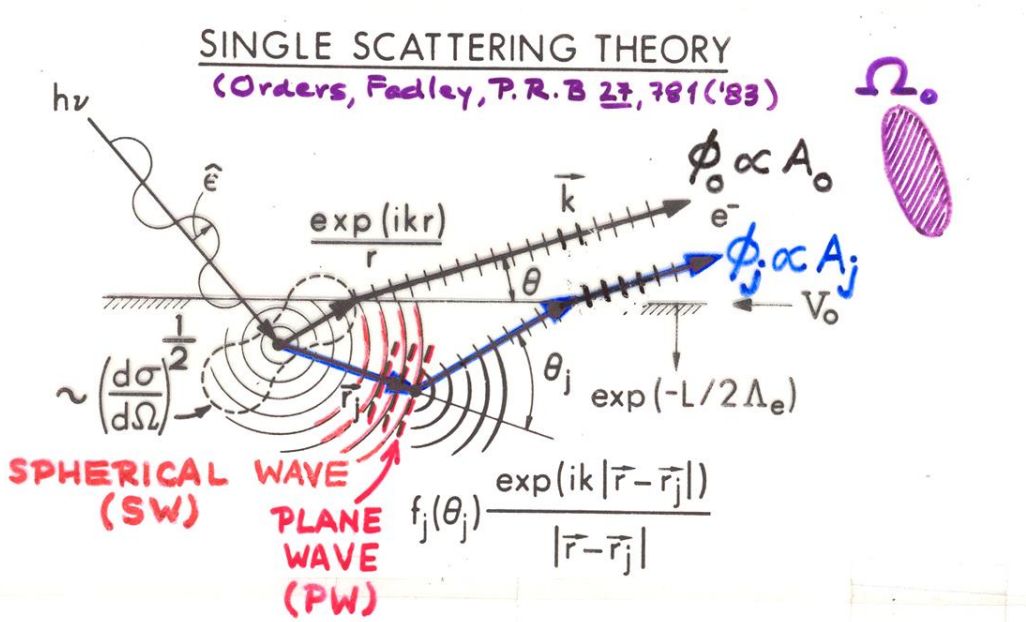

$$\chi(E \text{ or } \vec{k}) \propto \sum_{j\,(\text{CLUSTER})} \frac{F_j(k)}{F_0} \cos\left[k r_j (1-\cos\theta_j) + \Psi_j(\theta_j, k) \right]$$

PATH LENGTH DIFFERENCE (P.L.D.)

SCATTERING PHASE SHIFT

$$F_j(k) = (\hat{\varepsilon}\cdot\hat{r}_j)\frac{|f_j(\theta_j,k)|}{r_j} W_j(\theta_j,k) \exp(-L_j/2\Lambda_e)$$

ELASTIC e⁻–ATOM SCATTERING

DEBYE-WALLER

INELASTIC e⁻–e⁻ SCATTERING

= amplitude of scattered wave

$$F_0 = (\hat{\varepsilon}\cdot\hat{k}) \exp(-L_0/2\Lambda_e)$$

= amplitude of direct wave

∴ FOURIER TRANSFORM OF $\chi(k) \Rightarrow$ PEAKS AT ~ P.L.D. $= r_j(1-\cos\theta_j)$

Various papers by Shirley et al., Woodruff, Bradshaw et. al.

PATH-LENGTH DIFF'S. FROM FOURIER TRANSFORMS*

c(2x2)S/Cr(001): 45° off normal

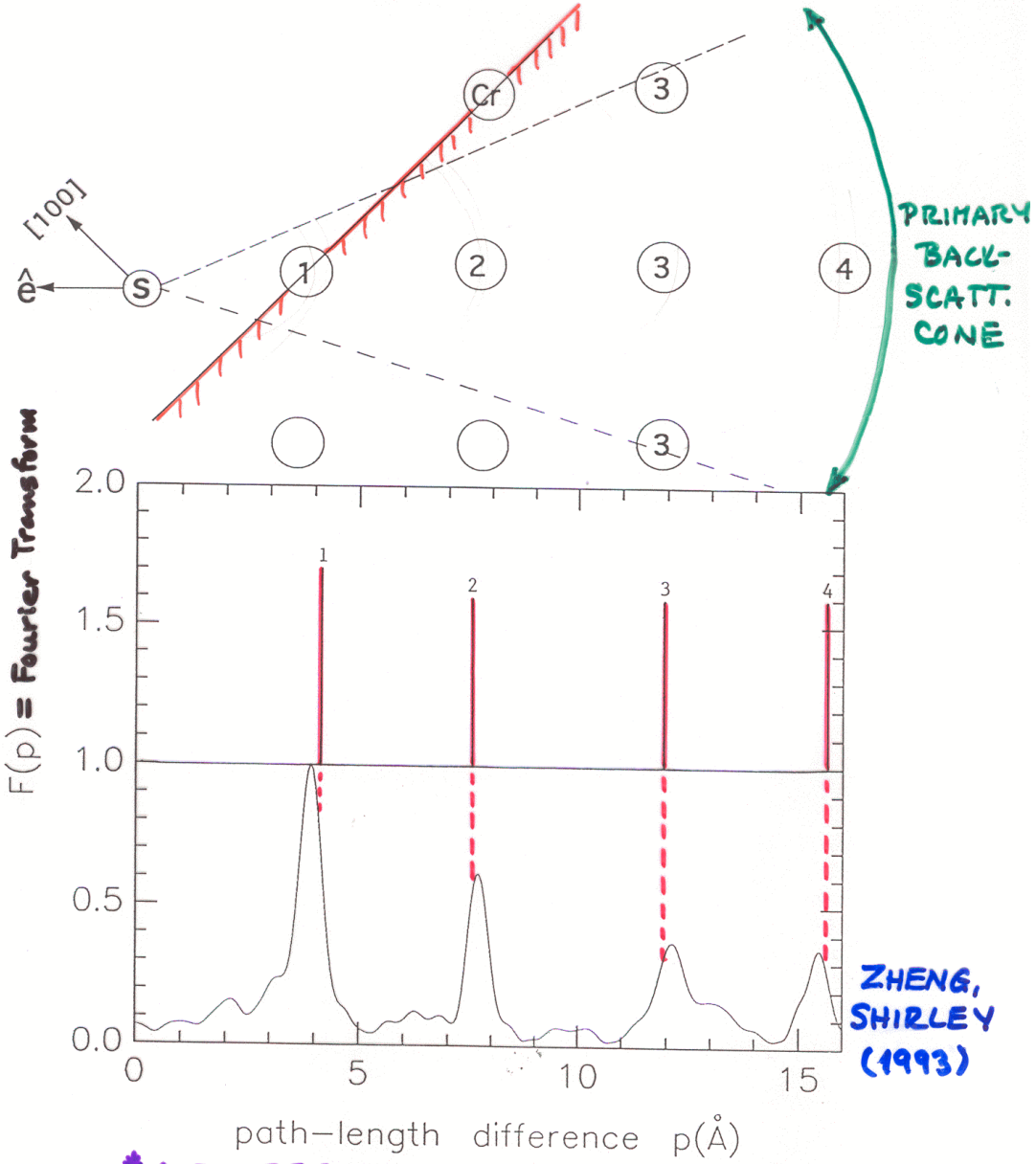

* AUTO-REGRESSIVE DATA EXTENSION

COMPARISON OF SCANNED-ENERGY PD TO EXTENDED X-RAY ABSORPTION FINE STRUCTURE

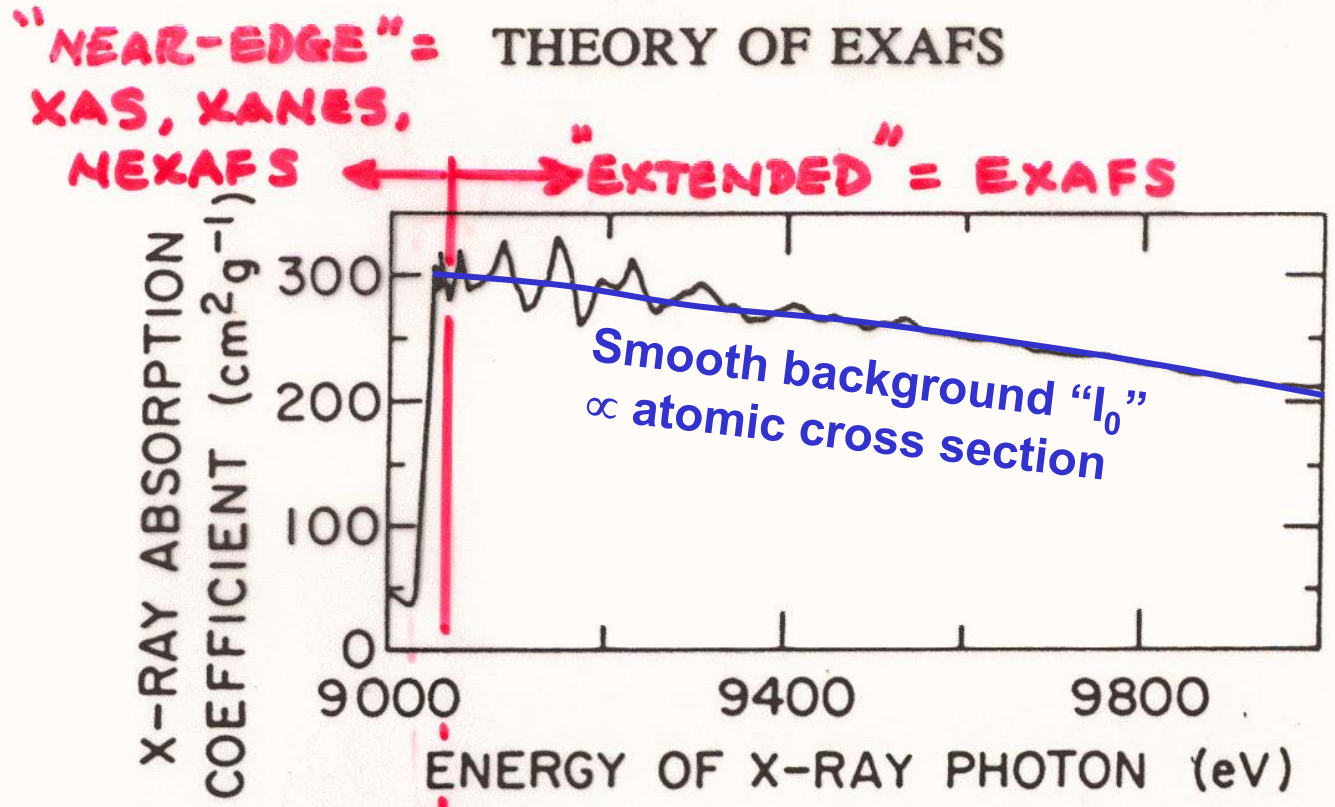

Figure 1.1. The x-ray absorption coefficient for the *K*-edge of copper metal.

Also scanned-energy, but integrates over all electron emission directions

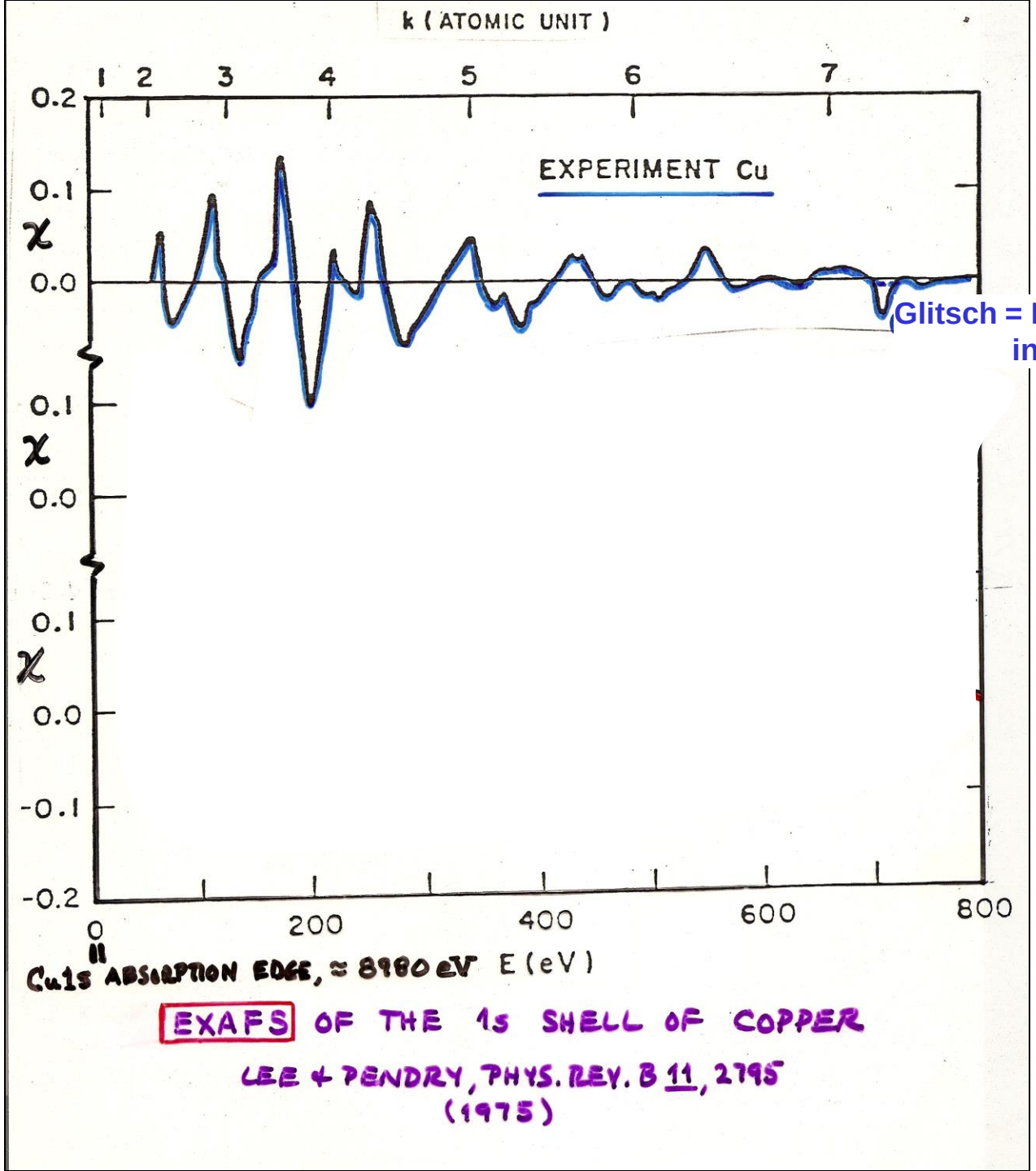

EXAFS OF THE 1s SHELL OF COPPER

LEE & PENDRY, PHYS. REV. B 11, 2795 (1975)

Glitsch = Bragg reflection in crystal

Theory of Extended X-Ray Absorption Fine Structure

SINGLE SCATTERING PLUS DOUBLE SCATTERING BACK TO EMITTER FROM A CLUSTER OF ~20–100 ATOMS ABOUT EMITTER –

SUM OVER ALL ϕ_1, ϕ_2, $I \propto |\phi_0 + \Sigma\phi_1 + \Sigma\phi_2|^2$,

THEN OVER ALL (UNOBSERVED) $\vec{k}$ DIRECTIONS

→

$$\chi(k) = \frac{\Delta\mu}{\mu_0} = -\sum_j \frac{N_j}{kr_j^2} |f_j(k,\pi)| S_0^2 \times \sin[2kr_j + \phi_j(k,\pi)] e^{-2\overline{u_j^2}k^2} e^{-2r_j/\Lambda_e(k)}$$

ALLOWS FOR SHAKEUP & SHAKEOFF LOST TO EXAFS SCATTERING

PHASES DUE TO: PATH LENGTH DIFF. | ELASTIC SCATT. | DEBYE-WALLER FACTOR | INELASTIC SCATT.

∴ FOURIER TRANSFORM OF $\chi(k)$ → PEAKS AT $\approx 2r_j$ → BOND DISTANCES

WITH: N_j = NO. SCATTERERS AT DISTANCE r_j

k = e^- WAVE VECTOR = $\sqrt{2mE}/\hbar$

$|f_j(k,\pi)|$ = BACKSCATTERING AMPLITUDE

$\phi_j(k,\pi) = \psi_j(k,\pi) + 2\delta_1$ = OVERALL BACKSCATT. PHASE SHIFT

S_0^2 = FRACTION FREE OF "SHAKE" $= |\langle \Psi_1 | \Psi_2 \rangle|^2$

$\overline{u_j^2}$ = MEAN-SQUARED VIBRATIONAL MOTION

$\Lambda_e(k)$ = INELASTIC MEAN FREE PATH

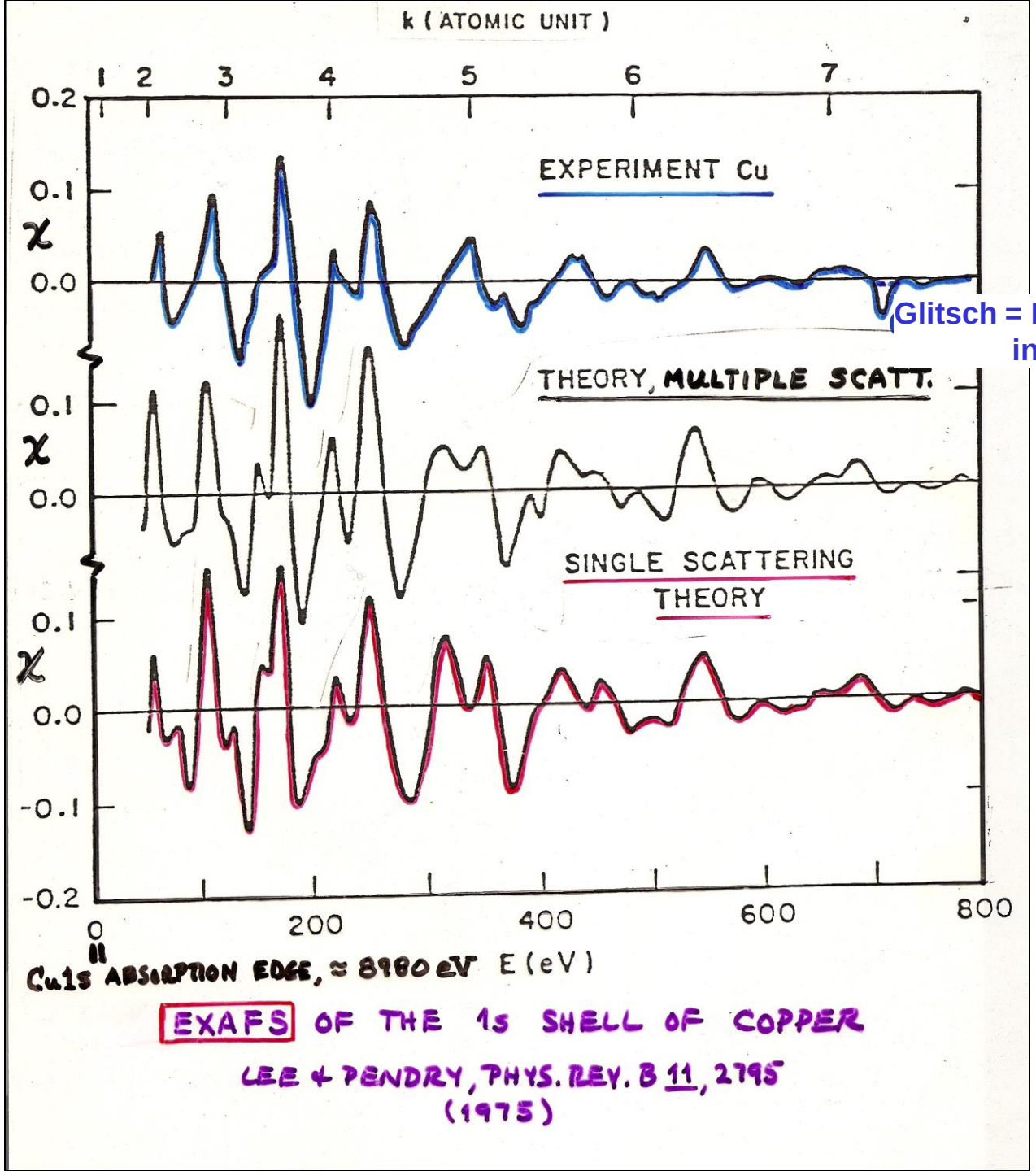

EXAFS OF THE 1s SHELL OF COPPER

LEE & PENDRY, PHYS. REV. B 11, 2795 (1975)

Glitsch = Bragg reflection in crystal

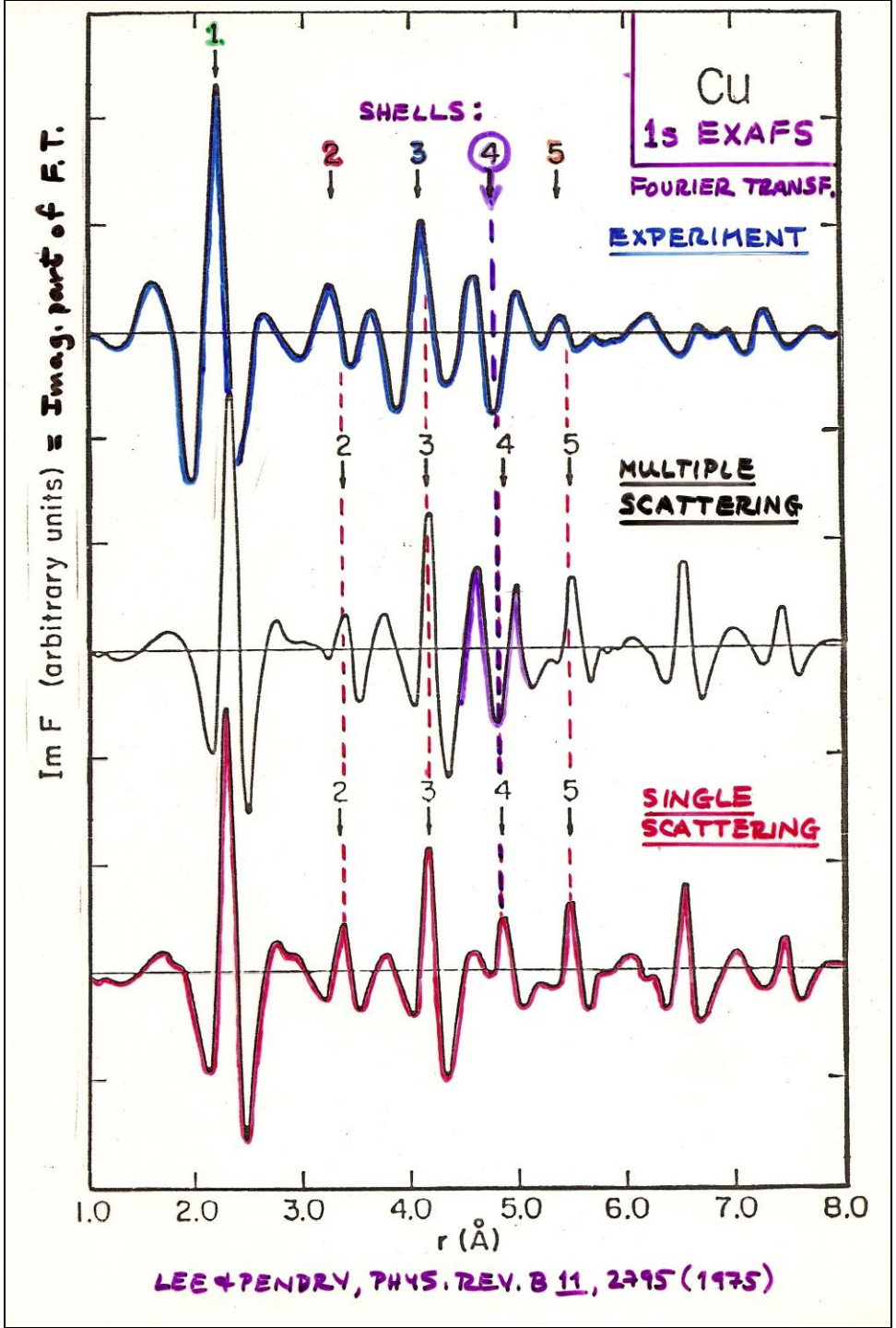

LEE & PENDRY, PHYS. REV. B 11, 2795 (1975)

Outline—Here to end of quarter

- Core-level chemical shifts: Koopmans', relaxation, the potential model
- Various other final state effects providing information in core-level spectra
- Photoelectron diffraction, extended x-ray absorption fine structure (EXAFS, XAFS)
- Photoelectron spectroscopy at realistic pressures in the multi-Torr range
- Photoelectron microscopy: adding lateral spatial resolution in 2 dimensions
- Valence-band spectra: low-energy UPS limit and high-energy XPS limit

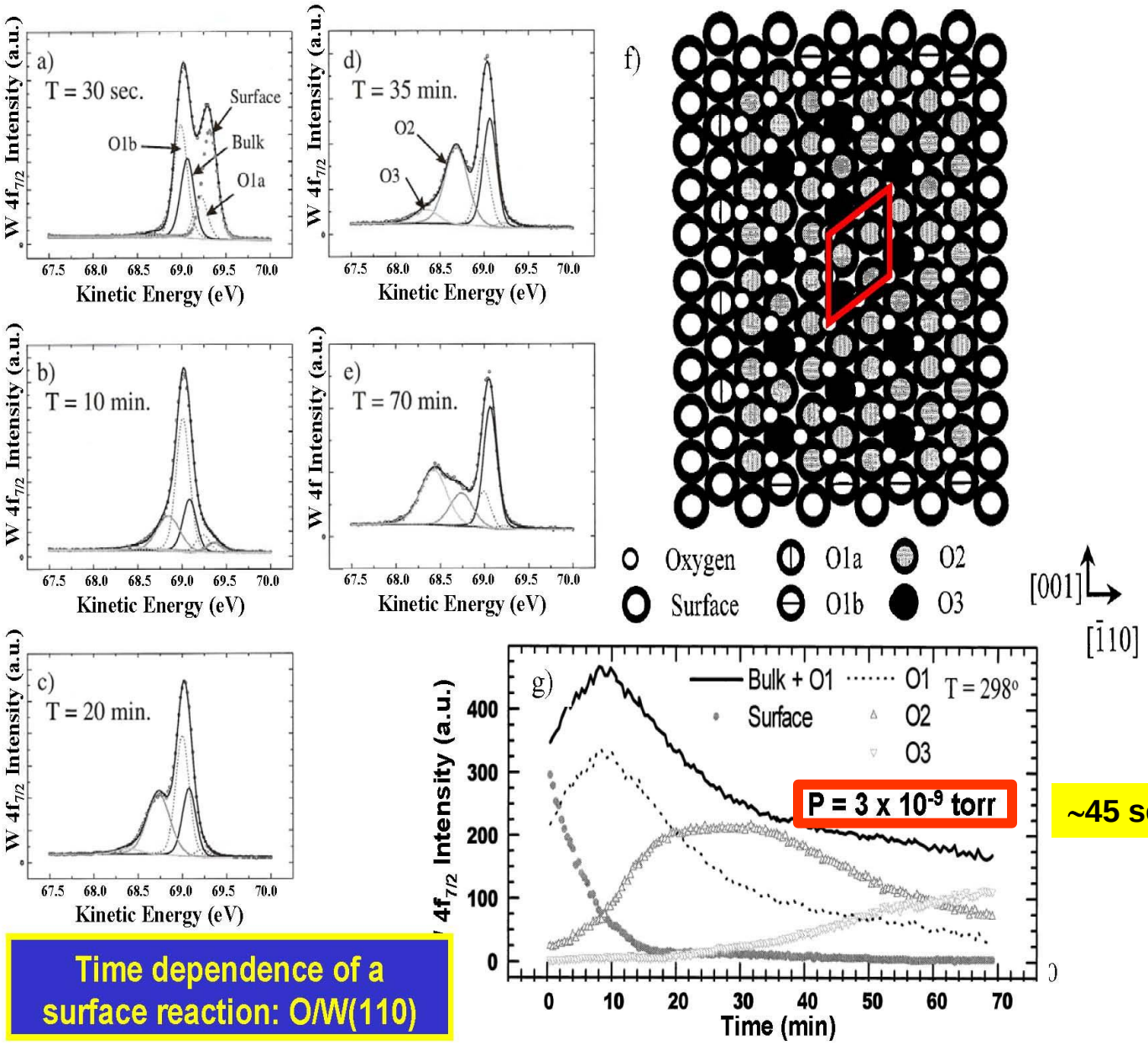

Time dependence of a surface reaction: O/W(110)

~45 sec/spectrum

Ynzunza et al., Surface Science 459, 69-92 (2000)

Ambient Pressure XPS-Bridging the Pressure Gap: State- and Time- Resolved Oxidation of Si at Multi-Torr Pressures

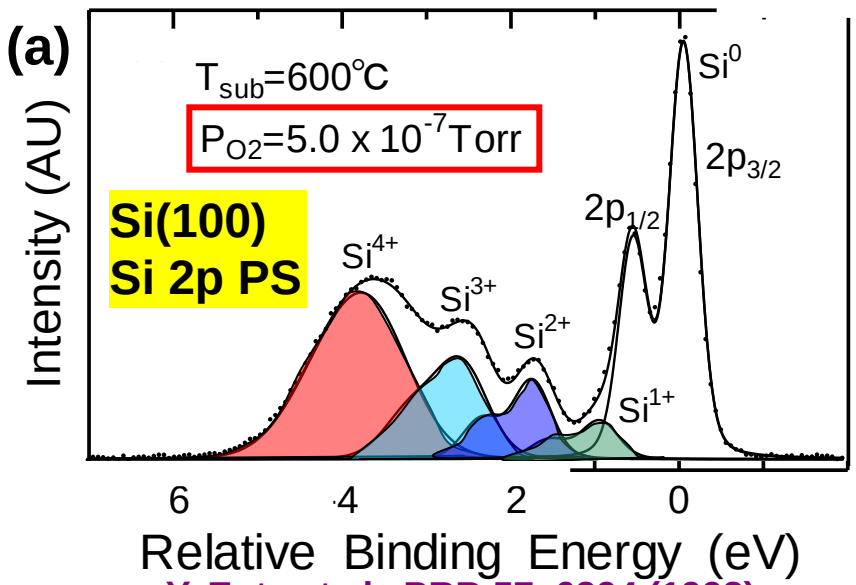

Y. Enta et al., PRB 57, 6294 (1998)

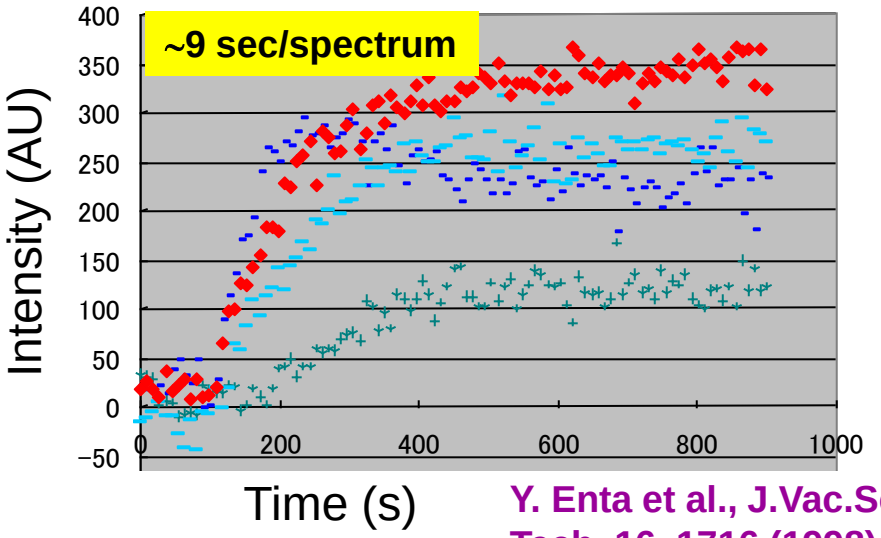

Y. Enta et al., J.Vac.Sci. Tech. 16, 1716 (1998)

Oxidation of Silicon: Time evolution at 580°C, Langmuir form

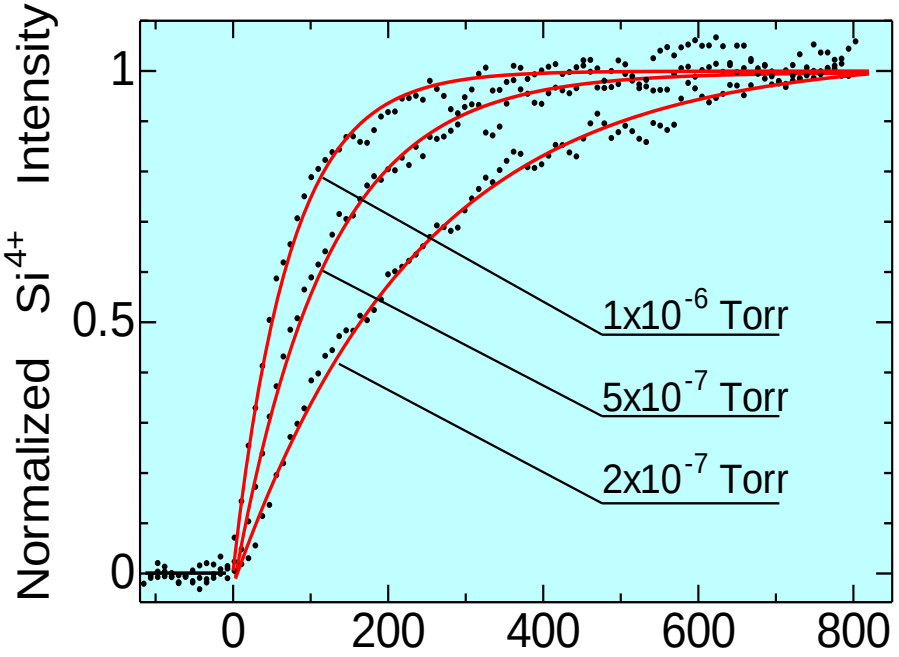

Langmuir-type adsorption: Growth rate is proportional to bare Si surface

How to go to higher, more realistic pressures?

$$\frac{d\theta}{dt} \propto P_S P (1-\theta)^n$$

θ = *oxide coverage*
P_S = *sticking probability*
P = *oxygen pressure*
n = *reaction order*

The time evolution follows $n = 1 \rightarrow$ first-order Langmuirian

Sticking probability, P_S = 0.016

Enta et al., PRB 57, 6294 (1998)

Challenges for high-pressure photoemission: analyzer pressure and short electron mean free fath

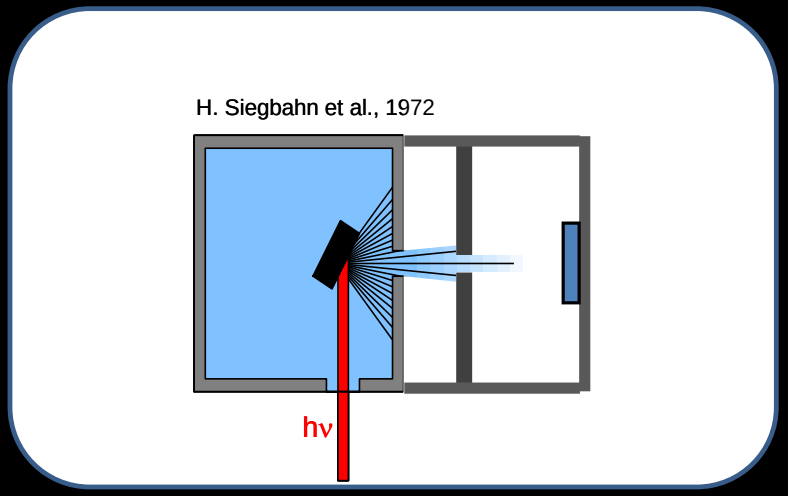

Very low efficiency

Better lens optics → Higher Pressure…

IMFP: N_2 @ 500 eV

1 atm ~ 0.003 mm = 3 microns

20 torr ~ 0.1 mm = 100 microns

1 torr ~ 2 mm

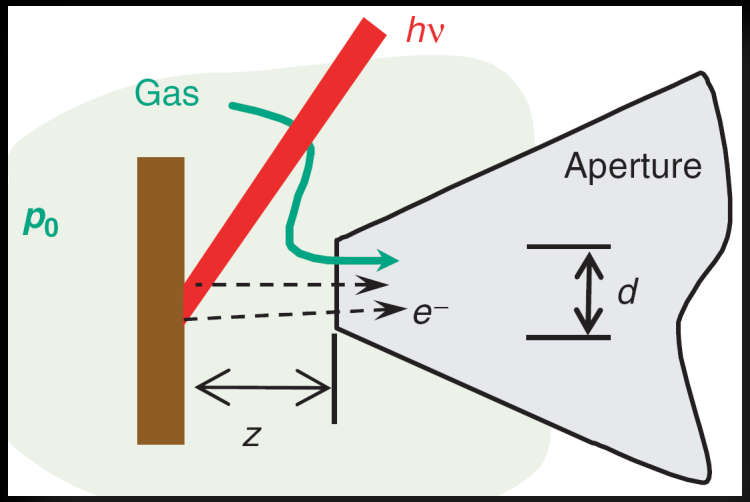

Smaller x-ray spot & z → Higher Pressure…

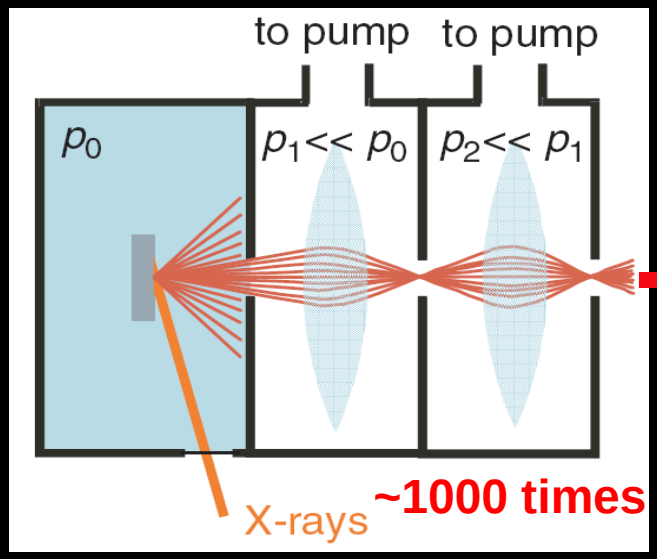

Detector

The first endstation at a SR facility (ALS, BL9.3.2):
D.F. Ogletree, H. Bluhm, G. Lebedev, C.S. Fadley, Z. Hussain, M. Salmeron, Rev. Sci. Instrum. 73 (2002) 3872.

A good review paper:
M. Salmeron and R. Schlögl, Surf. Sci. Rep. 63, 169-199 (2008).

Ambient Pressure XPS-Bridging the Pressure Gap: State- and Time- Resolved Oxidation of Si at Multi-Torr Pressures

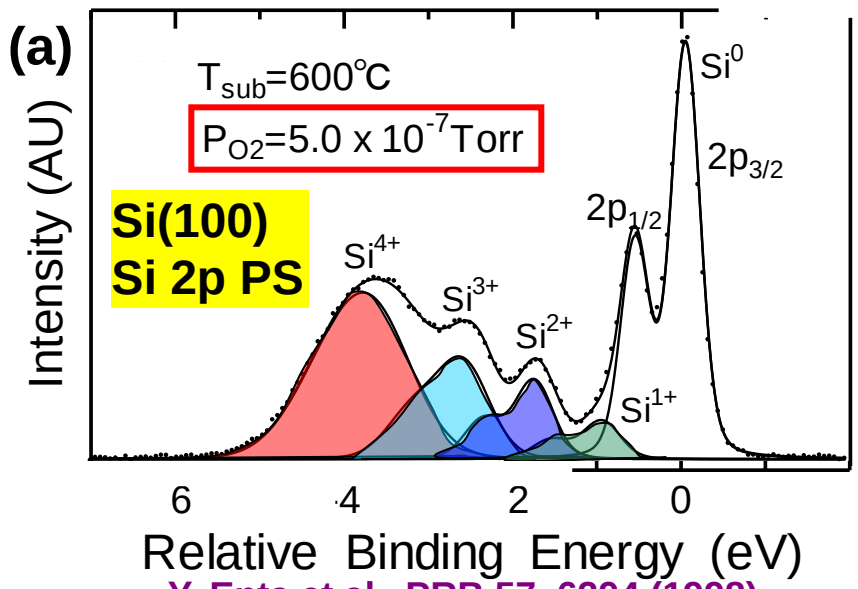

Y. Enta et al., PRB 57, 6294 (1998)

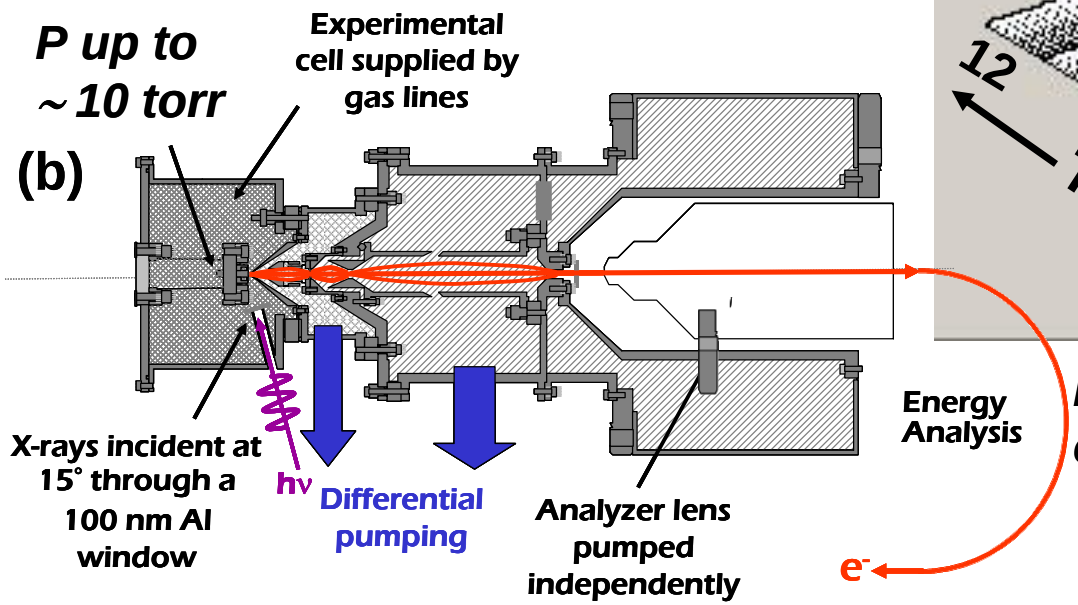

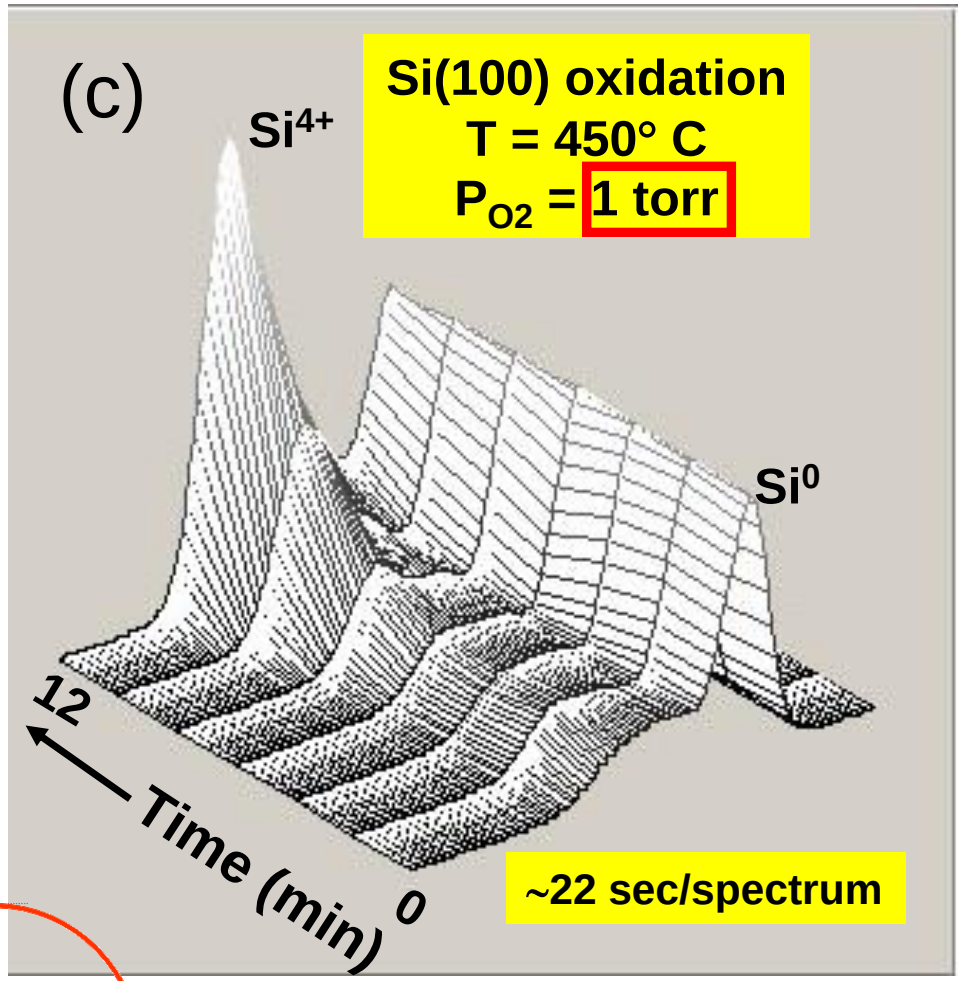

P ≈ 10^{-7} torr or better

Ogletree et al., Rev. Sci. Inst. 73, 3872 (2002)—SR, ALS
Bluhm, Salmeron, Schlögl—ALS, BESSY
Enta, Mun et al., Appl. Phys. Lett. 92, 012110 (2008); J. Appl. Phys. 103, 044104(2008)

Watching the oxide grow in real time: constant P, variable T

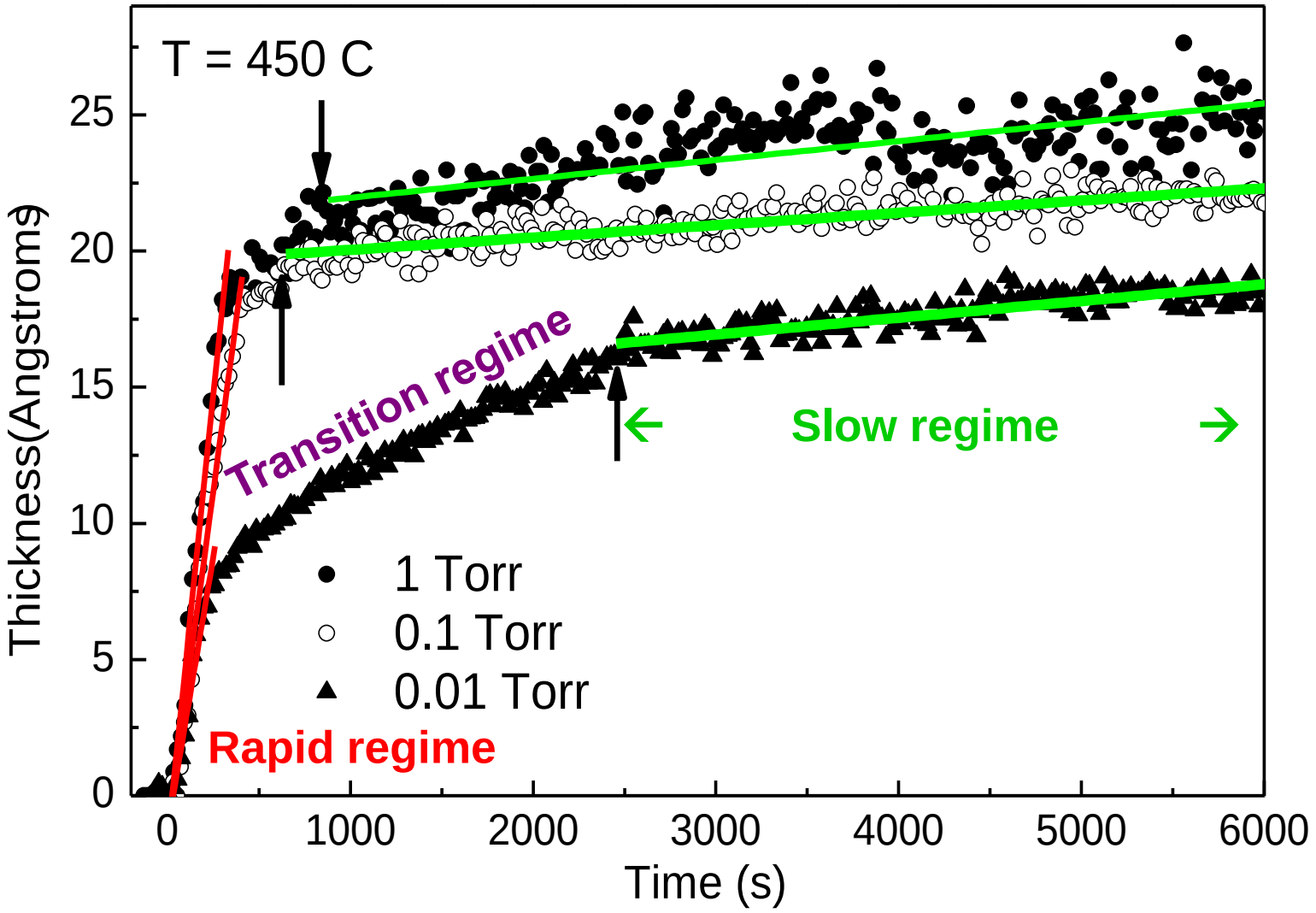

Enta, Mun et al., Appl. Phys. Lett. 92, 012110 (2008)

Measuring the concentration profile of ions near an aqueous surface

KBr (001) + H_2O

hν = 200 eV

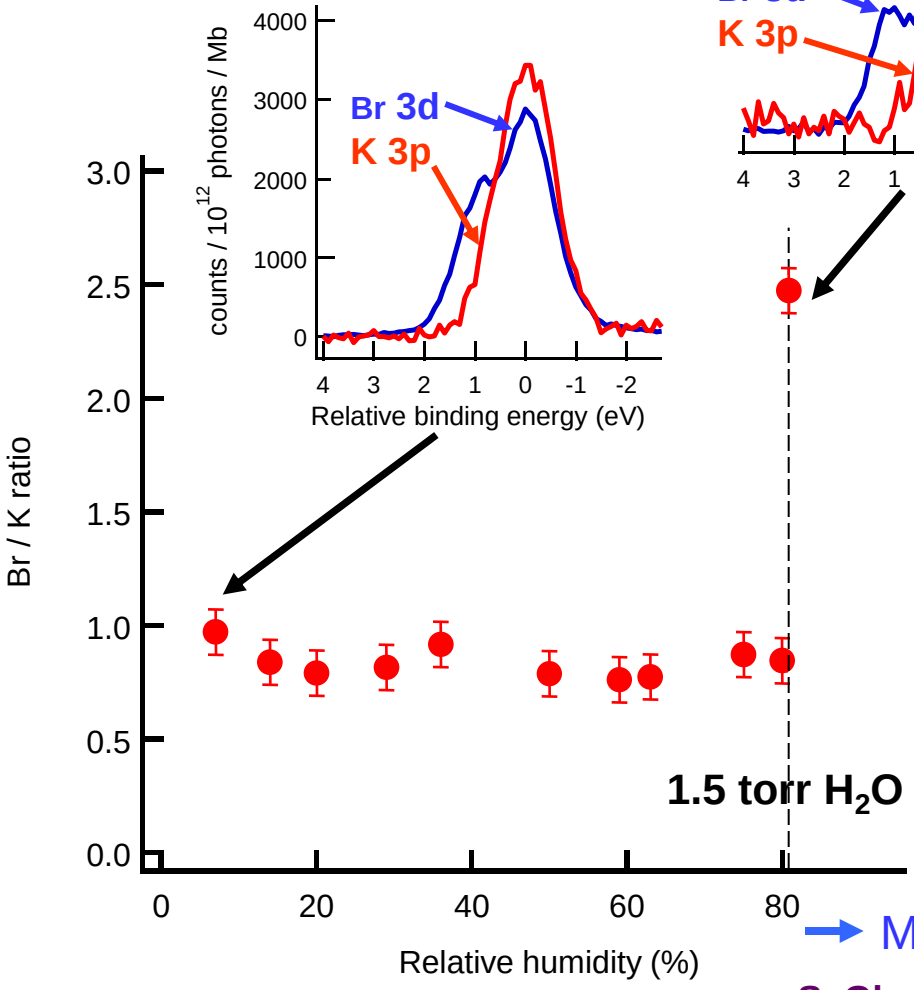

At deliquescence→
droplet formation

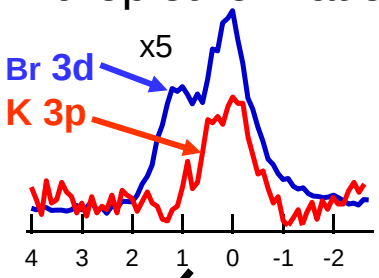

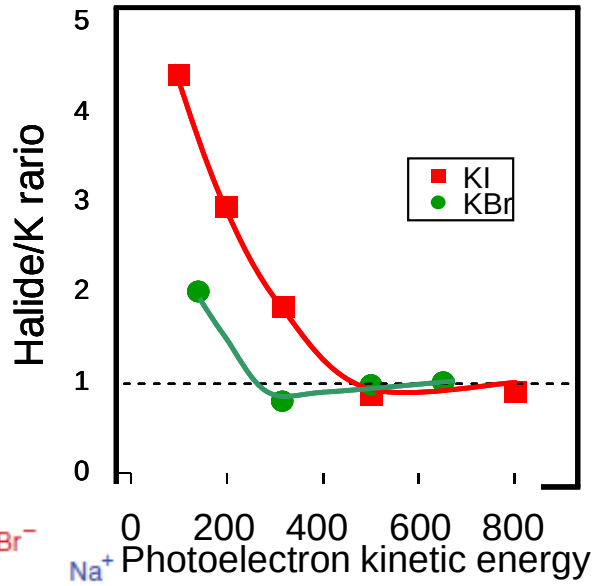

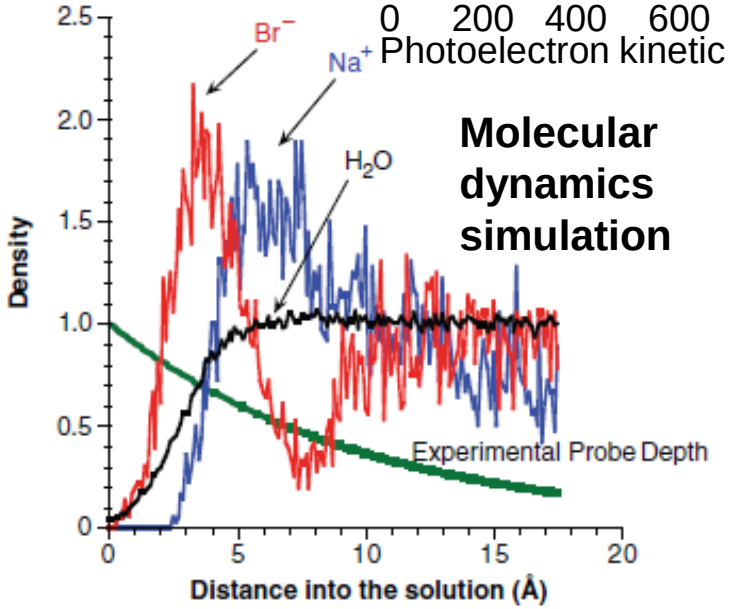

Molecular dynamics simulation

→ More halide near surface—marked change

S. Ghosal, J.C. Hemminger, et al., Science 307, 5709 (2005)

Outline—Here to end of quarter

- Core-level chemical shifts: Koopmans', relaxation, the potential model
- Various other final state effects providing information in core-level spectra
- Photoelectron diffraction, extended x-ray absorption fine structure (EXAFS, XAFS)
- Photoelectron spectroscopy at realistic pressures in the multi-Torr range
- Photoelectron microscopy: adding lateral spatial resolution in 2 dimensions
- Valence-band spectra: low-energy UPS limit and high-energy XPS limit

Imaging with soft x-ray microscopes—two types

Scanning X-ray Microscopy

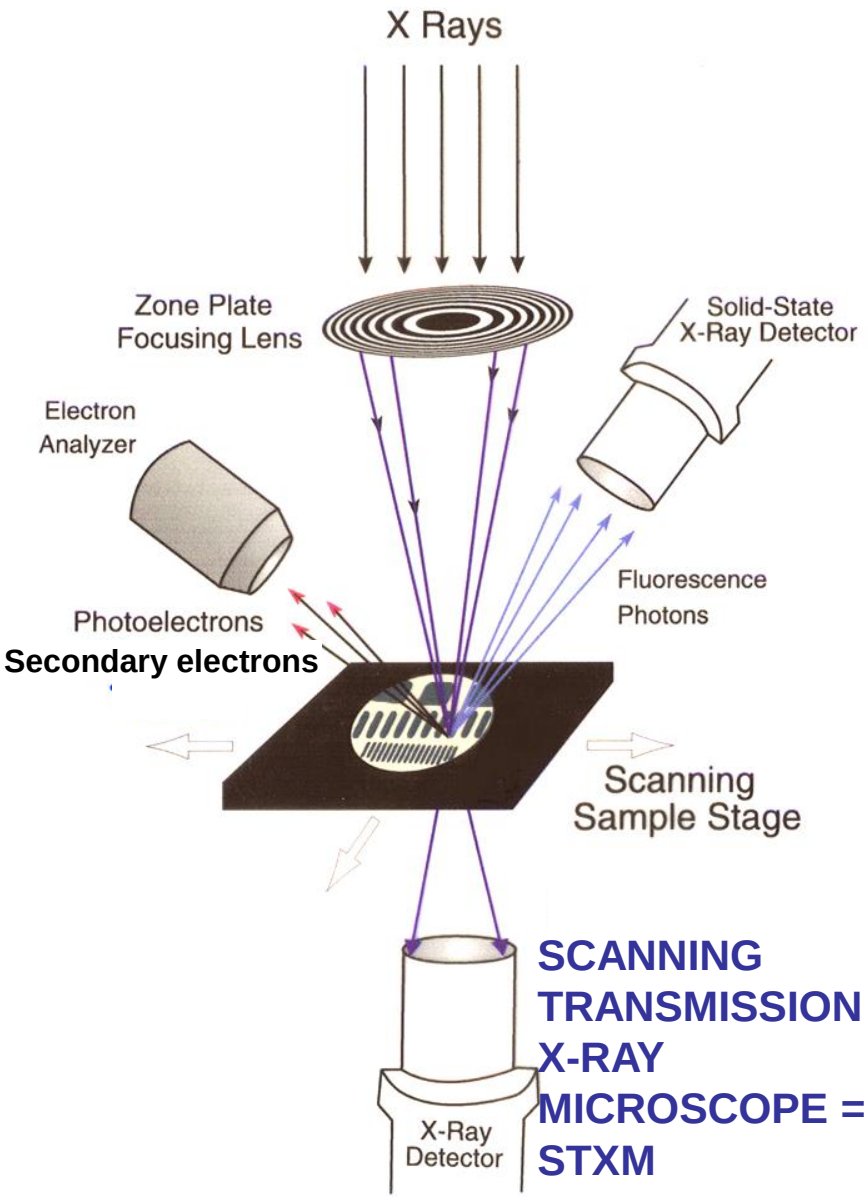

SCANNING TRANSMISSION X-RAY MICROSCOPE = STXM

X-Ray Photoelectron Microscopy

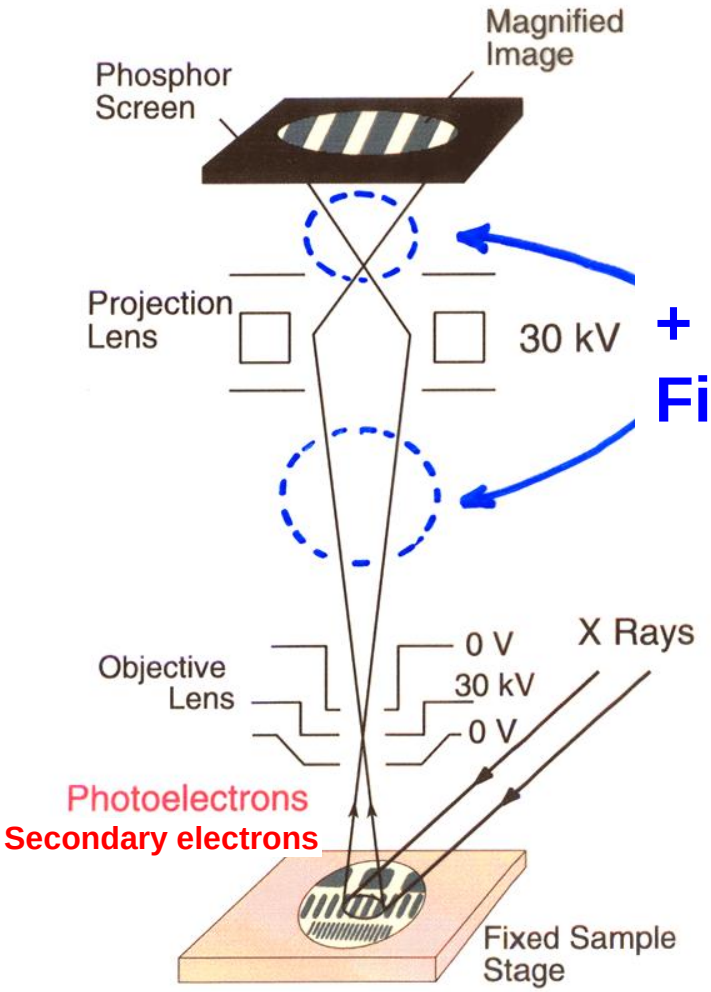

+ Energy Filter?

PHOTOELECTRON EMISSION MICROSCOPE = PEEM

Third type: Imaging Zone-Plate X-ray microscope XM-1 @ ALS

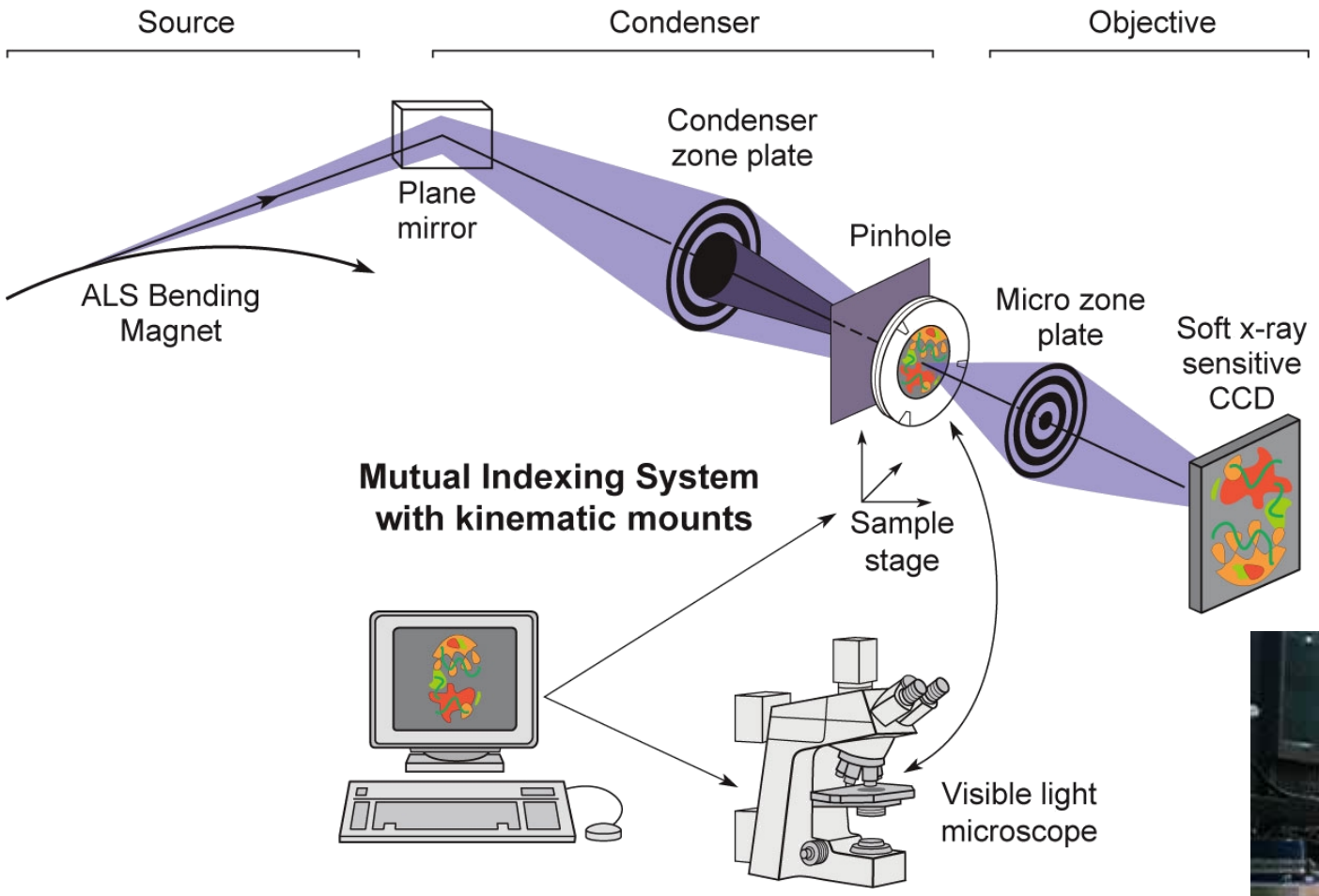

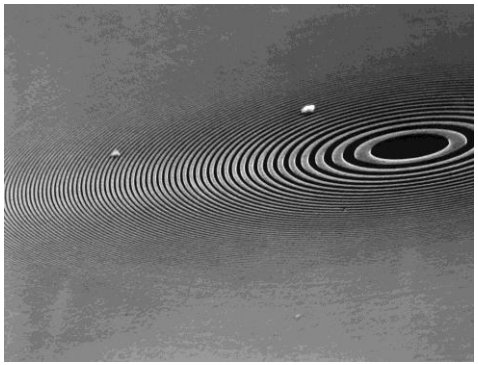

X-ray lens = zone plate
Outer rings 100 atoms apart

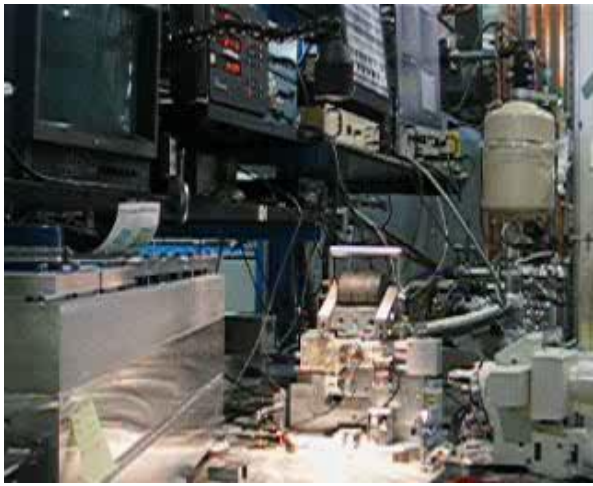

Fischer et al.

Imaging Iron Magnetic Domains with Circular-Polarized Light

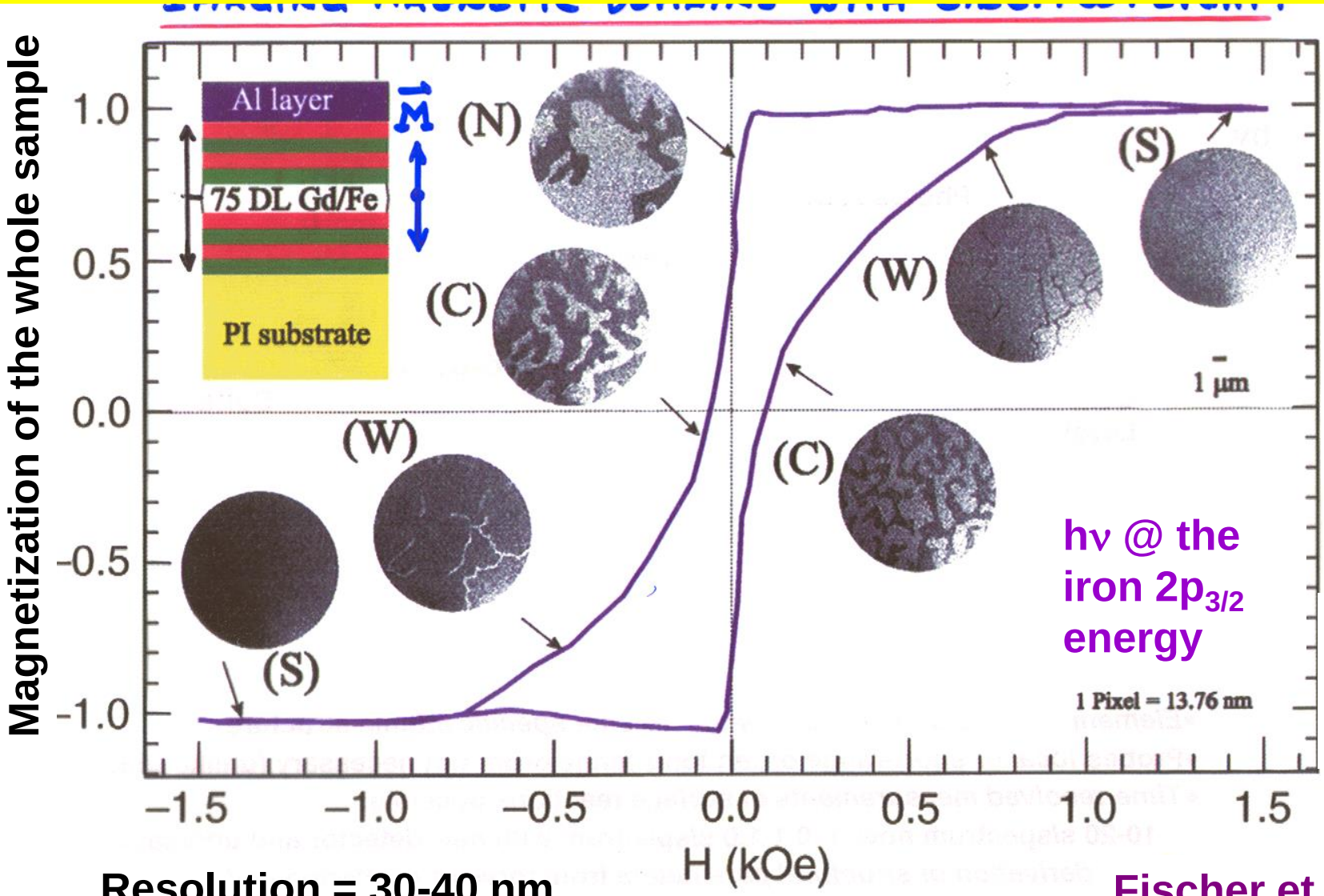

Resolution = 30-40 nm
Now 15 nm

Fischer et al.

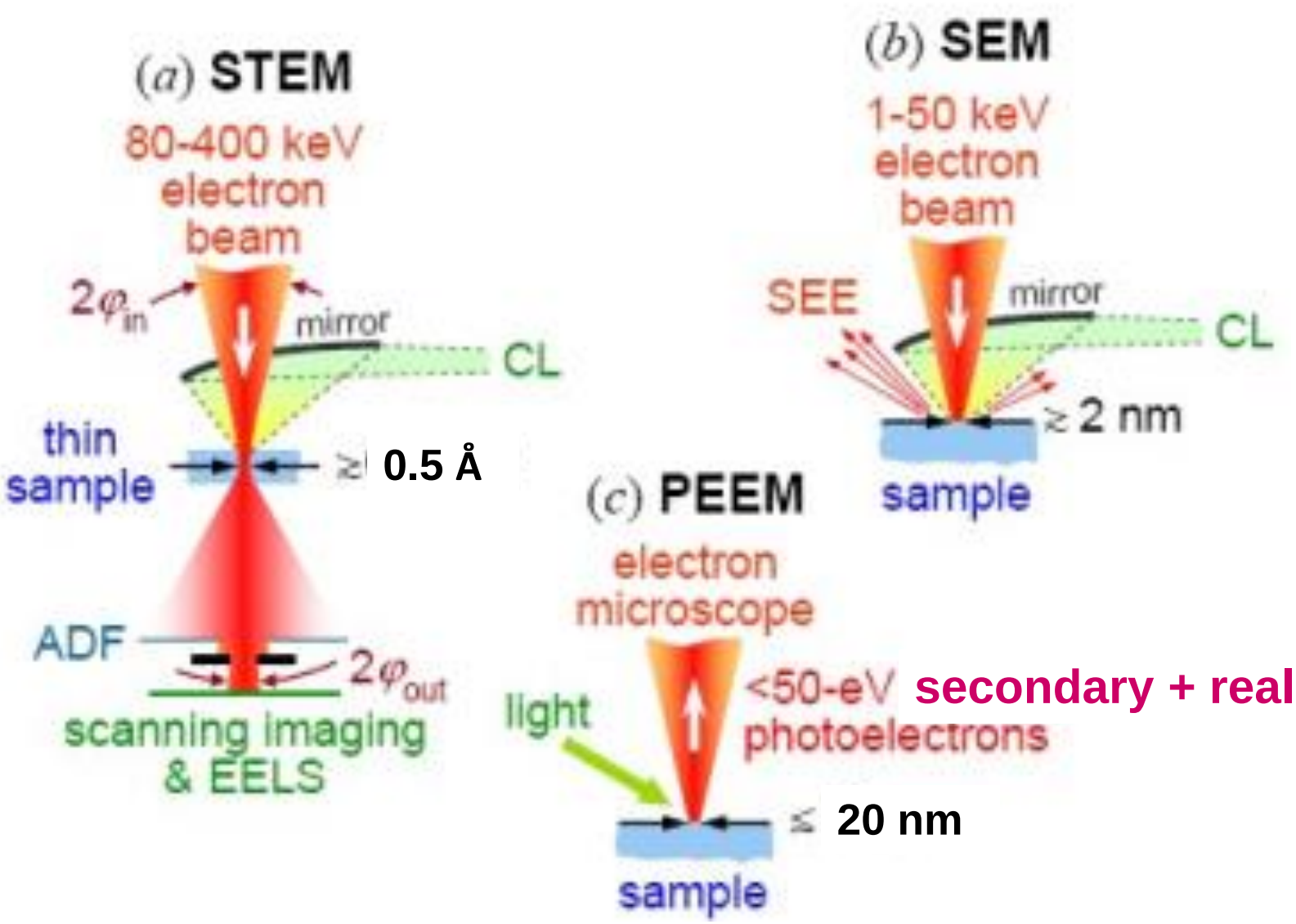
(a) STEM
80-400 keV electron beam
2φin
mirror
CL
thin sample
≳ 0.5 Å
ADF
2φout
scanning imaging & EELS
(b) SEM
1-50 keV electron beam
SEE
mirror
CL
≳ 2 nm
sample
(c) PEEM
electron microscope
light
<50-eV photoelectrons
secondary + real
≲ 20 nm
sample

Outline—Here to end of quarter

- Core-level chemical shifts: Koopmans', relaxation, the potential model
- Various other final state effects providing information in core-level spectra
- Photoelectron diffraction, extended x-ray absorption fine structure (EXAFS, XAFS)
- Photoelectron spectroscopy at realistic pressures in the multi-Torr range
- Photoelectron microscopy: adding lateral spatial resolution in 2 dimensions
- Valence-band spectra: low-energy UPS limit and high-energy XPS limit

PHOTOELECTRON EMISSION - BASIC MATRIX ELEMENTS & SELECTION RULES:

ATOMIC-LIKE (LOCALIZED) STATES ⇒ CORE:

$$\varphi_i(\vec{r}) = \varphi_{n_i l_i m_i}(r,\theta,\phi) = R_{n_i l_i}(r) Y_{l_i m_i}(\theta,\phi)$$

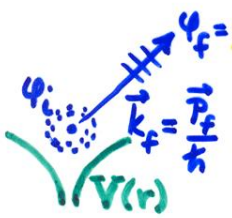

$$\varphi_f(\vec{r},\vec{k}_f) = \varphi_{E_f}(\vec{r},\vec{k}_f)$$

$$= 4\pi \sum_{l_f,m_f} i^{l_f} e^{-i\delta_{l_f}} Y^*_{l_f m_f}(\theta_{k_f},\phi_{k_f}) Y_{l_f m_f}(\theta,\phi) R_{E_f l_f}(r)$$

(PHASE SHIFT OF l_f WAVE IN V(r))

DIPOLE APPROX.: INT. $\propto |\langle\varphi_f|\hat{\varepsilon}\cdot\vec{r}|\varphi_i\rangle|^2 = |\hat{\varepsilon}\langle\varphi_f|\vec{r}|\varphi_i\rangle|^2 \Rightarrow$

- $\Delta l = l_f - l_i = \pm 1$ TWO CHANNELS
- $\Delta m = m_f - m_i = 0, \pm 1$ LINEAR POLARIZ.
- $\Delta m = \pm 1$, CIRCULAR POLARIZATION

EQUIVALENT WITHIN CONSTANT FACTOR ($\vec{p} \leftrightarrow \vec{\nabla} V(r)$)

VALENCE BANDS IN SOLIDS:

BLOCH-FUNCTION (DELOCALIZED) STATES ⇒ VALENCE:

$$\varphi_i(\vec{r}) = u_{\vec{k}_i}(\vec{r}) e^{i\vec{k}_i\cdot\vec{r}}$$

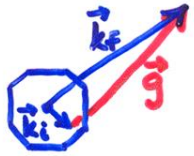

BRILLOUIN ZONE

$$\varphi_f(\vec{r}) = u_{\vec{k}_f}(\vec{r}) e^{i\vec{k}_f\cdot\vec{r}} \; ; \; E_f = \frac{p_f^2}{2m} = \frac{\hbar^2 k_f^2}{2m}$$ USUALLY NEGLIG.

$$|\langle\varphi_f|\hat{\varepsilon}\cdot\vec{p}|\varphi_i\rangle|^2 = |\hat{\varepsilon}\cdot\langle\varphi_f|\vec{p}|\varphi_i\rangle|^2 \Rightarrow \Delta\vec{k} = \vec{k}_f - \vec{k}_i - \vec{k}_{hv} + \vec{k}_{PHONON}$$

$$= \vec{g}_{BULK} \; (\text{OR } \vec{g}_{SURF})$$

"DIRECT" TRANSITIONS

BUT LATTICE VIBRATIONS ⇒ SUM OVER $\vec{k}_{PHONON}$

⇒ FRACTION DIRECT ≈ DEBYE-WALLER FACTOR

$$\approx \exp[-g^2 \overline{u^2}]$$

NEARLY-FREE ELECTRONS IN A WEAK PERIODIC POTENTIAL—1 DIM.

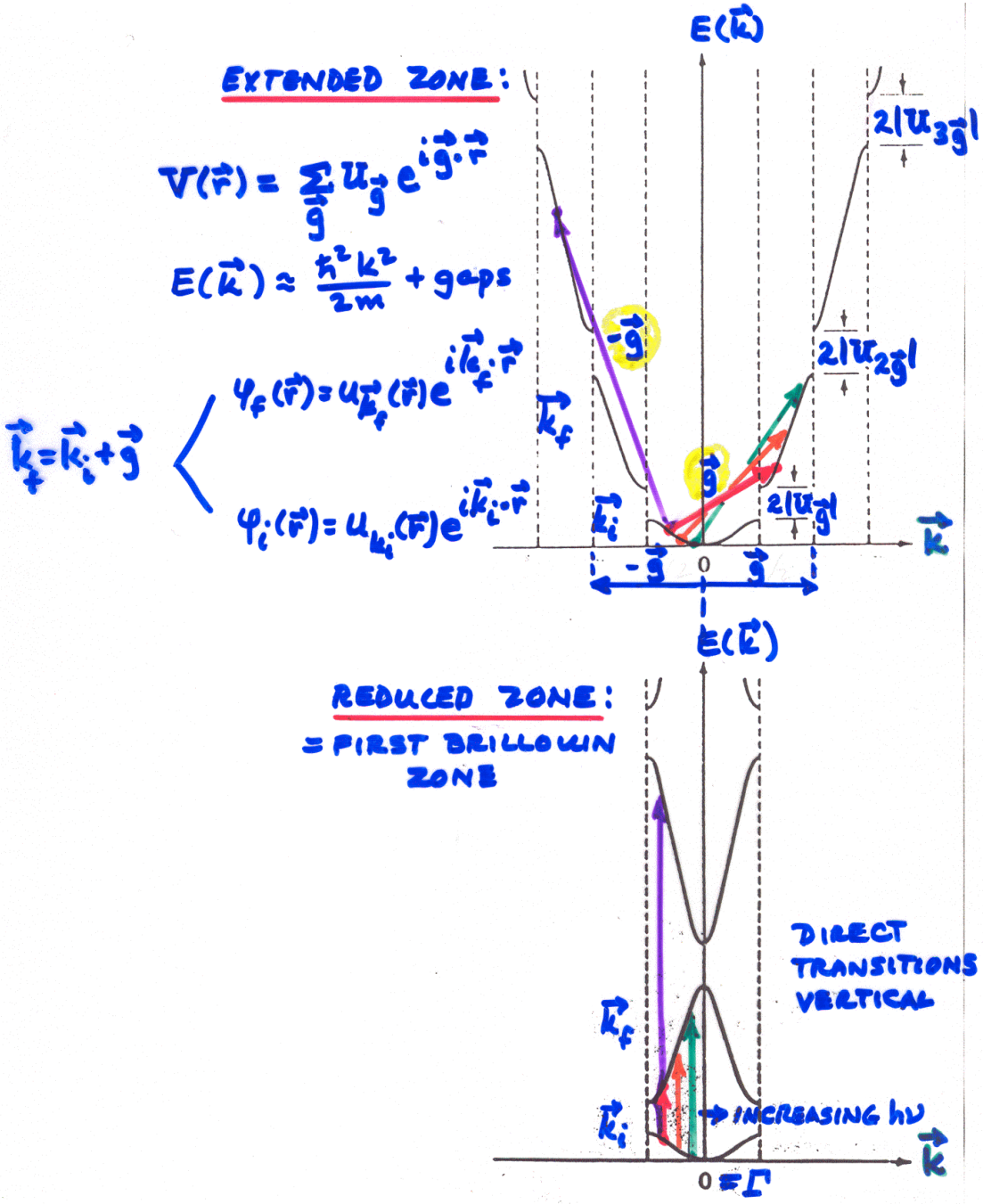

ALUMINUM – ELECTRONIC BANDS & D.O.S.

The electronic structure of a nearly free-electron metal—fcc Al

$$\phi(\vec{r}) = u_{\vec{k}}(\vec{r})\, e^{i\vec{k}\cdot\vec{r}}; \quad E(\vec{k}) \approx \frac{\hbar^2 k^2}{2m}$$

(Bloch)

3D Brillouin zone

REAL fcc:

↓

RECIP. bcc

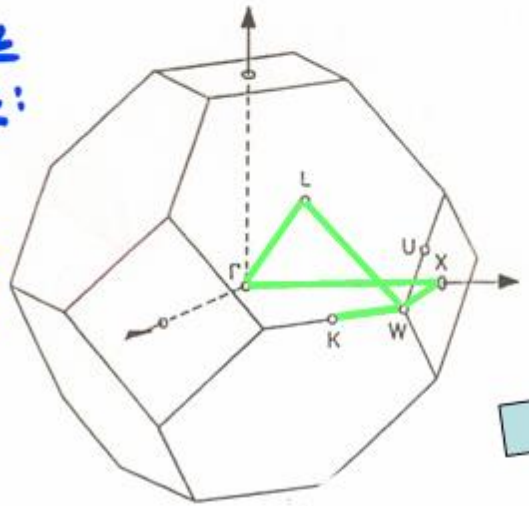

D.O.S.

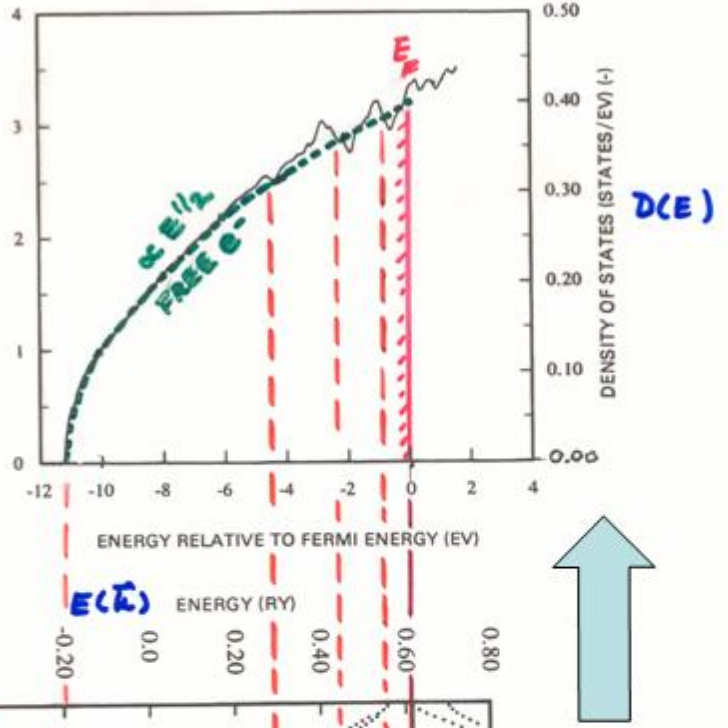

D(E)

BANDS

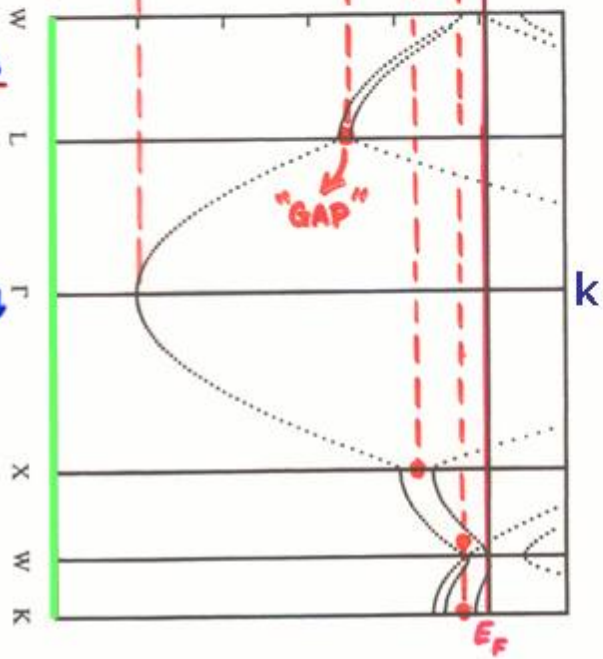

k = 0

Moruzzi, Janak, Williams, Pergamon, 1978

Conservation Laws in Valence-Band Photoelectron Spectroscopy:

$\vec{k}_{f,\parallel} = \vec{K}_{f,\parallel}$

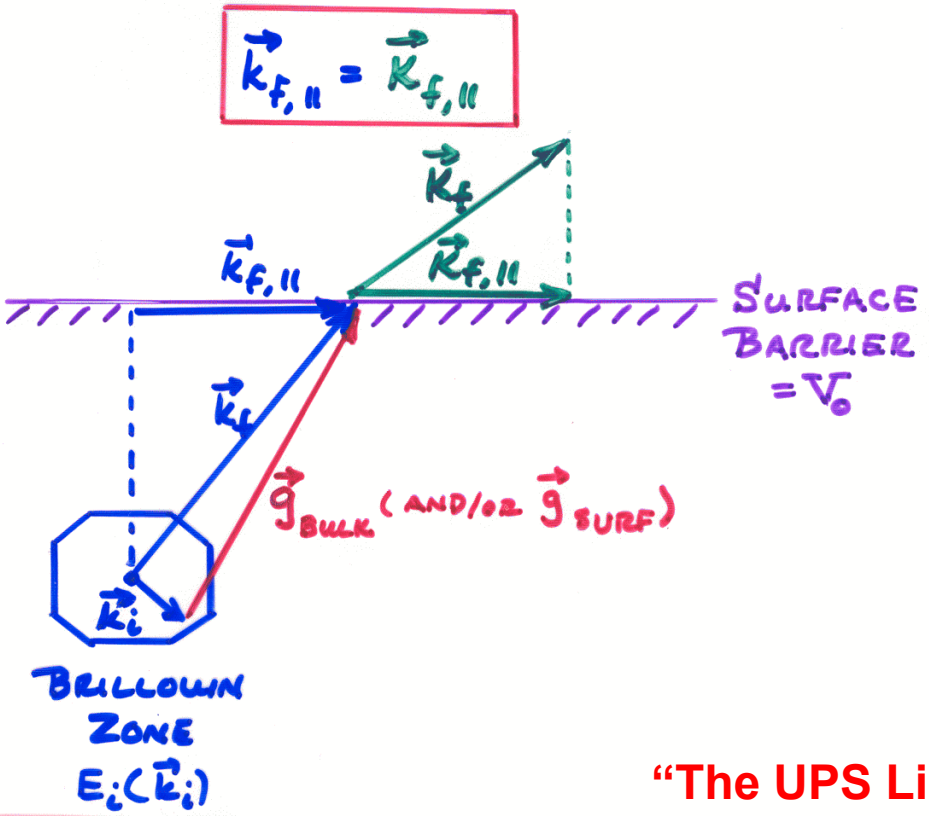

"The UPS Limit"

$$\vec{k}_f = \vec{k}_i + \vec{g}_{BULK}(\vec{g}_{SURFACE}) + \cancel{\vec{k}_{h\nu}} + \cancel{\vec{k}_{PHONON}}$$

NEGLIGIBLE IF: $h\nu \lesssim 500$ eV

$h\nu$ and/or T low enough

Basic energetics

$$h\nu = E_{binding}^{Vacuum} + E_{kinetic} = E_{binding}^{Fermi} + \varphi_{spectrometer} + E_{kinetic}$$

One-Electron Picture of Photoemission from a Surface

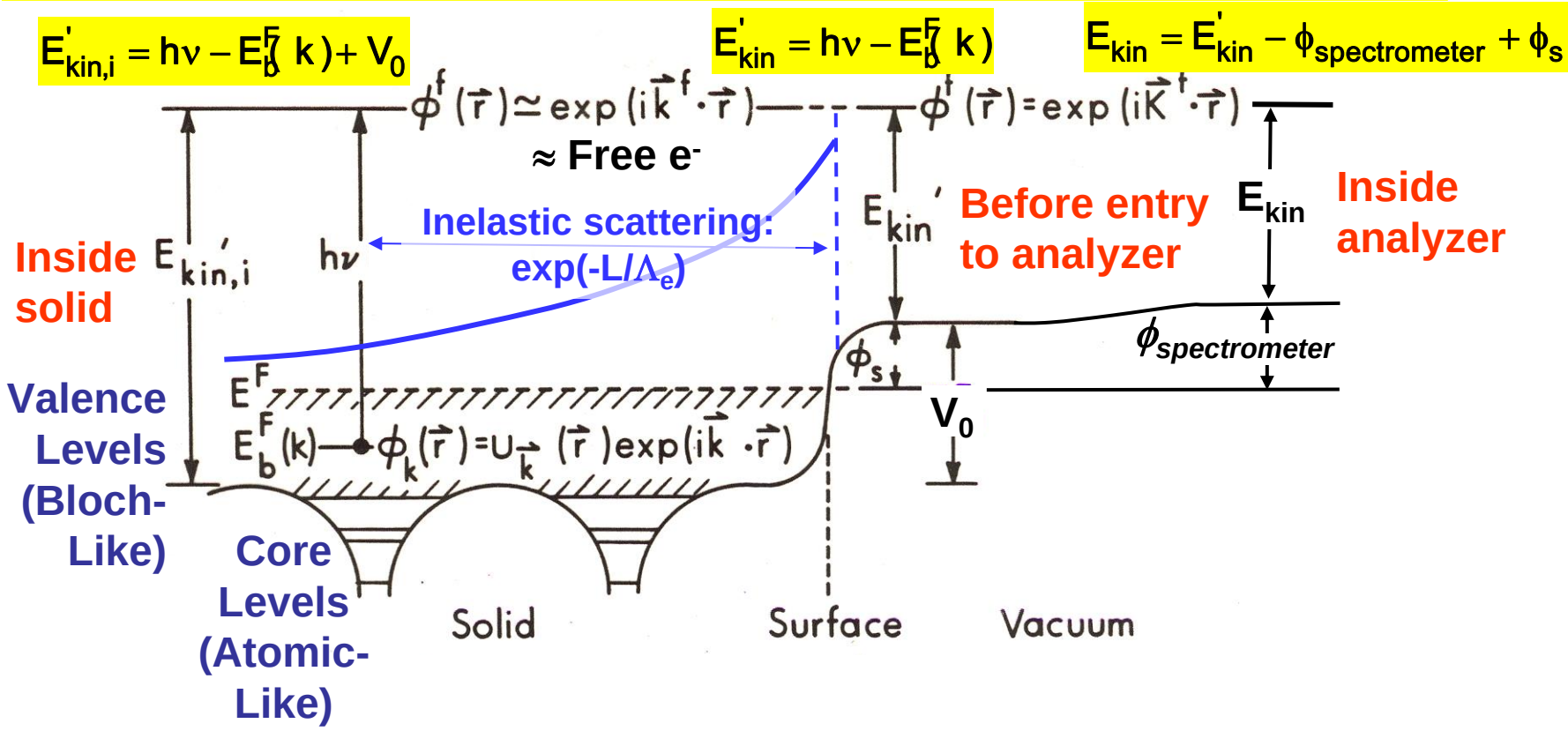

Valence-band photoemission: Angle-Resolved Photoemission (ARPES)

$E_f(\vec{K}_f) =$

$E_f(\vec{k}_f) - V_0 = h\nu - E_i(\vec{k}_i)$

$\approx \hbar^2 K_f^2 / 2m_e$

$\vec{k}_{f,\parallel} = \vec{K}_{f,\parallel}$

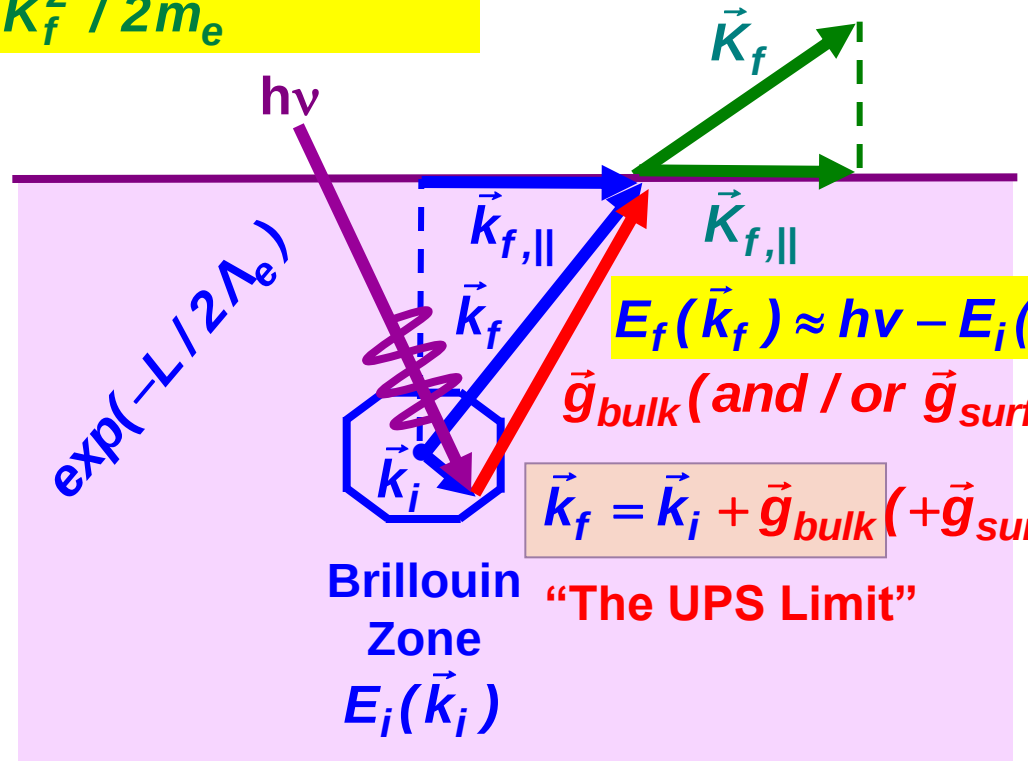

$E_f(\vec{k}_f) \approx h\nu - E_i(\vec{k}_i) + V_0 \approx \hbar^2 k_f^2 / 2m_e$

$\vec{g}_{bulk}$ (and / or $\vec{g}_{surf}$)

$\vec{k}_f = \vec{k}_i + \vec{g}_{bulk} (+\vec{g}_{surf}) + \vec{k}_{hv} + \vec{k}_{phonon}$

"The UPS Limit"

High energy a/o
High temp.

$$I(E_f, \vec{k}_f) \propto \left| \hat{\varepsilon} \bullet \left\langle \varphi_{photoe}(E_f = h\nu + E_i, \vec{k}_f = \vec{k}_i + \vec{g}) \left| \vec{r} \right| \varphi(E_i, \vec{k}_i) \right\rangle \right|^2$$

"Direct" or k-conserving transitions

EXAMPLE: NORMAL-EMISSION UPS FROM Cu(001)

$\Delta p_z \Delta z \approx \hbar/2$

$\Delta k_z \Lambda_e \approx ½$

$\Delta k_z \approx 1/(2\Lambda_e)$

For Cu @ $E_{kin} \approx 80$ eV,

$\Lambda_e \approx 4$ Å, $\Delta k_z \approx 0.12$ Å^{-1}

Compare $2\pi/a = 0.98$ Å^{-1}

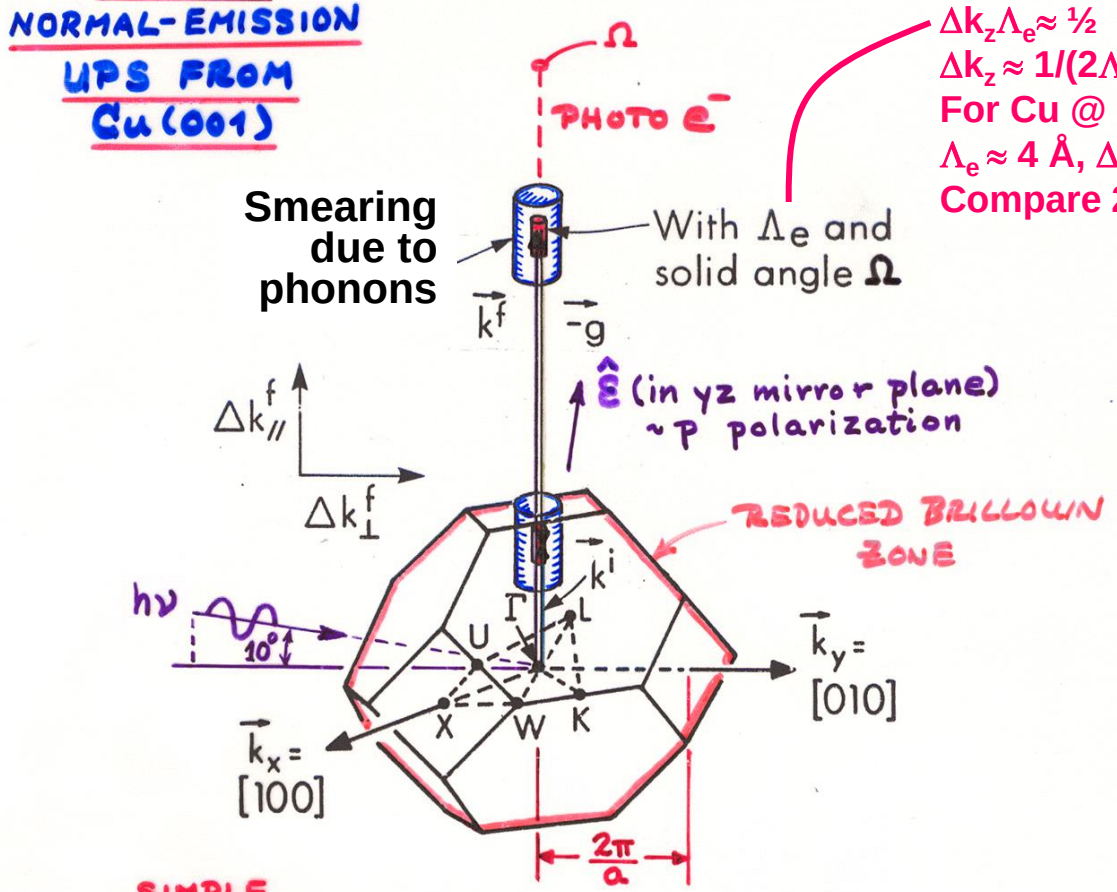

SIMPLE DT MODEL: Direct: $\vec{k}^f = \vec{k}^i + \vec{g} + \cancel{\vec{k}_{h\nu}}$

$E^i(\vec{k}^i)$ = initial band structure

$E^f(\vec{k}^f) \approx \hbar^2 (k^f)^2 / 2m$

Constant matrix elements

Expectations from simple direct-transition theory + symmetry considerations in matrix elements

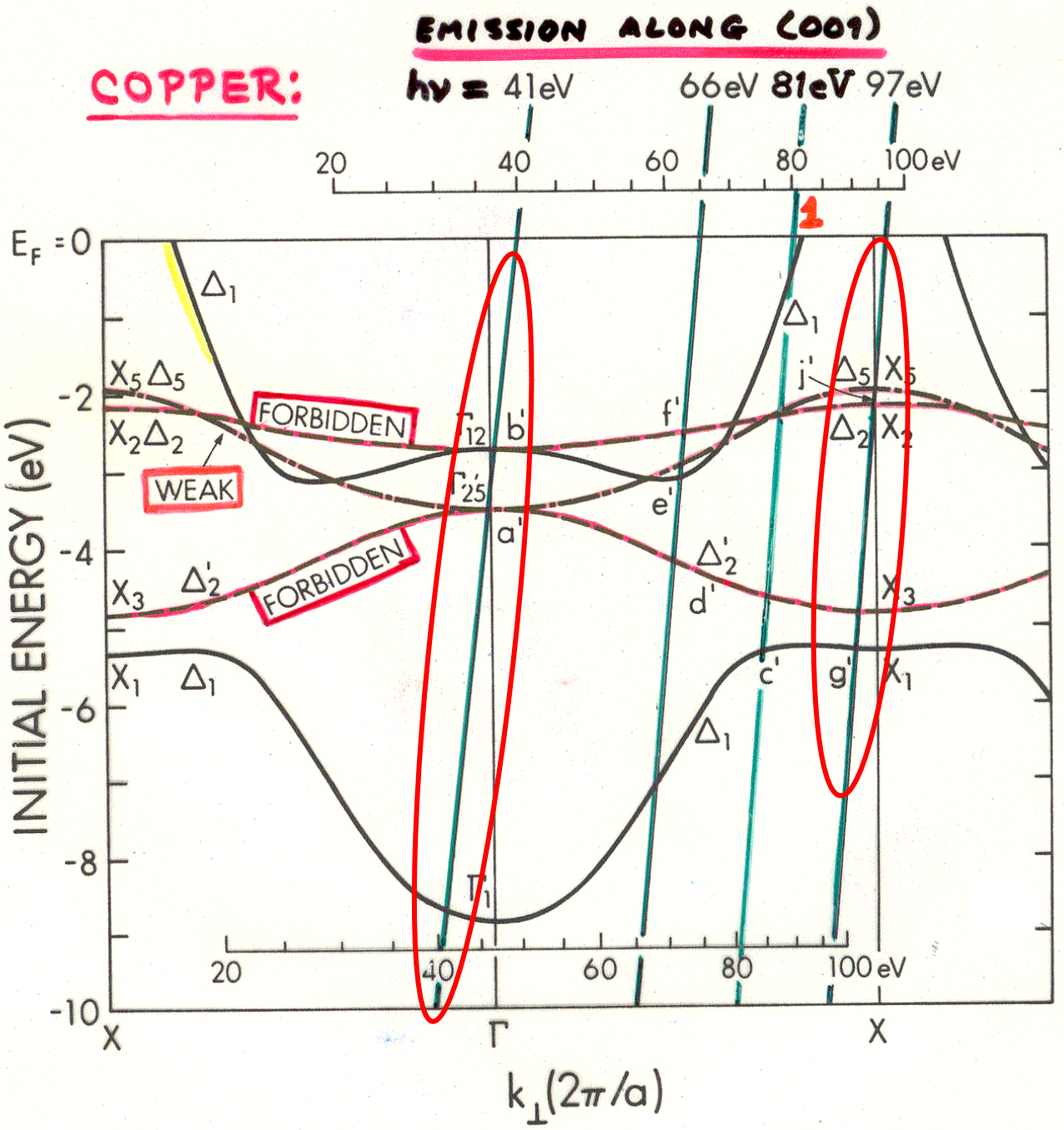

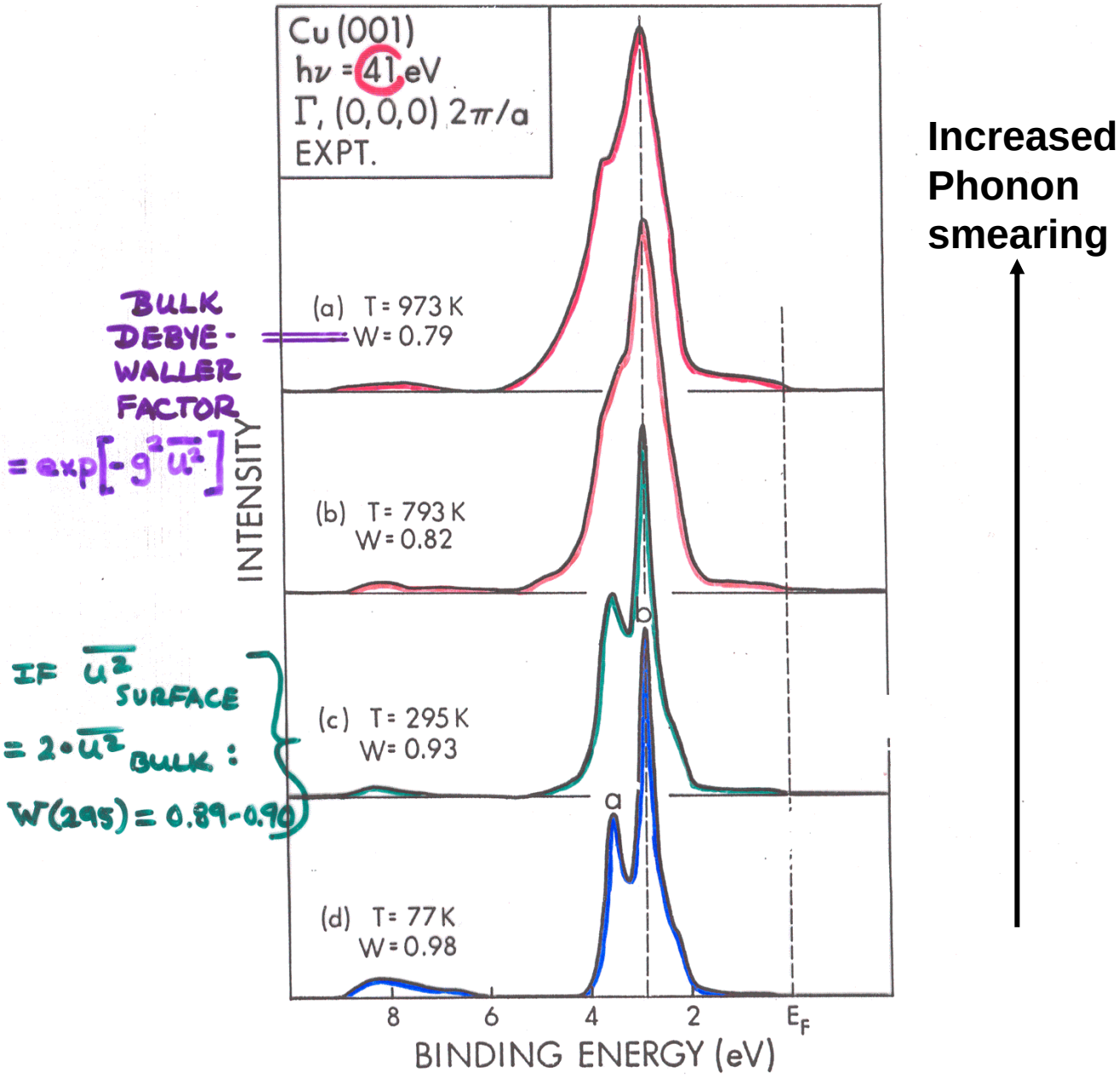

R.C. WHITE ET AL., PHYS. REV. B 35, 1147 (1987)

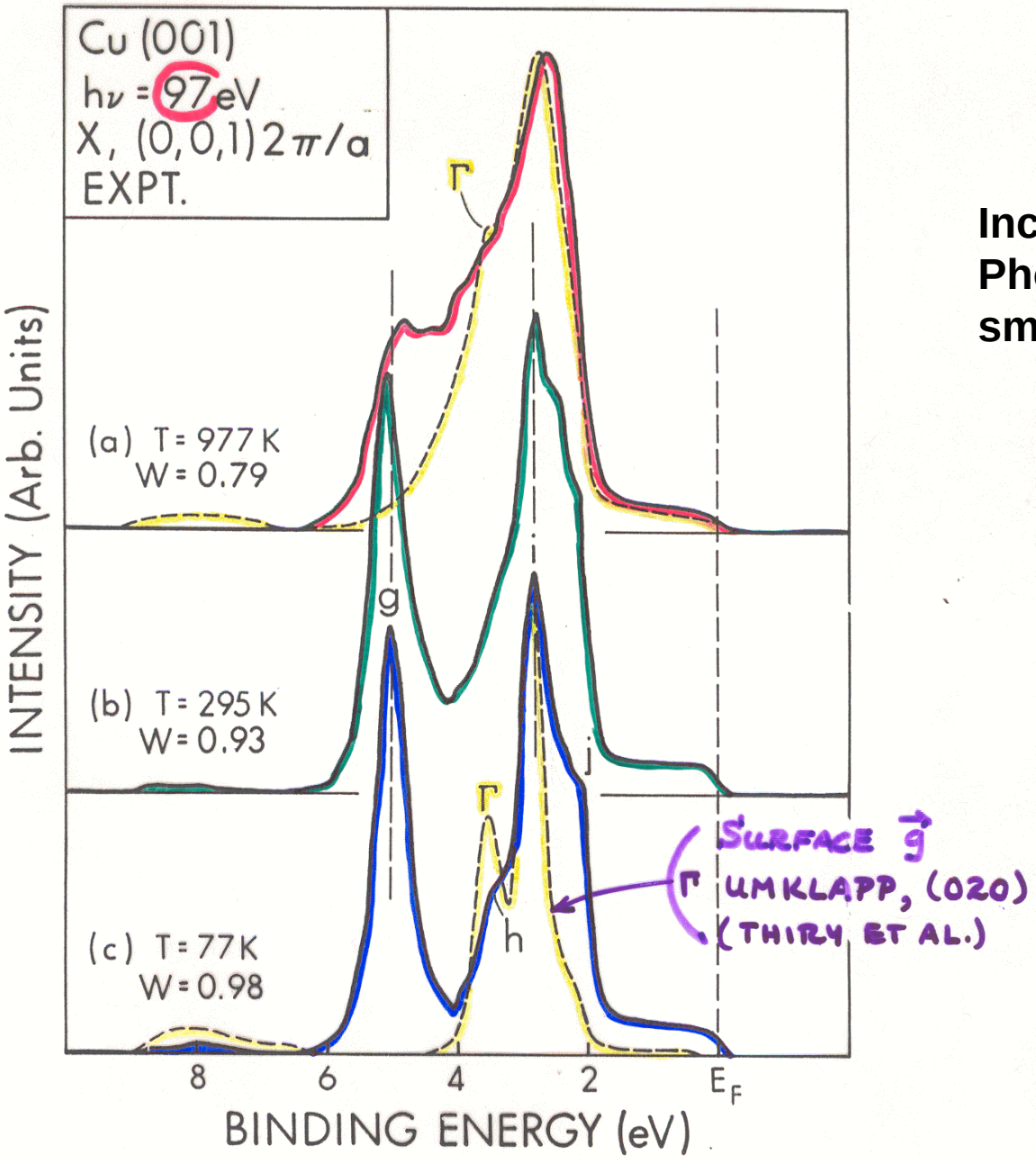

Increased Phonon smearing

Cu: ANGLE-RESOLVED PHOTOEMISSION AND BAND-MAPPING ALONG (001)

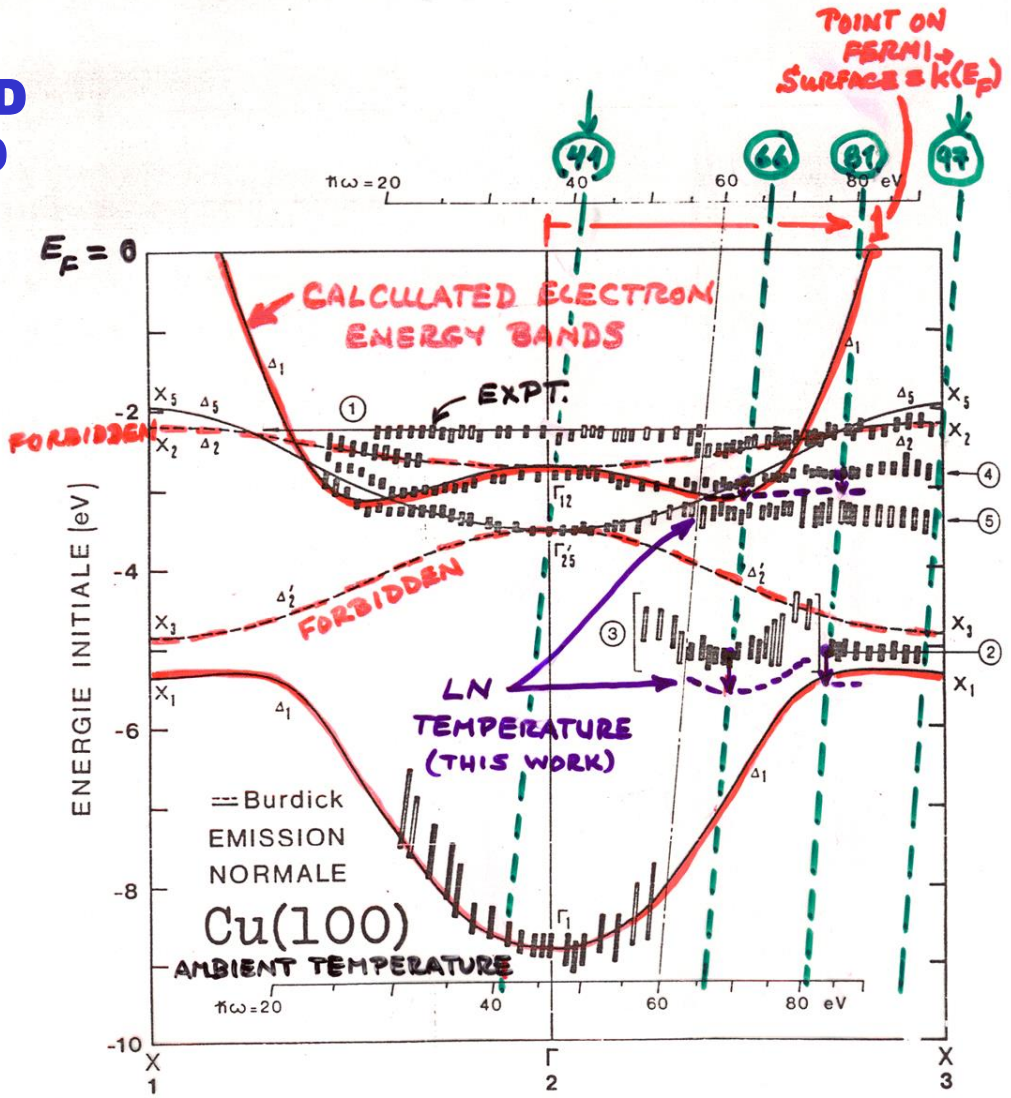

P. THIRY, THESIS, UNIV. OF PARIS (1980)
+ WHITE ET AL. P.R.B 35, 1147 (1987)

FIG. 56

Cu: ANGLE-RESOLVED PHOTOEMISSION AND BAND-MAPPING ALONG (110)

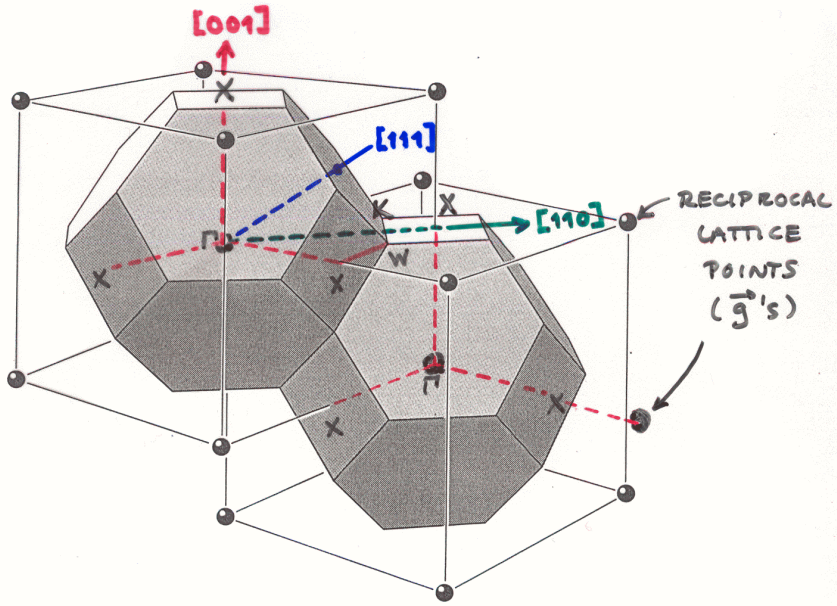

Figure 28 Brillouin zones of the face-centered cubic lattice. The cells are in reciprocal space, and the reciprocal lattice is body-centered, as drawn.

— STACKING OF fcc BRILLOUIN ZONES —

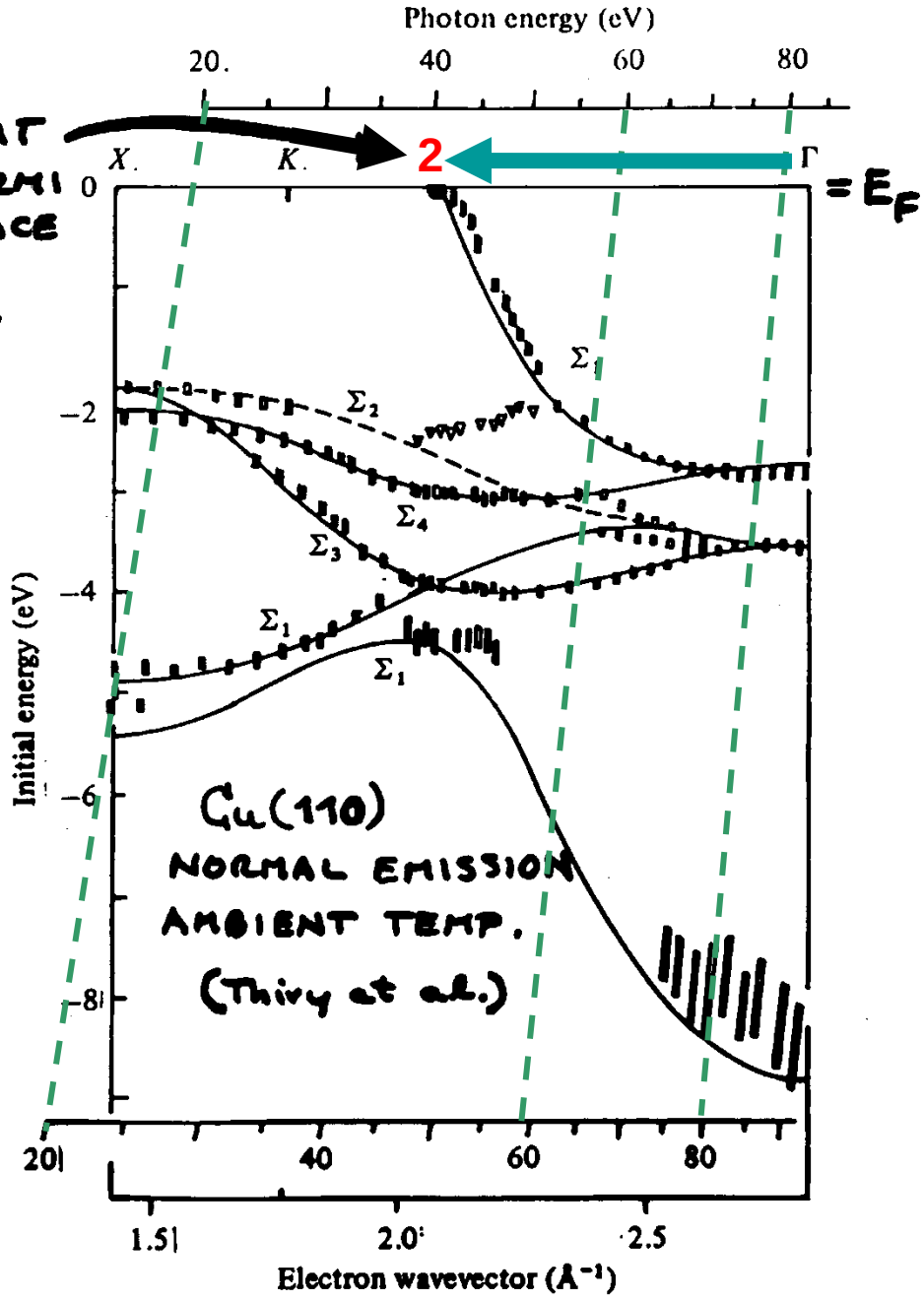

P.Thiry, Ph.D. thesis, Univ. of Paris (1980)

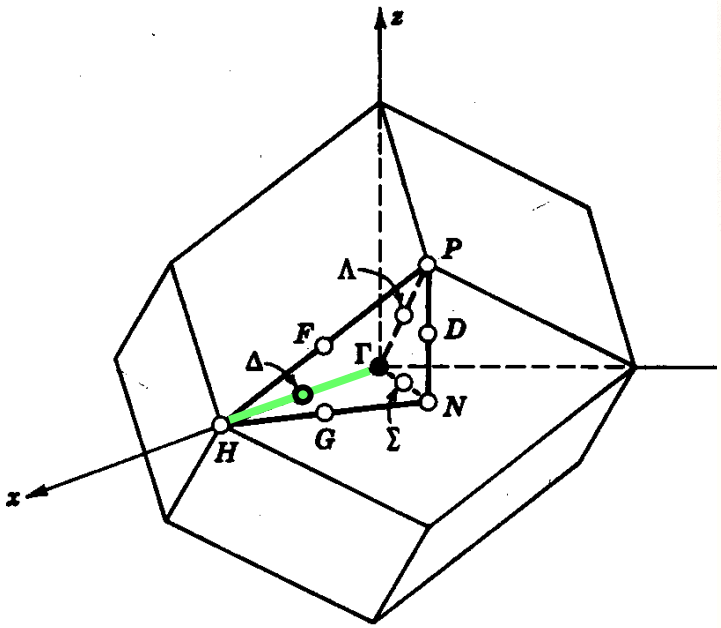

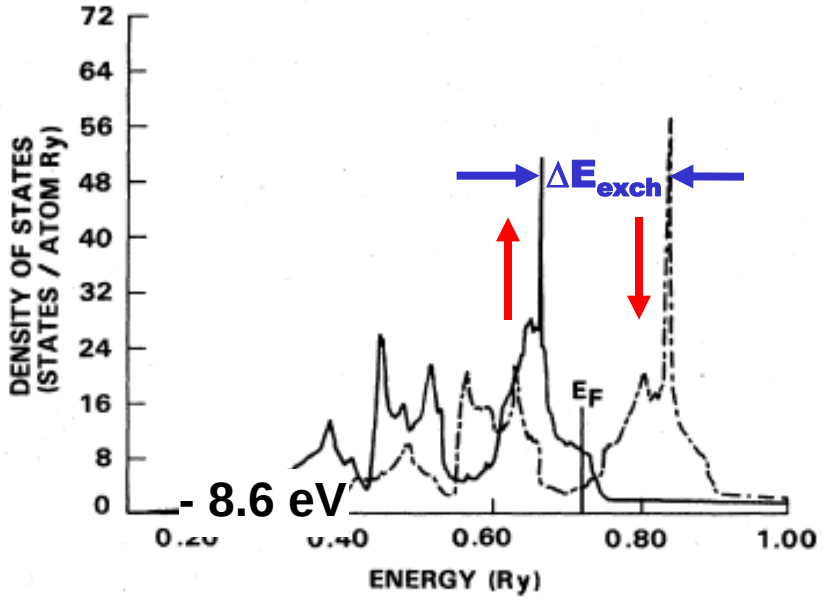

FIG. 4. Density of states at the equilibrium lattice constant of Fe for majority- (solid line) and minority- (broken line) spin states.

Hathaway et al., Phys. Rev. B 31, 7603 ('85)

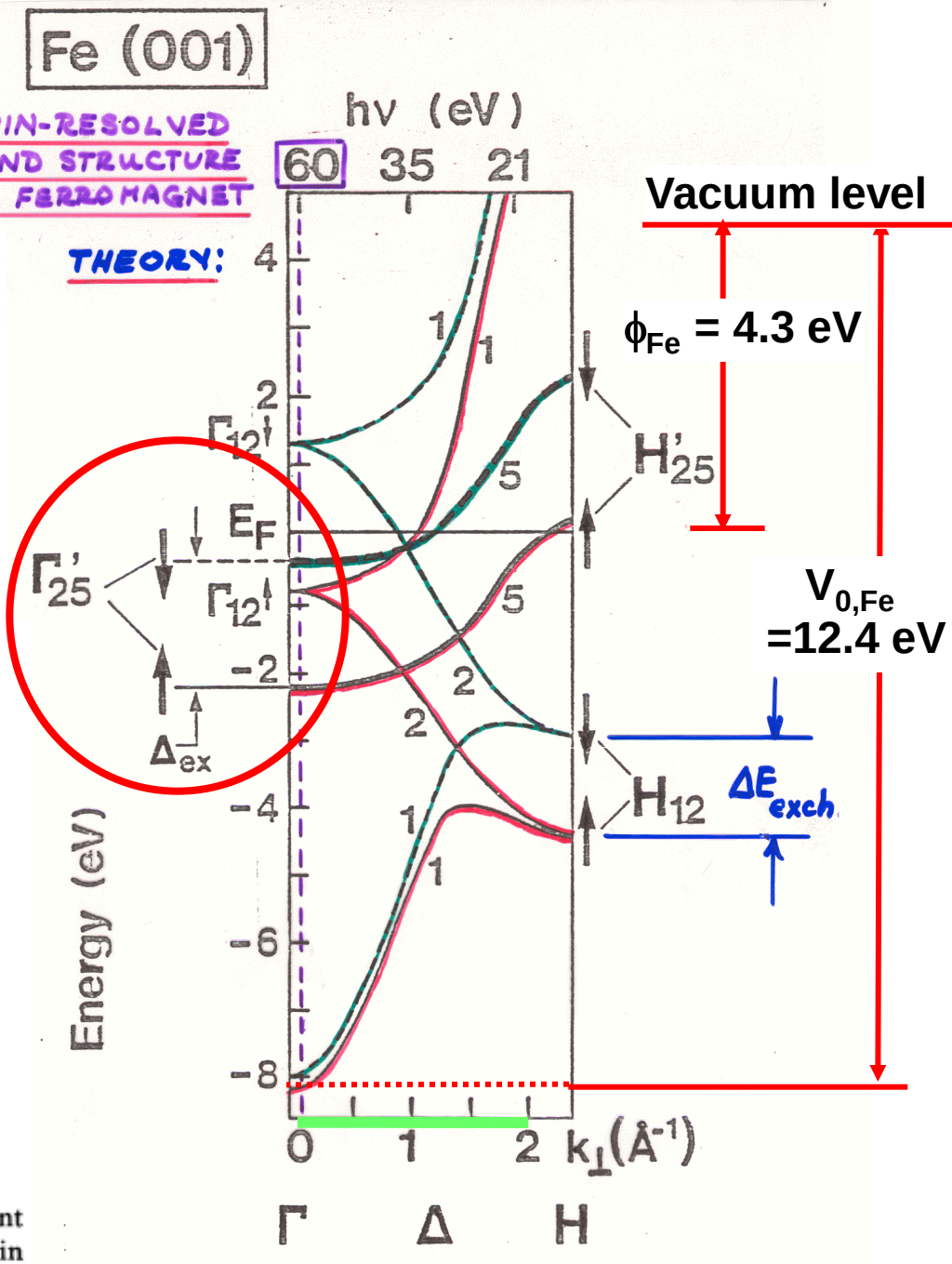

E. KISKER ET AL., PHYS. REV. B 31, 329 (1985)

Fe: ANGLE AND SPIN-RESOLVED SPECTRA AT Γ POINT

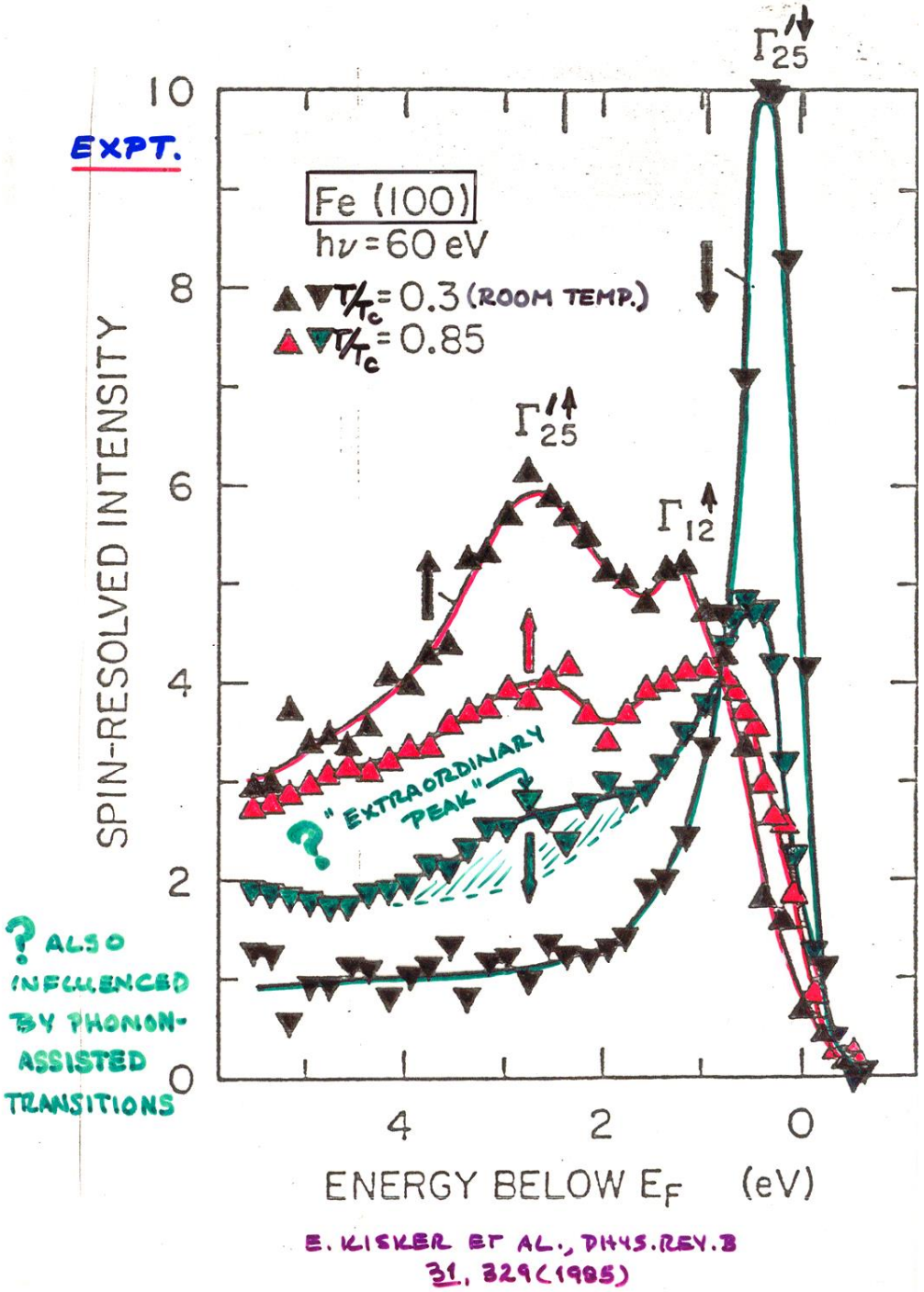

$SrTiO_3$ and $La_{0.67}Sr_{0.33}MnO_3$ band structures and DOS

$SrTiO_3$-band insulator

$La_{0.67}Sr_{0.33}MnO_3$- Half-Metallic Ferromagnet

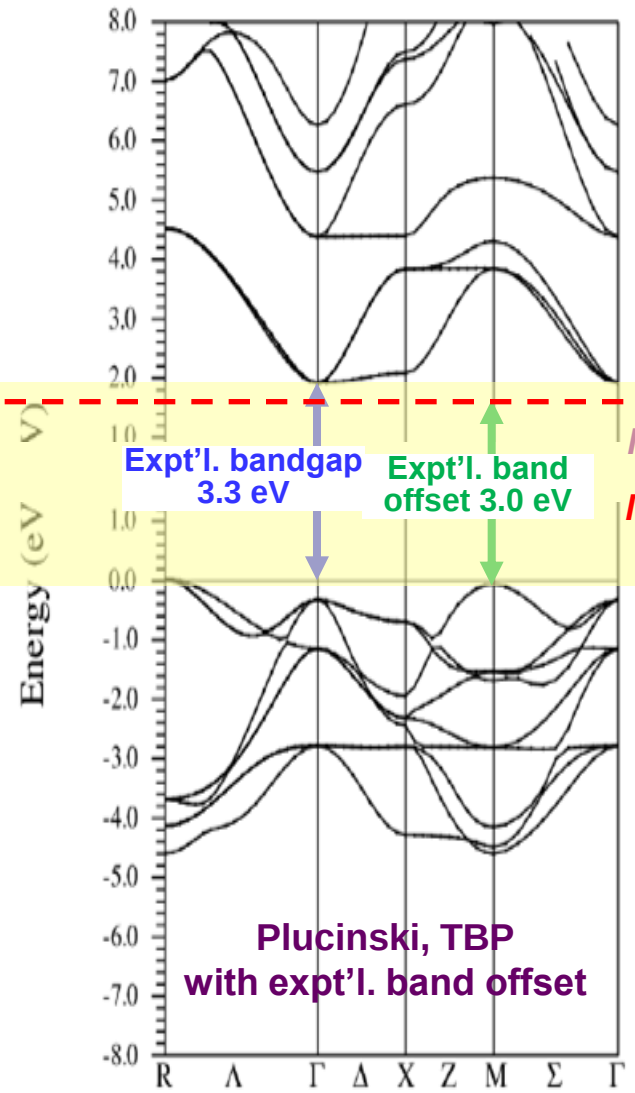

Plucinski, TBP
with expt'l. band offset

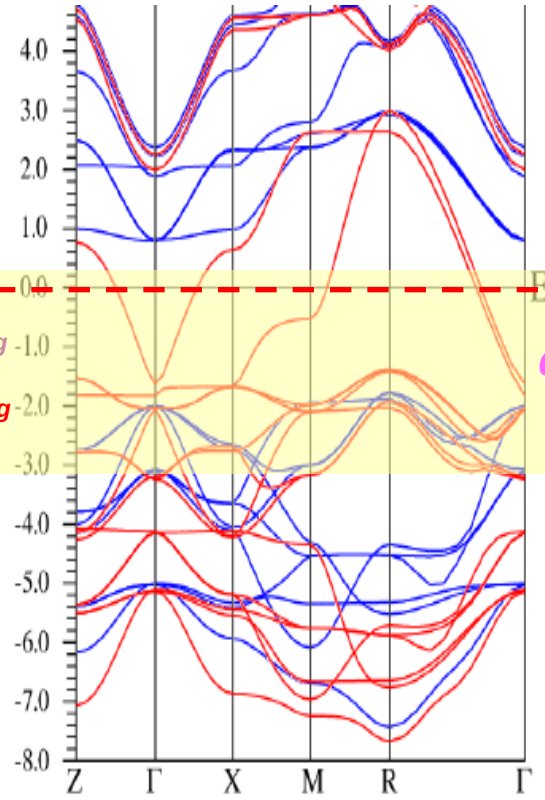

Spin-up
Spin-down
Chikamatsu et al.,
PRB 73, 195105 (2006);
Plucinski, TBP

Projected DOSs

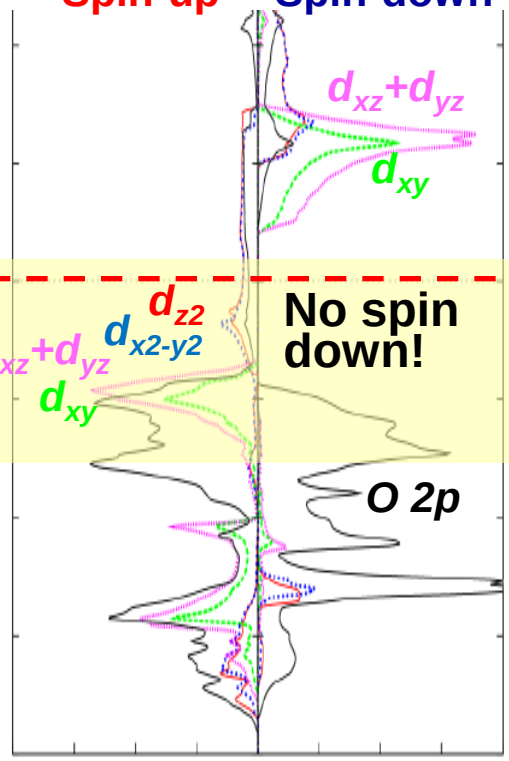

Zheng, Binggeli, J. Phys.
Cond. Matt. 21, 115602 (2009)
Plucinski, TBP

Half-Metallic Ferromagnetism

***LDA theory*- FM $La_{0.75}Ca_{0.25}MnO_3$**

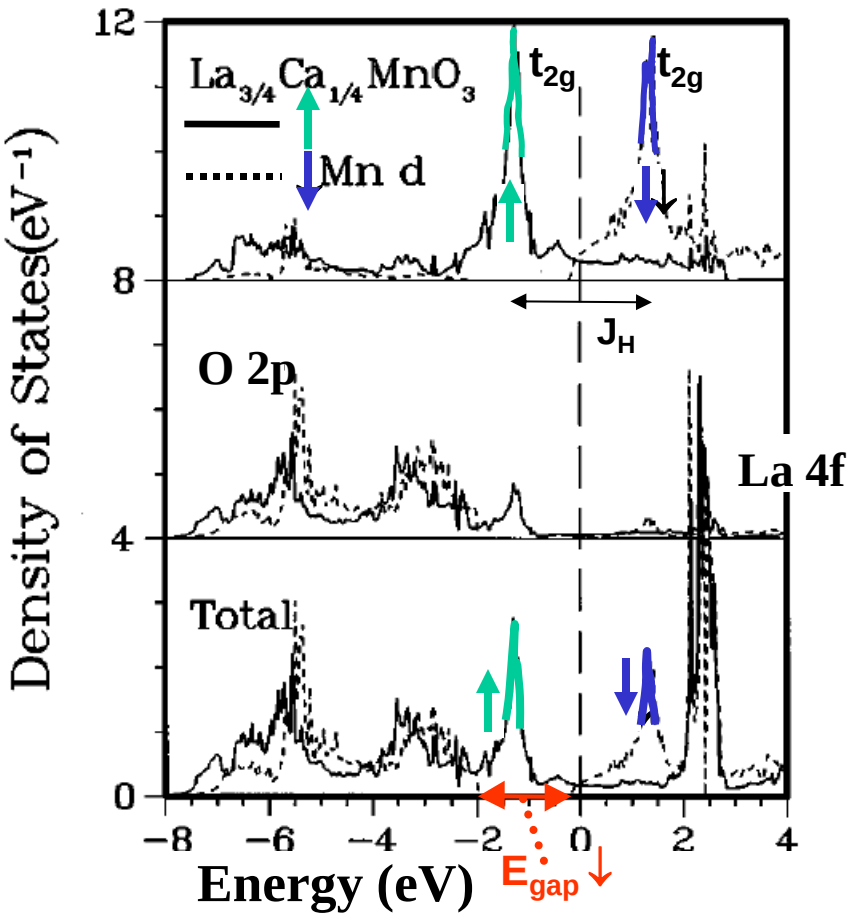

Pickett and Singh, PRB 53, 1146 (1996)

***Experiment*- spin-resolved PS $La_{0.70}Sr_{0.30}MnO_3$ as thin film**

Park et al., Nature, PRB 392, 794 (1998)

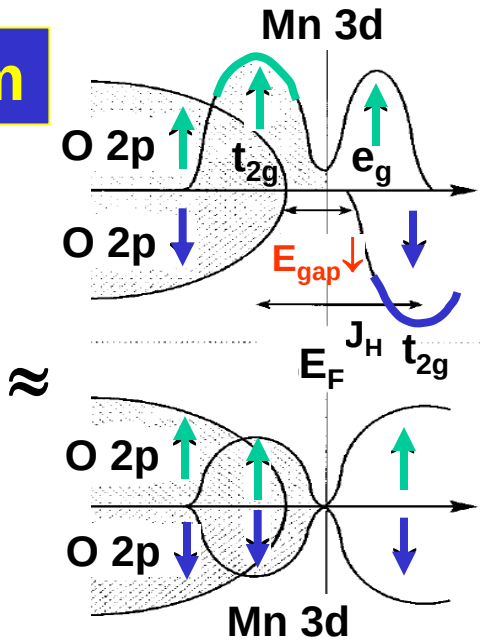

FM : $T \ll T_C$

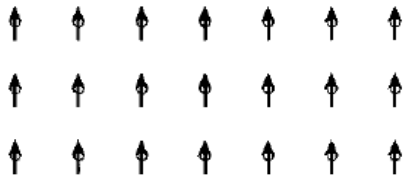

PM : $T > T_C$

$T \ll T_C$

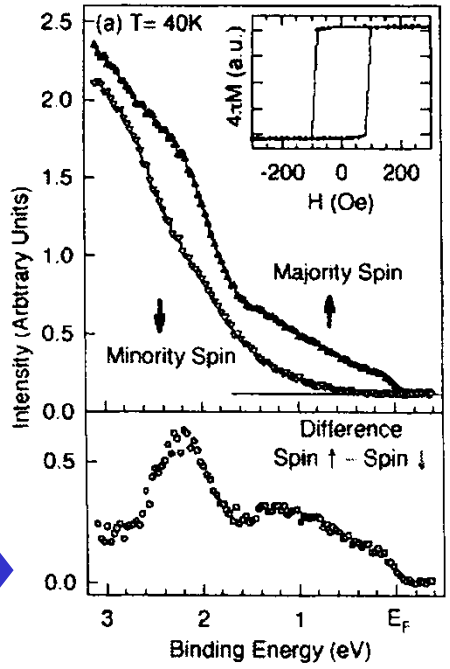

$T > T_C$

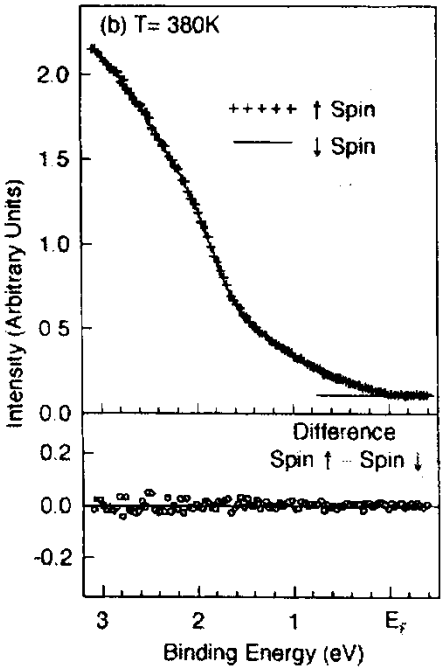

SURFACE ELECTRONIC STATES

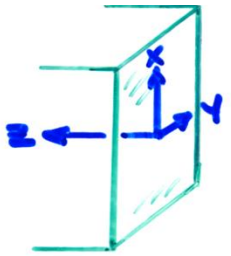

$k_x, k_y \Rightarrow \vec{k}_{\parallel}$

$k_z \Rightarrow \vec{k}_{\perp}$

- STRONGLY LOCALIZED NEAR SURFACE
- BLOCH FUNCTION IN x+y, BUT DECAYING IN z:

$$\varphi_{\vec{k}_{\parallel}}(\vec{r}) = u_{\vec{k}_{\parallel}}(\vec{r})\, e^{i\vec{k}_{\parallel}\cdot\vec{r}}\, e^{-\kappa_{\perp} z}$$

($\kappa_{\perp}$: DECAY CONSTANT)

- TWO LIMITING TYPES: TAMM STATE, SHOCKLEY STATE (OSCILLATES INTO BULK A LITTLE)

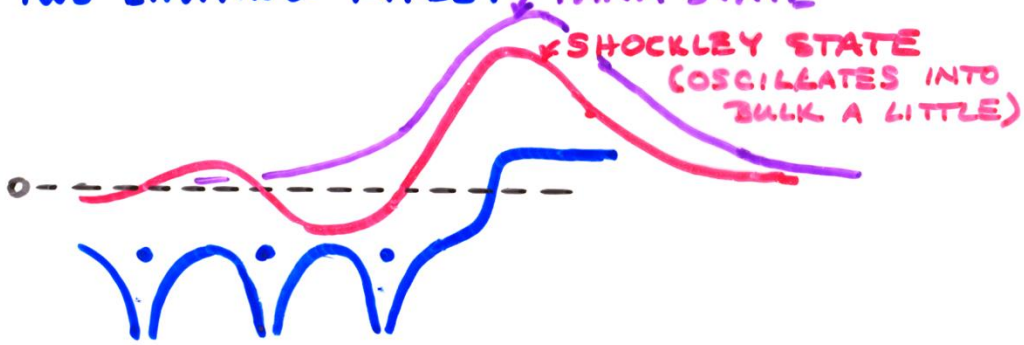

- ONLY EXIST WHEN NO BULK STATE EXISTS AT SAME $\vec{k}_{\parallel} = k_x\hat{i} + k_y\hat{j}$; OTHERWISE MIXING OCCURS + NOT SURFACE-LOCALIZED

Conservation Laws in Valence-Band Photoelectron Spectroscopy:

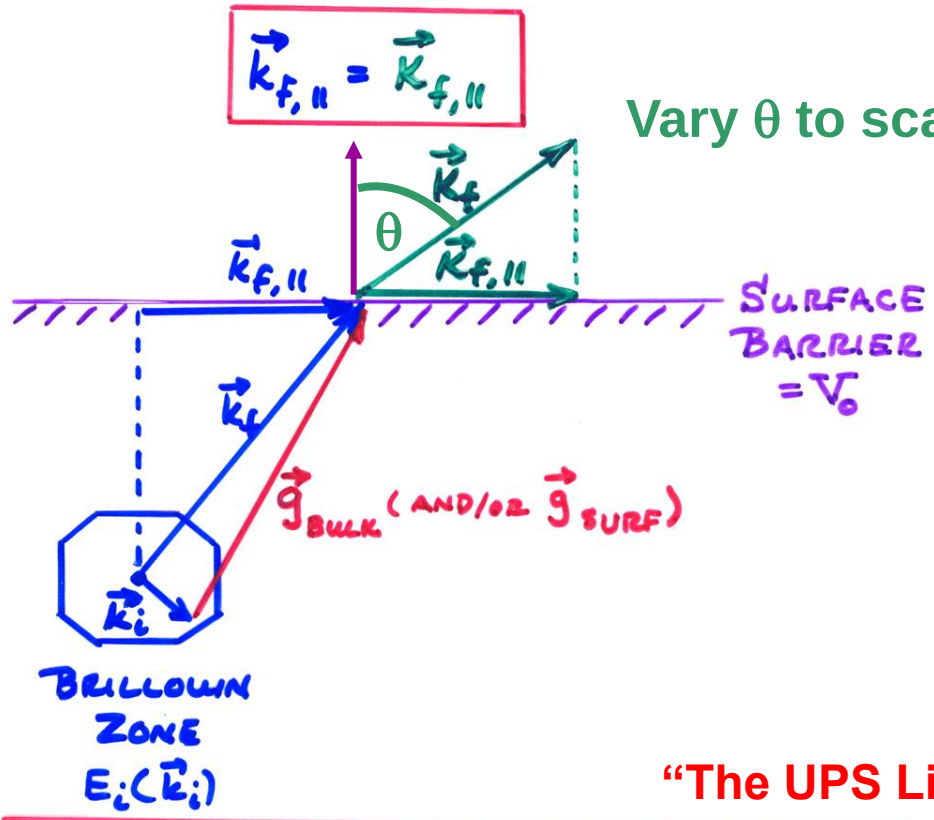

Vary θ to scan $\vec{K}_{f,\parallel} = \vec{k}_{f,\parallel}$

"The UPS Limit"

$$\vec{k}_f = \vec{k}_i + \vec{g}_{BULK}(\vec{g}_{SURFACE}) + \cancel{\vec{k}_{h\nu}} + \cancel{\vec{k}_{PHONON}}$$

NEGLIGIBLE IF: $h\nu \lesssim 500$ eV; $h\nu$ and/or T low enough

The electronic structure of a transition metal—fcc Cu

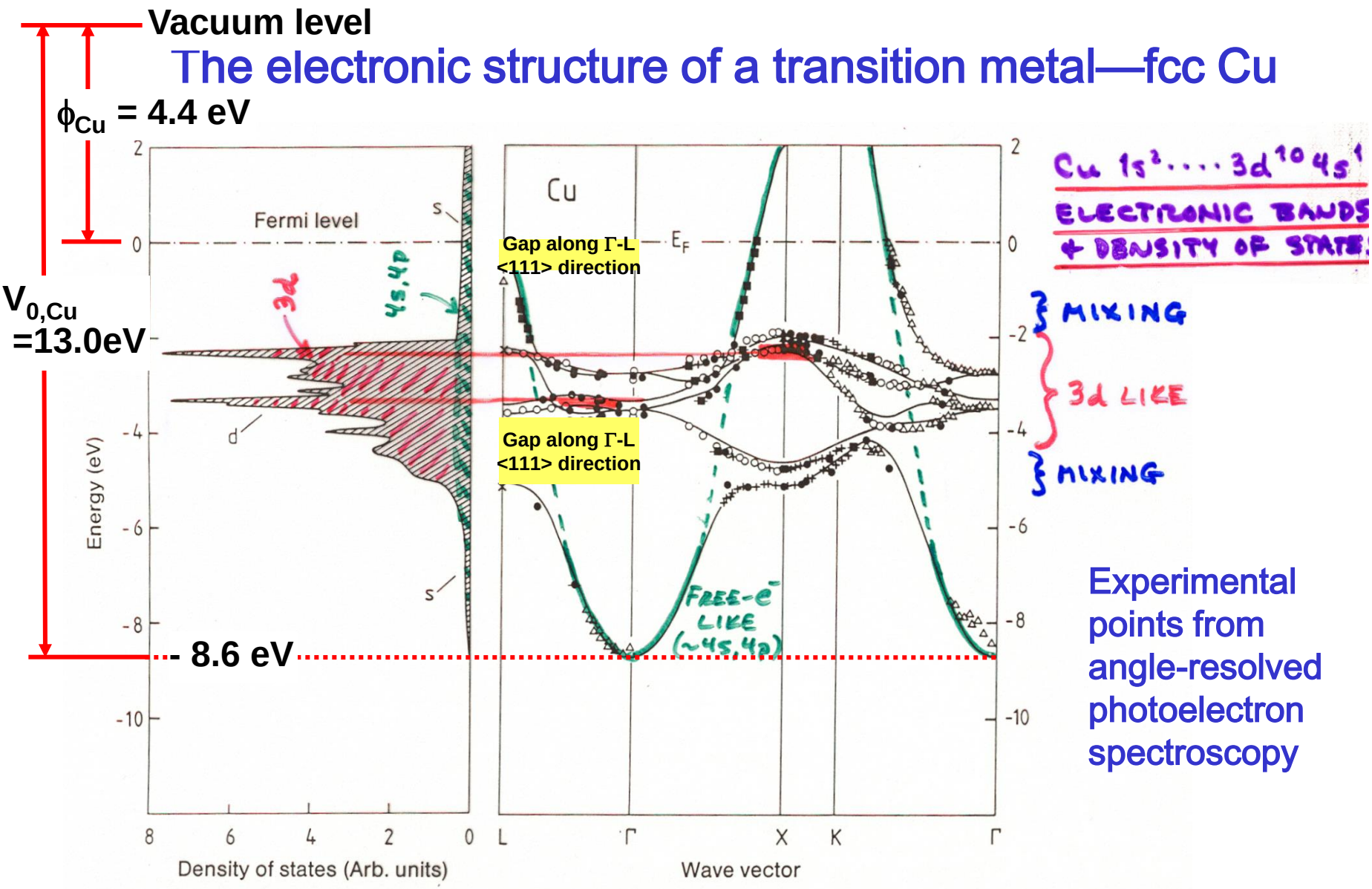

Experimental points from angle-resolved photoelectron spectroscopy

Fig. 7.12. Bandstructure $E(k)$ for copper along directions of high crystal symmetry (*right*). The experimental data were measured by various authors and were presented collectively by Courths and Hüfner [7.4]. The full lines showing the calculated energy bands and the density of states (*left*) are from [7.5]. The experimental data agree very well, not only among themselves, but also with the calculation

Surface states on Cu(111)

Shockley surface state

Tamm surface state

Fig. 4.21. Experimental dispersion of Cu(111) surface states plotted with a projection of the bulk bands: (*a*) Shockley state near the zone center (Kevan, 1983); (*b*) Tamm state near the zone boundary (Heimann, Hermanson, Miosga and Neddermeyer, 1979). Compare with Fig. 4.17.

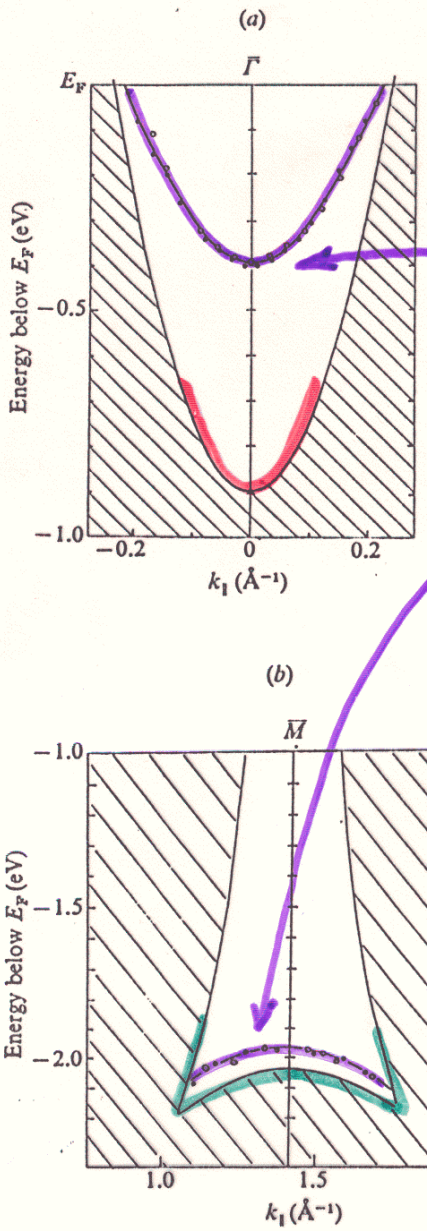

EXPT.

EXPT.

THEORY

Fig. 4.17. Surface states (dashed curves) and bulk projected ban Cu(111) surface according to a six-layer surface band structure calculation (Euceda, Bylander & Kleinman, 1983).

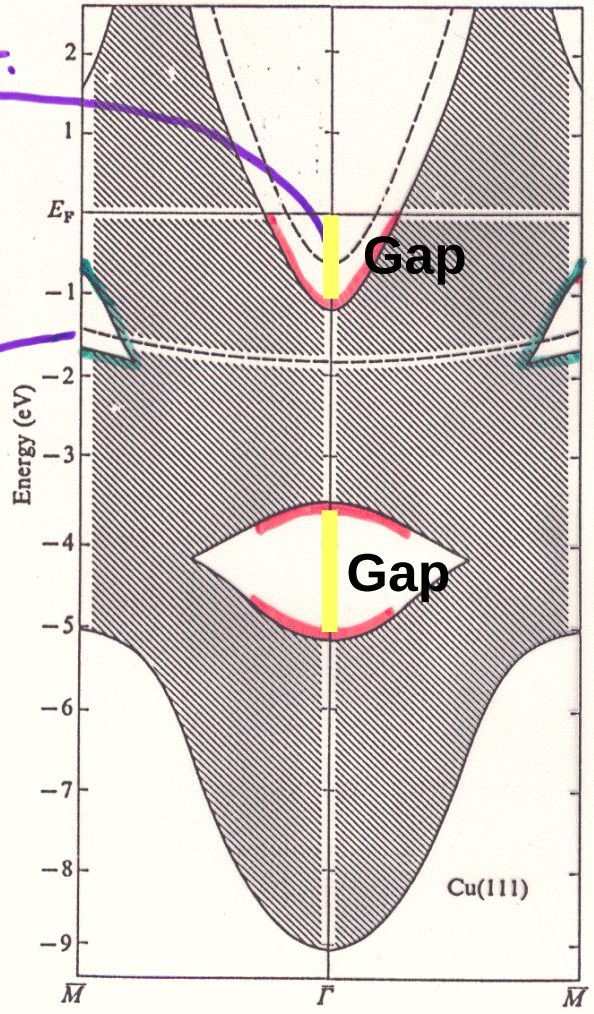

Zangwill, Surface Physics,

Fig. 4.20. Photoemission energy distribution curves from Cu(111) at different collection angles. Equation (4.32) has been used to express the electron kinetic energy in terms of the binding energy of the electron state (Kevan, 1983).

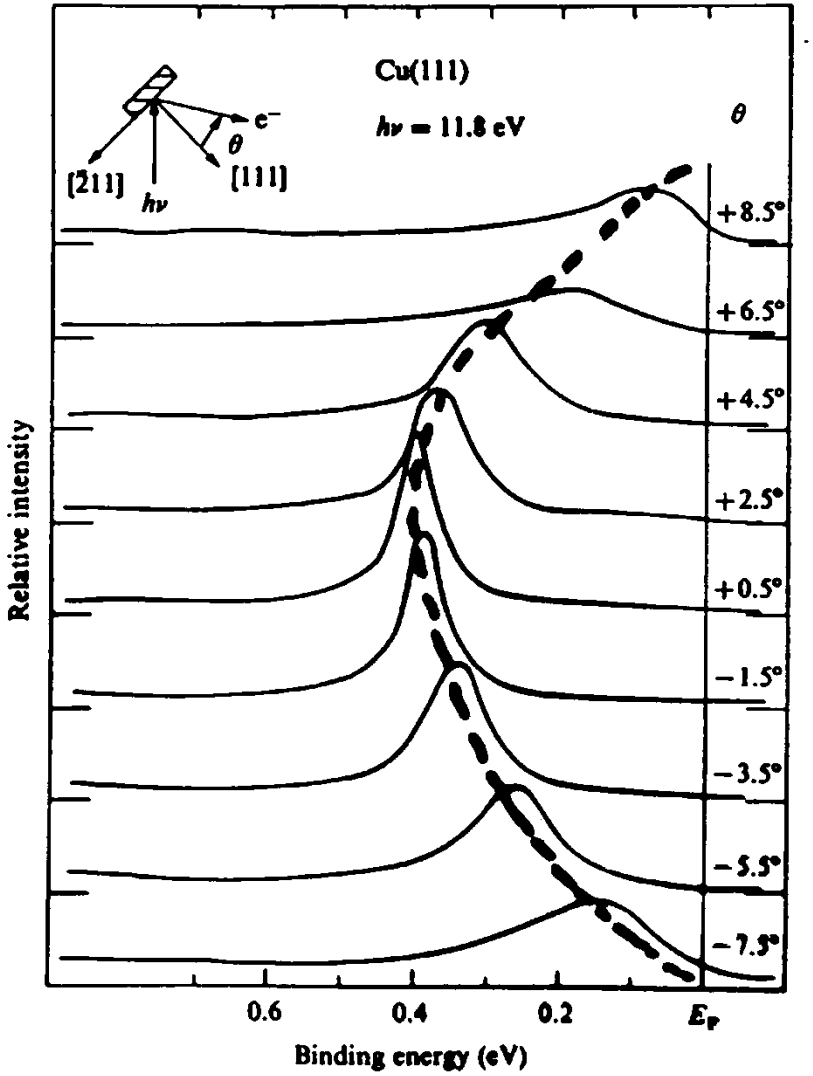

Zangwill,
Surface Physics,

Valence-Band Photoemission at High Energy--What & Where is the "XPS Limit"?:

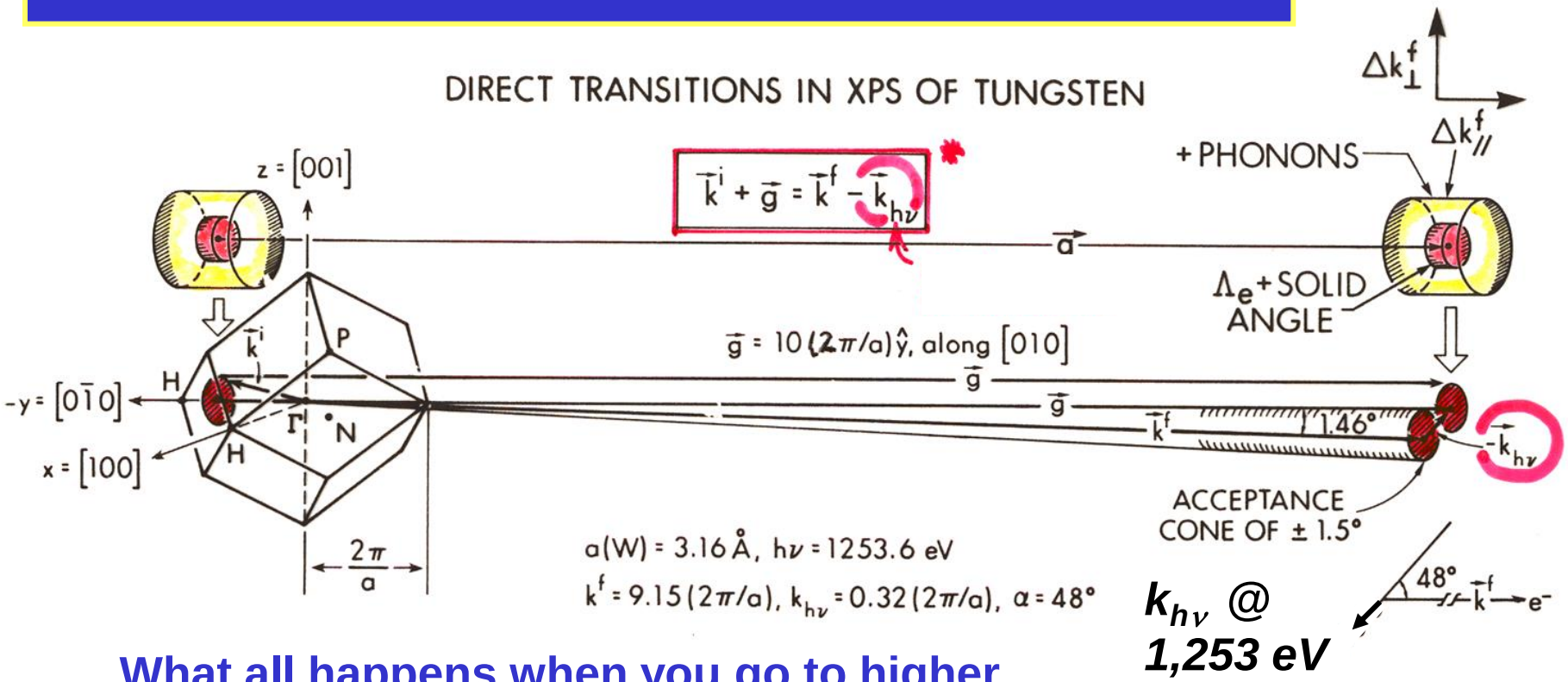

$k_{h\nu}$ @ 1,253 eV

What all happens when you go to higher photon energies?

- **non-dipole effect→the photon momentum**
- **angular acceptance→B.Z. averaging**
- **lattice recoil, phonon creation→more B.Z. averaging, energy loss**

….the XPS limit of full B.Z. averaging and D.O.S. sensitivity

Hussain et al., Phys. Rev. B 22, 3750 ('80)

Valence-band photoemission—at higher energy

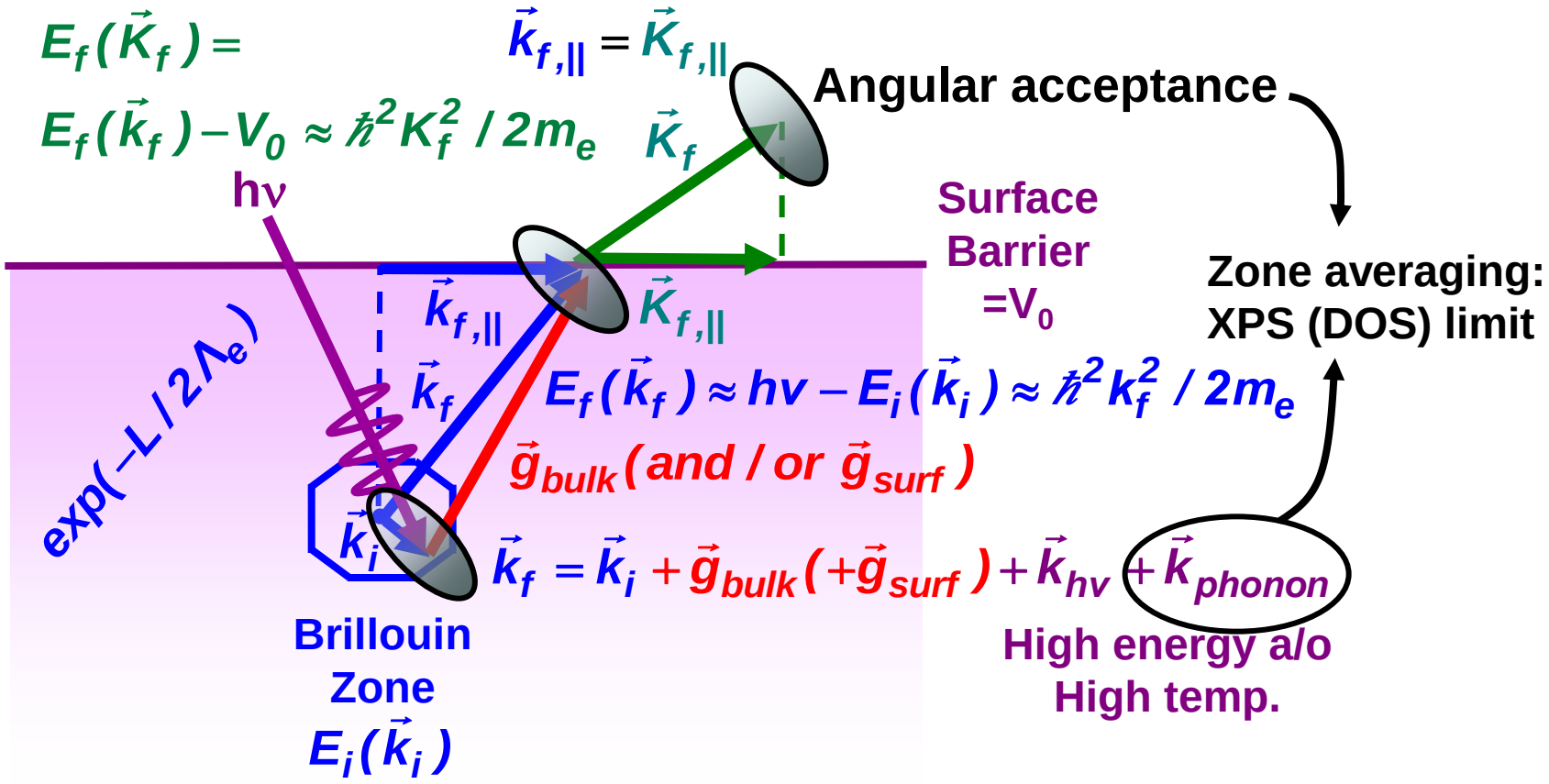

$$I(E_f, \vec{k}_f) \propto \left| \hat{\varepsilon} \bullet \left\langle \varphi_{photoe}(E_f = h\nu + E_i, \vec{k}_f = \vec{k}_i + \vec{g}) \middle| \vec{r} \middle| \varphi(E_i, \vec{k}_i) \right\rangle \right|^2$$

Hussain et al., Phys. Rev. B 34 (1986) 5226.

Angle-Resolved Photoemission at High Energy--

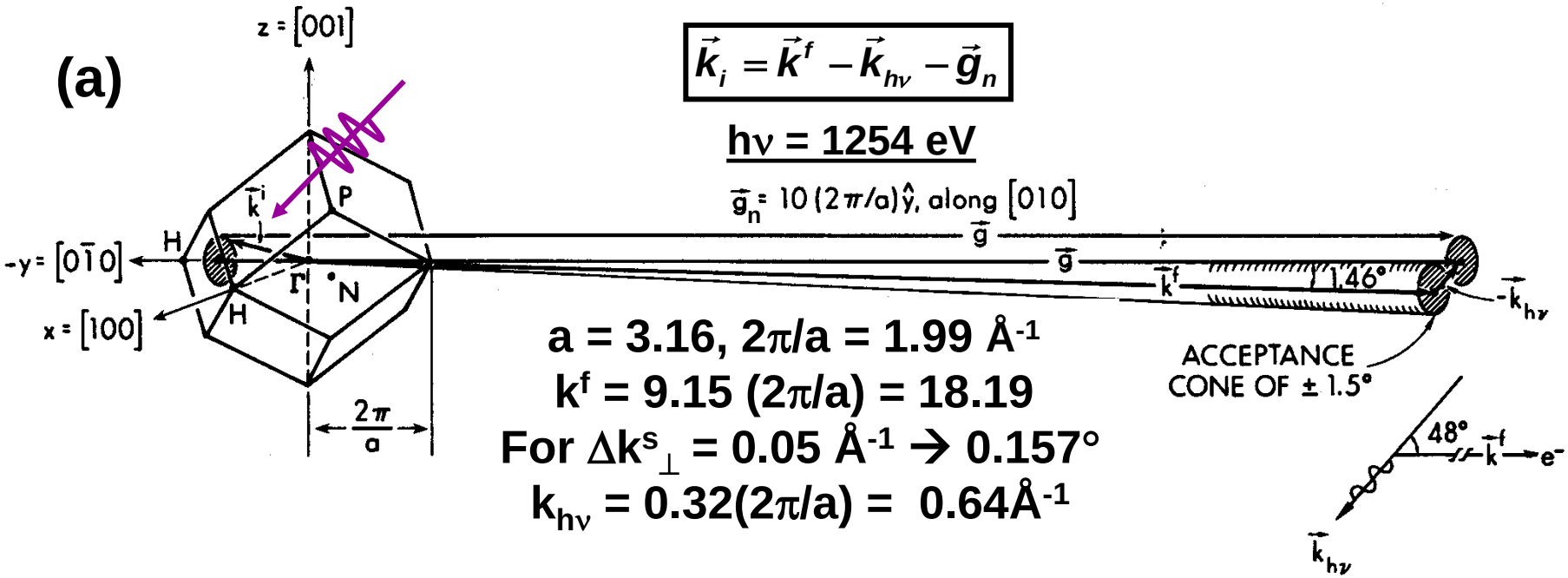

Hussain et al.….CF, Phys. Rev. B 22 3750 (1980) Phys. Rev. B 34, 5226 (1986)

Additional effects at higher energies:

- **Non-dipole--the photon momentum $k_{h\nu}$**
- **Angular acceptance→B.Z. averaging**
- **Lattice recoil→phonon creation→more B.Z. averaging,**

Fraction DTs ≈ Debye-Waller factor $= W(T) \approx exp[-(k^f)^2 \langle u^2(T)\rangle]$

$\approx exp[-C_1 (k^f)^2 T/(m\Theta_D^2)] \approx exp(-C_2 E_{kin} T)$

Shevchik, Phys. Rev. B 16, 3428 (1977)

Takata et al., Phys. Rev. B 75, 233404 (2007)

→the "XPS limit" of full B.Z. averaging and D.O.S. sensitivity

→core-like photoelectron diffraction Alvarez et al., PR*B* 54, 14703 (1996)

- **Recoil leads to peak shifts and broadening:** $E_{recoil}(eV) \approx \left[\frac{m_e}{M}\right] E_{kin} \approx 5.5 \times 10^{-4} \left[\frac{E_{kin}(eV)}{M(amu)}\right]$

Table 1 Debye temperature and thermal conductivity[a]

Li	Be											B	C	N	O	F	Ne
344	1440												2230				75
0.85	2.00											0.27	1.29				
Na	Mg											Al	Si	P	S	Cl	Ar
158	400	Low temperature limit of θ, in Kelvin										428	645				92
1.41	1.56	Thermal conductivity at 300 K, in W $cm^{-1}K^{-1}$										2.37	1.48				
K	Ca	Sc	Ti	V	Cr	Mn	Fe	Co	Ni	Cu	Zn	Ga	Ge	As	Se	Br	Kr
91	230	360.	420	380	630	410	470	445	450	343	327	320	374	282	90		72
1.02		0.16	0.22	0.31	0.94	0.08	0.80	1.00	0.91	4.01	1.16	0.41	0.60	0.50	0.02		
Rb	Sr	Y	Zr	Nb	Mo	Tc	Ru	Rh	Pd	Ag	Cd	In	Sn $_w$	Sb	Te	I	Xe
56	147	280	291	275	450		600	480	274	225	209	108	200	211	153		64
0.58		0.17	0.23	0.54	1.38	0.51	1.17	1.50	0.72	4.29	0.97	0.82	0.67	0.24	0.02		
Cs	Ba	La β	Hf	Ta	W	Re	Os	Ir	Pt	Au	Hg	Tl	Pb	Bi	Po	At	Rn
38	110	142	252	240	400	430	500	420	240	165	71.9	78.5	105	119			
0.36		0.14	0.23	0.58	1.74	0.48	0.88	1.47	0.72	3.17		0.46	0.35	0.08			
Fr	Ra	Ac															

Ce	Pr	Nd	Pm	Sm	Eu	Gd	Tb	Dy	Ho	Er	Tm	Yb	Lu
						200		210				120	210
0.11	0.12	0.16		0.13		0.11	0.11	0.11	0.16	0.14	0.17	0.35	0.16

Th	Pa	U	Np	Pu	Am	Cm	Bk	Cf	Es	Fm	Md	No	Lr
163		207											
0.54		0.28	0.06	0.07									

[a] Most of the θ values were supplied by N. Pearlman; references are given the *A.I.P. Handbook*, 3rd ed; the thermal conductivity values are from R. W. Powell and Y. S. Touloukian, Science **181**, 999 (1973).

Silicon--Debye-Waller Factors

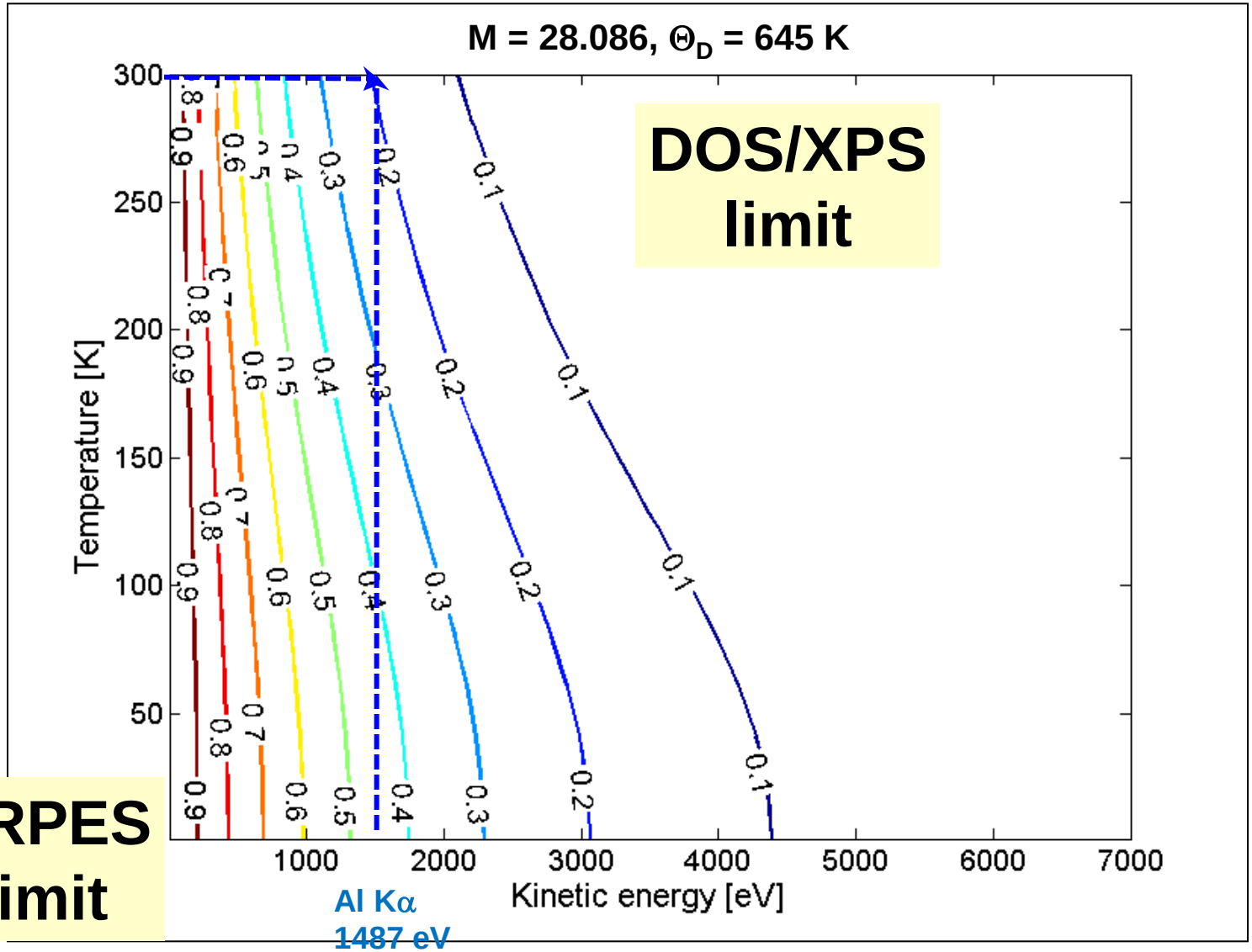

Plucinski, et al. PRB 78, 035108 (2008);
Phys. Rev. B 84, 045433 (2011)

Some classic cases in the XPS limit:

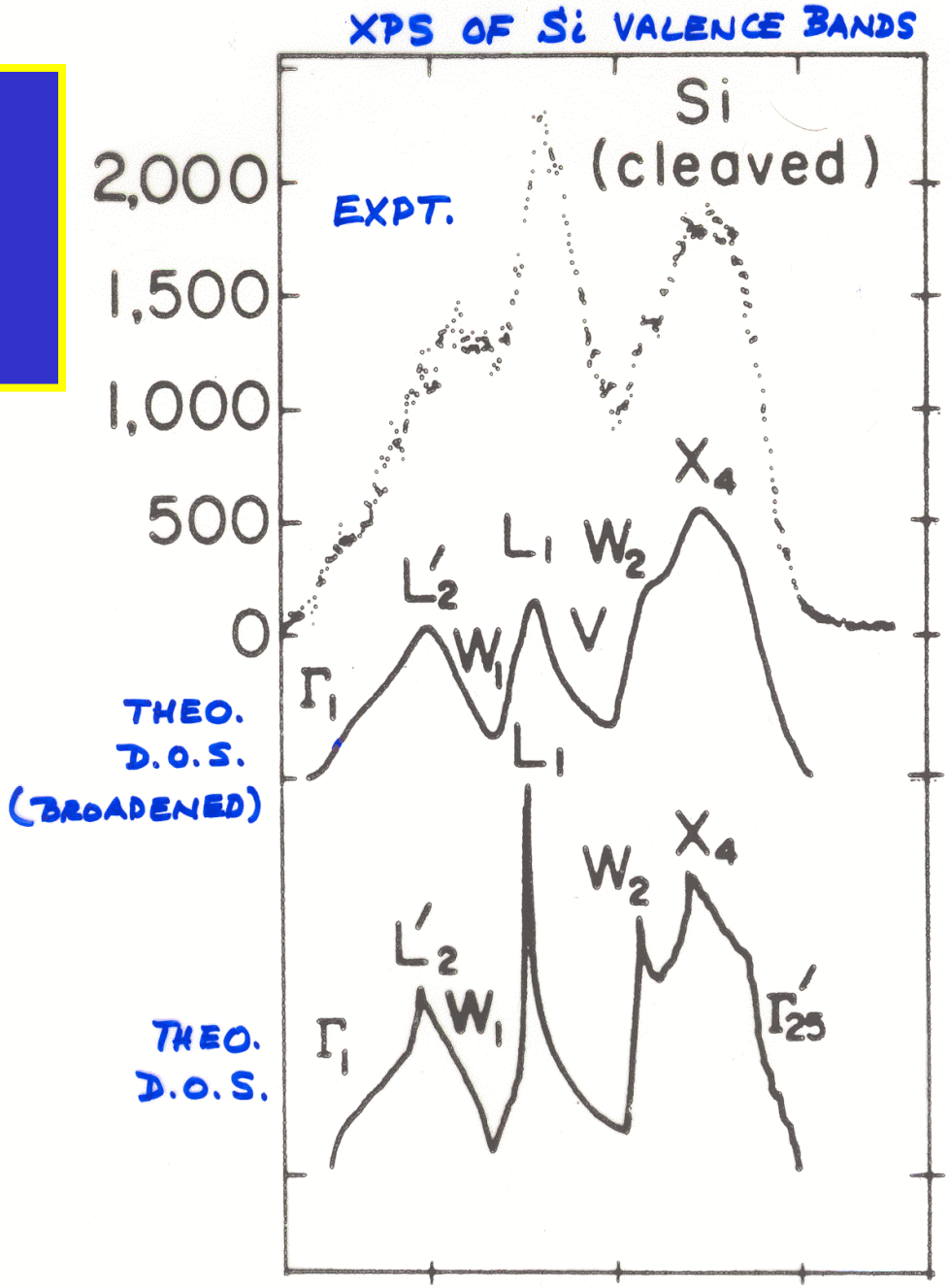

"Basic Concepts of XPS"
Figure 14

Densities of states From XPS spectra

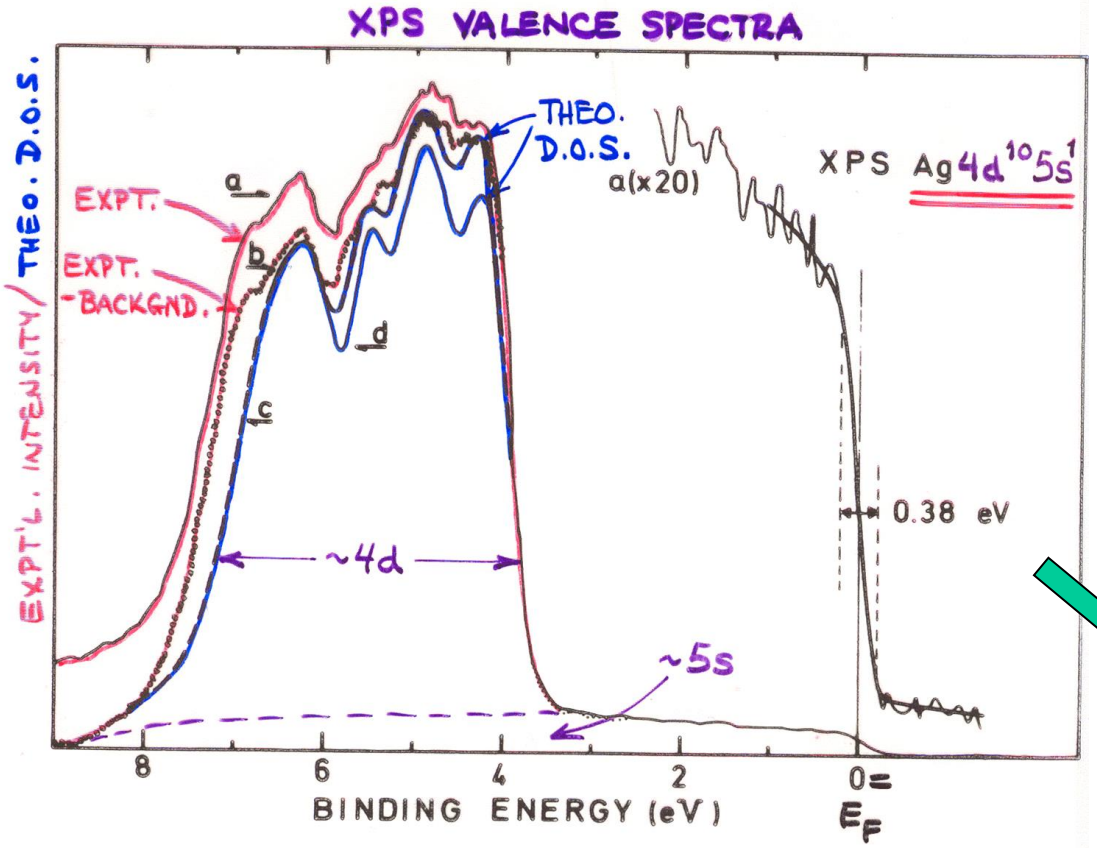

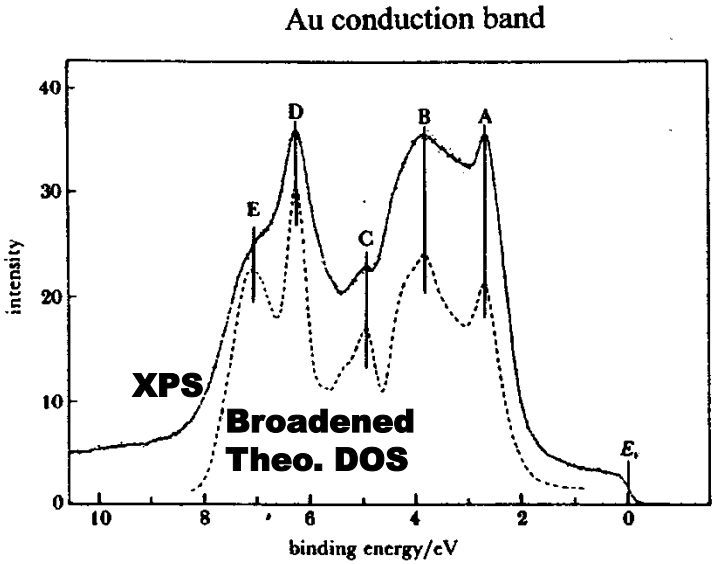

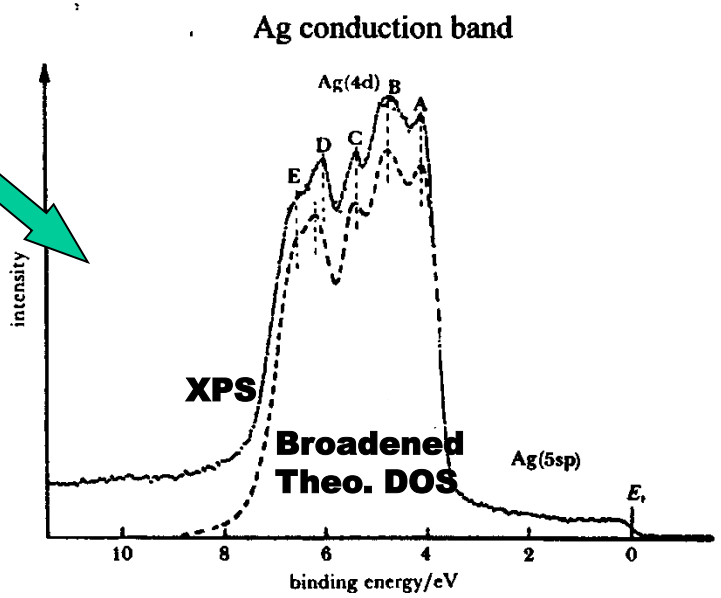

"Basic Concepts of XPS"
Figure 13

Siegbahn, 2003

Tungsten--Debye-Waller Factors and Recoil Energies

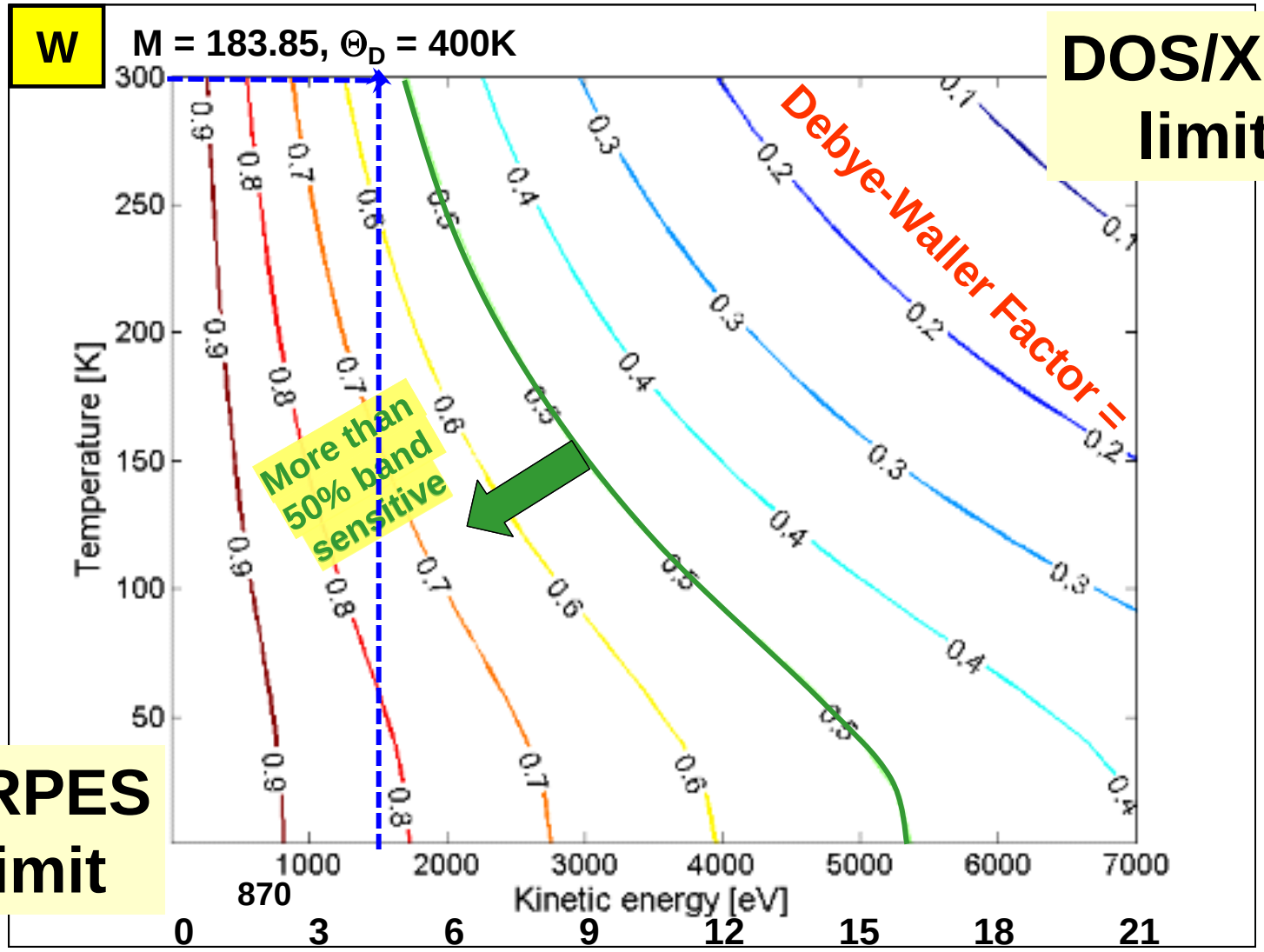

Plucinski, et al. PRB 78, 035108 (2008); Phys. Rev. B 84, 045433 (2011)

Direct-transition effects in XPS: W(110) at 1253.6 eV

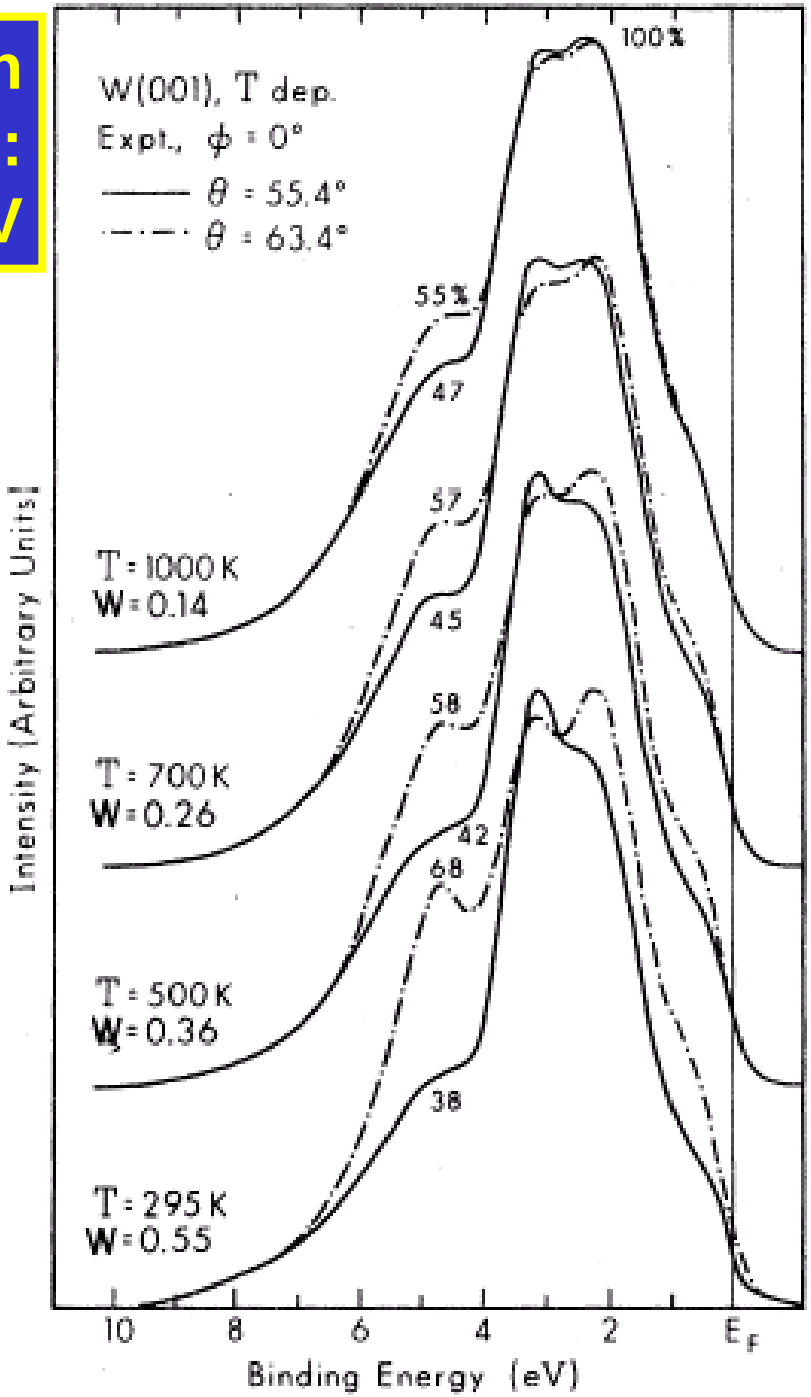

Present if vibrations stiff enough (Debye T high enough), but suppressed as temperature is raised.

Hussain et al., Phys. Rev. 22, 3750 (1980)

Effect of photon momentum on k conservation: W(110) at 1253.6 eV

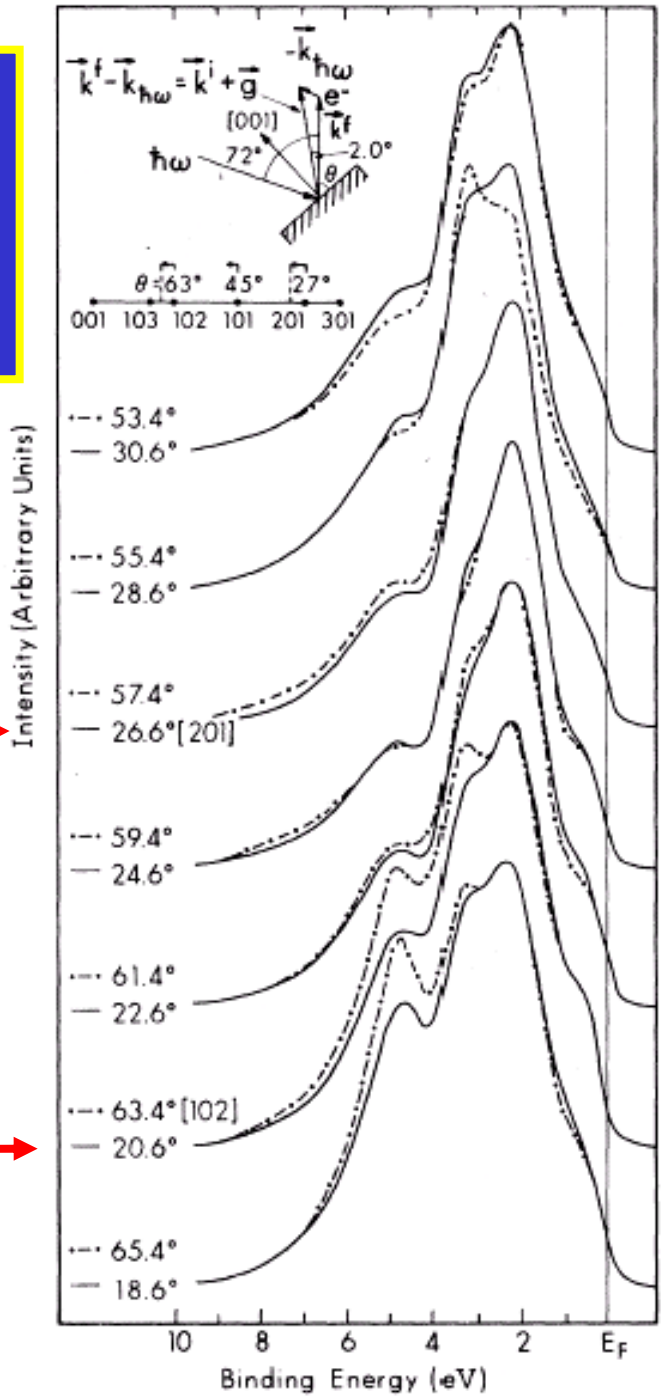

Symmetry-related spectra shifted by 6.0° for best match. Theoretical 4.8° due to $k_{h\nu}$

Hussain et al., Phys. Rev. 22, 3750 (1980)

Tungsten--Debye-Waller Factors and Recoil Energies

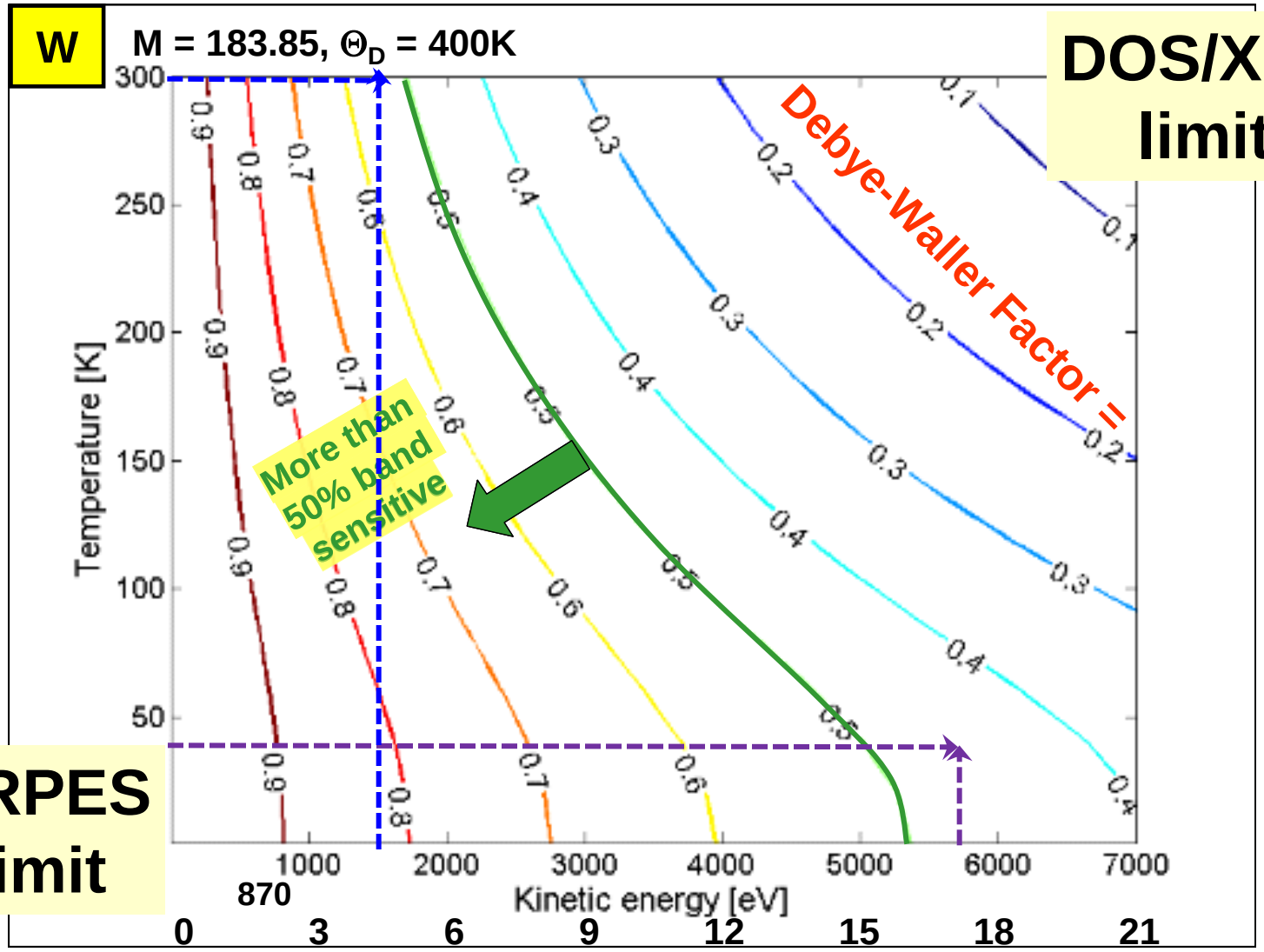

Plucinski, et al. PRB 78, 035108 (2008);
Phys. Rev. B 84, 045433 (2011)

Hard x-ray ARPES for W(110): 5.96 keV

(i)

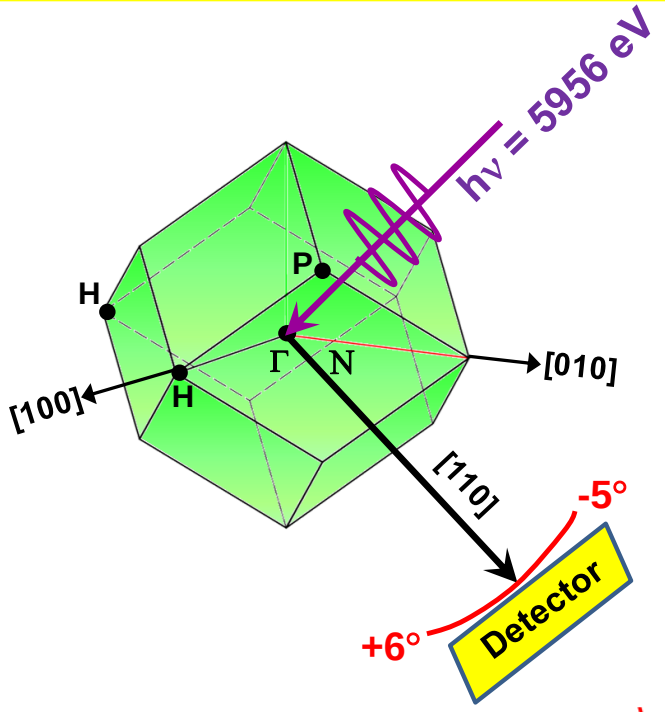

(ii)

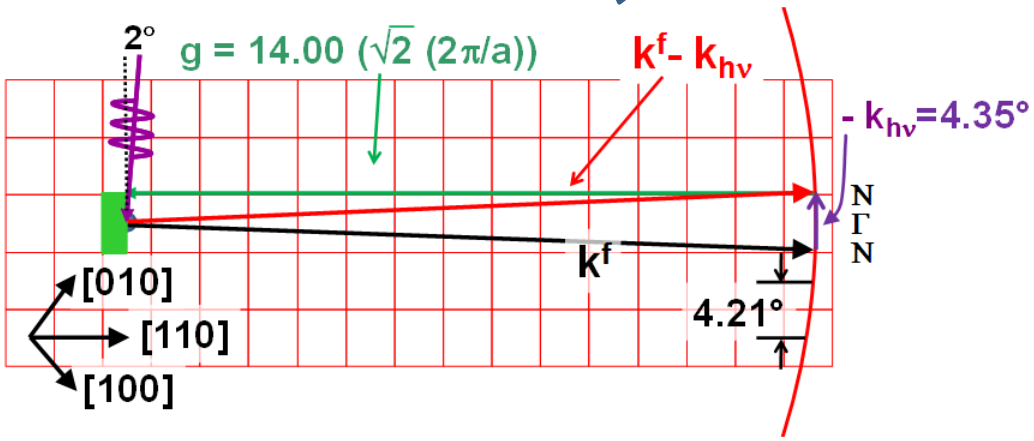

(iii)

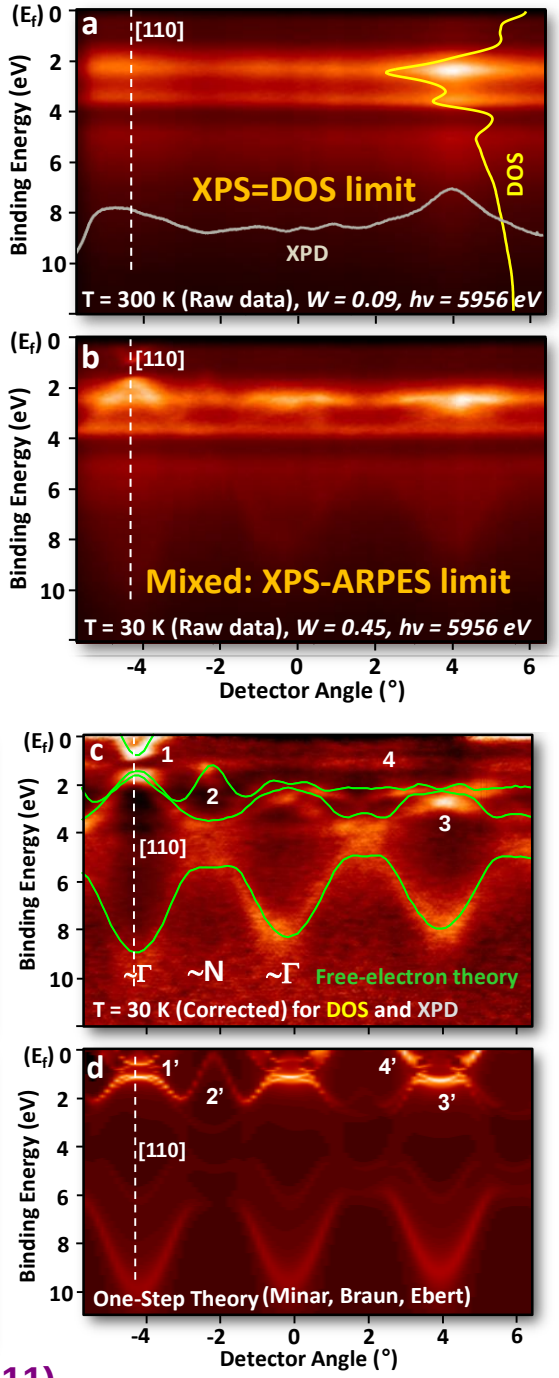

Gray, Minar et al., Spring-8, Nature Materials 10, 759 (2011)

Photon energy for D-W = O.5 @ 20K

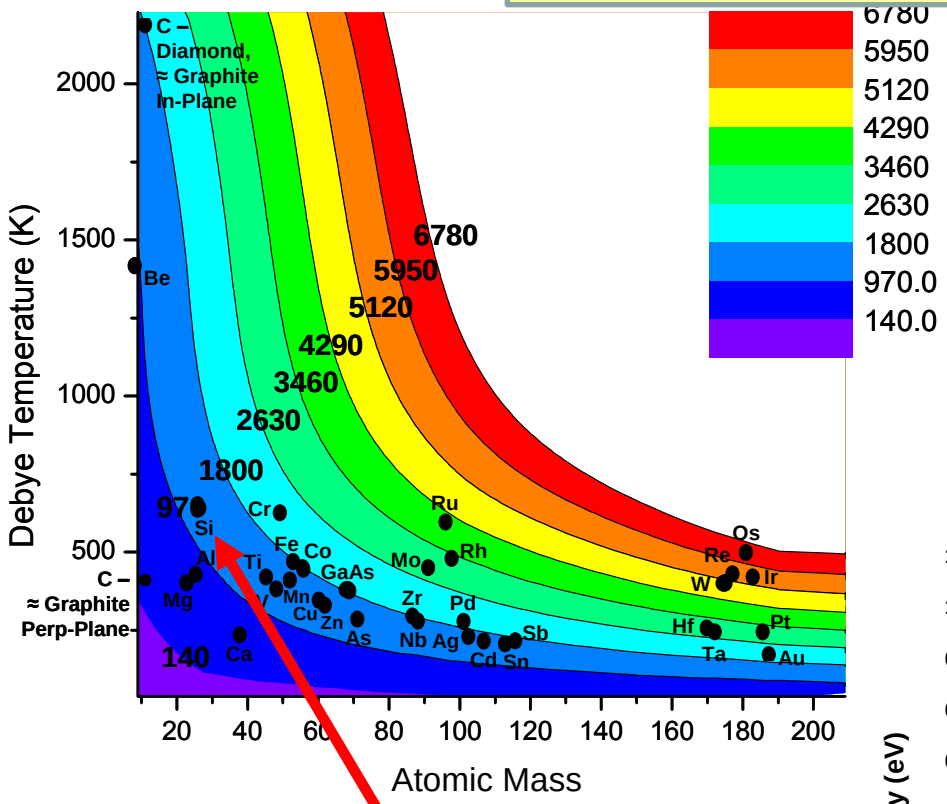

HARPES-How high can we go? Photoemission Debye-Waller Factors and Recoil Energies

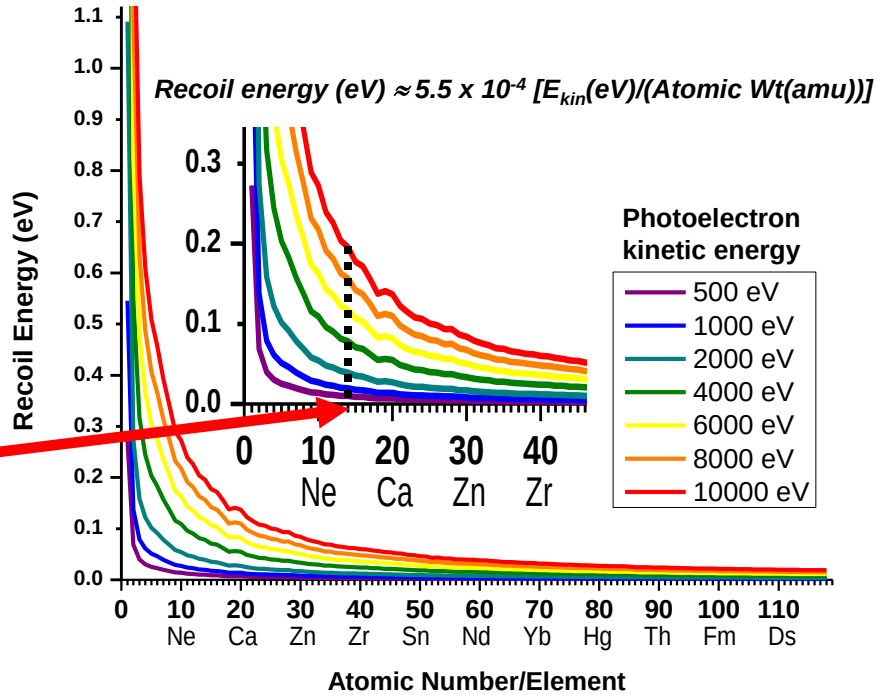

E.g.-Si

C. Papp. L. Plucinski, et al.,
Phys. Rev. B 84, 045433 (2011)

Thank you for your attention and all your efforts!